Function of the C. elegans T-box Transcription Factor TBX-2 Depends on SUMOylation and Groucho

BY

Paul B. Huber

B.S., University of Illinois at Chicago, 2006

THESIS

**Submitted as partial fulfillment of the requirements
for the degree of Doctor of Philosophy in Biological Sciences
In the Graduate College of the
University of Illinois at Chicago 2016**

Chicago, Illinois

Defense Committee:

Jennifer Schmidt, Chair
Peter Okkema, Advisor
Teresa Orenic
Jeremy Lynch
Hans-Georg Simon, Northwestern University

ACKNOWLEDGEMENTS

First and foremost I would like to thank my advisor Peter Okkema for his guidance and tutelage in science and in life. Pete is an excellent scientist and mentor and without his enthusiasm and support this work could not have been completed.

I would like to thank all members of the Okkema lab, past and present. On top of the splendid friendships I've made with them, their advice and ideas were a big part of my successes in the laboratory. This can be said too about all members of the Alfonso lab, and I thank them as well.

I would also like to thank my thesis committee members, Jennifer Schmidt, Teresa Orenic, Qun-Tian Wang, Jeremy Lynch, and Hans-Georg Simon for their time and insights over the years.

Finally, I would like to thank my parents for their unconditional love and support through all of my trials and tribulations throughout life and my older sister Allison for instilling in me the drive to excel academically.

CONTRIBUTIONS OF CO-AUTHORS

In Chapter 3, of which a portion was previously published in the journal Cellular and Molecular Life Sciences in an article entitled “Function of the T-box factor TBX-2 depends on SUMOylation”, the co-authors are Tanya Crum, Lynn Clary, Tom Ronan, Adelaide Packard, and Peter Okkema. The figures or tables contributed by each co-author are specified as such.

In Chapter 4, Tanya Crum is a co-author and contributed yeast two-hybrid data.

TABLE OF CONTENTS

LIST OF TABLES

LIST OF FIGURES

LIST OF ABBREVIATIONS

BiFC	bimolecular fluorescence complementation
BME	β-Mercaptoethanol
bp	base pair
cDNA	complimentary DNA
CIAP	Calf Intestinal Alkaline Phosphatase
CMV	Human *cytomegalovirus*
DIC	differential interference contrast
DNA	deoxyribonucleic acid
dNTPs	deoxynucleotides
dsRNA	double stranded RNA
EDTA	ethylenediaminetetraacetic acid
Eh1	engrailed homology 1
F1	first filial generation
F2	second filial generation
FBS	fetal bovine serum
GFP	green fluorescent protein
HA	Human influenza hemagglutinin
HF	high fidelity
HRP	horseradish peroxidase
L1	larval stage 1
L4	larval stage 4
mRNA	messenger RNA
MS	mass spectrometry
NB	nuclear body
NEP	enriched peptone plates with nystatin
NFDM	non-fat dry milk

NF-Y	nuclear transcription factor Y
NGM	nematode growth media
ONPG	ortho-Nitrophenyl-β-galactoside
PBS	phosphate-buffered saline
PCR	polymerase chain reaction
PML	promyelocytic leukemia
PMSF	phenylmethanesulfonyl fluoride
PVDF	polyvinylidene fluoride
RNA	ribonucleic acid
RNAi	RNA interference
RNAP II	RNA polymerase II
RPM	rotations per minute
RT	room temperature, or refers to RT (dicistronic counter-selection) cassette
SDS	sodium dodecyl sulfate
SDS-PAGE	sodium dodecyl sulfate polyacrylamide gel electrophoresis
SIM	SUMO interaction motif
SUMO	small ubiquitin-like modifier
TAE	tris base, acetic acid, and EDTA
TBP	TATA binding protein
TE	tris base and EDTA
TEV	Tobacco Etch Virus
TSS	transcription start site
ULP	ubiquitin-like protease
VC and VN	C-terminal Venus protein and N-terminal Venus protein
w/t	wild type
WD	tryptophan-aspartic acid

SUMMARY

T-box transcription factors are critical regulators of development in all animals, and reduction of their function underlies a number of known diseases (Papaioannou, 2014). Overexpression of T-box factors has been identified in several cancers, indicating their actions must be tightly regulated for normal function, however relatively little is known about the molecular mechanisms of their activity. In this work we show that the *C. elegans* T-box transcription factor TBX-2 depends on SUMOylation and interaction with a Groucho corepressor for its function in pharyngeal development.

tbx-2 is required for a subset of cells in the anterior pharynx, those which give rise to pharyngeal muscle from the ABa lineage (Roy Chowdhuri et al., 2006; Smith and Mango, 2007). Complete loss of *tbx-2* results in a loss of anterior pharyngeal muscles and larval lethality. In a yeast two-hybrid screen we identified the SUMO-conjugating enzyme UBC-9 and the Groucho-like corepressor UNC-37 as interactors of TBX-2, and reduction of their function *in vivo* also leads to a loss of anterior pharyngeal muscles (Roy Chowdhuri et al., 2006). Furthermore, *tbx-2* interacts genetically with both *ubc-9* and *unc-37*, as partial reduction of *tbx-2* and *ubc-9* or *tbx-2* and *unc-37* causes a *tbx-2* null-like phenotype. TBX-2 is a transcriptional repressor which regulates its own expression via a negative autoregulatory loop, and *tbx-2* is the only direct TBX-2 target known to date (Milton and Okkema, 2015). Knockdown of *tbx-2*, *ubc-9*, or *unc-37* by RNA interference similarly leads to deregulation of *tbx-2*. Taken together, these results suggest TBX-2 may function in a repressor complex with SUMO and UNC-37 during pharyngeal development, and because we show TBX-2 and its mammalian orthologs can be SUMOylated, we propose this as a novel mechanism to regulate T-box factor activity.

1 BACKGROUND AND INTRODUCTION

1.1 *C. elegans* is an excellent model system to study development

One of the most fascinating events in biology is the development of a complex organism, consisting of multiple cell types and differentiated organs, from one single cell. The molecular mechanisms that coordinate and drive development have only begun to be examined in depth as of recent, and the ever-expanding plethora of model organisms which are used to elucidate such mechanisms have proven to be key tools facilitating the expansion of this rapidly growing field of study. The free-living nematode *C. elegans* has proven to be an excellent model organism for developmental studies (Brenner, 1974). In addition to being well-suited for experimentation in the laboratory, many of the molecular pathways uncovered in the worm are well conserved in higher eukaryotes, and such discoveries have contributed to current knowledge about diseases in humans (Ogg et al., 1997; Sundaram and Greenwald, 1993).

Several characteristics of *C. elegans* make it uniquely adept for developmental studies. First, the worms are easy to maintain because they are small (reaching about 1 mm in length as full grown adults) and can flourish on a diet consisting strictly of *E. coli*, which can easily and quickly be cultured in the lab (Lewis and Fleming, 1995). *C. elegans* reproduction is rapid and robust, with a life cycle of about three days from egg to adult (Figure 1) and self-fertilizing hermaphrodites producing average progeny broods of 300 or more animals. Because *C. elegans* exist primarily as hermaphrodites, of which the cell lineage is completely known and essentially invariant, researchers have been able to track the fate of every cell throughout every stage of development (Kimble and Hirsh, 1979; Sulston and Horvitz, 1977; Sulston et al., 1983). *C. elegans* is a transparent animal, and the use of green fluorescent protein (GFP) reporters with

compound or confocal microscopy has facilitated the understanding of how the onset of specific gene expression at the single cell level can correlate with developmental timing (Chalfie et al., 1994). This technique, combined with the ability to proficiently reduce the function of any gene by RNA interference (RNAi) (Fire et al., 1998), has greatly advanced the knowledge of gene function in *C. elegans*. As it is estimated that about 60-80% of human genes have clear orthologs in the *C. elegans* genome (Kaletta and Hengartner, 2006), *C. elegans* is an ideal model organism for metazoan developmental studies.

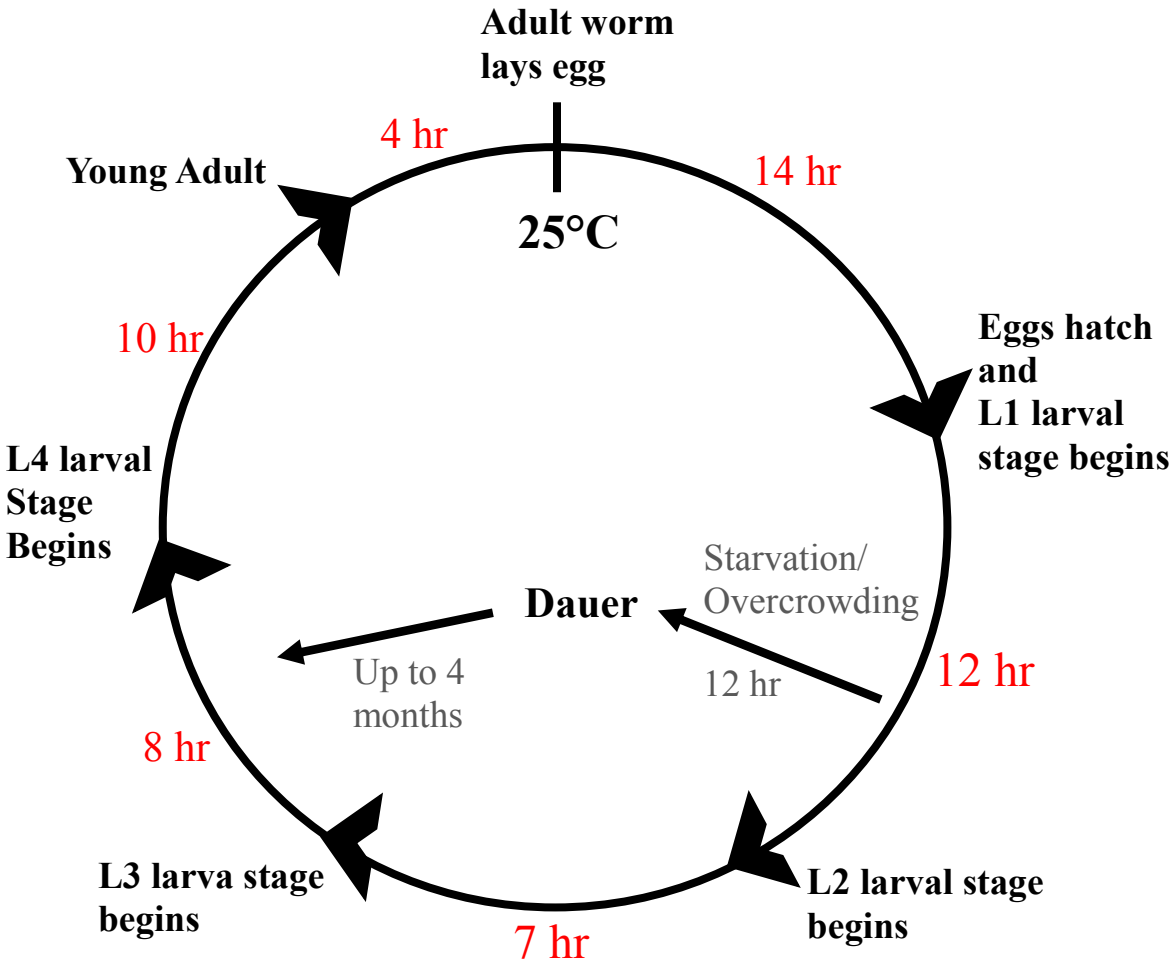

Figure 1. Schematic of the *C. elegans* life cycle

This schematic depicts the life cycle of a single *C. elegans* grown at 25°C, beginning from the time an embryo is laid by an adult hermaphrodite (0 hr) to the time it grows to a fertile adult capable of laying eggs (approximately 2.5 days) (Corsi, 2006). The length of time spent in embryonic, larval, and adult developmental stages are indicated in red. There are 4 larval stages between the embryonic and adult stages, with an alternative path to the dauer stage in the case of stresses such as starvation or overcrowding.

1.2 The *C. elegans* pharynx as a model for organogenesis

The *C. elegans* pharynx is a great model for organogenesis for numerous reasons (Mango, 2007). The pharynx is a neuromuscular organ used for feeding, and can easily be seen as a large bi-lobed structure at the anterior end of the worm using a dissecting microscope. Because the worms are transparent and the cell lineage is completely known, one can observe the entire development of the pharynx, starting from initial formation of the pharyngeal primordium. The pharynx is anatomically well characterized, thanks, in large part, to extensive examination of pharyngeal serial cross section images obtained using electron microscopy (Albertson and Thomson, 1976). Although a simple organ, the pharynx contains a total of 80 nuclei of five different cell types, and, because these cells can have different embryonic origins (Sulston et al., 1983), it faces similar developmental challenges as organs in higher eukaryotes.

The *C. elegans* pharynx is a neuromuscular organ that contracts rhythmically throughout the life of the worm to pump material (bacteria) through a lumen, and, as such, has drawn comparisons to the vertebrate heart (Mango, 2007). While it has been proposed that their similarities are likely a result of convergent evolution to fulfill similar biological roles, the pharynx can be used as a model to study gene function in cardiac muscle development. For example, in both the zebrafish heart and the *C. elegans* pharynx, Nkx homeodomain transcription factors, Nkx2.5 and CEH-22, respectively, activate genes involved in terminal differentiation of muscle cells (Chen and Fishman, 1996; Okkema and Fire, 1994; Okkema et al., 1997). Furthermore, Nkx2.5 can rescue *ceh-22* mutants and activate the CEH-22 target gene *myo-2* when introduced into *C. elegans*, confirming similar molecular mechanisms regulate genesis of the heart and pharynx (Haun et al., 1998).

1.2.1 Anatomy and function of the pharynx

Essentially, the pharynx is a bi-lobed muscular tube, surrounded by a basement membrane and innervated by a nervous system which is almost completely separate from that of the rest of the worm (Albertson and Thomson, 1976). Its function is to pump food (bacteria) to a structure called the grinder, where the food is masticated before being passed into the gut. Bacterial cells are initially taken in through the buccal cavity at the mouth of the worm, then pumped by contraction of the pharyngeal muscles through a cuticle-lined central lumen in the procorpus to the metacorpus (also called anterior bulb). There, a bolus of food develops, and, after a variable number of pumps, is transported through the isthmus in a peristaltic wave-like motion to the grinder in the terminal bulb (Figure 2) (Avery and Horvitz, 1987; Ray et al., 2008).

The pharynx is comprised of several non-equivalent cell types, muscle cells, marginal cells, gland cells, epithelial cells, and neurons, but marginal and muscle cells comprise the bulk of the structure (Albertson and Thomson, 1976). Marginal and muscle cells display a 3-fold radial symmetry around the pharyngeal lumen along the anterior-posterior axis, and can be sub-divided into 3 and 8 sections, respectively (Figure 3). These cells attach to the basement membrane on their basal side by half desmosomes, and they form the apical side of the pharyngeal cells (closest to the lumen) and secrete the cuticle which lines the inside of the pharynx, which indicates that they similarly possess epithelial properties (Albertson and Thomson, 1976). Large projections anchor muscle cells to neighboring marginal cells, and they communicate via gap and adherens junctions (Avery and Thomas, 1997). Marginal cells

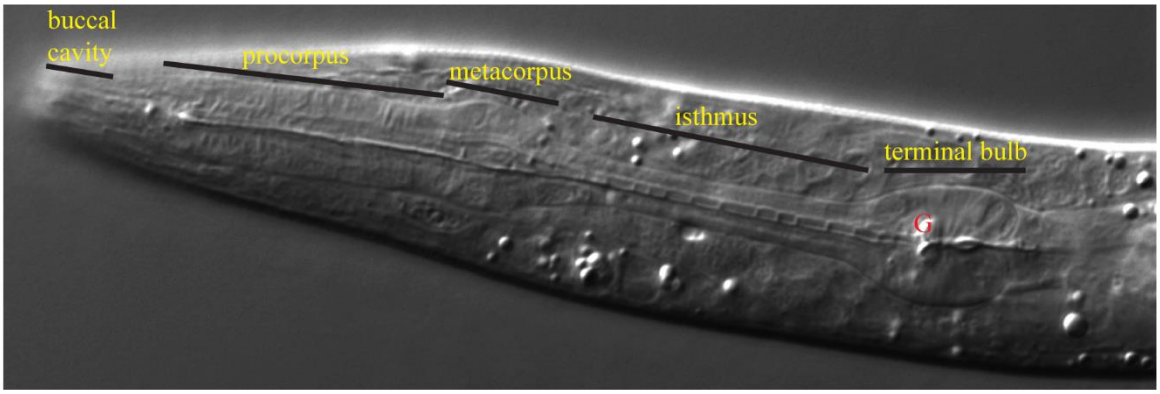

Figure 2. The *C. elegans* pharynx

DIC image of a *C. elegans* pharynx at the L1 larval stage at 100x magnification (anterior at left). By the L1 stage, the pharynx is fully differentiated and can be divided into the five sub-sections indicated: the buccal cavity, procorpus, metacorpus (anterior bulb), isthmus, and terminal bulb. The grinder (G), which pulverizes ingested bacteria, is in the center of the terminal bulb.

A. **B.**

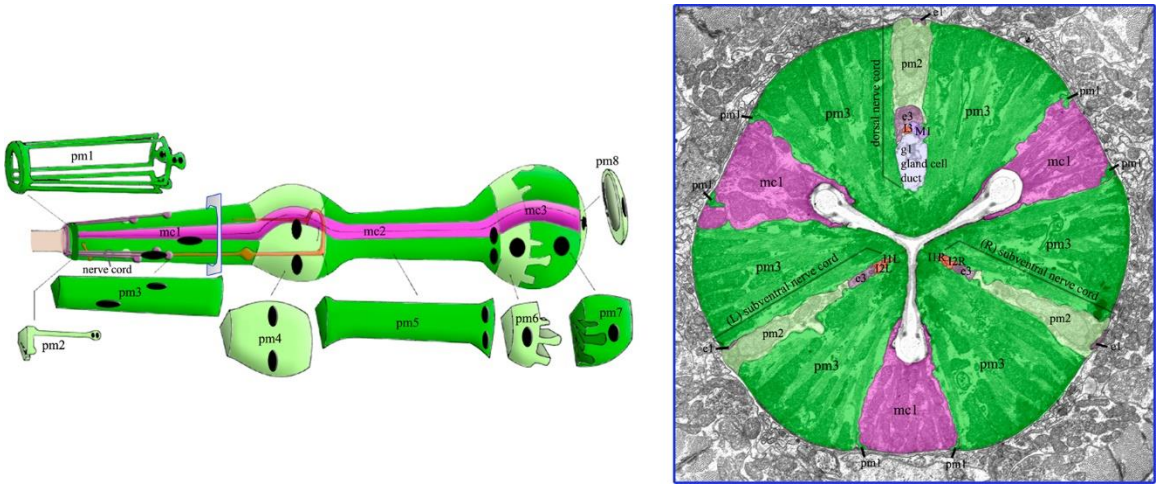

Figure 3. Positioning of muscle and marginal cells in the pharynx

Schematics depicting the positions of muscle and marginal cells within the pharynx [adapted from WormBook (http://www.wormbook.org/)]. A) Location of pharyngeal muscles, pm1-8, (in green), and their nuclei are indicated. Marginal cells, mc1-3, (in purple) lie between pharyngeal muscles. B) Micrograph obtained by electron microscopy of a pharyngeal cross section (mid-procorpus), depicting the 3-fold radial symmetry of pharyngeal muscle and marginal cells. The dorsal and subventral nerve cords [containing the cell bodies of epithelial cells (e3), gland cells (g1), and neurons (M1)] are embedded in clefts within the pharyngeal muscle layers.

primarily aid in structural support, giving the muscles a surface to bind, which permits the opening of the lumen upon muscle contraction during pumping (Albertson and Thomson, 1976).

1.2.2 Specification of pharyngeal identity

Formation of the pharynx occurs during embryogenesis (Sulston et al., 1983). Following gastrulation, the pharyngeal primordium exists as a tightly packed ball of cells near the anterior end of the embryo (Sulston et al., 1983). This group of cells, bound to one another by adherens junctions, undergoes re-orientation and elongation, forming a bi-lobed tube recognizable as the pharynx by the 3-fold embryonic stage, just prior to hatching (Portereiko and Mango, 2001). Cell division in the pharynx stops at this point, but the pharyngeal cells continue to grow larger until the worm is a full grown adult (Sulston and Horvitz, 1977). Unlike the midgut, which is derived from the single blastomere EMS of the 4 cell stage embryo, the pharynx (also called the foregut) is polyclonal, with contributions from both the ABa and EMS blastomeres forming the anterior and posterior regions of the pharynx, respectively (Figure 4) (Sulston et al., 1983). Although both blastomeres can produce identical cell types within these regions, they employ separate and distinct molecular pathways to activate the pharyngeal organ selector gene, *pha-4* (Bowerman et al., 1993; Bowerman et al., 1992; Broitman-Maduro et al., 2006; Broitman-Maduro et al., 2005; Calvo et al., 2001; Christensen et al., 1996; Evans et al., 1994; Gaudet and Mango, 2002; Good et al., 2004; Goszczynski and McGhee, 2005; Hutter and Schnabel, 1994; Kalb et al., 1998; Lambie and Kimble, 1991; Lin et al., 1995; Lo et al., 2004; Maduro et al., 2007; Maduro et al., 2002; Maduro et al., 2001; Mango et al., 1994; Mann and Carroll, 2002; Moskowitz et al., 1994; Priess et al., 1987; Priess and Thomson, 1987; Roy Chowdhuri et al., 2006; Shetty et al., 2005; Smith and Mango, 2007; Sulston et al., 1983).

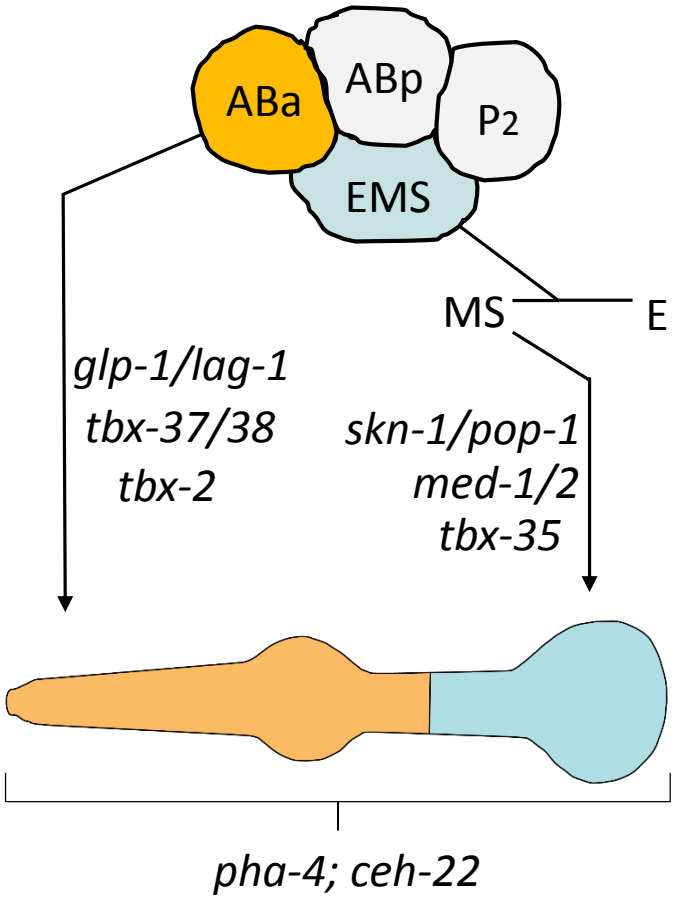

Figure 4. The pharynx is formed polyclonally.

Schematic depicting embryonic origins of the pharynx. The ABa and EMS blastomeres of the 4 cell stage embryo give rise to the anterior and posterior regions of the fully differentiated pharynx, respectively, by employment of separate and distinct molecular pathways to activate pharyngeal identity gene *pha-4* and pharyngeal muscle selector *ceh-22*.

The EMS blastomere, whose daughter cells, E and MS, give rise to gut and mesoderm including posterior pharynx, respectively, is autonomously specified by the maternally provided bZIP-related transcription factor *skn-1* (Figure 4) (Bowerman et al., 1993; Bowerman et al., 1992). *skn-1* is also required for anterior pharyngeal development, as a loss of *skn-1* causes EMS daughters to adopt the fate of their cousin, the C blastomere, which lacks the Notch signaling ligand necessary for ABa-derived pharynx, resulting in a complete loss of pharynx (Priess et al., 1987; Priess and Thomson, 1987). The HMG box protein POP-1 is enriched in the nucleus of the MS daughter cell and specifies MS fate by repressing genes which promote E fate (Broitman-Maduro et al., 2005; Calvo et al., 2001; Lin et al., 1995; Lo et al., 2004; Maduro et al., 2002; Shetty et al., 2005). Reduction of *pop-1* leads to a loss of posterior pharynx. In MS, SKN-1 activates zygotic expression of the GATA family transcription factors *med-1* and *med-2*, whose expression leads to activation of the T-box transcription factor *tbx-35*, marking the transition to total zygotic control of posterior pharyngeal development (Broitman-Maduro et al., 2006; Broitman-Maduro et al., 2005; Goszczynski and McGhee, 2005; Maduro et al., 2007). TBX-35 activates the NK-2 class homeodomain gene *ceh-51*, and TBX-35 and CEH-51 have overlapping functions in the MS lineage (Broitman-Maduro et al., 2009). Inactivation of *med-1* and *med-2* or *tbx-35* and *ceh-51* similarly leads to a loss of posterior pharynx.

In contrast to MS-derived pharynx, ABa-derived pharynx is specified conditionally, via activation of the GLP-1/Notch receptor at the 12-cell stage by intercellular signals from EMS descendant, MS (Priess et al., 1987; Priess and Thomson, 1987). *glp-1* RNA is provided maternally, and then translated only in ABa and its sister cell ABp (Evans et al., 1994). GLP-1 activation leads to activation of the LAG-1 transcription factor, which in turn activates *pha-4*

expression (Christensen et al., 1996; Hutter and Schnabel, 1994; Lambie and Kimble, 1991; Mango et al., 1994; Moskowitz et al., 1994; Smith and Mango, 2007).

Functioning in parallel to the GLP-1/Notch signaling pathway, the redundant T-box genes *tbx-37* and *tbx-38* are also required for ABa-derived pharynx, as a combined reduction of their function leads to a loss of *pha-4* activation in the ABa lineage (Good et al., 2004). *tbx-37* and *tbx-38* are activated at the 24-cell stage in 8 ABa descendants, and their expression is restricted to these cells because REF-1 family members repress their expression in non-ABa descendants (Neves and Priess, 2005). TBX-37/38 and LAG-1 both activate *pha-4*, indicating that induction of ABa pharyngeal fate relies on two parallel pathways (Christensen et al., 1996; Good et al., 2004; Kalb et al., 1998; Mango et al., 1994).

The closely related T-box factors *tbx-35* and *tbx-37/38* are similarly required in early embryogenesis for pharyngeal specification, although it remains unclear whether or not *tbx-35* directly activates *pha-4*, and it is likely that other factors are involved in commitment to pharyngeal fate (Broitman-Maduro et al., 2006). Interestingly, another T-box factor, *tbx-2*, which is first expressed around the 100-cell stage, is crucial for a subset of cells from the ABa lineage, those which give rise to anterior pharyngeal muscle (Roy Chowdhuri et al., 2006; Smith and Mango, 2007). *tbx-2* is necessary for ABa-derived pharyngeal muscle precursors to maintain *pha-4* expression, and *pha-4* is necessary for *tbx-2* expression in the same cells, indicating that these two factors regulate each other's expression in a positive feedback loop. However, *tbx-2* and its vertebrate orthologs repress transcription of target genes, and since targets of TBX-2 remain largely unidentified, it is unclear how this feedback loop works (Christoffels et al., 2004; Huber et al., 2013).

1.3 T-box transcription factors are highly conserved regulators of development

T-box factors regulate organogenesis and tissue specification during the early development of all vertebrates and invertebrates alike [reviewed in (Showell et al., 2004)]. This family of proteins is characterized by a highly conserved DNA binding domain, termed the T-box, consisting of approximately 180 amino acids, and can act as activators or repressors of transcription. The family is named after the founding member *Brachyury*, or *T* (Greek for short tail), which was the first T-box gene to be characterized (Herrmann, 1991). Many more T-box genes have since been identified in various species [reviewed in (Naiche et al., 2005)]. In vertebrates, there are currently about 20 known T-box factors, which can be subdivided in 5 distinct subfamilies based on sequence homology within the T-box (Figure 5). Many of the vertebrate T-box factors have clear orthologs in invertebrates, indicating that their function is evolutionarily conserved across different species (Ruvinsky et al., 2000). For example, the closely related mammalian Tbx2 subfamily *Tbx2* and *Tbx3* genes have clear orthologs in *Drosophila* and *C. elegans*, *omb* (optomotor blind) and *tbx-2*, respectively, and all are crucial for viability and regulate similar cell fate decisions in development (Bakker et al., 2008; Harrelson et al., 2004; Pflugfelder et al., 1992; Roy Chowdhuri et al., 2006; Smith and Mango, 2007).

The genes of the Tbx2 subfamily are involved in many aspects of mammalian development and are crucial for viability, as homozygous mutants perish during embryogenesis and heterozygous mutants display various dysmorphisms and generally have shorter expected life spans [reviewed in (Naiche et al., 2005)]. In particular, normal heart development depends on the Tbx2 subfamily genes *Tbx2*, *Tbx3*, and *Tbx5*, as mutations in these genes leads to phenotypes characterized by debilitating cardiac defects [reviewed in (Greulich et al., 2011)]. Tbx2 and Tbx3 are both repressors, and lead to inhibition of cardiac chamber myocardium, while

Tbx5 is an activator that induces chamber formation and cardiomyocyte differentiation. Interestingly, Tbx2/Tbx3 and Tbx5 regulate similar target genes (such as *Nppa* and *Cx40*), and can even interact with the same proteins (Nkx2-5, for example) in developing cardiac tissue, suggesting specific protein-protein interactions and possibly post-translational modifications guide their functionality (Christoffels et al., 2004; Ghosh et al., 2001; Habets et al., 2002; Hiroi et al., 2001; Hoogaars et al., 2008; Hoogaars et al., 2004; Takeuchi et al., 2003). T-box factors often require other factors to function properly, and understanding how they function and which protein-protein interactions are important for the Tbx2 subfamily members will shed light on how and which downstream targets they regulate during development [reviewed in (Naiche et al., 2005)].

1.3.1 Misregulation of T-box factors causes diseases and cancer

T-box factors have gained the attention of researchers, in large part, because their misregulation is known to cause a number of human congenital diseases and cancer [reviewed in (Naiche et al., 2005; Wansleben et al., 2014)]. The Tbx1 subfamily gene *TBX22* is required for human palatogenesis, and haploinsuffiency of this gene is known to cause X-linked cleft palate with ankyloglossia, or CPX (Braybrook et al., 2001; MarÁano et al., 2004). Patients with DiGeorge syndrome, an unfortunate consequence of haploinsuffiency of *TBX1*, are also afflicted with craniofacial dysmorphisms, as well as heart defects (Papangeli and Scambler, 2013). In fact, haploinsuffiency of T-box genes underlies a number of known human diseases and syndromes, with the most well characterized of those genes hailing from the Tbx2 subfamily.

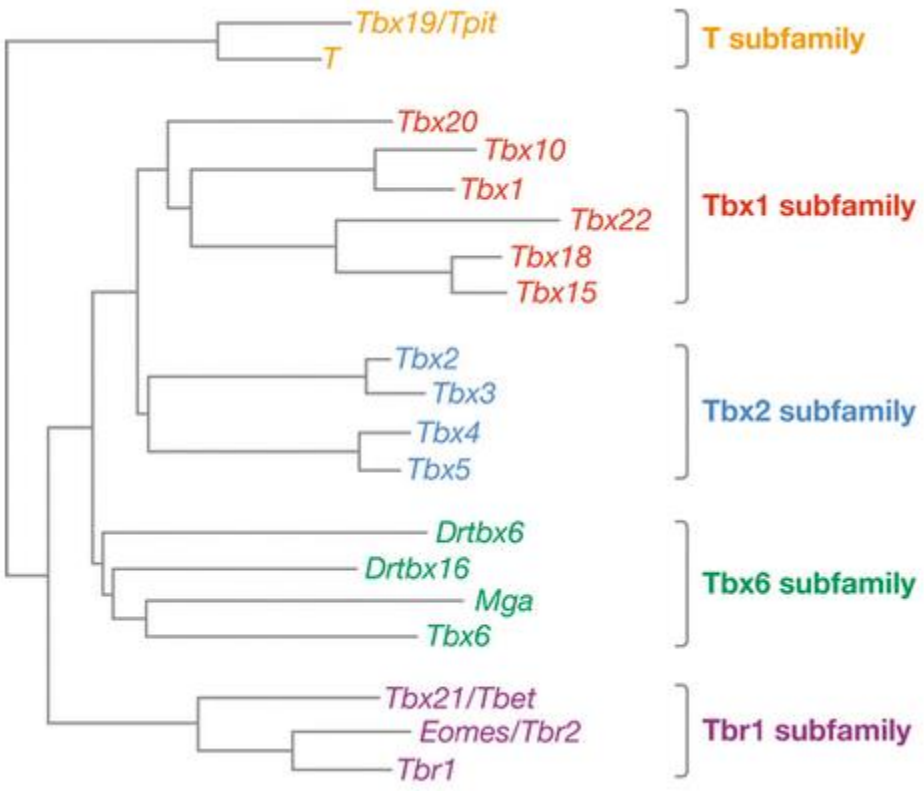

Figure 5. The 5 evolutionarily conserved vertebrate T-box factor subfamilies

Schematic depicting a phylogenetic tree of the vertebrate T-box genes [adapted from (Naiche et al., 2005), which can subdivided into 5 distinct subfamilies based on sequence homology within the T-box. All of these genes exist in mammals, except for the zebrafish genes *Drtbx6* and *Drtbx16*, which have no mammalian orthologs.

Patients with Ulnar-mammary syndrome, caused by mutations in *TBX3*, suffer from defects in limb, apocrine, and genital development (Bamshad et al., 1997). Mutations in *TBX4* cause small patella syndrome, which is characterized by underdevelopment of the patella and abnormalities in the pelvic region and feet (Bongers et al., 2004). Lastly, *TBX5* mutations lead to Holt-Oram syndrome, and afflicted patients suffer from cardiac and upper limb defects (Basson et al., 1997; Li et al., 1997).

Interestingly, overexpression of the Tbx2 subfamily genes can be as detrimental as reduction of their function [reviewed in (Wansleben et al., 2014)]. *TBX2* is overexpressed in breast, pancreatic, colorectal, and ovarian cancers, as well as melanomas. A pro-proliferative factor, high levels of Tbx2 leads to direct repression of components of the cell senescence pathway, $p19^{ARF}$ ($p14^{ARF}$ in humans) and *p21* (Dobrzycka et al., 2006; Jacobs et al., 2000; Prince et al., 2004; Vance et al., 2005; Vormer et al., 2008). *TBX2* has also been shown to promote epithelial to mesenchyme transition (EMT), which can lead to the initiation of metastasis in cancer progression (Chaffer and Weinberg, 2011; Wang et al., 2012). Unsurprisingly, *TBX3*, which is the most closely related Tbx2 family member to *TBX2*, is also heavily implicated in cancer progression [reviewed in (Wansleben et al., 2014)]. In addition to its ability to repress $p19^{ARF}$ and *p21*, Tbx3 can indirectly promote cell proliferation and survival by repression of the tumor suppressor phosphatase and tensin homolog (PTEN) (Brummelkamp et al., 2002; Burgucu et al., 2012; Carlson et al., 2001; Hoogaars et al., 2008; Lingbeek et al., 2002). In summary, what we know about T-box factors is that their activity must be tightly regulated throughout development, and studies geared towards understanding how they function could lead to novel therapies for the diseases and cancers associated with their misregulation.

1.3.2 The sole *C. elegans* Tbx2 subfamily member *tbx-2* is required for ABa-derived pharyngeal muscle

In *C. elegans*, there is only one representative gene of the Tbx2 subfamily, *tbx-2*, and like its mammalian orthologs, it is an essential gene that is crucial for viability (Roy Chowdhuri et al., 2006; Smith and Mango, 2007). The T-box domain of TBX-2 is closely related to the T-boxes of human TBX2/3 and TBX4/5, sharing approximately 70% and 60% amino acid sequence identity, respectively, suggesting their function is conserved across metazoan species. *tbx-2* is expressed dynamically throughout the majority of a worm's life (approximately from 100 cell stage and onward) and is involved in many processes, including behavioral adaptation and neural fate specification, and, as previously mentioned, is required for ABa-derived pharyngeal muscle development (Miyahara et al., 2004; Roy Chowdhuri et al., 2006; Singhvi et al., 2008; Smith and Mango, 2007). Using a full length *tbx-2::gfp* fosmid, we have observed onset of expression in the nuclei of pharyngeal precursors around the 100 cell stage, which persists in the developing pharynx throughout pharyngeal extension and numerous cells in the head and pharynx during adulthood. Null *tbx-2(ok529)* mutants display a striking phenotype in that they appear to completely lack the anterior portion of the pharynx and thereby arrest as L1 larva, presumably due to the inability to feed. Using a nuclear-localized CEH-22::GFP marker, which fluoresces in the 21 nuclei of pm3,4,5,7 pharyngeal muscles, it has been shown that the 7 ABa-derived muscles specifically are lacking in *tbx-2* loss of function animals, while the 14 MS-derived muscles are retained (Roy Chowdhuri et al., 2006; Smith and Mango, 2007). It is unclear whether these missing cells have adopted an alternative cell fate, although they do not appear to have undergone apoptosis. It is equally unclear as to exactly how TBX-2 promotes pharyngeal development, as direct downstream targets and protein interaction partners remain largely unidentified.

Although relatively little is known about the mechanisms of TBX-2 activity, we have identified two proteins which affect TBX-2 function, the small ubiquitin-like modifier (SUMO) protein and the Groucho-like corepressor UNC-37 (Huber et al., 2013; Roy Chowdhuri et al., 2006). SUMO becomes covalently attached to target proteins via an enzymatic cascade similar to ubiquitination in a process referred to as SUMOylation (Figure 6). SUMOylation can affect a substrate protein in numerous ways, such as altering that protein's stability, nuclear or subnuclear localization, or involvement with particular protein complexes (Gill, 2004; Park et al., 2016; Pferdehirt and Meyer, 2013; Shen et al., 2006; Zhang et al., 2004; Zhong et al., 2000). SUMO plays a large role in the regulation of gene expression and is generally associated with gene repression, which is accomplished largely by promoting interaction with proteins [transcriptional co-repressors or histone deacetylases (HDACs), for example] that repress transcription (Ahn et al., 2009; Ng et al., 2015). Also in contrast to ubiquitination, for which there are several different E2 conjugating enzymes, for SUMOylation there is only 1, UBC9 (Figure 6) [reviewed in (Gill, 2004; van Wijk and Timmers, 2010)], so genetic ablation of this enzyme in living cells inhibits SUMOylation of all the proteins therein. We found that, in *C. elegans*, knockdown of *ubc-9* by RNAi leads to a pharyngeal phenotype identical to that seen in *tbx-2* mutants, and we hypothesize that *tbx-2* function to promote ABa-derived pharyngeal muscles is SUMO-dependent (Roy Chowdhuri et al., 2006). *ubc-9(RNAi)* embryos also exhibit mislocalization of a TBX-2::GFP translational fusion to subnuclear puncta, suggesting SUMOylation of TBX-2 could be required for proper distribution throughout the nucleoplasm, although it is possible that this mislocalization was due to indirect negative effects on nuclear structure in a strong mutant. Interestingly, our most recent evidence is consistent with a role for

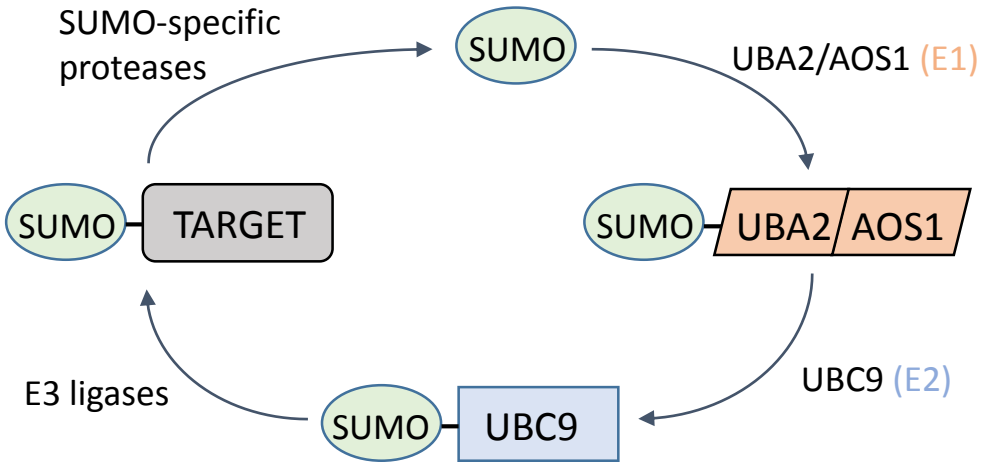

Figure 6. The SUMOylation pathway

Diagram of the reversible enzymatic pathway responsible for SUMO-conjugation to target substrate proteins [reviewed in (Gill, 2004)]. SUMO first forms a thioester conjugate with the heterodimeric E1 activating enzyme UBA2/AOS1. SUMO is then transferred to the E2 conjugating enzyme UBC9. SUMO is then conjugated to a target protein through an isopeptide bond at a lysine residue on the target, and this step is sometimes aided by E3 ligases which promote transfer to specific substrates. SUMO-specific proteases containing isopeptidase activity are responsible for removal of SUMO from substrates, as well as initial maturation of the SUMO peptide.

SUMOylation in the promotion of TBX-2 interaction with the Groucho-like corepressor UNC-37. *unc-37(RNAi)* animals, like *ubc-9(RNAi)* and *tbx-2* loss of function animals, lack ABa-derived pharyngeal muscles (Roy Chowdhuri et al., 2006). Knockdown of *ubc-9* or *unc-37* by RNAi also leads to deregulation of the TBX-2 target gene, *tbx-2* (Milton and Okkema, 2015). As TBX-2 can interact directly with UBC-9 and UNC-37 in yeast two-hybrid assays (Roy Chowdhuri et al., 2006), we propose that SUMO promotes TBX-2 interaction with UNC-37 in a repressor complex to regulate target genes during pharyngeal development, and this will be discussed in further detail in the following chapters. The function of mammalian T-box factors, such as TBX22, Tbx5, Tbx15, and Tbx18, have been shown to rely on SUMO or Groucho, suggesting similar interactions occur during the development of other organisms (Andreou et al., 2007; Beketaev et al., 2014; Farin et al., 2007).

1.4 Post-translational modification by SUMOylation

Post-translational modifications such as acetylation, methylation, phosphorylation, and ubiquitination have been widely studied in the context of cell biology, and since the discovery of the first SUMOylated protein, the GTPase activating protein RanGAP1, in 1996, SUMOylation has also been identified as an essential regulator of protein activity in numerous cellular processes (Hay, 2005; Mahajan et al., 1997; Matunis et al., 1996). SUMOylation has been linked to proteins involved in the DNA damage response, cell division, DNA replication, nuclear trafficking, and transcription [reviewed in (Eifler and Vertegaal, 2015)]. Due to recent advancements in proteomic approaches, more than 1,600 SUMO substrates were identified in an immortalized human cell line (Hendriks et al., 2014). A whopping 4,361 sites of SUMO-conjugation were identified in these substrates, with many of those overlapping with previously reported sites of acetylation, methylation, and ubiquitination, indicating cross-talk among SUMO and other post-translational modifications.

Interestingly, the majority of SUMO targets reside in the nucleus or shuffle between the nucleus and cytoplasm, emphasizing the importance of SUMO in nuclear processes (Hendriks et al., 2014). Absent from this list of nuclear SUMO targets is the T-box factor TBX5, which was recently shown to depend on SUMOylation for its transcriptional activity, indicating the limitation of large-scale SUMO pulldowns in correctly identifying all functional SUMO target substrates and that we have only scratched the surface of understanding the roles SUMO plays in the cell (Beketaev et al., 2014).

1.4.1 The SUMOylation pathway

SUMO becomes covalently attached to target proteins in an enzymatic cascade very similar to that of ubiquitination (Figure 6) [reviewed in (Gill, 2004)]. As its name would

suggest, SUMO is a relatively small protein at approximately 100 amino acids in length. At its C-terminal is a Glycine-Glycine (GG) motif, followed by a small, but variable number of amino acids (varies among SUMO homologs), which is cleaved by SUMO-specific proteases, thereby producing mature SUMO protein [reviewed in (Gill, 2004)]. Once mature, SUMO first forms a thioester conjugate (through its C-terminus) with the heterodimeric E1 activating enzyme UBA2/AOS1. SUMO is then transferred to the E2 conjugating enzyme UBC9, forming another thioester intermediate. UBC9 recognizes the SUMO consensus motif ΨKX(D/E) (where Ψ represents a bulky, hydrophobic amino acid, K is the point of SUMO-conjugation, X can be any amino acid, and either aspartic or glutamic acid can fill the fourth position) in target proteins and catalyzes SUMO conjugation at these same sites [reviewed in (Gill, 2004)]. SUMOylation has been shown to occur at non-consensus sites, which is thought to be facilitated by E3 ligases, which promote the transfer of SUMO from UBC9 to specific targets by acting as docking stations for UBC9.

SUMO-modification is both a dynamic and reversible process, and SUMO-specific proteases are responsible for deconjugation of SUMO from substrates (Figure 6) [reviewed in (Gill, 2004)]. Only a minimal number of SUMO proteases have been identified to date [reviewed in (Eifler and Vertegaal, 2015)]. In mammals, for example, there are 6 SUMO-specific proteases (SENP1, 2, 3, 5, 6, and 7) involved in the maturation and deconjugation of SUMO, and although they are all classified as cysteine isopeptidases, they can differ in their cellular localization and ability to recognize specific SUMO peptides and target substrates.

1.4.2 Function of SUMO

Because SUMO is involved in a multitude of cellular processes, it is crucial for viability in most organisms, which is evidenced by the pervasiveness of lethal phenotypes among

eukaryotic developmental models lacking essential components of the SUMO pathway, UBC9 or SUMO itself [reviewed in (Lomelí and Vázquez, 2011)]. In mice, Zebrafish, and *C. elegans*, UBC9 loss of function mutants exhibit early embryonic lethality (Nacerddine et al., 2005; Nowak and Hammerschmidt, 2006; Roy Chowdhuri et al., 2006). As not all eukaryotes possess the same number of SUMO-encoding genes, mutation of a single SUMO gene can cause embryonic arrest or no observable phenotype, depending on the organism [reviewed in (Lomelí and Vázquez, 2011)]. There are 4 SUMO genes in humans and mice (*SUMO-1-4*), 3 in Zebrafish (*sumo1-3*), and only 1 in yeast (*SMT3*), *Drosophila* (*smt3*), and *C. elegans (smo-1)*, and only in these 3 latter species is the loss of the single SUMO gene lethal, suggesting SUMO-1-3 can fill each other's role in the absence of either one of them (Giaever et al., 2002; Nie et al., 2009; Zhang et al., 2004). Based on phylogenetic evidence, SUMO-2, 3 (which are more similar in amino acid sequence to each other than SUMO-1) arose as duplications of SUMO-1 during metazoan evolution, which is consistent with observations of their functional redundancy in mouse single gene KO models, and suggests that SUMO likely performs similar functions in different species (Lomelí and Vázquez, 2011; Ureña et al., 2016). This was recently shown to be true in an insect model, as defects in wing and puparian formation observed in s*mt3*-deficient tissues of the holometabolous *Drosophila* were rescued by overexpression of the SUMO homolog, *BgSUMO3*, from the more distantly related, hemimetabolous cockroach *B. germanica*.

An interesting and suprisingly common finding about SUMO-modified proteins is that "a little can go a long way", as most target substrates exist primarily in a non-SUMOylated state, with only a small portion being SUMOylated at any given time (under non-stress conditions), yet a large biological response is achieved [reviewed in (Hay, 2005)]. For example, though the SUMO target and transcriptional repressor TBX22 is mostly non-SUMOylated (even upon

overexpression with SUMO-1) when transiently transfected in COS-1 cells, mutation of the SUMO acceptor lysine abolished both SUMOylation and repressor activity in GAL4-driven luciferase reporter assays (Andreou et al., 2007). One theory to explain this observation is that SUMO may promote the interaction of transcription factors in a repressor complex, but once that complex is formed, it is stable and SUMO-specific proteases can deconjugate SUMO from the target substrate without disturbing the complex [reviewed in (Hay, 2005)]. SUMO conjugating and deconjugating enzymes are similarly located in the nucleus, so rapid, reversible conjugation of DNA-bound targets is feasible.

An alternative theory, which is not mutually exclusive from that previously mentioned, is that simultaneous SUMOylation of individual components of a complex, or group of functionally related proteins, leads to a quick, cellular response [reviewed in (Eifler and Vertegaal, 2015)]. In this model, as long as some of the components are SUMOylated, the complex can fulfill its biological role, and which components are SUMOylated can differ at any given time. Consistent with this idea, many cofactors of SUMOylated transcription factors can also be SUMOylated, and similar observations have been made in other SUMO-dependent complexes as well [reviewed in (Gill, 2004)]. The most well characterized example of a SUMO-dependent complex is that of promyelocytic leukemia nuclear bodies (PML NBs) [reviewed in (Cheng and Kao, 2013)]. The presence of SUMO interaction motifs (SIMs) as well as SUMO-conjugation sites in PML NB components contribute to PML NB formation, as this assembly is mediated by the combination of non-covalent interactions between SUMOylated substrates as well as SUMOylation of PML and many of the other NB components (Ishov et al., 1999; Seeler and Dejean, 2003; Shen et al., 2006; Zhong et al., 2000). Other examples of SUMOylation of multiple components within a complex have been reported in yeast and *C. elegans*, for a

Groucho-dependent repressor complex and the X chromosome dosage compensation complex, respectively, indicating the function of SUMO to hold transcriptional complexes together is conserved among eukaryotes (Ng et al., 2015; Pferdehirt and Meyer, 2013).

1.5 The evolutionarily conserved Groucho/Transducin-Like Enhancer of split (Gro/TLE) family of corepressors interact with many transcription factors

Drosophila Groucho, named after a mutant which developed supernumerary supraorbital bristles resembling the large, bushy eyebrows of the late American film star Groucho Marx, was the first member identified from the highly conserved Groucho/Transducin-like Enhancer of split (Gro/TLE) family of proteins [reviewed in (Kaul et al., 2015)]. This family is found in all animals and participates in a wide range of biological processes, including neurogenesis, osteogenesis, somitogenesis, haematopoiesis, proliferation, stem cell maintenance, and organogenesis [reviewed in (Agarwal et al., 2015)]. Gro/TLE proteins lack the ability to bind DNA directly and instead act as repressive cofactors for DNA-binding transcription factors. Transcription factors of the Pax, Six, Nkx, Runx, Hes, LEF1/Tcf, Fox, and T-box families have been shown to interact with Gro/TLE proteins, several of which function in cell fate specification. For example, two mouse T-box factors from the Tbx1 subfamily, *Tbx15*, which is involved in skin and skeletal development, and *Tbx18*, which is involved in axial skeletal formation, both depend on Groucho for repressor activity (Farin et al., 2007). Some Groucho effectors are also involved in pathways which are known to be misregulated in human cancers, further emphasizing the importance of Groucho for normal cell functions [reviewed in (Agarwal et al., 2015; Kaul et al., 2015)].

Although different species have differing numbers of Groucho-encoding genes [1 in *Drosophila* and *C. elegans* (*unc-37*), and 4 in humans (*TLE1-4*) and mice (*Grg1-4*)], the primary structure of Groucho protein remains the same in all animals [reviewed in (Agarwal et al., 2015)]. At the N-terminus is a glutamine-rich Q domain containing two coiled-coil motifs which is primarily involved in oligomerization of Groucho proteins. At the C-terminus is a WD-repeat

domain, which forms a seven-bladed β propeller that mediates the bulk of Groucho interactions with transcription factors via the central pore of the propeller (Jennings et al., 2006).

Transcription factors primarily interact with the WD domain of Groucho through either of two short peptide motifs; the WRPW (Trp-Arg-Pro-Trp) or engrailed homology 1, or "eh1" motif [FS(I/V)XXΨΨX, with X representing a non-polar or charged amino acid and Ψ representing a branched hydrophobic amino acid] (Jennings et al., 2006; Yaklichkin et al., 2007). Interestingly, even though these two classes of motif form drastically different peptide conformations, crystal structure data has revealed both motifs interact with the central pore of the WD domain β propellor, and mutations in the β propeller of Groucho or the WRPW or eh1 motifs of Groucho interactors can abrogate this interaction. Both WRPW and eh1 motifs are highly conserved in a diverse array of transcription factors of all metazoa, indicating similar interactions likely occur in all animals (Agarwal et al., 2015; Copley, 2005)

1.5.1 Groucho function

Groucho recruitment and repression of target gene expression is thought to be achieved via multiple mechanisms [reviewed in (Kaul et al., 2015)]. In *Drosophila*, Groucho was initially shown to act as a corepressor for Dorsal and Hairy genes from long-range, or distances more than 1 kb. Although subsequent evidence was shown that Groucho can repress from short distances (less than 1 kb), long-range repression has been the canonical model for nearly 2 decades [reviewed in (Kaul et al., 2015)]. In this proposed "spreading" model, Groucho is recruited by a transcription factor to a target gene promoter, and oligomerizes with other Groucho molecules via the Q domain over several kilobases of DNA to block the transcription start site (TSS) and thereby silence gene expression. However, more recent studies employing ChIP-seq in two independent *Drosophila*-derived cell lines (Kc167 and S2) found that Groucho

frequently bound the genome with peak widths of less than 1 kb, with median peak widths of 708 and 425 bp in Kc167 and S2 cells, respectively (Kaul et al., 2014). Groucho was also frequently found at the TSS of genes, although these genes were not completely silenced and still produced transcripts, albeit in a limited capacity.

One might predict that the binding of Groucho at a TSS could silence gene expression by interfering with the occupancy of RNA polymerase II (RNAP II) at those sites, however, RNAP II actually often co-localizes with Groucho at the TSS, suggesting Groucho's presence there does not inhibit RNAP II recruitment (Kaul et al., 2014). At times, the checkpoint to transfer from initation of transcription to elongation for many genes being transcribed during development is rate-limiting, such that more RNAP II molecules are positioned at the TSS than elsewhere on the gene, and this event is referred to as "promoter proximal RNAP II pausing" [reviewed in (Kaul et al., 2015). In this context, transcripts can be assigned a "pause ratio", defined by the total amount of RNAP II at the TSS to the amount of RNAP II at other regions within the gene. Interestingly, in Kc167 cells, nearly half of the transcripts for which Groucho was bound over the TSS were found to have a "very high" pause ratio (in the top 10 percentile of all transcripts), suggesting Groucho may reduce gene expression by increasing promoter proximal RNAP II pausing (Kaul et al., 2014). Consistent with this hypothesis, depletion of Groucho by RNAi in the same cells reduced RNAP II pausing at the high confidence Groucho target locus *E(spl)mβ-HLH*.

While recent ChIP-seq experiments have provided insights into possible new mechanisms of Groucho-mediated repression, they have also provided evidence supporting the long-standing model that Groucho represses target genes, at least in part, through modulation of chromatin structure by the recruitment of HDAC1 (called Rpd3 in *Drosophila*) (Chen et al., 1999; Kaul et

al., 2014). In 1999, Groucho was shown to interact physically and genetically with Rpd3, indicating that functions of Groucho which are essential for normal development are Rpd3-dependent, although Groucho has since been shown to act independently of Rpd3 in some contexts [reviewed in (Kaul et al., 2015)]. In ChIP-seq assays, Groucho is generally associated with regions in the genome that are not highly acetylated, and 59% of Groucho binding peaks overlap with peaks of Rpd3 binding, which is highly consistent with a model in which Groucho partially depends on the recruitment of histone deacetylases for gene inactivation (Kaul et al., 2014).

Previous studies in other organisms, like *C. elegans*, have indicated that the mechanisms of Groucho corepressor activity are conserved. The *C. elegans* Groucho ortholog *unc-37* was shown to genetically interact with components of the transcriptional mediator complex, a regulator of RNAP II which plays a role in nearly all aspects of transcription, including RNAP II pausing (Allen and Taatjes, 2015; Zhang and Emmons, 2002). UNC-37 depends on interaction with the truncated Groucho-like protein LSY-22 via the Q domain to specify neural fates, and interaction with LSY-22 is thought to promote UNC-37 interaction in a repressor complex (Flowers et al., 2010). UNC-37 is also known to interact with the homeodomain proteins UNC-4 and COG-1 (through their eh1 motifs) in neuronal fate specification, further indicating that the biological functions of Groucho are conserved among metazoans, and *C. elegans* can be a powerful tool for elucidating the mechanisms of Groucho repression (Chang et al., 2003; Winnier et al., 1999).

1.5.2 SUMO affects Groucho and Groucho-interacting proteins

Groucho proteins are known to function in a variety of tissues throughout development, and it is likely that functional specificity in certain tissues at particular times is accomplished by

its ability to interact with different macromolecular protein complexes at target promoters [reviewed in (Agarwal et al., 2015)]. Interestingly, HDAC-dependent Groucho repression has recently been linked to SUMOylation (Ahn et al., 2009). Groucho can be SUMOylated at 4 lysine residues, and mutation of these residues to arginines abolishes Groucho repressor activity in luciferase reporter assays. Fusion of SUMO to a SUMO-deficient Groucho mutant completely restores repressor activity, indicating that Groucho function depends on SUMO-modification (Ahn et al., 2009). HDAC1 possesses a highly conserved SIM, which mediates interaction with SUMOylated Groucho in GST pull-downs, suggesting SUMO may increase Groucho repressor activity by promoting interaction with histone deactelyases. However, other proteins which interact physically and genetically with Groucho (in yeast and Xenopus, for example) have recently been shown to be SUMO substrates as well, and these observations suggest SUMOylation may be a conserved modulator of Groucho corepressor complexes (Lee et al., 2012; Ng et al., 2015).

2 GENERAL MATERIAL AND METHODS

2.1 Nematode Handling

Worm strains were maintained in 16-25°C incubators on nematode growth media (NGM) plates which were seeded with *E. coli* strain OP50 (Lewis and Fleming, 1995). For passaging, 4-6 young adult hermaphrodites were moved to new plates every 5-7 days. For long term storage, starved worms were washed from 5 NGM plates with a 1:1 mixture of M9 buffer and worm freezing buffer. The solution of worms was then transferred to 5 cryostorage vials (Nunc) and temporarily frozen at -80°C before being transferred to liquid nitrogen.

2.2 General microscopy

Worms and mammalian cells were examined, manipulated, and/or imaged using a Zeiss Stemi 2000 dissecting microscope equipped with a 100IL-PS power supply (Diagnostic Instruments), a Zeiss Axiovert 100 inverted microscope, a Leica DMIL inverted microscope equipped with fluorescence and an ebq100 ISOLATED power supply, or a Zeiss AxioImager or Axioskop fluorescence microscope (with 10X, 40X, 63X, and 100X objectives). Images were acquired with AxioVision or Zen software.

2.3 *C. elegans* germline transformation

Germline transformation by injection (at a DNA concentration range between 2.5 – 100 ng/µl) was performed as described (Mello and Fire, 1995). pRF4, a plasmid containing the dominant co-injection marker *rol-6(su1006)* was used to identify transformants, via the *rol-6* rolling phenotype, in the F1 generation. Arrays which were passed to the F2 generation were assumed to be stable and worms carrying the array segregated both progeny that carry and do not carry the array, at varying segregation efficiencies. Animals which expressed *rol-6* were

assumed to possess all co-injected plasmids in the array at high copy number, this was verified by fluorescence microscopy, DNA sequencing, or western blotting in some cases. Transgenic strains were maintained by passaging rolling worms.

Germline transformation by biolistic transformation (also called microparticle bombardment) was performed following parts from two existing protocols, *Biolistic Transformation of C. elegans* on the Transgeneome Project website (https://docs.google.com/document/d/1xsgu6U0MpEhWIghiwTlrgNMDm_uuvCTYtm65vgC9Eyo/edit) and the bombardment protocol in *Transgenic solutions for the germline* on WormBook (Merritt and Seydoux, 2010). Special parts and equipment employed for particle delivery are the Biolistic PDS-1000/He particle delivery system (Bio-Rad 165-2257) with Hepta adapter (Bio-Rad 165-2225), 1.1 µm tungsten M-17 microcarrier beads (Bio-Rad 165-2267), 1 µm gold microcarrier beads (Bio-Rad 165-2263), biolistic microcarriers (Bio-Rad 165-2335), 1550 psi rupture discs (Bio-Rad 165-2333), and hepta stopping screens (Bio-Rad 165-2226). Tungsten beads were successfully used to bombard plasmids, and gold beads were successfully used to bombard fosmids.

Prior to the day of bombardment, the hepta adapter, stopping screens, microcarrier holder, microcarriers (placed in a glass petri dish with forceps), and a pair of forceps were individually wrapped in aluminum foil and autoclaved on the Dry20 cycle for sterilization. Tungsten and gold bead stocks were also prepared in advance in and were stored at 4°C for up to 4 months. For bead stock preparation, 30-50 mg beads were carefully measured into a 1.7 ml low retention, siliconized tube (Denville Scientific) and 1 ml 70% ethanol was added, followed by a 5 minute high speed vortex. The tube was allowed to sit on the bench for 15 minutes, and then centrifuged at 1500 RPM for 1 minute to pellet beads. The supernatant was discarded and

beads were washed 3 times with sterile water. After decanting final wash, the beads were resuspended in 500 µl sterile 50% glycerol, giving a final concentration of 60 mg/ml.

Mutant strain DP38 (*unc-119(ed3)*) worms were grown in large numbers for use in all bombardments. Transformation by bombardment has a low frequency of success (approximately 1 in 200,000), which requires large numbers of worms to be synchronized in the adult stage at the moment of particle delivery (500,000-1,000,000 per bombardment). DP38 grow very slowly, so worms were maintained at 25°C to facilitate the accumulation of such a large number of worms in a timely manner. Amplification of DP38 began by picking 10 piles of starved DP38 to each of 2 small NGM plates seeded with OP50. Once the worms on these plates began to starve and formed piles, the worms were resuspended in 6 ml M9 buffer and spread evenly to 6 large NEP (enriched peptone plates with nystatin) [1.2 g NaCl, 20 g peptone, 25 g agar, dH_2O to 1 liter, autoclave, cool, add 1 ml cholesterol (5 mg/ml in EtOH), 1 ml 1 M $MgSO_4$, 25 ml 1 M potassium phosphate (pH 6.0), 10 ml Nystatin suspension (Sigma-aldrich)] plates with NA22 *E. coli* bacterial lawn (0.5-1 ml bacterial solution added to plates 4-5 days before plating worms). Worms were grown until most were freshly starved L1s, and each plate was then resuspended in 10 ml M9 buffer giving a total of 60 ml, which was transferred to 50 ml conical tubes. To enrich for L1s, the suspension was allowed to sit for 5-10 minutes so that adult worms would settle to the bottom of the tubes. The supernatant was then pipetted into new 50 ml conical tubes, and spread evenly over 60 NEP plates with NA22. Once the worms on these plates reached adulthood, they were collected by resuspension in M9 and split into three 50 ml conical tubes (60 plates is good for 3 bombardments). After letting the worms settle for 10 minutes, the supernatant was aspirated and worms were washed with M9. Supernatant was then aspirated such that no more than 2 ml of worm suspension remained in each tube, and each suspension was

spread evenly over chilled, dry, unseeded large NGM plates. The plates were then gently placed on top of an ice bucket filled with ice and covered with saran wrap, and as soon as the worm solution dried, plates were bombarded.

DNA coated beads were prepared on the day of bombardment in low retention tubes to minimize the loss of DNA. The bead stock solution was vortexed for 5 minutes, and 100 µl was added to a 1.7 ml siliconized tube. 20-50 µl DNA was added and the tube was vortexed (all vortexing steps were performed on the lowest setting from this point on to avoid DNA shearing) for 1 minute. 100 µl 2.5 M $CaCl_2$ was added and the tube was again vortexed for 1 minute. 60 µl 0.1 M spermidine was added and the tube vortexed for 30 minutes. The DNA coated beads were then pelleted at 1000 RPM for 30 seconds, and the supernatant was discarded. The beads were washed with 300 µl 70% ethanol, then 100% ethanol. The supernatant was discarded, and 170 µl 100% ethanol was added, giving the final DNA coated bead solution which was ready for immediate bombardment.

Once DNA coated beads were prepped and worms were dried on unseeded NGM plates, the particle delivery system was prepared for bombardment. The apparatus was turned on by activating the vacuum pump and the helium tank valve was opened and set to 1750 psi. The bombardment chamber was wiped with 70% ethanol to ensure sterile conditions during delivery. The coated bead prep was mixed by flicking the tube and 20 µl was distributed to each of 7 autoclaved microcarriers on top of autoclaved foil for 1 bombardment. These microcarriers were then allowed to air dry to remove any remaining ethanol. Once the microcarriers were dried, they were transferred with forceps to the microcarrier holder, which was assembled with a stopping screen as described in the Bio-rad manual. A rupture disk (1550 PSI) was dipped in isopropanol, then placed into the hepta adapter. The hepta adapter was inserted into the chamber

and tightened with a torque wrench. The microcarrier holder was placed on a rung in the bombardment chamber directly below the hepta adaptor and aligned such that each of the adaptor pins was directly overhead the microcarriers. The worm plate to be bombarded was placed on and taped to the plate holder in the second rung of the bombardment chamber. The chamber was closed, the vacuum button pushed to upper position until vacuum reached 28 inches, and then moved to the lower position to hold the vacuum. The fire button was pressed until a popping noise was heard. Then the vacuum button was moved to the middle position to vent the chamber, at which point the hepta adapter, microcarrier holder, and the bombarded plate were removed from the chamber. The particle delivery system and vacuum pump were then turned off and the helium tank valve was closed after ensuring pressure was released from the line.

Following bombardment, worms were allowed to recover by incubation at room temperature for 1 hour. Worms from each bombarded plate were then resuspended in 5 ml M9 buffer and spread evenly onto 20 large NEP plates with NA22, such that not too many worms were placed on the plates that they would starve sooner than 3 days at 25°C. The plates were checked over the next 2-4 weeks for transformants by screening for non Unc animals, which were picked to individual plates when found. Because all DNA constructs that were bombarded contained GFP, non Uncs which segregated progeny that expressed GFP were considered to be successfully transformed lines. Non Uncs which segregated progeny that did not express GFP were considered to be non-transgenic revertants and were discarded. 10-100 worms were cloned from each independent GFP(+) line, those that segregated no Unc worms were considered to be chromosomally integrated transformants and integrations were sometimes mapped, those that always segregated some percentage of Unc worms were considered stable extrachromosomal array transformants and segregation efficiencies were determined.

2.4 Single worm PCR

Worm lysis reactions were carried out by picking a single worm into a PCR tube containing 2.5 µl 1x single worm lysis buffer (50 mM KCl, 10 mM Tris pH 8.3, 2.5 mM $MgCl_2$, 0.45% Triton x-100, 0.45% Tween 20, 0.1% gelatin) with 120 µg/ml Proteinase K (Beaster-Jones and Okkema, 2004). Tubes were placed in a thermal cycler at 60ºC for 1 hour, then 95ºC for 15 minutes for Proteinase K deactivation. PCR was then carried out by adding worm lysis reaction to PCR mix (2.5 µl 10x PCR buffer, 0.75 µl 50 mM $MgCl_2$, 0.2 µl 25 mM dNTPs, 1 µl 100 ng/µl primer 1, 1 µl 100 ng/µl primer 2, 1 µl 100 ng/µl primer 3, 18.4 µl dH_2O, and 0.25 µl Taq DNA polymerase), including appropriate primers, for a final volume of 25 µl. PCR programs were designed based on the primers being used and the PCR products being amplified, and PCR products were separated by 1-2% agarose gel electrophoresis for analysis.

2.5 DNA sequencing

DNA constructs were sequenced at the University of Illinois at Chicago Research Resources Center (UIC-RRC) using a 3730xl Capillary Sequencer (Applied Biosystems). For each sample to be sequenced, 10 µl of approximately 100 ng/µl sample DNA and 10 µl of approximately 5 pmol/µl sequencing primer were provided to sequencing facility. MacVector software (MacVector) was used to open and analyze received electronic sequence files.

2.6 DNA isolation

Plasmids and fosmids were isolated from various bacterial strains using standard plasmid and fosmid isolation kits according to manufacturer's instructions. Kits used include the High Pure Plasmid Isolation Kit (Roche), QIAprep Spin Miniprep Kit (Qiagen), Wizard Plus SV Miniprep System (Promega), FosmidMAX DNA Purification Kit (Epicentre). Single bacterial colonies containing plasmid or fosmid DNA grown on appropriate selective media were picked,

grown in the appropriate selective media, and pelleted for purification. PCRs and gels were purified and DNA was isolated using the Wizard SV Gel and PCR Clean-up System (Promega), according to manufacturer's instructions.

2.7 Quantitation of DNA concentration

DNA concentrations were typically quantified using a Nanodrop Lite spectrophotometer (Thermo Scientific) according to the manufacturer's manual. In some cases, DNA concentrations were estimated by comparison to a known standard. Briefly, a particular volume of sample DNA was digested and visualized on an agarose gel along with DNA ladder of a known volume and concentration. DNA concentrations were then estimated based on comparison of the sample DNA band intensity to DNA ladder band intensities.

2.8 DNA analysis by agarose gel electrophoresis

DNA constructs were separated on 1-2.2% agarose gels based on fragment size in 1X TAE buffer (40 mM Tris base, 30 mM acetic acid, 5 mM sodium acetate, 1 mM EDTA) with 0.3 µg/ml ethidium bromide. For fragments exceeding 1,000 base pairs, HindIII/KpnI-digested lambda phage DNA was used for molecular weight marker. For DNA fragments less than 1,000 base pairs, commercially bought DNA molecular weight markers from Fermentas, New England Biolabs, or Invitrogen were used.

2.9 General vector construction

Vector and insert DNA were digested with appropriate restriction enzymes for 2 hours in a water bath. Only vector DNA was treated with calf intestinal alkaline phosphatase (CIAP) (Invitrogen) for 1 hour at 37°C, then CIAP was deactivated by incubation at 70°C for 20 min. Restriction digests producing fragments of varying sizes (over 300 bp) were typically gel

purified to retrieve only desired fragments. After separation of fragments by agarose gel electrophoresis, the desired vector and insert fragments were excised by removal from the agarose gel with a razor blade on top of a UV illuminator. The fragments were then purified and isolated from the gel slice using a Wizard SV Gel and PCR Clean-up System (Promega). Varying ratios of purified vector and insert fragments were then added to 1 µl 10X ligation buffer and 0.5 µl T4 DNA ligase (New England Biolabs) and diluted to a final reaction volume of 10 µl with dH_2O. Ligations were incubated at room temperature for 15 minutes, or 16°C overnight, before being transformed into competent DH5α *E. coli* cells.

2.10 Site Directed Mutagenesis

Site directed mutagenesis reactions were performed using the Quikchange II Site-directed Mutagenesis kit (Stratagene), according to manufacturer's instructions. Briefly, primers were designed which were 24-45 bp in length with a melting temperature ≥78°C and the desired mutation positioned directly in the middle of the primer sequence. PCR mutagenesis reactions contained 5 µl 10x reaction buffer, 25 ng template DNA, 125 ng forward mutagenesis primer, 125 ng reverse mutagenesis primer, 1 µl dNTPs, 3 µl Quiksolution, 1 µl Pfu Ultra HF DNA polymerase, and were filled to a total reaction volume of 50 µl with dH_2O. The PCR program used was as follows: step (1) 95°C for 30 seconds, 16 x [(2) 95°C for 30 seconds, (3) 55°C for 1 minute, (4) 68°C for 1 minute per Kb of template]. Amplified products were digested with DpnI for 1 hour to digest template DNA, and then transformed into XL1-Blue supercompetent cells provided in the kit as described in the manufacturer's instructions (Strategene).

2.11 Primer design and preparation

All primers were designed using MacVector software and then purchased from either Sigma Genosys or IDT. Lyophilized oligonucleotides were then resuspended in dH_2O or TE buffer and stored in a -20°C freezer.

2.12 Preparation of competent DH5α *E. coli*

A single DH5α colony was used to inoculate 3 ml 2xTY and the culture was grown overnight. The next day 100 ml of pre-warmed 2xTY was added to a sterile 500 ml flask and inoculated with 0.5 ml of overnight culture and shaken at 37ºC for about 2.5 hours, or until $OD_{600} = 0.6$. The culture was transferred to 50 ml conical tubes (BD Falcon), incubated on ice for 15 minutes, and centrifuged for 4 minutes at 4,000 rpm and 4ºC to pellet bacteria. The supernatant was aspirated and the pellets were resuspended in 2 ml ice cold Buffer 1 (10 mM MES pH 6.2, 100 mM $RbCl_2$, 10 mM $CaCl_2$, 50 mM $MnCl_2$) and consolidated into a single tube. After adding an additional 14 ml of Buffer 1, the tube was incubated on ice for 15 minutes, then centrifuged for 4 minutes at 4,000 rpm and 4ºC. The supernatant was aspirated, the pellet was resuspended in 1.6 ml ice cold Buffer 2 (10 mM MOPS, 75 mM $CaCl_2$, 10 mM $RbCl_2$, 15% glycerol), and the tube was incubated on ice for 15 minutes. Aliquots of 100-200 µl were frozen in a dry ice ethanol bath and stored at -80ºC.

To make Buffer 1, 0.390 g MES was dissolved in 100 ml dH_2O and the pH was adjusted to 6.2. In a separate flask, 2.42 g $RbCl_2$, 1.98 g $MnCl_2$, and 2 ml 1M $CaCl_2$ was dissolved in 50 ml of dH_2O. The solutions were then combined, diluted to 200 ml with dH_2O, pH adjusted to 5.8 with 1M HOAc, filter sterilized, and stored at 4ºC.

To make Buffer 2, 0.419 g MOPS, 15 ml 1 M $CaCl_2$, 0.242 g $RbCl_2$, and 30 ml glycerol was dissolved in 100 ml dH_2O. The solution was then diluted to 200 ml, pH adjusted to 6.5, filter sterilized, and stored at 4ºC.

2.13 Plasmid transformation into DH5α competent cells

Pre-prepared DH5α competent cells (DH5α) were thawed on ice, and the entire ligation reaction was added to 50-100 µl of cells in pre-chilled Eppendorf tubes. After incubation on ice for 30 minutes, the mixture was heat shocked for 30 seconds at 42°C, and transferred back to ice for 2 minutes. Then 100 µl 2xTY media was added, and cells were recovered for 1 hour at 37°C with shaking, before being plated on 2xTY media containing the appropriate antibiotics and returned to 37°C for incubation overnight.

2.14 Mammalian cell passaging

Mammalian cell cultures were maintained in 37°C incubator with 5% CO_2 in 0.22 µm filter-sterilized growth medium (3.1 ml Antibiotic-Antimyotic, 6.25 ml HEPES, 30 ml FBS, 250 ml D-MEM (Invitrogen)). When plates reached 80-90% confluency, cells were passaged to fresh 10 cm cell culture tissue plates (Corning) in a sterilized biosafety cabinet. Growth medium was aspirated, then the plate was washed twice with 1xPBS, and wash aspirated. 1 ml of 0.25% EDTA-trypsin (Invitrogen) was added to the plate before incubation at 37°C for 5-7 minutes. Then 9 ml growth media was added to the plate with gentle pipetting until cells were no longer in clumps. 1-2.5 ml of this suspension was added to fresh plates, and diluted with growth medium to final volume of 10-15 ml. After pipetting to disperse cells in media, plates were placed back in 37°C CO_2 incubator.

2.15 Transient Transfection of mammalian cells

2-3 days prior to day of transfection, cell cultures were split so cells will be 90% confluent at time of transfection. Transfection was performed with Lipofectamine 2000 (Invitrogen) according to manufacturer's instructions, using a ratio of 1 µg DNA per 2 µl Lipofectamine. Briefly, appropriate amounts of DNA and Lipofectamine were separately diluted in Opti-MEM (1.5 ml for 10 cm plate) (Invitrogen), and incubated at room temperature for 20 minutes. During this time, growth media was removed from plates to be transfected, pre-warmed (37°C) transfection media (growth media minus anti-anti) was added to plates, and plates placed back at 37°C CO_2 incubator. DNA and Lipofectamine dilutions were then mixed together and incubated for an additional 30 minutes at room temperature. The DNA/Lipofectamine mixture was then added to the appropriate transfection plates/wells and allowed to incubate at 37°C for 4-6 hours, at which point transfection media was aspirated and replaced with pre-warmed growth media, and returned back to the 37°C CO_2 incubator until harvesting of cells 24 or 48 hours later.

2.16 SDS-PAGE

Proteins were separated by SDS-polyacrylamide gel electrophoresis (SDS-PAGE) at 100-200 volts with a Mini-PROTEAN TGX Precast gel system (Bio-Rad) using pre-cast Ready Gels (Bio-Rad), and Precision Plus Protein Dual Color Standards (Bio-Rad) as a molecular weight marker.

2.17 Western Blotting

After completion of SDS-PAGE, gels were briefly rinsed in transfer buffer (14.42 g glycine, 3 g Tris base, 150 ml methanol, in 1 liter dH_2O). Immobilon-P polyvinylidene diflouride (PVDF) membrane (Cat. # IPVH15150, Millipore) was cut to the same size as gel, put in 100% methanol for 1 min, rinsed with dH_2O 3x, then put in 10 ml transfer buffer. The gel was

placed on top of the membrane, sandwiched between 3MM Whatman paper, rolled over with a pencil to remove trapped air bubbles, and secured in the gel holder cassette before placement in the BioRad Mini-Transblot cell holder cassette (Cat. # 170-3930, Bio-Rad) (see manual for assembly instructions). Transfer was carried out at 100 V for 1 hour, then the blot was removed and immediately placed in 10 ml block [1xPBS, 0.5% non-fat dry milk (NFDM)] on a nutator for 1 hour. Blot was then removed, washed 3x in 5 ml wash buffer (1xPBS, 0.05% NFDM, 0.025% Tween 20), then put in 5 ml antibody buffer (same as wash) with the appropriate primary antibody dilution for 2 hours on a nutator. The blot was then washed in 5ml wash buffer 3x, and put in 5 ml antibody buffer with the appropriate secondary antibody dilution on a nutator for 1 hour. The blot was then rinsed in 5 ml wash buffer 3x and left in wash buffer solution until application of detection reagent.

2.18 Protein detection

For western blots, after completion of antibody staining and final washes, the detection reagent applied was Amersham ECL Plus (GE Healthcare Life Sciences), and proteins were imaged using the STORM phosphorimager (GE Healthcare Life Sciences) or on film (Amersham ECL Hyperfilm, GE Healthcare Life Sciences) using an SRX-101A developer (Konica Minolta).

For Coomassie staining (Current Protocols in Molecular biology), after completion of SDS PAGE, the pre-cast gel was removed from casing and placed in about 15 ml fix (250 ml methanol, 50 ml acetic acid, 200 ml dH_2O) with gentle shaking for 10-15 minutes. The fix was then discarded and just enough Coomassie solution [50% methanol, 0.05% Coomassie brilliant blue R-250 (Rio-Rad), 10% acetic acid, 40% dH_2O], was added to completely cover gel, and the gel was stained with gentle shaking until blue in color. The stain was then discarded and a Kimwipe tissue was rolled up and placed along the length of the container with the gel. Destain

(25 ml methanol, 35 ml acetic acid, 440 ml, dH_2O) solution was then added to completely cover gel, and gel was gently shaken until clear background on gel was obtained. The gel was then wrapped in saran wrap, photographed using an Alpha Imager, and kept at 4°C.

3 FUNCTION OF THE *C. ELEGANS* T-BOX FACTOR TBX-2 DEPENDS ON SUMOYLATION

(Portions of the work from this chapter were contributed by co-authors Tanya Crum, Lynn Clary, Tom Ronan, and Adelaide Packard, and were published in: Huber, P., Crum, T., Clary, L., Ronan, T., Packard, A., and Okkema, P., 2013. Function of the C. elegans T-box factor TBX-2 depends on SUMOylation. Cellular and Molecular Life Sciences. 70, 4157-4168.)

3.1 Abstract

T-box transcription factors are critical developmental regulators in all multi-cellular organisms, and altered T-box factor activity is associated with a variety of human congenital diseases and cancers. Despite the biological significance of T-box factors, their mechanism of action is not well understood. Here we examine whether SUMOylation affects the function of the *C. elegans* Tbx2 sub-family T-box factor TBX-2. We have previously shown that TBX-2 interacts with the E2 SUMO-conjugating enzyme UBC-9, and that loss of TBX-2 or UBC-9 produces identical defects in ABa derived pharyngeal muscle development. We now show that TBX-2 is SUMOylated in mammalian cell assays, and that both UBC-9 interaction and SUMOylation depends on two SUMO consensus sites located in the T-box DNA binding domain and near the TBX-2 C-terminus, respectively. Mutation of both consensus sites did not affect nuclear localization or protein stability, and a conservative mutation of the SUMO-conjugating lysine residue at the C-terminal site does not affect rescue of a *tbx-2* null, indicating SUMOylation at either site can facilitate TBX-2 function. In co-transfection assays, a TBX-2:GAL4 fusion protein represses expression of a 5xGal4:tk:luciferase construct. However, this activity does not require SUMOylation, indicating SUMO is not generally required for TBX-2 repressor activity. In *C. elegans*, reducing SUMOylation enhances the phenotype of a temperature sensitive *tbx-2* mutant and results in ectopic expression of a gene normally repressed by TBX-2, demonstrating that SUMOylation is important for TBX-2 function *in vivo*. Finally,

we show mammalian orthologs of TBX-2, TBX2 and TBX3, can also be SUMOylated, suggesting SUMOylation may be a conserved mechanism controlling T-box factor activity.

3.2 Introduction

T-box proteins are a family of transcription factors found in all multicellular animals where they play important roles in the development of a variety of tissues (Greulich et al., 2011; Naiche et al., 2005). The defining feature of this family is the conserved T-box DNA-binding domain, and T-box factors are grouped into distinct sub-families based on sequence conservation within this domain. In many cases, the level of T-box factor activity is crucial to normal function. For example, reduced expression of the human Tbx2 subfamily genes *TBX3*, *TBX4* and *TBX5* resulting from loss of one functional allele results in ulnar-mammary syndrome, small patella syndrome, and Holt-Oram syndrome, respectively (Bamshad et al., 1997; Basson et al., 1997; Bongers et al., 2004; Li et al., 1997; Packham and Brook, 2003). In contrast, over-expression of the Tbx2 subfamily genes *TBX2* and *TBX3* is found in a number of human cancers (Lu et al., 2010). Despite their developmental and clinical importance, relatively little is known about the mechanism by which T-box factors function.

We are interested in the role that SUMOylation plays in T-box factor activity. SUMOylation is the covalent and reversible post-translational attachment of the small ubiquitin-like modifier peptide (SUMO) to specific lysine residues in target proteins (Gareau and Lima, 2010; Wilkinson and Henley, 2010), and it has been implicated in diverse processes, including modifying function, nuclear localization, and sub-nuclear localization of transcriptional regulators (Gill, 2004). SUMOylation of transcription factors is typically associated with repression (Gill, 2005), but it has also been implicated in transcriptional activation by some factors (Wang et al., 2004; Wang et al., 2007). The SUMO conjugation pathway is analogous to

the ubiquitination pathway and involves an E1 activating enzyme (Aos1/Uba2) and an E2 conjugating enzyme (Ubc9) sufficient for specific SUMO attachment *in vitro* (Desterro et al., 1999; Okuma et al., 1999). In addition, a variety of E3 ligases have been identified that promote SUMO transfer from E2 to specific substrates *in vivo*. Ubc9 recognizes the ΨKX(D/E) SUMO consensus site (where Ψ is a large hydrophobic amino acid and K is the residue attached to SUMO) (Bernier-Villamor et al., 2002; Sampson et al., 2001), and many SUMOylation substrates have been identified by their interaction with Ubc9 in yeast 2-hybrid screens (Johnson, 2004). SUMOylation also occurs at non-consensus sites, and non-covalent SUMO/substrate or E3 ligase/substrate interactions are involved in directing SUMOylation at these sites (Gareau and Lima, 2010).

We hypothesize that function of the *C. elegans* T-box factor TBX-2 depends on SUMOylation (Roy Chowdhuri et al., 2006). TBX-2 is the sole *C. elegans* member of the Tbx2 subfamily and is necessary for formation of anterior pharyngeal muscles. In yeast two-hybrid assays, TBX-2 interacts with the E2 SUMO conjugating enzyme UBC-9, and loss of UBC-9 produces pharyngeal phenotypes identical to those resulting from *tbx-2* loss-of-function. In addition, sub-nuclear localization of a TBX-2::GFP fusion protein is altered when SUMOylation is reduced.

Here, we ask if TBX-2 is SUMOylated and whether SUMOylation affects TBX-2 activity *in vivo*. We first used the two-hybrid assay to map interaction sites between TBX-2 and UBC-9 and found two SUMO consensus sites in TBX-2 that mediate interaction with UBC-9. One of these sites is located near the TBX-2 C-terminus, while the other is located in a highly conserved region of the T-box DNA binding domain. We next showed that TBX-2 is SUMOylated in mammalian cell assays, and that TBX-2 SUMOylation depends on both of these UBC-9

interaction sites. Mutation of these sites does not affect nuclear localization or protein stability in COS-1 cells, and a lysine to arginine mutation at the C-terminal consensus site, which reduces overall SUMOylation in COS-1 cells, does not affect the ability of TBX-2 to rescue *tbx-2(ok529)* nulls, suggesting SUMOylation at both sites can facilitate TBX-2 function *in vivo*. We then examined TBX-2 transcriptional activity and found that in mammalian cells a TBX-2:GAL4 DNA-binding domain (GAL4-DBD) fusion protein represses expression of a GAL4-responsive reporter, but surprisingly this repression did not require SUMOylation. To determine whether SUMOylation is important for TBX-2 activity *in vivo*, we asked if *tbx-2* and *ubc-9* interact genetically. We found that reduction of SUMOylation enhances the effect of a *tbx-2* hypomorphic mutant on embryonic viability and pharyngeal muscle development, and that repression of a downstream target of TBX-2 depends on SUMOylation. Finally we examined SUMOylation of two mammalian orthologs of TBX-2 and found that human TBX2 and mouse TBX3 can also be SUMOylated. We suggest SUMOylation is a common mechanism regulating activity of T-box transcription factors.

3.3 Materials and Methods

3.3.1 Nematode handling, transformation and strains

C. elegans were grown under standard conditions (Lewis and Fleming, 1995). Germ line transformation was performed using standard techniques with pRF4 containing *rol-6(su1006)* as a dominant marker for transformation (Mello and Fire, 1995), or by biolistic transformation of DP38 strain [*unc-119*(ed3)] with fosmids containing [*unc-119(+)*]. Biolistic transformation was performed using biolistic transformation with a PDS-1000/He (Bio-Rad) particle delivery system equipped with a Hepta adapter (Bio-Rad) as described in the Transgeneome project manual, "Biolistic Transformation of *C. elegans*", with the exception of using NEP plates seeded with

NA22 strain of *E. coli* to facilitate the growth of larger populations of DP38 worms at the time of bombardment, an adjustment taken from the Wormbook protocol, "Transgenic solutions for the germline".

The following strains were used in these studies: OK0660 *tbx-2(bx59)* was obtained by outcrossing from EM207 *tbx-2(bx59); him-5(e1490)*, OK0666 *cuEx553[D2096.6::gfp]*, OK0692 *tbx-2(bx59); cuEx553[D2096.6::gfp]*, OK0741 *tbx-2(ok529)/dpy-17(e164) unc-32(e189); cuEx553[D2096.6::gfp]*, DP38 *unc-119(de3)*, OP159 *unc-119(ed3); wgIs159 [tbx-2::TY1::EGFP::3xFLAG+unc-119(+)]*, OK0460 *tbx-2(ok529)/ dpy-17(e164)unc-32(e189).*

The following strains were generated for this study: OK0873 *tbx-2(ok529); wgIs159*, OK1034 *unc-119(ed3); cuIs38 [tbx-2::TY1::EGFP::3xFLAG+unc-119(+)]*, OK1044 *tbx-2(ok529); cuIs38*, OK1039 *unc-119(ed3); cuIs39 [tbx-2^{K400R}::TY1::EGFP::3xFLAG+unc-119(+)]*, OK1051 *tbx-2(ok529); cuIs39*

3.3.2 Genotyping *tbx-2* mutants

tbx-2(bx59) is a G->A substitution located at position 24,597 of the cosmid F21H11 (accession FO081200) (K. Chow, personal communication) and disrupts a BstCI restriction enzyme site. Animals were genotyped by single worm PCR (Beaster-Jones and Okkema, 2004) using primers PO931 [AGTTTGACACCGATTTTCTCG] and PO932 [GTGATGATGGATCTTGTTCCG] followed by digestion with BstC1 and gel electrophoresis. PCR contained 2.5 µl single worm lysis reaction, 1X PCR buffer, 2.5 mM MgCl2, 0.2 mM dNTPs, 100 ng each of PO931 and PO932, and 0.1 µl Platinum Taq DNA polymerase (Invitrogen) in dH_2O to a final volume of 25 µl. PCR program was as follows: 94°C for 30 seconds, (92°C for 30 seconds, 52.3°C for 30 seconds, 72°C for 30 seconds) X 40, 72°C for 5

minutes. BstC1 digestion contained 5 µl PCR reaction, 1x NEB buffer 4, and 0.5 µl BtsC1 in dH_2O to a final volume of 20 µl, and was done at 50°C water bath for 2 hours.

To generate rescue strains in the *tbx-2(ok529)* background, individual animals were genotyped for the *tbx-2(ok529)* allele as previously described (Roy Chowdhuri et al., 2006). Briefly, animals were genotyped by single worm PCR (Beaster-Jones and Okkema, 2004) using primers PO604, PO605 and PO606 followed by gel electrophoresis. PCR contained 2.5 µl single worm lysis reaction, 1X PCR buffer, 2.5 mM MgCl2, 0.2 mM dNTPs, 100 ng each of PO604, PO605 and PO606, and 0.1 µl Platinum Taq DNA polymerase (Invitrogen) in dH_2O to a final volume of 25 µl. PCR program was as follows: 94°C for 30 seconds, (92°C for 30 seconds, 55°C for 30 seconds, 72°C for 30 seconds) X 40, 72°C for 5 minutes. *tbx-2(ok529)* homozygotes were distinguished from heterozygotes by progeny tests in which rescued hermaphrodites were crossed into N2 males, and 100% of male progeny possessed the *ok529* allele.

3.3.3 General methods for nucleic acid manipulations and plasmid construction

Standard methods were used to manipulate plasmid DNAs and oligonucleotides (Ausubel, 1990). For yeast two hybrid assays, the LKIE and VKKE SUMOylation sites were separately mutated using the Stratagene QuikChange II Kit in the *tbx-2* bait plasmid pOK187.01 containing the full-length *tbx-2* orf (Roy Chowdhuri et al., 2006) to generate pOK222.01 and pOK222.06, respectively. The LKIE/VKKE->AAAA double mutant was constructed by ligation of fragments pOK222.01 and pOK226.06 to create the plasmid pOK225.02.

Plasmids for expressing TBX-2 (pOK241.05), TBX-$2^{LKIE->AAAA}$ (pOK241.10), TBX-$2^{VKKE->AAAA}$ (pOK241.13), and TBX-$2^{LKIE/VKKE->AAAA}$ (pOK241.17) were constructed by inserting the PCR amplified *tbx-2* orf from the two-hybrid vectors into pCDNA3.1 using TOPO cloning (Invitrogen). The PCR reaction contained 1 µl DNA template (1/50 dilution of a mini-

prep in dH_2O), 0.5 µl 25 mM dNTPs, 5 µl 10x PCR buffer, 1.5 µl 50 mM $MgCl_2$, 1 µl primer PO821 (100 ng/µl), 1 µl primer PO822 (100 ng/µl), 39.5 µl dH_2O, 0.5 µl Platinum Taq DNA polymerase (NEB) for a total volume of 50 µl. The thermocycler program used was as follows: step (1) 95°C for 2 minutes, 39 x [(2) 95°C for 45 seconds, (3) 55.5°C for 45 seconds, (4) 72°C for 1.5 minutes], (5) 72°C for 5 minutes. TOPO kit cloning reactions were performed in PCR tubes and contained 1 µl PCR product, 1 µl provided salt solution, 3 µl sterile dH_2O, 1 µl TOPO vector, and were incubated for 5 minutes at room temperature. Reactions were then placed on ice, transformed into dH5α *E. coli*, and plated on 2xTY+Amp (100ng/µl). Single colonies were then picked, grown overnight in selective media, and DNA was isolated from the pelleted culture. DNA was then subjected to restriction digest with HindIII to confirm insertion of the PCR product in the correct orientation (producing two bands of 5611 and 1184 bp). Those with correctly oriented insertions were sequenced with primers PO4, PO448, PO449, and PO824 to verify the plasmids contained only the desired mutation.

Plasmids for expressing TBX-2^{K231R} (pOK263.01), TBX-2^{K400R} (pOK244.18) and the TBX-2^{2KR} double mutant (pOK261.03) were made by site directed mutagenesis of pOK241.05 using the Stratagene QuikChange II Kit according to manufacturer's instructions. The PCR program used was as follows: step (1) 95°C for 30 seconds, 16 x [(2) 95°C for 30 seconds, (3) 55°C for 1 minute, (4) 68°C for 9 minute]. The primer pair PO1021/PO1022 was used to make the TBX-2^{K231R} mutation, primer pair PO833/PO834 was used to make the TBX-2^{K400R} mutation. Sequencing primers PO4, PO448, and PO835 were used to verify the mutagenized plasmids contained only the desired mutation.

The plasmid encoding HA::SUMO-1 (pcDNA3 HA SUMO-1, pOK251.01) was a gift from Jorge A. Iñiguez-Lluhí (University of Michigan), and it was mutated using the Stratagene

QuikChange II Kit according to manufacturer's instructions to encode HA::SUMO-1(ΔGG) (pOK263.05). The PCR program used was as follows: step (1) 95°C for 30 seconds, 16 x [(2) 95°C for 30 seconds, (3) 55°C for 1 minute, (4) 68°C for 9 minute]. The mutagenesis primer pair used was PO1067/PO1068. Sequencing primer PO4 was used to verify only the (ΔGG) mutation was present in pOK263.05.

cDNA clones for human TBX2 (IMAGE:6339405) and mouse TBX3 (IMAGE:30547736) were purchased from Open Biosystems, PCR amplified with primers PO859/PO860 and PO861/862, respectively, and inserted into pCDNA3.1 using TOPO cloning to make pOK246.01 and pOK245.01. For amplification of cDNA, the PCR reaction contained 1 µl DNA template (1/50 dilution of a mini-prep in dH_2O), 0.5 µl 25 mM dNTPs, 5 µl 10x PCR buffer, 1.5 µl 50 mM $MgCl_2$, 1 µl forward primer (100 ng/µl), 1 µl reverse primer (100 ng/µl), 39.5 µl dH_2O, and 0.5 µl Platinum Taq DNA polymerase (NEB) for a total volume of 50 µl. To amplify the cDNA clone of TBX2, 5 µl of PCRx Enhancer (Invitrogen) was added to the PCR reaction mix. The thermocycler program used was as follows: step (1) 95°C for 2 minutes, 39 x [(2) 95°C for 45 seconds, (3) 62.5°C for 45 seconds, (4) 72°C for 1.5 minutes], (5) 72°C for 5 minutes. TOPO kit cloning reactions were performed in PCR tubes and contained 1 µl PCR product, 1 µl provided salt solution, 3 µl sterile dH_2O, 1 µl TOPO vector, and were incubated for 5 minutes at room temperature. Reactions were then placed on ice, transformed into dH5α *E. coli*, and plated on 2xTY+Amp (100ng/µl). Single colonies were then picked, grown overnight in selective media, and DNA was isolated from the pelleted culture. DNA was then subjected to restriction digest to confirm insertion of the PCR product in the correct orientation. For TBX-2, NotI was used, and correctly oriented TOPO clones produced a digest pattern of 5.6 and 2 kb. For Tbx3, EcoRV was used, and correctly oriented TOPO clones produced a digest pattern of

6227 and 1463 bp. Those with correctly oriented insertions were sequenced with primers PO4 and PO824, and PO871 (for Tbx3) or PO876 and PO877 (both for TBX2) to verify the plasmids contained no point mutations.

Plasmids for expressing TBX-2::GAL4 (pOK253.01) and TBX-2$^{LKIE/VKKE->AAAA}$::GAL4 (pOK253.04) for co-transfection assays were made by cloning the amplified *tbx-2* orf from pOK241.05 and 241.17, respectively, into pcDNA HA:GAL4(1-100), named pOK251.04 (provided by Jorge A. Iñiguez-Lluhí, University of Michigan). Primers used for amplification were PO933 (with an XbaI linker) and PO934 (with a BamHI linker). The PCR program used was as follows: step (1) 94°C for 2 minutes, 4 x [(2) 94°C for 30 seconds, (3) 54.8°C for 30 seconds, (4) 72°C for 1.3 minutes], 34 x [(5) 94°C for 30 seconds, (6) 57.4°C for 30 seconds, (7) 72 °C for 1.3 minutes], (8) 72°C for 5 minutes. PCR reaction contained 1 µl DNA template (1/10 dilution in dH_2O), 5 µl 10x PCR buffer, 1.5 µl $MgCl_2$, 0.5 µl 25 mM dNTPs, 1 µl PO933 (100ng/µl), 1 µl PO934 (100 ng/µl), 0.5 µl Platinum Taq, and 39.5 µl dH_2O. Amplified products and vector pOK251.04 were both digested with XbaI and BamHI, and the 1.2 kb gel purified insertions were ligated into the 5.7 kb vector, transformed into dH5α *E. coli*, and plated on 2xTY+Amp (100ng/µl). Single colonies were then picked, grown overnight in selective media, and DNA was isolated from the pelleted culture. DNA was then subjected to restriction digest with HindIII to confirm insertion of the PCR product in the correct orientation (producing two bands of 5791 and 1184 bp). Those with correctly oriented insertions were sequenced with primers PO4, PO593, PO587, and PO824 to confirm clones had no point mutations.

For mock transfections, the HA::GAL4 fragment was removed from pcDNA HA::GAL4(1-100) (plasmid pOK251.04) by restriction digest with PmeI, and subsequent re-ligation of the gel-purified vector. The resulting plasmid was named pOK293.03, and was

sequenced with PO4 to confirm the deletion of HA::GAL4. The 5xGAL4:tk:luc reporter (pOK269.04) and CMV β-GAL plasmid (pOK269.09) used for normalization were gifts from the Elizaveta Benevolenskaya and Brad Merrill labs at the University of Illinois at Chicago, respectively.

3.3.4 Fosmid handling and recombineering

Recombineering was performed essentially as described to introduce the *tbx-2*^{K400R} mutation into the *tbx-2::gfp* rescue fosmid WRM063aG09, and is outlined below (Dolphin and Hope, 2006). We received as a gift from the Sarov lab a construct containing the *tbx-2* fosmid, WRM063aG09 (pOK313.05), fused in-frame with a 2xTY1::GFP::3xFLAG tag at the 3' end of *tbx-2*, as well as *unc-119(+)*, in the copy-number inducible vector pCC1Fos, harbored in EP1300 *E. coli* (clone 9347172996193398 G10) (Sarov et al., 2012). This construct was isolated with using a standard DNA mini prep kit (Promega) and the sequence was verified with primers PO1403, PO1404, PO1405, PO1406, and PO1407, and then 100-150 ng was transformed via electroporation (2400 V), using an Eppendorf Electroporator 2510, into MW005 *E. coli* (a gift from Colin Dolphin, Addgene #24545), and, after an addition of 1 ml LB and 1 hour recovery at 30°C, plated on 2XTY+Cm(10µg/ml) for a 48 hour incubation at 32°C (Hirani et al., 2013; Sarov et al., 2012). A glycerol stock prepared from an individually selected colony was used to grow a 1 ml overnight culture (LB+Cm(10µg/ml)) for inoculation of 100 ml the same media in a 500 ml flask, followed by incubation until OD_{600} = 0.6 (32°C, 220 RPM). 50 ml of culture was then transferred to a pre-warmed 500 ml flask and incubated in a 42°C water bath (Haake C-10, Thermo Electron) for 20 minutes to induce lambda-Red recombinase function. The culture flask was then chilled on ice with occasional swirling for 15-30 minutes while the centrifuge rotor and chamber cooled to 4°C, before being pelleted in an ice-cold 50 ml conical tube (BD Falcon) at

3,000 RPM for 10 min. The pellet was then re-suspended in ice-cold dH_20, re-pelleted in the same fashion, and then washed twice with ice-cold 10% glycerol. The final pellet was re-suspended in 1 ml ice-cold GYT medium, and 100 µl aliquots of the freshly made competent cells were frozen in 1.5 ml micro-centrifuge tubes resting in a dry ice ethanol bath and stored at -80°C.

For the positive-selection recombineering step, a PTC-200 Peltier thermal cycler (MJ Research) was used to PCR amplify [94°C for 5 minutes, 40x(94°C for 30 sec, 60°C for 30 sec, 72°C for 2 min), 72°C for 5 min] the RT cassette from the plasmid pNH034 (a gift from Colin Dolphin, Addgene 42150) using forward primer PO1408, of which the first 50 bases are homologous to the *tbx-2* sequence just 5' to the VKKE site and the remaining 22 bases bind to the 5' region of the RT cassette in pNH034, and reverse primer PO1409, of which the first 50 bases are homologous to the opposite strand of the *tbx-2* sequence just 3' to the VKKE site and the remaining 23 bases bind to the 3' region of the RT cassette on the opposite strand in pNH034, giving a product of about 2.1 kb (Hirani et al., 2013). Excised, gel-purified (Wizard SV gel and PCR clean-up system, Promega) RT cassette (100 ng) was electroporated as described above into an aliquot of *tbx-2* fosmid-containing electro-competent cells, which were allowed to recover 1 hour at 32°C after the addition of 1 ml SOB[-Mg], and undiluted or a 1:10 dilution in SOB[-Mg] of recovered cells were plated on LB+Tc(5 µg/ml)+Cm(10 µg/ml) for a 48 hour incubation at 32°C. 8 colonies total were found on the "undiluted" plates, all were re-streaked on the same antibiotic plates, and sequencing with primer PO1403 and PO1404 verified that 1/8 colonies had the correct RT cassette insertion in *tbx-2* (more may have contained the cassette, however sequencing reactions failed in all but for this clone). A glycerol stock was

prepared from this clone and lambda-Red recombinase-induced electro-competent cells were prepared as described above from this stock for use in the next step in recombineering.

For the negative-selection recombineering step, a small replacement cassette containing the *tbx-2*^{K400R} mutation was generated for replacement of the RT cassette by annealing 2 µl concentrated primer PO1410, of which the first 50 bases match the homology arm of primer PO1408 and the remaining 15 bases span the bases encoding the mutated VKKE site plus a few additional bases to allow for sufficient annealing, to 2 µl concentrated primer PO1411, of which the first 50 bases match the homology arm of primer PO1409 and the remaining 15 bases complement and base pair with the final 15 bases of PO1410, in a 2.5 mM NaCl solution in a 95°C heat block for 5 minutes followed by a cool-down at RT for 1 hour. Annealed oligos were then end-filled using T4 DNA polymerase (New England Biolabs) at 12°C for 15 minutes, and the 115 bp product was gel-purified and 500 ng electroporated into the earlier prepared MW005 competent cells containing the *tbx-2* fosmid with RT cassette insertion, and plated on NSLB+Strep(500µg/ml)+Cm(10µg/ml), as described above. Only 1 out of 6 re-streaked colonies from a 1:100 dilution plate was confirmed to have the *tbx-2*^{K400R} mutation by sequencing with PO1403. A glycerol stock was prepared from one of these clones, and the recombineered fosmid DNA (pOK313.06) was later isolated for biolistic transformation.

3.3.5 Yeast 2-hybrid assays

Yeast 2-hybrid assays were carried out in L40 yeast containing HIS3 and *lacZ* reporters regulated by LexA binding sites with the *ubc-9* prey plasmid pOK193.11 in the pACT vector and *tbx-2* bait plasmids pOK187.01 (wild-type *tbx-2*), pOK222.01 (*tbx-2*$^{LKIE->AAAA}$), pOK222.06 (*tbx-2*$^{VKKE->AAAA}$), or pOK225.02 (*tbx-2*$^{LKIE/VKKE->AAAA}$) in the pLexA-NLS vector as previously described (Roy Chowdhuri et al., 2006). ß-galactosidase expression in yeast was quantified in at least three assays as previously described (Amberg et al., 2005).

3.3.6 Assays for TBX-2 nuclear localization in COS-1 cells

COS-1 cells were maintained in D-MEM with 10% FBS, 10 mM HEPES, and 1x Antibiotic-Antimycotic (Invitrogen). For localization assays, ~2x10^5 cells were seeded into the wells of 2-chamber Lab-Tek chamber slides (Cat.# 177380, Nunc) 24 hours prior to transfection. Wells were transfected with plasmids expressing wild type TBX-2 (pOK241.05, 800 ng) or TBX-2$^{LKIE/VKKE->AAAA}$ (pOK241.17, 800 ng), and SUMO-1 or SUMO-1(ΔGG) (pOK251.05 or pOK263.05, 800 ng), using Lipofectamine 2000 in OPTI-MEM according to manufacturer's instructions (Invitrogen). 48 hours later, media was aspirated from the wells and cells were fixed in 1 ml freshly made 3.7% formaldehyde (in PBS, pH 7.0) for 10 minutes. The fix was aspirated, and cells were washed twice with 1 ml PBS (pH 7.4). After aspirating the final wash, cells were permeabilized in 1 ml 0.2% Triton-X-100 (in PBS) for 5 minutes. The solution was aspirated, and 1 ml block buffer [10% FBS (Invitrogen) in PBS] was added to each well and incubated for 20-30 minutes. Block buffer was then removed, and 1 ml primary antibody solution [1:200 anti-V5 (Invitrogen) in 0.2% Triton-X-100, 10% FBS (in PBS)] was added to the appropriate wells and incubated for 1 hour. Primary antibody solution was then aspirated, and all wells were washed with 1 ml 10% FBS in PBS three times. The final wash was aspirated,

and 1 ml secondary antibody solution [1:150 Texas Red-conjugated Goat anti-mouse and 0.5 µg/ml DAPI in 0.2% Triton-X-100, 10% FBS (in PBS)] was added to the appropriate wells and incubated for 1 hour. Secondary antibody solution was then aspirated, and all wells were washed with 1 ml 10% FBS in PBS three times. After aspiration of the final wash, the chambers were removed from the slides, 1 drop of mounting solution (Bio-Rad) was placed on each slide, and coverslips were carefully placed over the slides before sealing the edges with nail polish. The slides were immediately viewed on a fluorescent microscope, images were captured, and the slides were stored at 4°C.

3.3.7 TBX-2 protein turnover assays

COS-1 cells were maintained in D-MEM with 10% FBS, 10 mM HEPES, and 1x Antibiotic-Antimycotic (Invitrogen). For turnover assays, ~$2x10^6$ cells were seeded into 10 cm plates 24 hours prior to transfection. 2 plates were transfected with 20 µg plasmids expressing either TBX-2 (pOK241.05) or TBX-$2^{LKIE/VKKE->AAAA}$ (pOK241.17) using Lipofectamine 2000 in OPTI-MEM according to manufacturer's instructions (Invitrogen). 24 hours later, each transfected plate was split and cells were re-distributed evenly to 5 plates for each construct (one plate for each time point after cycloheximide treatment, which were 0 hr, 3 hr, 6 hr, 9 hr, and 12 hr). The following morning, 100 µl of 10 mg/ml cycloheximide (in 100% ethanol) was added to each plate (except for the 0 hr plates which received 100 µl of 100% ethanol and were harvested at the same time as the 3 hr plates). Cells were harvested at the time points indicated above. Briefly, the media was aspirated and cells were collected in 5 ml PBS using a cell scraper before being centrifuged into a pellet in Eppendorf tubes for 5 minutes at 1K RPM at 4°C. The tubes were then brought to the cold room (the remainder of the protocol was carried out at 4°C). The supernatant was aspirated, and 100 µl of freshly made 1x lysis buffer [1 ml 2x lysis buffer (800

mM NaCl, 100 mM Tris-HCl at pH 7.5, 0.4% NP40, 20% glycerol, 10 mM EDTA), 20 µl 100 mM Sodium orthovanadate, 40 µl 100 mM PMSF in isopropanol, 286 µl complete mini protease inhibitor cocktail (Sigma P8465), 50 µl 0.4 M NEM, 2 µl 1 M DTT in dH_20, 20 µl 100 mM NaF in dH_20, 582 µl dH_20] was added to each tube, followed by pipetting up and down to facilitate efficient cell lysis. Tubes were kept on ice for 50 minutes, with occasional vortexing at high speed, before being centrifuged for 10 minutes at 14K RPM and 4°C. The supernatant was transferred to fresh Eppendorf tubes and frozen in a dry ice/ethanol bath, then stored at -80°C. Bradford assays (Bio-Rad) were used to determine the protein concentrations of all samples according to manufacturer's instructions. 1 µg/µl stock protein samples were prepared in 1x SDS buffer by the addition of a determined volume of protein sample (based on concentration from Bradford assay) to 100 µl of 2x SDS sample buffer, and heated on a 95°C heat block for 5 minutes. Protein samples were then resolved by SDS-PAGE, and transferred to PVDF membrane by western blot. Proteins were detected using monoclonal anti-V5 (1:5,000) (Invitrogen) or anti-TBP (1:5,000) (Sigma) primary antibodies (anti-TBP was used an internal control), HRP-conjugated secondary antibody (1:2000) (Goat anti-mouse, Millipore), and ECL Plus (GE Healthcare) detection reagent. Chemilluminescence was recorded using Amersham ECL hyperfilm (GE Healthcare) or recorded and quantified using a STORM 860 Molecular Imager and ImageQuant software (Molecular Dynamics).

3.3.8 RNAi analyses

Feeding RNAi was performed as previously described (Kamath et al., 2001) using plasmids obtained from Geneservice containing genomic fragments of *ubc-9* or *smo-1* cloned into L4440 (Timmons et al., 2001). To assess enhancement of the *tbx-2(bx59)* mutant phenotype, N2 or OK0660 [*tbx-2(bx59)*] L4 hermaphrodites raised at 16˚C were transferred to

plates seeded with RNAi feeding *E. coli* or OP50 and incubated at 25˚C for 24 hr. These animals were transferred to fresh feeding plates at 25˚C and allowed to lay eggs for 4 hrs. Progeny embryos were transferred to fresh feeding plates and counted. Larvae and terminally arrested embryos were counted 24 hr later to assay embryonic lethality, or examined by DIC microscopy after hatching to assess the pharyngeal phenotype.

To examine *D2096.6::gfp* expression, OK0666 [*cuEx553*] L4 hermaphrodites were transferred to plates seeded with *ubc-9* RNAi feeding *E. coli* or OP50 and grown 20 hr at 20˚C. These animals were transferred to fresh feeding plates, and GFP expression was examined in progeny embryos and larvae.

3.3.9 SUMOylation and co-transfection assays

COS-1 cells were maintained in D-MEM with 10% FBS, 10 mM HEPES, and 1x Antibiotic-Antimycotic (Invitrogen). For SUMOylation assays, ~$2x10^6$ cells were seeded into 10 cm plates 24 hours prior to transfection. Plates were transfected with plasmids expressing wild type or mutant TBX-2 (10 µg), HA-SUMO-1 or HA-SUMO-1(ΔGG) (10 µg), and pEGFP-N3 (4 µg; Clontech) using Lipofectamine 2000 in OPTI-MEM according to manufacturer's instructions (Invitrogen). After 48 hours, transfected plates were checked on a Leica inverted microscope for GFP expression as a control for transfection. Then COS-1 cells were harvested with a cell scraper in PBS and transferred to 50 ml conical tubes (BD Falcon). Once all plates were harvested, the tubes were spun down at 1K RPM to obtain cell pellets, then the pellets were resuspended in 1 ml PBS and transferred to 1.5 ml Eppendorf tubes, which were centrifuged for 5 minutes at 1K RPM. The supernatant was aspirated and 0.75 ml lysis buffer [8 M urea, 0.5 M NaCl, 45 mM Na_2HPO_4, 5 mM NaH_2PO_4,10 mM imidazole, 10 mM NEM (pH 8.0)] was added. The suspension was then sonicated, and the tubes were centrifuged at 14K RPM for 15 minutes

at 4°C. The supernatant was transferred to fresh Eppendorf tubes, and incubated with 50 µl Ni-NTA magnetic beads (Qiagen) for 1 hour on an end-over-end shaker. The beads were then washed twice with 1 ml wash buffer [8 M urea, 0.4 M NaCl, 17.6 mM Na_2HPO_4, 32.4 mM NaH_2PO_4, 10 mM imidazole, 10 mM NEM (pH 6.75)]. For each wash, the tubes were placed directly next to the magnets on a MagnaRack (Invitrogen), and the supernatant was aspirated. The tubes were moved away from the magnet, at which point 1 ml of wash was added to all tubes, which were then briefly vortexed and placed back against the magnets. After aspiration of the final wash, the tubes were kept against the magnets, and proteins were eluted by addition of 50 µl elution buffer (250 mM imidazole, 5% SDS, 0.15 M Tris pH6.7, 30% glycerol, 0.72 M ßME). The eluate was transferred to fresh Eppendorf tubes with 50 µl 2x SDS sample buffer, and heated on a 95°C heat block for 5 minutes. Protein samples were then resolved by SDS-PAGE, and transferred to PVDF membrane by western blot. Proteins were detected using anti-V5 (1:5,000) (Invitrogen) or anti-HA (1:1000) (Covance) primary antibodies, HRP-conjugated secondary antibody (1:2000) (Goat anti-mouse, Millipore), and ECL Plus (GE Healthcare) detection reagent. Chemilluminescence was recorded using Amersham ECL hyperfilm (GE Healthcare) or recorded and quantified using a STORM 860 Molecular Imager and ImageQuant software (Molecular Dynamics).

For co-transfection assays, $2x10^5$ COS-1 cells were seeded to wells of a 24 well-plate 24 hours prior to transfection. Wells were transfected in triplicate with plasmids expressing TBX-2 (25-500 ng), 5xGAL4:tk:luc (280 ng), and CMV ß-gal (20 ng) using Lipofectamine 2000 in OPTI-MEM using manufacturer's instructions (Invitrogen). 48 hours later, media was aspirated from the wells, and 150 µl of Steady Glo Luciferase lysis buffer (Promega) was added and pipetted up and down to break up cells. 50 µl of lysate of each sample was then transferred from

a well of the 24 well plate to an Eppendorf tube (for ß-gal assay) and to a well in a white 96 well plate with 50 µl Steady Glo Luciferase substrate. Luminescence was measured on the 96 well plate immediately with a Clarity Luminescence Micro-plate reader (BIO-TEK) using the Simple Reads feature. Luciferase values were normalized over ß-gal activity. The Eppendorfs containing 50 µl of lysate were mixed with 180 µl Z buffer mix [3.524 ml Z buffer (ph 7.0) (4.27 g Na_2HPO_4, 2.75 g NaH_2PO_4-H_2O, 0.375 g KCl, 0.125 g $MgSO_4$-$7H_2O$ in 500 ml dH_2O), 996 µl ONPG, 24 µl BME] for 10 minutes at 37°C in the dark. The yellowish solution was then transferred to disposable cuvettes (Thermo-Fisher) and ß-gal values were measured with a Genesys 10 UV spectrophotometer (Thermo-Fisher) at $OD_{414\ nm}$ (Rogers et al., 2012).

3.3.10 Microarray and data analysis

Mixed stage populations of N2 and OK0660 [*tbx-2(bx59)*] animals grown at 25˚C were treated with bleach/sodium hypochlorite to isolate embryos (Lewis and Fleming, 1995). Aliquots of embryos were examined to verify comparable age distributions, and RNA was isolated using TRIzol (Invitrogen) and further purified using RNeasy Kit (Qiagen) following manufacturers' protocols.

Total RNA from 2 independent populations of N2 embryos and 3 independent *tbx-2(bx59)* embryos were labeled and hybridized to Affymetrix *C. elegans* Genome GeneChips by the UIC Core Genomic Facility (CGF). The microarray data was analyzed using the R statistical programming language, using the Bioconductor suite of tools (Gentleman et al., 2004), and the Affy package. Normalization to correct for chip-to-chip variation was done using the Robust Multiarray Averaging (RMA) method of microarray normalization (Bolstad et al., 2003). Microarray results were pre-filtered using the genefilter function (25% of the probes have a measured intensity of at least 100 on the original scale and the coefficient of variation is between

0.7 and 10 on the original scale) (Chiaretti et al., 2004). The limma package (Smyth, 2004) was used to calculate differentially expression using the limma linear model fit, eBayes smoothing of standard errors, and Benjamini-Hochberg (BH) multiple test correction with a false discovery rate of 5% (Benjamini and Hochberg, 1995). Probes were matched to genes using the Affymetrix-to-WormBase ID table for WS210 (www.wormbase.org). Probes mapping to more than one gene were discarded. When one or more probes mapping to a gene were differentially expressed, that gene was considered to be differentially expressed. One GeneChip hybridized with *tbx-2(bx59)* RNA exhibited high variation in the spiked in control probes (TBXa) compared to the other samples, and data from this chip was not included in our analysis.

3.3.11 Microscopy

Worms were visualized using a Zeiss Axioskop microscope equipped for DIC and fluorescence microscopy, and images were captured using an Axiocam MRm camera and AxioVision software.

3.4 Results

3.4.1 TBX-2 interacts with UBC-9 via two SUMO consensus sites

We previously showed using yeast two-hybrid assays that TBX-2 specifically interacts with the E2 SUMO-conjugating enzyme UBC-9 (Roy Chowdhuri et al., 2006), and we used this assay to identify sites in TBX-2 mediating this interaction. TBX-2 contains several sites matching the SUMO consensus site ψKX(D/E) (Table I) (Bernier-Villamor et al., 2002; Sampson et al., 2001). The two highest-scoring matches to this consensus are an $LK_{231}IE$ sequence located near the C-terminus of the T-box DNA binding domain and a $VK_{400}KE$ sequence located near the TBX-2 C-terminus (Figure 7A). LKIE is located in a conserved region

TABLE I: POTENTIAL SUMOYLATION SITES IN TBX-2 PROTEIN PREDICTED BY SUMOplot, SUMOhydro AND SUMOsp 2.0

Rank	Position	Group	SUMOplot Score
1	K400	AEKPE **VKKE** QKSVT	0.93 [a]
2	K231	EKVTE **LKIE** NNPFA	0.91 [a]
3	K133	RWMIA **GKAD** PEMPK	0.67
4	K248	RDAGA **GKRE** KKRQL	0.67
5	K62	GVTDD **PKVE** LDERE	0.61 [a]
6	K396	DSEEA **EKPE** VKKEQ	0.50
7	K239	ENNPF **AKGF** RDAGA	0.44
8	K410	KSVTP **PKKG** GFDVL	0.43
9	K174	TNNIS **DKHG** YTILN	0.33
10	K411	SVTPP **KKGG** FDVLD	0.31

The TBX-2 protein sequence (Accession CCD69847) was analyzed for matches to the SUMO consensus site ΨKX(D/E) using SUMOplot at http://www.abgent.com/tools/. The top-scoring matches VKKE and LKIE were characterized in this study.

[a] Also predicted as a potential SUMOylation site by SUMOhydro and SUMOsp 2.0 at high threshold (Chen et al., 2012; Ren et al., 2009).

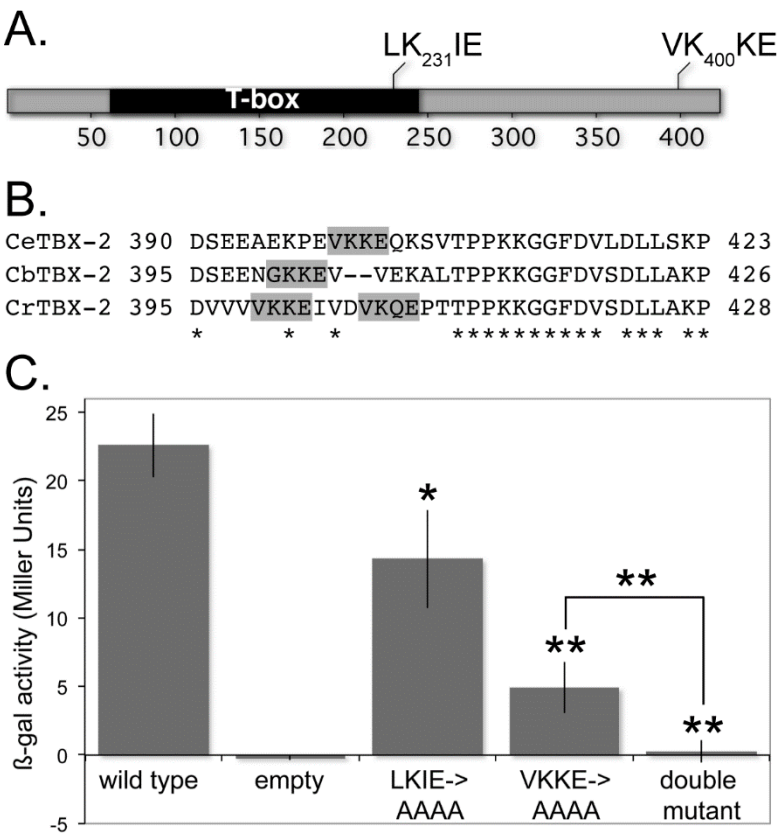

Figure 7. TBX-2 interacts with UBC-9

(A) Schematic diagram of the TBX-2 protein (Accession CCD69847) indicating the location of the T-box DNA binding domain (black) and the positions of the $LK_{231}IE$ and $VK_{400}KE$ SUMO consensus sites. (B) T-Coffee alignment of the C-terminus of TBX-2 proteins from *C. elegans* (CeTBX-2), *C. briggsae* (CbTBX-2; WormBase ID CBP05056), and *C. remanei* (CrTBX-2; WormBase ID RP21057) (Notredame et al., 2000). High scoring SUMO consensus sites are indicated in grey, and identical residues are marked with asterisks. (C) Quantification of ß-galactosidase activity in yeast expressing the indicated TBX-2 protein or the empty pLexA as bait and UBC-9 prey in replicate samples from 3 independent experiments (n=7). Differences between mutants and wild-type TBX-2 or different mutants (bracket) are statistically significant at $p<0.05$ (*) or $p< 0.005$ (**). The double mutant is TBX-$2^{LKIE/VKKE->AAAA}$. The error bars indicate the standard error of the mean.

Panel C of this figure was contributed by co-author Tanya Crum.

of the T-box, and a SUMO consensus site is found at this position in many T-box factors, including all members of the Tbx2 subfamily (Papaioannou, 2001). VKKE is located in a region that is not highly conserved among T-box factors, although high scoring SUMO consensus sites are found near the C-terminus of TBX-2 proteins from *C. elegans*, *C. briggsae*, and *C. remanei*, suggesting this site may be functionally conserved (Figure 7B). We mutated each of these two sites in *C. elegans* TBX-2 to all alanines either in single mutants (LKIE->AAAA or VKKE->AAAA) or in a double mutant (LKIE/VKKE->AAAA) and tested whether these mutants affected the ability of a TBX-2 bait to interact with UBC-9 prey. Interactions were scored in plate assays for histidine prototrophy and ß-galactosidase (ß-gal) expression, and the level of interaction was quantified by measuring ß-gal activity.

We found that UBC-9 interaction with TBX-2 was affected by mutations affecting both the LKIE and VKKE sites. UBC-9 interacted with both the TBX-2$^{LKIE->AAAA}$ and TBX-2$^{VKKE->AAAA}$ single mutants in plate assays, but this interaction was reduced to 63% and 22% of the levels observed for wild-type TBX-2, respectively (Figure 7C). In comparison, UBC-9 failed to interact with the TBX-2$^{LKIE/VKKE->AAAA}$ double mutant in plate assays, and the ß-gal activity was close to that obtained using an empty bait plasmid (Figure 7C). As a control, we found that wild-type and all of the mutant TBX-2 proteins retained the ability to interact with an unrelated protein, UNC-37, in yeast two-hybrid assays indicating the mutant proteins were expressed. Thus, both the LKIE and VKKE sites can interact with UBC-9. Because mutating both of these sites reduces interaction to near background, we believe they are the primary sites in TBX-2 that mediate this interaction. We have not tested other potential TBX-2 SUMOylation sites for interaction with UBC-9 in two-hybrid assays.

3.4.2 TBX-2 can be SUMOylated in mammalian cell assays

To determine if TBX-2 can be SUMOylated, we co-expressed full-length TBX-2 and human SUMO-1 in COS-1 cells. TBX-2 was fused to poly-histidine and pulled down using Ni^{2+}-beads under denaturing conditions, while TBX-2 and SUMO-1 were tagged with V5 and HA epitope tags, respectively, for detection on western blots. A SUMO-1ΔGG mutant lacking the C-terminal Gly-Gly motif required for conjugation to target lysine residues was used as a control to demonstrate SUMO conjugation.

When co-expressed with SUMO-1, wild-type TBX-2 formed several more slowly migrating bands detectable with both anti-HA and anti-V5 (Figure 8A). These bands likely represent mono- and multi-SUMOylated TBX-2, although proteins SUMOylated at different sites can also migrate at different positions due to the branched nature of the SUMOylated protein (Costa et al., 2011). In comparison, no SUMOylated TBX-2 was detected when co-expressed with SUMO-1ΔGG. As for many SUMOylated proteins, we found only a fraction of TBX-2 (~10%) is SUMOylated in these assays. Similar results were obtained when TBX-2 was co-expressed with human SUMO-2 or SUMO-3 (Figure 9).

We next asked how mutations in the UBC-9 interaction sites affected TBX-2 SUMOylation. SUMOylation of TBX-$2^{LKIE->AAAA}$ and TBX-$2^{VKKE->AAAA}$ were reduced to approximately 30% and 70% the level of wild-type TBX-2, respectively, while SUMOylation of the TBX-$2^{LKIE/VKKE->AAAA}$ double mutant was further reduced to a level comparable to background (Figure 8A, lanes 2 and 9). These results indicate that TBX-2 can be SUMOylated, and that the LKIE and VKKE sites for UBC-9 interaction are required for TBX-2 SUMOylation.

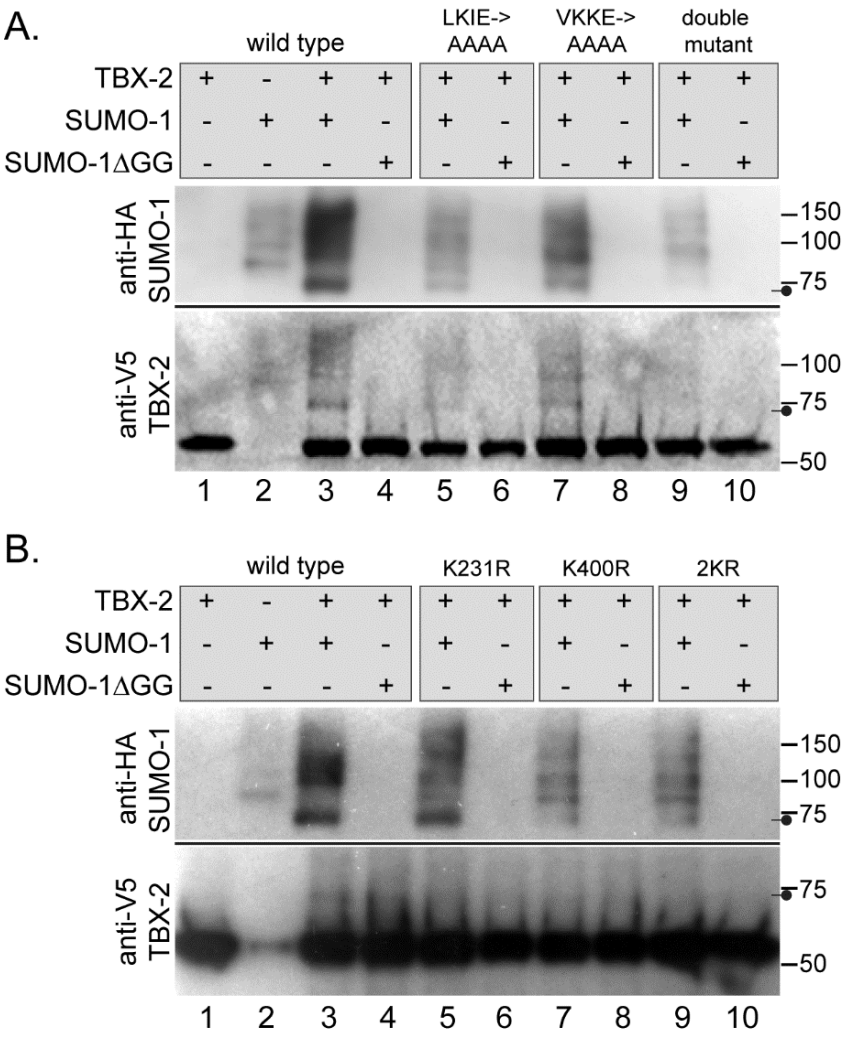

Figure 8. SUMOylation of TBX-2 is mediated via two SUMO consensus sites.

Western blots of Ni-NTA pulled-down wild-type and mutant TBX-2/V5/HIS probed to detect TBX-2 (bottom) or SUMO-1 (top). Combinations of proteins (grey boxes) were expressed in COS-1 cells. (A) Wild-type TBX-2 and mutants with SUMOylation sites converted to all alanines. (B) Wild-type TBX-2 and mutants with SUMO acceptor lysines converted to arginines. The position of the fastest migrating SUMOylated form of TBX-2 is indicated (bar & circle) and the position of molecular weight markers are indicated in kDa (bars). Signal in the lower panel in A was detected using a STORM Molecular Imager and clearly demonstrates more slowly migrating TBX-2 bands when co-transfected with SUMO-1. TBX-2/V5/HIS is ~52 kDa, and HA-SUMO-1 is ~13 kDa. The fastest migrating SUMOylated form migrates somewhat slower than predicted by its molecular weight, which is a common feature of SUMOylated proteins.

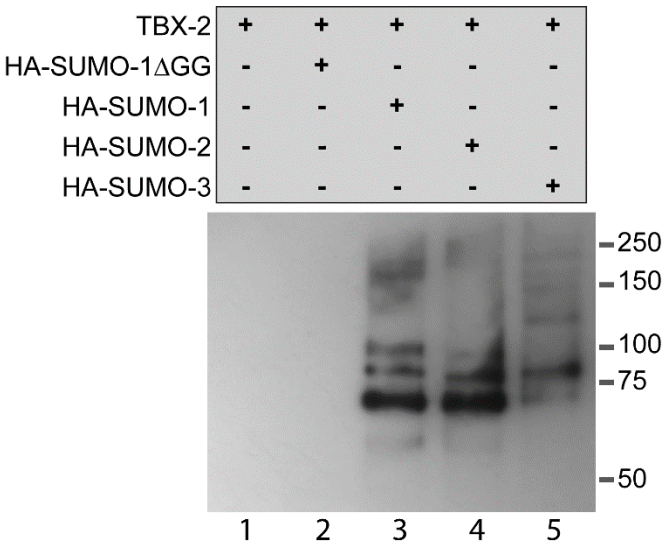

Figure 9. *C. elegans* TBX-2 conjugation to SUMO-1, SUMO-2, SUMO-3

Western blot of Ni-NTA pulled-down TBX-2/V5/HIS probed with anti-HA to detect SUMO-1 (lane 3), SUMO-2 (lane 4), or SUMO-3 (lane 5) conjugated TBX-2 protein. Combinations of proteins (grey box) were expressed in COS-1 cells. The positions of MW markers are indicated (kDa). Mono-SUMOylated TBX-2 is seen just below 75 kDa, and poly-SUMOylated TBX-2 migrates between 75 and 100 kDa.

We next mutated the SUMO-conjugated lysine residues in the LKIE and VKKE sites to arginine, which is a conservative substitution that cannot be conjugated to SUMO, and we examined SUMOylation in COS-1 cells (Figure 8B). The TBX-2^{K231R} mutant affecting LKIE exhibited reduction of the more slowly migrating SUMOylated products, but these products were not eliminated, while the fastest migrating band appeared unaffected. In comparison, overall SUMOylation of the TBX-2^{K400R} mutant affecting VKKE was strongly reduced, and the fast migrating form of SUMOylated TBX-2 was nearly completely eliminated. SUMOylation of the TBX-2^{2KR} double mutant containing K231R and K400R was similar to that of the TBX-2^{K400R} single mutant, but this mutant was still SUMOylated above background levels (compare Figure 8B, lanes 2 and 9). Because both of these conservative mutations affect the pattern of TBX-2 SUMOylation, we believe lysine residues in both the LKIE and VKKE SUMO consensus sites are SUMOylated.

3.4.3 Reduced SUMOylation does not affect TBX-2 nuclear localization pattern or stability

TBX-2$^{LKIE/VKKE->AAAA}$ does not interact with the SUMO-conjugating enzyme UBC-9, and thereby is incapable of being SUMOylated, and we wanted to ask how these mutations might affect TBX-2 activity in order to determine a mechanistic role for SUMOylation. We previously reported that *ubc-9(RNAi)* animals appear to mislocalize a TBX-2::GFP translational fusion protein to subnuclear puncta *in vivo* (Roy Chowdhuri et al., 2006), suggesting SUMOylation may affect subnuclear localization of TBX-2, as is the case for the *C. elegans* Polycomb group protein SOP-2 (Zhang et al., 2004). We expressed V5-tagged full length TBX-2 or TBX-2$^{LKIE/VKKE->AAAA}$ in COS-1 and stained cells with antibodies against the V5 epitope to detect if there was a difference in the nuclear localization pattern between wild type TBX-2 and the non-SUMOylatable mutant. As expected, TBX-2 staining was specific to the nucleus, although

TBX-2$^{LKIE/VKKE->AAAA}$ also localized to the nucleus in an indistinguishable pattern from that of the wild type protein (Figure 10A). Co-expression with SUMO-1 also did not affect this pattern (Figure 10B). Our lab previously observed similar localization patterns when over-expressing TBX-2 and TBX-2$^{LKIE/VKKE->AAAA}$ in *C. elegans* via heat shock promoters (Crum, 2011), and we conclude that SUMO site mutations do not affect TBX-2 localization.

Recent advancements in the understanding of regulation by SUMOylation have uncovered novel mechanisms involving cross-talk between SUMO and other important post-translational modifications, such as ubiquitination, phosphorylation, and acetylation (Eifler and Vertegaal, 2015). One such mechanism is that employed by sumo-targeted ubiquitin ligases, or STUbLs, which provide a regulatory link between ubiquitination and SUMOylation. Essentially, STUbLs catalyze poly-ubiquitination of SUMO-modified targets by the addition individual ubiquitin moieties to an existing SUMO peptide, resulting in targets which are modified by both SUMO and ubiquitin (Sriramachandran and Dohmen, 2014). Although these targets can undergo non-proteolytic fates, the addition of ubiquitin chains is generally thought to result in degradation at the proteasome. In this capacity, STUbLs act to negatively regulate the existing pool of their substrates, and we were interested in the possibility that TBX-2 was similarly regulated by STUbL activity. It was observed that a TBX-2$^{LKIE/VKKE->AAAA}$::GFP translational fusion seemed to perdure longer than TBX-2::GFP in the worm (Crum, 2011), and we hypothesized this perdurance could be a consequence of resistance of the non-SUMOylatable mutant to degradation by the proteasome. To address this possibility, we transfected COS-1 cells with V5-tagged TBX-2 or TBX-2$^{LKIE/VKKE->AAAA}$, terminated protein biosynthesis with the addition of cycloheximide, then harvested cells at successive time points and probed the whole cell lysates

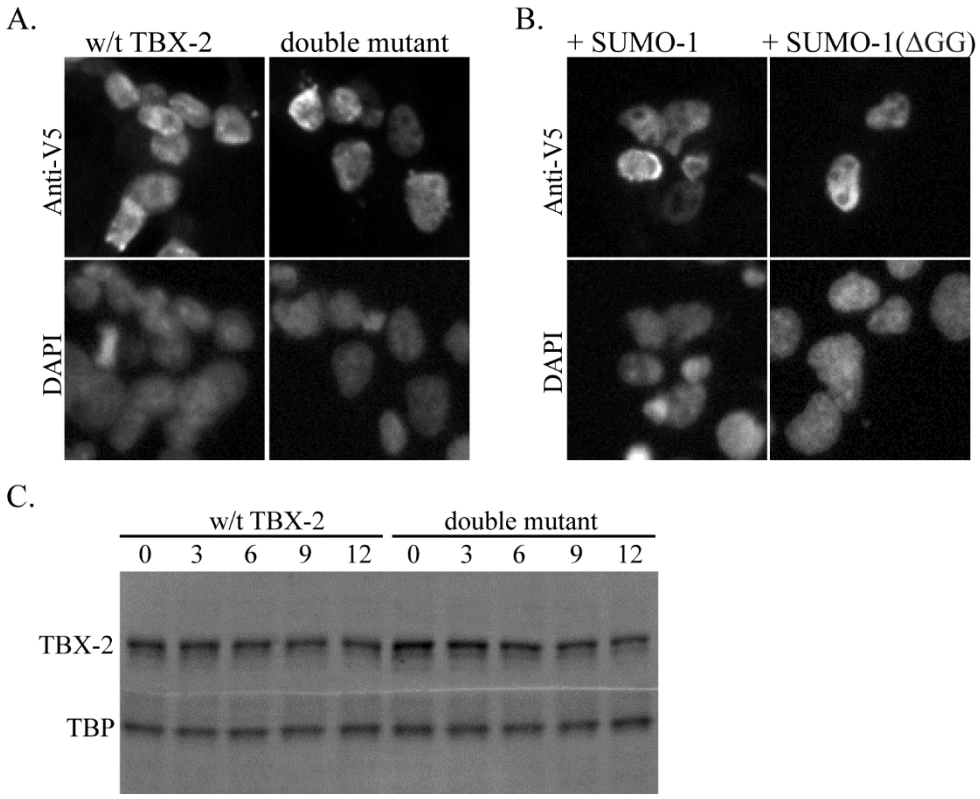

Figure 10. SUMOylation does not affect TBX-2 localization or stability

Assaying the effect of mutation of both TBX-2 SUMO consensus sites to AAAA on protein localization and stability in COS-1 cells. Panels A & B depict immunostained COS-1 cells transfected with wild type TBX-2/V5/His or TBX-2$^{LKIE/VKKE->AAAA}$/V5/His (panel A), or co-transfected with TBX-2/V5/His and SUMO-1 or SUMO-1(ΔGG) (panel B). Upper panels depict staining with anti-V5/Texas Red to visualize TBX-2, and lower panels depict DAPI staining to identify nuclei positions. Compared red fluorescent within panels A & B were obtained at nearly identical exposure times (within 1 ms), and were brightened for publication by equivalent methods using Zen lite software. Panel C is a western blot of whole COS-1 cell lysates transfected with either wild type TBX-2/V5/His or TBX-2$^{LKIE/VKKE->AAAA}$/V5/His. The hours cells were harvested after cycloheximide treatment are indicated above the blot in the appropriate lanes, as well as the transfected construct. Anti-V5 was used to visualize TBX-2 protein (upper bands), and anti-TBP (TATA binding protein) was used to verify total protein concentrations were equivalent in all lanes (lower bands).

with anti-V5 to determine if TBX-2 protein levels were affected over time by the LKIE/VKKE->AAAA mutation. We did not observe a significant difference in the protein levels between wild type and mutant proteins, and conclude that SUMO site mutations do not affect TBX-2 stability or turnover in COS-1 cells (Figure 10).

3.4.4 TBX-2 is a transcriptional repressor in mammalian cells

C. elegans TBX-2 is most closely related to the mammalian T-box repressors Tbx2 and Tbx3 (Roy Chowdhuri et al., 2006). We wanted to ask if TBX-2 functions similarly to repress transcription and, if so, whether this activity depends on SUMOylation. Because mutations affecting the LKIE SUMOylation site would likely affect DNA binding, we asked if TBX-2 fused to the heterologous GAL4 DNA binding domain (TBX-2:GAL4) could repress expression of the 5xGAL4:tk:luc reporter. This reporter contains 5 copies of the GAL4 binding site upstream of thymidine kinase promoter:luciferase reporter, and TBX-2:GAL4 repressed expression of this reporter up to 5-fold (Figure 11). SUMOylation is most often associated with transcriptional repression, and we expected that mutation of the LKIE and VKKE SUMO sites would reduce this repressor activity. However, we found that the TBX-2$^{LKIE/VKKE->AAAA}$ double mutant repressed 5xGAL4:tk:luc similarly to wild-type TBX-2. Co-expressing SUMO-1 did not affect repression of 5xGAL4:tk:luc with either wild-type or mutant TBX-2 (Figure 12). Thus, SUMOylation is not required for TBX-2:GAL4 repressor activity in COS-1 cells.

3.4.5 TBX-2 function is SUMO-dependent in *C. elegans*

mab-22(bx59) is a temperature sensitive mutant that exhibits defects in male tail ray formation and partially penetrant larval lethality. *bx59* has recently been identified as a missense mutation in *tbx-2* (King Chow, personal communication), and we subsequently refer to this mutation as *tbx-2(bx59)*. We examined the viability and pharyngeal morphology of *tbx-2(bx59)*

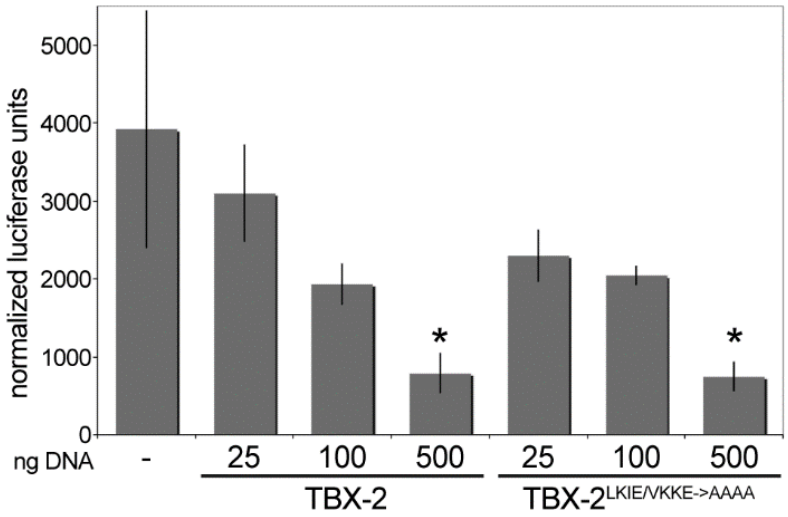

Figure 11. Dose dependent transcriptional repression by TBX-2:GAL4.

Relative luciferase activity in experiments co-transfecting increasing amounts of wild-type and mutant TBX-2:GAL4 with the 5xGAL4:tk:luc reporter. Data shown is the average of three assays and is representative of multiple independent experiments. Error bars indicate standard deviation. Statistically significant differences from control transfections are marked (*) ($p<0.05$).

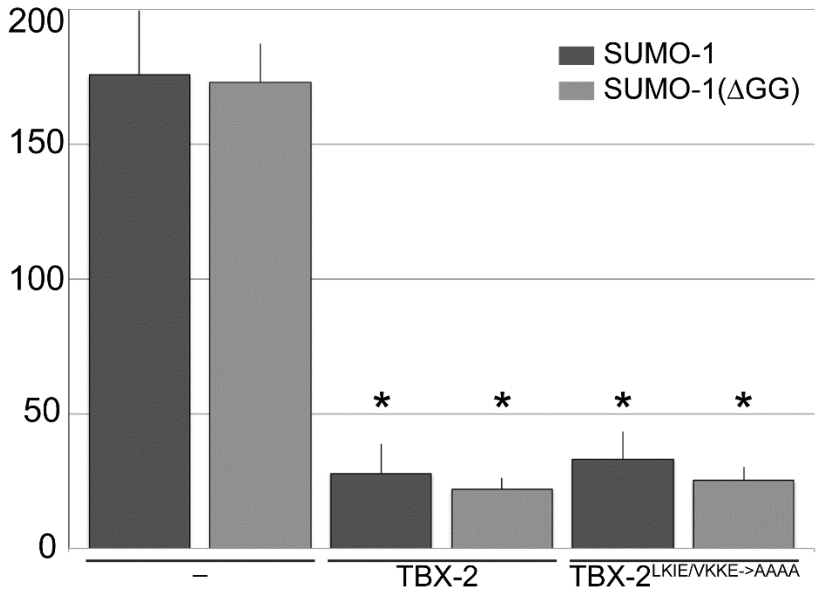

Figure 12. Co-transfection with SUMO-1 or SUMO-1(ΔGG) does not affect TBX-2 repressor activity

Normalized relative luciferase activity in experiments co-transfecting 500 ng wild-type or mutant TBX-2:GAL4 and the 5xGAL4:tk:luc reporter with either wild-type SUMO-1 or the non-conjugable SUMO-1(ΔGG). Data shown is the average of three assays and is representative of multiple independent experiments. Error bars indicate standard deviation. Statistically significant differences from control transfections are marked (*) ($p<0.005$).

mutants produced from hermaphrodites shifted to the non-permissive temperature (25˚C) at the L4 stage. Forty-four percent of these animals arrested at the L1 stage (n = 64) with variable pharyngeal abnormalities (Figure 13A-C). These phenotypes are similar to those observed in *tbx-2(RNAi)* animals and are not as severe as those observed in *tbx-2* null mutants (Roy Chowdhuri et al., 2006; Smith and Mango, 2007), and we conclude that *tbx-2(bx59)* is a hypomorphic allele.

We hypothesize that TBX-2 function depends on SUMOylation. To test this hypothesis we asked if inhibiting SUMOylation by reducing UBC-9 or the SUMO protein SMO-1 by RNAi could enhance the phenotype of *tbx-2(bx59)* mutants. Using the RNAi-feeding method we found that *ubc-9(RNAi)* produced a relatively low frequency of embryonic arrest in a wild-type background (Table II) (Kamath et al., 2001). In comparison, *tbx-2(bx59); ubc-9(RNAi)* double mutants exhibited a synergistic increase in the frequency of arrested embryos (Table II). *tbx-2(bx59); smo-1(RNAi)* double mutants also exhibited an increased frequency of embryonic lethality compared to each single mutant; however, the *smo-1(RNAi)* lethality alone was higher making it difficult to determine if the double mutant lethality was more than additive (Table II).

Many of the *tbx-2(bx59)* mutants that hatch grow to adulthood, but nearly all of the *tbx-2(bx59); ubc-9(RNAi)* and *tbx-2(bx59); smo-1(RNAi)* arrested as L1 larvae. We examined newly hatched larvae to determine if this enhanced L1 arrest results from pharyngeal defects. We found that both *tbx-2(bx59); ubc-9(RNAi)* and *tbx-2(bx59); smo-1(RNAi)* double mutants exhibited a synergistic increase in the frequency of animals with a severe anterior pharyngeal defect compared to the single mutants (Table II; Figure 13). Together, these results strongly suggest SUMOylation is necessary for TBX-2 function in anterior pharyngeal development.

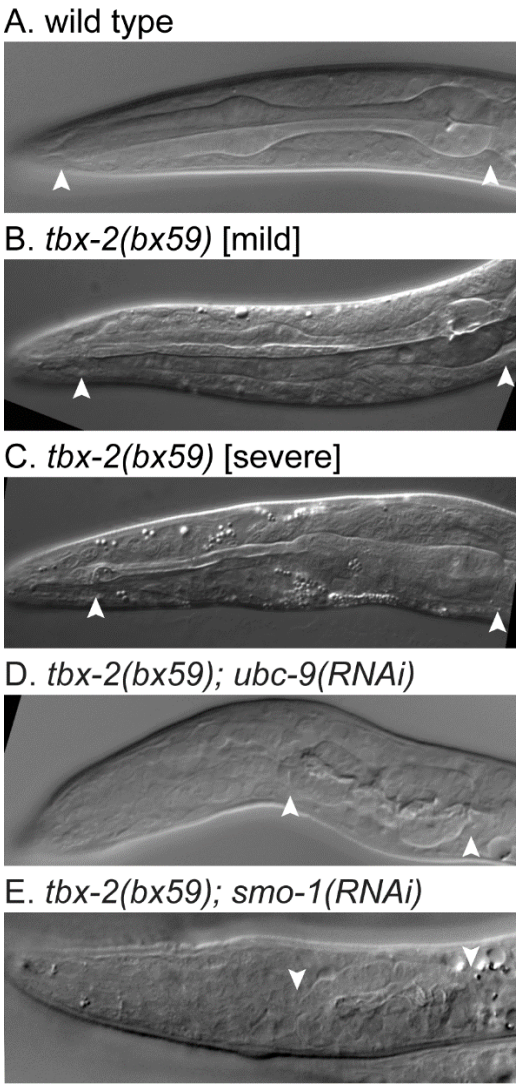

Figure 13. Pharyngeal defects in *tbx-2(bx59)* mutant are enhanced by reduced SUMOylation

DIC micrographs of the pharynx of L1 larvae of the indicated genotypes raised at the non-permissive temperature (25˚C). (A) wild type N2. (B) *tbx-2(bx59)* exhibiting a mild pharyngeal defect. (C) *tbx-2(bx59)* exhibiting a more severe pharyngeal defect. (D, E) *tbx-2(bx59); ubc-9(RNAi)* (D) and *tbx-2(bx59); smo-1(RNAi)* (E) L1 larvae exhibiting very severe defects resembling those of *tbx-2* null mutants. Arrowheads mark the extent of pharyngeal tissue. Anterior is left. The frequency of these phenotypes are indicated in Table II.

This figure was contributed by co-author Tanya Crum.

TABLE II: REDUCTION OF SUMOYLATION ENHANCES *tbx-2(bx59)* EMBRYONIC LETHALITY AND PHARYNGEAL DEFECTS

genotype [a]	% embryonic arrest (n)	Pharyngeal phenotypes in hatched L1s (percentage of total hatched animals)			
		Severe Tbx-2 pharynx	Mild Tbx-2 pharynx	Wild-type pharynx	n
tbx-2(bx59)	7 (120)	19	56	25	54
ubc-9(RNAi)	19 (186)	7	6	87	69
tbx-2(bx59); ubc-9(RNAi)	78 (200)	70	30	0	47
smo-1(RNAi)	65 (347)	22	39	39	49
tbx-2(bx59); smo-1(RNAi)	75 (359)	69	26	5	64

[a] L4 animals raised at 16˚C were shifted to 25˚C, and defects were scored in the F1 progeny.

This table was contributed by co-author Tanya Crum.

3.4.6 WRM063aG09 *tbx-2::gfp* fosmid rescues *tbx-2* null mutants

There is a wide range of pharyngeal defects and overall viability seen between different *tbx-2* mutants. While the hypomorphic *tbx-2(bx59)* mutants described earlier display only minor pharyngeal abnormalities and most can grow, albeit slowly, to adulthood, animals homozygous for the *tbx-2(ok529)* null allele, which possesses a deletion of a large part of the DNA binding domain predicted to make major contacts with the major groove of DNA, completely lack anterior pharyngeal muscle derived from the ABa lineage and thereby arrest soon after hatching, presumably due to the inability to feed (Coll et al., 2002; Roy Chowdhuri et al., 2006). Rescuing these mutant phenotypes has indeed been a struggle for us and others, as multiple attempts using various *tbx-2* cDNA and genomic transgenes generated by microinjection have proven unsuccessful in this endeavor. We now report rescue of *tbx-2(ok529)* mutants with 2 independent transgenic lines expressing an integrated *tbx-2::gfp* fosmid (WRM063aG09), both generated by biolistic transformation (Sarov et al., 2012). Rescued worms displayed a completely formed pharynx with a normal morphology (Table III, Figure 14). The fosmid WRM063aG09 was created by the modENCODE Project, and contains approximately 36 kb of genomic DNA centered roughly over *tbx-2* (http://www.wormbase.org/species/c_elegans/clone/WRM063aG09#02--10) with *gfp* fused in frame at the 3' end and an *unc-119(+)* marker to facilitate the generation of transgenic animals using biolistic transformation.

3.4.7 TBX-2^{K400R} rescues *tbx-2(ok529)* anterior pharyngeal defects

To test if SUMOylation is required for TBX-2 function *in vivo*, we introduced the *tbx-2* ^{K400R} mutation, which reduces SUMOylation of TBX-2, into the *tbx-2::gfp* rescue fosmid via recombineering (Dolphin and Hope, 2006), and using biolistic transformation, generated a

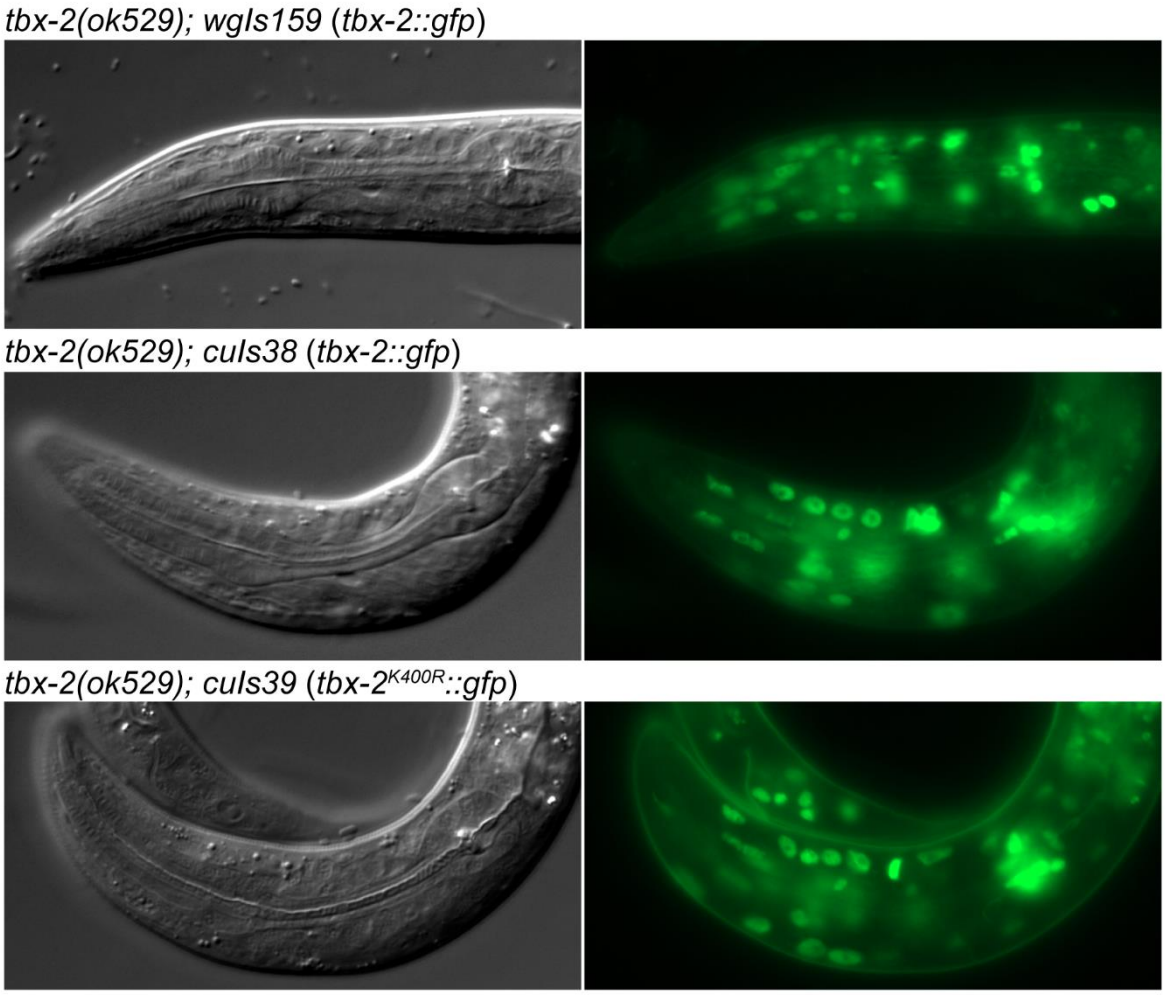

Figure 14. TBX-2^{K400R} rescues *tbx-2(ok529)* mutants

DIC (left panels) and fluorescence (right panels) images of synchronized hermaphrodite L1 *tbx-2(ok529)* homozygotes expressing the indicated integrated rescue constructs. The frequency of pharyngeal phenotypes for these strains are indicated in Table III.

TABLE III: PHARYNGEAL MORPHOLOGY OF L1 ANIMALS RESCUED WITH WILD TYPE AND MUTANT *tbx-2::gfp* CONSTRUCTS

Genotype	% wild type pharynx	% mild Tbx-2 pharynx[a]	% severe Tbx-2 pharynx[b]	n
+/+	100	0	0	36
tbx-2(ok529); wgIs159[tbx-2::gfp]	100	0	0	52
tbx-2(ok529); cuIs38[tbx-2::gfp]	100	0	0	48
tbx-2(ok529); cuIs39[tbx-2^{K400R}::gfp]	92.5	7.5	0	40

[a] Animals exhibiting a mild Tbx-2 phenotype had a complete pharynx extending to the anterior tip of the head but had an abnormally short and thick isthmus.
[b] Animals exhibiting a severe Tbx-2 phenotype had a clear decrease in the amount of anterior pharyngeal tissue and more extensive morphological defects in the pharynx.

chromosomally integrated *tbx-2* ^{K400R}*::gfp* expressing strain. We observed the GFP expression level of *tbx-2* ^{K400R}*::gfp* is similar to that of *tbx-2::gfp* expressing strains (Figure 14), and the *tbx-2* ^{K400R}*::gfp* transgene was crossed into the *tbx-2(ok529)* mutant background. We found that it also restored viability and normal pharyngeal morphology, similar to both *tbx-2::gfp* expressing strains, although a small percentage of animals exhibited a mild Tbx-2 phenotype similar to *tbx-2(bx59)* mutants (Table III, Figure 14).

3.4.8 TBX-2 and SUMOylation are required for repression of *D2096.6* gene expression

To identify genes downstream of TBX-2, we used microarrays to compare mRNA levels in populations of wild-type and *tbx-2(bx59)* embryos grown at 25˚C. We found 1276 protein coding genes that are differentially expressed in *tbx-2(bx59)* (BH corrected $p \leq 0.05$). 1030 of these genes (80.7%) are upregulated in *tbx-2(bx59)*, consistent with our hypothesis that TBX-2 functions as a transcriptional repressor.

We focused on the gene *D2096.6*, which had previously been shown to be specifically expressed in the pharyngeal muscles, marginal cells and epithelial cells under control of the FoxA-family transcription factor PHA-4 (Gaudet and Mango, 2002; Nakano et al., 2010). We observed an approximately 1.8-fold increase in *D2096.6* expression in *tbx-2(bx59)* mutants in our microarray (BH corrected p=0.03). While several candidate T-box binding sites are located upstream of *D2096.6*, our preliminary characterization of this promoter suggests it is indirectly regulated by TBX-2.

To determine how TBX-2 regulates *D2096.6* expression, we compared expression of a *D2096.6::gfp* reporter in wild-type and *tbx-2* mutants. Consistent with previous studies (Gaudet and Mango, 2002), we observed that a *D2096.6::gfp* reporter was expressed in wild-type embryos specifically in the pharynx at beginning approximately at the bean stage when the

pharyngeal primordium forms. Expression was typically observed in one to two cells in the pharynx in one and one-half fold embryos (Figure 15), and no expression was observed outside the pharynx. The number of GFP-expressing cells increased and animals hatched as L1s with GFP expression in pharyngeal muscles, marginal cells and epithelial cells (Figure 15D). In comparison, in *tbx-2(bx59)* and *tbx-2(ok529)* embryos *D2096.6::gfp* was expressed in more cells in the pharynx, and expression was observed in many cells outside the pharynx, including body wall muscles and hypodermal cells (Table IV; Figure 15B,C). Ectopic *D2096.6::gfp* expression continued into the L1 larval stage where it was observed in body wall muscle, hypodermal and gut cells (Figure 15E, F). These results indicate TBX-2 is an upstream regulator that represses *D2096.6* expression both temporally and spatially.

To ask if SUMOylation is necessary for TBX-2 function, we examined *D2096.6* expression in animals where activity of UBC-9 was reduced using feeding-RNAi. The most severely affected *ubc-9(RNAi)* animals have a highly disorganized morphology that makes it difficult to identify specific tissues (Roy Chowdhuri et al., 2006). Therefore we characterized *D2096.6::gfp* expression in older embryos that had undergone morphogenesis and the surviving L1 larvae. *ubc-9(RNAi)* resulted in *D2096.6::gfp* expression in posterior body wall muscles in embryos in a pattern similar to that which we have observed in *tbx-2(bx59)* and *tbx-2(ok529)* embryos (Figure 16A,B). In larvae we observed expression in body wall muscles and hypodermal cells in the posterior of the worm similar to the expression pattern we see in *tbx-2* mutants (Figure 16C,D). Thus SUMO-dependent mechanisms repress *D2096.6::gfp* expression, and the similarities in the pattern of ectopic expression in *ubc-9(RNAi)* and *tbx-2* mutants strongly suggests TBX-2 function depends on SUMOylation.

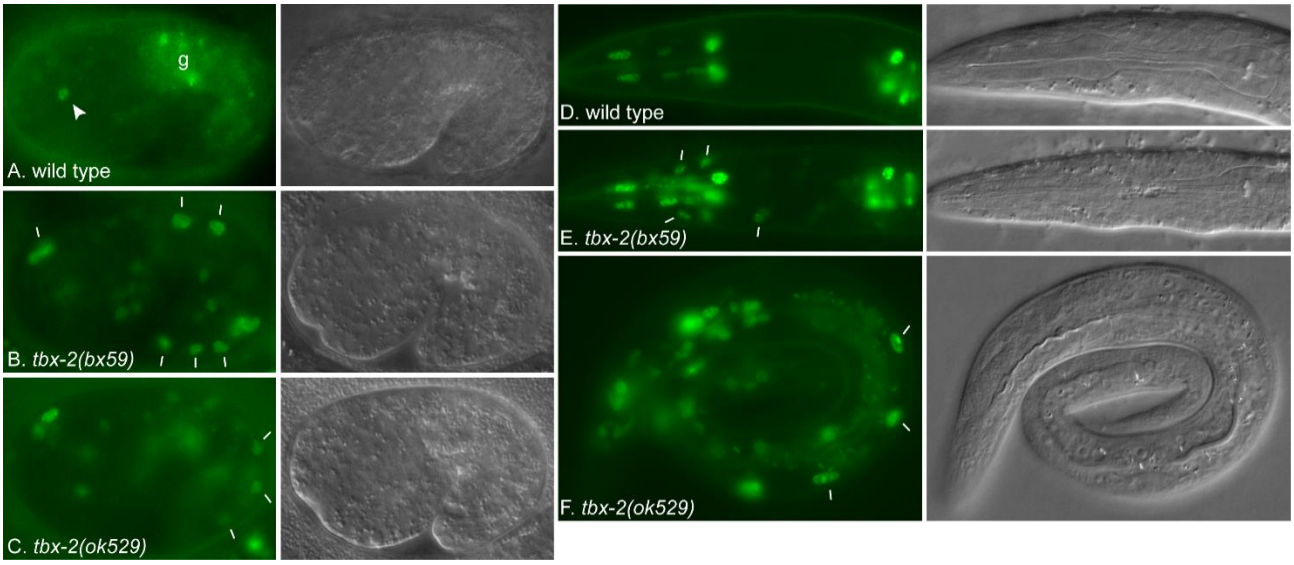

Figure 15. *D2096.6::gfp* is ectopically expressed in *tbx-2* mutants.

Fluorescence (left) and DIC (right) micrographs of 1.5-fold stage embryos (A-C) and L1 larvae (D-F) expressing *D2096.6::gfp*. (A) *tbx-2(+); cuEx553[D2096.6::gfp]* embryo containing a single GFP-expressing pharyngeal nucleus (arrowhead) and auto-fluorescent gut granules (g). (B) and (C) *tbx-2(bx59); cuEx553* and *tbx-2(ok529); cuEx553* embryos exhibiting widespread *D2096.6::gfp* expression outside the pharynx. (D) *tbx-2(+); cuEx553* L1 with GFP expression in pharyngeal nuclei. (E,F) *tbx-2(bx59); cuEx553* and *tbx-2(ok529); cuEx553* L1 larvae Representative bodywall muscle and hypodermal nuclei ectopically expressing *D2096.6::gfp* are marked (bars).

This figure was contributed by co-author Lynn Clary.

TABLE IV: REDUCTION OF UBC-9 LEADS TO ECTOPIC EXPRESSION OF *D2096.6::gfp*

Genotype	% animals with ectopic *D2096.6::gfp* expression (n)
cuEx553[D2096.6::gfp]	5 (136)
tbx-2(bx59); cuEx553 [a]	71 (55)
tbx-2(ok529); cuEx553 [b]	20 (35)
ubc-9(RNAi); cuEx553	75 (48)

[a] L4 animals raised at 16˚C were shifted to 25˚C, and defects were scored in the F1 progeny.
[b] Progeny segregating from *tbx-2(ok529)/dpy-17(e164) unc-32(e189)* hermaphrodites were scored. Twenty-five percent of these progeny are expected to be *tbx-2(ok529)* homozygotes.

This table was contributed by co-author Lynn Clary.

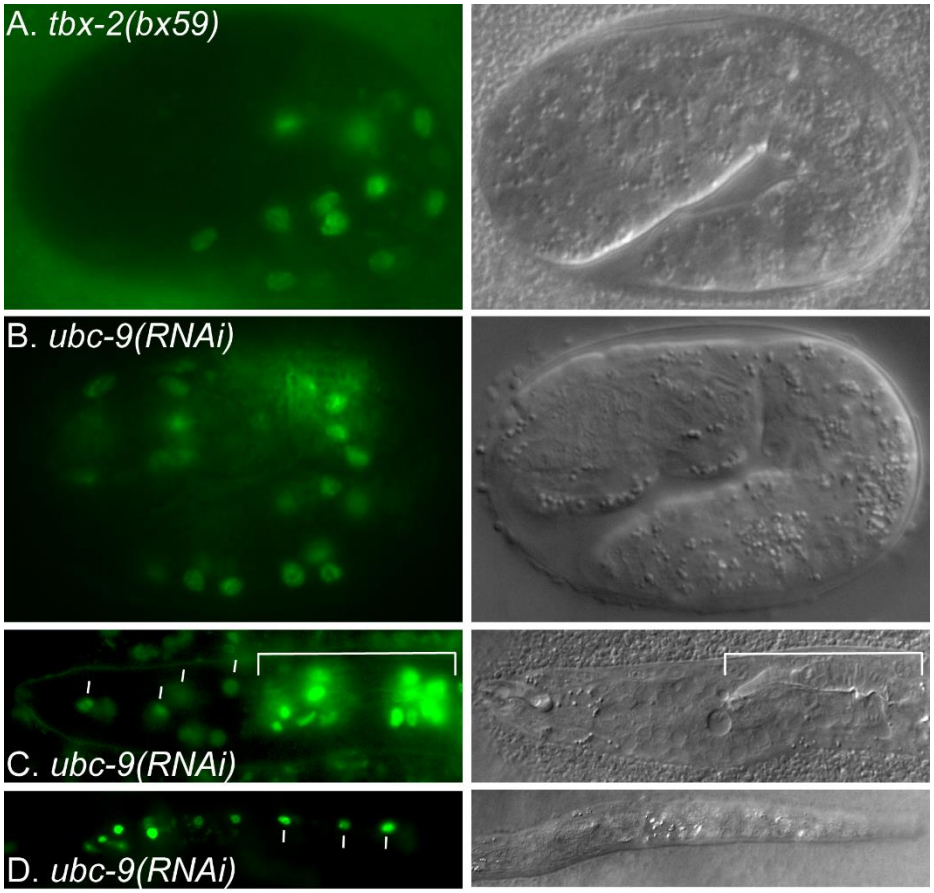

Figure 16. *D2096.6::gfp* is ectopically expressed in *ubc-9(RNAi)* animals

Fluorescence (left) and DIC (right) micrographs of a *tbx-2(bx59); cuEx553* embryo (A) and a *ubc-9(RNAi); cuEx553* embryo (B) and L1 larva (C, D) expressing *D2096.6::gfp* in body wall muscle and hypodermal nuclei (bars). A white bracket indicates the partial pharynx in C.

This figure was contributed by co-author Lynn Clary.

3.4.9 Mammalian Tbx2 subfamily members can be SUMOylated

To determine if SUMOylation is a conserved mechanism regulating T-box factor activity, we asked if mammalian orthologs of TBX-2 could be SUMOylated. Human TBX2 or mouse TBX3 tagged with poly-histidine and V5 were co-expressed in COS-1 cells with or without HA:SUMO-1 and pulled down using Ni^{2+}-beads under denaturing conditions similarly to *C. elegans* TBX-2. When co-expressed with SUMO-1 both TBX2 and TBX3 formed two more slowly migrating SUMOylated bands (Figure 17). This data indicates that other Tbx2 subfamily members can be SUMOylated, and we hypothesize that SUMOylation may be a common regulatory method of T-box factor activity.

3.5 Discussion:

Here we show that *C. elegans* TBX-2 and its mammalian orthologs human TBX2 and mouse TBX3 can be SUMOylated, and that TBX-2 SUMOylation depends on two SUMO consensus sites, LKIE and VKKE, which mediate interaction with the E2 SUMO conjugating enzyme UBC-9. We further demonstrate that *C. elegans* TBX-2 can function as a transcriptional repressor when fused to a heterologous DNA-binding domain; however mutations that eliminate SUMOylation do not affect this repressor activity. We note that these same mutations also do not affect TBX-2 nuclear localization or stability in COS-1 cells. The K400R mutation which reduces overall TBX-2 SUMOylation does not abrogate the ability of a *tbx-2*^{K400R}*::gfp* fosmid to rescue *tbx-2* nulls, suggesting SUMOylation at either site can facilitate TBX-2 function. Finally, we provide genetic evidence that SUMOylation is required for TBX-2 function *in vivo* by showing that reduction of SUMOylation enhances the phenotype of a hypomorphic *tbx-2* mutant and phenocopies the loss of *tbx-2* on expression of one gene that is downstream of TBX-2.

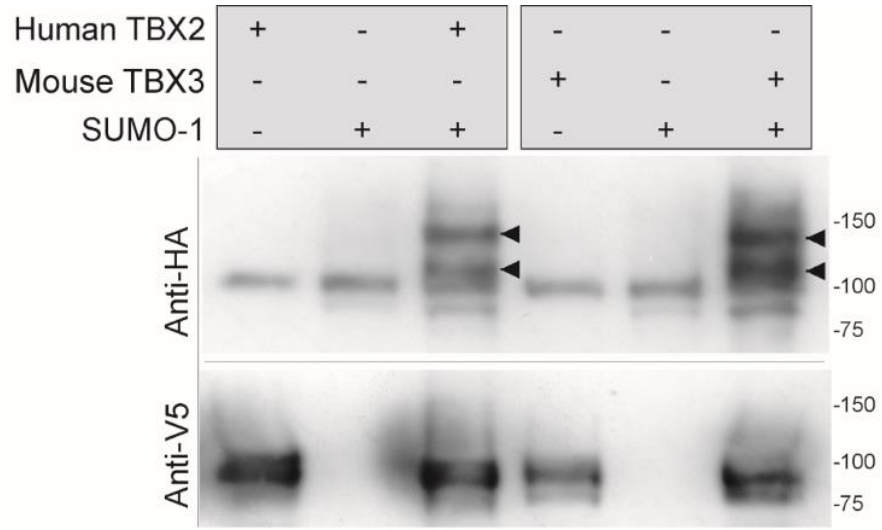

Figure 17. SUMOylation of mammalian Tbx2 subfamily members.

Western blots of Ni-NTA pulled-down human TBX2/V5/HIS and mouse TBX3/V5/HIS probed to detect TBX2 and TBX3 (bottom) or SUMO-1 (top). Combinations of proteins expressed in COS-1 cells are indicated (grey boxes). SUMOylated forms of TBX2 and TBX3 are marked with arrowheads, and MW weight markers are indicated (kDa). A cross-reacting background band was detected in all lanes using anti-HA.

3.5.1 Two TBX-2 SUMO consensus sites interact with UBC-9 and mediate SUMOylation

TBX-2 contains two predicted high scoring SUMO consensus sites. VKKE located near the C-terminus and LKIE located within the T-box DNA-binding domain. Each of these sequences interacts with the E2 SUMO-conjugating enzyme UBC-9 in yeast 2-hybrid assays, and they are the only sites that can mediate this interaction.

Our data strongly suggests that both of these sites are SUMOylated. We observed multiple SUMOylated forms of TBX-2 in COS-1 cells, and mutations affecting either SUMO site reduce the amount of SUMOylated TBX-2. However, there are differences in how specific mutations in these sites affect TBX-2 SUMOylation. For VKKE, mutation of the acceptor lysine (K400R) results in a more severe reduction in SUMOylation than mutating this site completely to alanines. In comparison, mutating the LKIE site to alanines results in a large decrease in SUMOylation whereas mutation of the acceptor lysine (K231R) has a moderate affect and preferentially affects the more slowly migrating SUMOylated forms of TBX-2. Mutations affecting only the acceptor lysine likely retain interaction with UBC-9 (Sampson et al., 2001), whereas mutations converting the SUMO site to alanines eliminate UBC-9 binding, and this difference likely underlies the different effects we observed on TBX-2 SUMOylation when these two sites are mutated.

T-boxes have a highly conserved structure when bound to DNA (Coll et al., 2002; El Omari et al., 2011; Muller and Herrmann, 1997; Stirnimann et al., 2010), and TBX-2 LKIE is located within the α3 helix that spans the DNA backbone. While SUMOylation can occur in α helices (Knipscheer et al., 2008; Pichler et al., 2005), this is an unusual 2˚ structure for UBC-9 interaction and SUMOylation, as UBC-9 has been shown to bind SUMO consensus sites in extended loops (Bernier-Villamor et al., 2002; Lin et al., 2002). However, recent evidence

indicates that some T-boxes have significant structural flexibility that might allow SUMOylation at LKIE. The Tbx20 T-box exists as a molten globule with an unstable tertiary structure allowing flexibility between 2˚ structural domains (Macindoe et al., 2009). Likewise in TBX5, the 3_{10}-helix located just C terminal to the α3 helix is unstructured in the absence of DNA (Stirnimann et al., 2010). While the α3 helix remains structured when TBX5 is not bound to DNA, the LKIE site would be more accessible to bind UBC-9.

LKIE was also investigated as a potential SUMOylation site in the human T-box factor TBX22 (Andreou et al., 2007). Interestingly mutation of this site eliminated TBX22 SUMOylation, however this is believed to result indirectly from possible effects on DNA binding as was observed with several DNA-binding defective mutants. Biochemical analyses of SUMOylated T-box factors is necessary to explicitly determine if this site is SUMOylated in different proteins.

3.5.2 *tbx-2* genetically interacts with *ubc-9* and *smo-1*

tbx-2(bx59); ubc-9(RNAi) and *tbx-2(bx59); smo-1(RNAi)* animals exhibit penetrant embryonic arrest and enhanced pharyngeal defects, indicating that reduced SUMOylation affects TBX-2 activity *in vivo*. In particular, the enhanced pharyngeal phenotype of these animals resembles that of *tbx-2* null mutants, strongly suggesting that *tbx-2* and SUMOylation function in the same pathway to specify pharyngeal muscle fate (Herman and Yochem, 2005). These observations are consistent with the hypothesis that TBX-2 function is SUMO-dependent.

In comparison, we do not know why enhanced embryonic lethality was observed in *tbx-2(bx59); ubc-9(RNAi)* and *tbx-2(bx59); smo-1(RNAi)* animals. Neither *tbx-2* null mutants nor *tbx-2(RNAi)* animals exhibit embryonic lethality (Roy Chowdhuri et al., 2006), indicating lethality does not result from loss of zygotic *tbx-2(bx59)* activity. One possibility is that *tbx-*

2(bx59) may have a partial gain-of-function character, and reducing SUMOylation deregulates this activity. *tbx-2(bx59)* mutates a conserved histidine residue within the dimerization domain of the T-box to a tyrosine (H145Y; accession CCD69847), and mutations affecting this domain in human TBX1 result in gain-of-function associated with some cases of DiGeorge and velocardiofacial syndromes (Zweier et al., 2007). Alternatively, decreased SUMOylation of a parentally-provided, RNAi-resistant protein or mRNA *tbx-2* gene product might be required for viability. Finally, decreased SUMOylation may affect SUMO-dependent activity of both TBX-2 and another factor with a partially redundant activity required for embryogenesis.

3.5.3 How might SUMOylation affect TBX-2 activity?

SUMO-modification can affect substrate protein activity by a variety of mechanisms, such as altering cellular localization, protein stability, DNA-binding capacity, or protein-protein interactions. In our COS-1 assays, TBX-2 and non-SUMOylatable TBX-2$^{LKIE/VKKE->AAAA}$ mutants exhibited identical nuclear localization patterns and protein stability. SUMOylation of transcription factors is commonly associated with transcriptional repression, and it can promote recruitment of chromatin remodeling and histone modifying complexes (Garcia-Dominguez and Reyes, 2009; Gill, 2005). Indeed, SUMOylation of the *C. elegans* Ets-domain factor LIN-1 leads to interaction with MEP-1 and the NuRD chromatin repressor complex (Leight et al., 2005). However our results argue that SUMOylation affects TBX-2 function by a different mechanism. Unlike LIN-1, repressor activity of TBX-2:GAL4 fusion protein in mammalian cells is independent of SUMOylation, and in extensive yeast 2-hybrid screens TBX-2 has not been observed to interact with MEP-1 (Roy Chowdhuri et al., 2006).

SUMOylation at the LKIE site in the T-box would likely affect the ability of TBX-2 to bind sites in the genome and to interact with other factors binding TBX-2 regulated promoters.

If this is the case, our assays for TBX-2:GAL4 repressor activity would be insensitive to SUMOylation, since they depend on a heterologous DNA-binding domain targeting a synthetic promoter. Indeed, SUMOylation has been shown to affect DNA-binding activity of specific transcription factors (Anckar and Sistonen, 2007; Campbell et al., 2008; Hong et al., 2001).

It is difficult to predict how SUMOylation at the VKKE site would affect TBX-2 activity. T-box proteins are poorly conserved outside of the DNA-binding domain, and the function of the TBX-2 C-terminus is unknown. Interestingly, our preliminary results indicate VKKE is located near an interaction site for the Groucho-family co-repressor UNC-37 (Crum, 2011). SUMOylation can regulate interaction with Groucho-family proteins (Lee et al., 2012; Sung et al., 2005), and we hypothesize SUMOylation at VKKE has a similar function. Groucho-interaction motifs are enriched in T-box factors from *C. elegans*, Drosophila, and humans (Copley, 2005), and several T-box factors have been shown to interact with Groucho-family proteins (Farin et al., 2007; Formaz-Preston et al., 2012; Kawamura et al., 2008; Miller and Okkema, 2011). SUMOylation may be a common mechanism for regulating T-box factor interaction with Groucho, and this will be discussed further in the following chapters.

4 FUNCTION OF THE C.*ELEGANS* T-BOX FACTOR TBX-2 DEPENDS ON INTERACTION WITH THE UNC-37/GROUCHO COREPRESSOR

(Portions of the work from this chapter were contributed by co-author Tanya Crum.)

4.1 Abstract

T-box transcription factors are important regulators of development in all animals, and altered expression of T-box factors has been identified in an increasing number of diseases and cancers. Despite these important roles, the mechanism of T-box factor activity is not well understood. We have previously shown that the *C. elegans* Tbx2 subfamily member TBX-2 functions as a transcriptional repressor to specify ABa-derived pharyngeal muscle, and that this function depends on SUMOylation. Here we show that TBX-2 function also depends on interaction with the Groucho-family corepressor UNC-37. TBX-2 interacts with UNC-37 in yeast two-hybrid assays via a highly conserved engrailed homology 1 (eh1) motif located near the TBX-2 C-terminus. Reducing *unc-37* phenocopies *tbx-2* mutants, resulting in a loss of anterior pharyngeal muscles and derepression of the *tbx-2* promoter. Moreover, double mutants containing hypomorphic alleles of *unc-37* and *tbx-2* exhibit enhanced phenotypes, providing strong genetic evidence that *unc-37* and *tbx-2* share common functions *in vivo*. To test whether interaction with UNC-37 is necessary for TBX-2 activity, we developed a transgene rescue assay using a *tbx-2* containing fosmid and found that mutating the *tbx-2* eh1 motif reduced rescue of a *tbx-2* null mutant. These results indicate that TBX-2 function *in vivo* depends on interaction with UNC-37. Lastly, we show that reduction of SUMO pathway components and UNC-37 similarly leads to a loss of *tbx-2* repression, suggesting SUMO may promote TBX-2 interaction with UNC-37, and as many T-box factors contain eh1 motifs, we suggest that interaction with Groucho-family corepressors is a common mechanism contributing to their activity.

4.2 Introduction

T-box proteins are a family of transcription factors found in all animals that play important roles in development [reviewed in (Papaioannou, 2014)]. They are characterized by a conserved 180-200 residue T-box DNA-binding domain. A number of T-box genes have been implicated in human congenital diseases and cancers, and in most cases the level of T-box factor function is a crucial determinant of disease. For example, patients heterozygous for loss-of-function mutations in the Tbx2 sub-family genes *TBX3*, *TBX4*, and *TBX5* are affected by Ulnar-mammary, Small patella, and Holt-Oram syndromes, respectively (Bamshad et al., 1997; Basson et al., 1997; Bongers et al., 2004; Li et al., 1997). In contrast, over expression of the closely related Tbx2 subfamily genes *TBX2* and *TBX3* has been found in many different human cancers, where it may inhibit cellular senescence and promote metastasis [reviewed in (Wansleben et al., 2014)]. While these observations suggest therapies affecting T-box factor activity would be effective in treating these diseases, we need a better mechanistic understanding of how these factors function to adequately target these diseases.

T-box protein function often depends on interactions with other factors and chromatin regulatory proteins (Boogerd et al., 2009; Papaioannou, 2014). In particular, several T-box factors have been shown to interact with the Groucho-family of transcriptional corepressors (Farin et al., 2007; Formaz-Preston et al., 2012; Hitachi et al., 2009; Kaltenbrun et al., 2013; Kawamura et al., 2008; Miller and Okkema, 2011). Further, so-called engrailed homology 1 (eh1) motifs that can mediate interaction with Groucho-family factors are frequently found in T-box factors (Copley, 2005), suggesting that Groucho interaction is an important mechanism of T-box factor function.

In this report, we examine physical and genetic interactions between the *C. elegans* Groucho-family factor UNC-37 and the T-box factor TBX-2. UNC-37 is a ubiquitously expressed factor that has been shown to interact with eh1 motifs in several transcriptional repressors (Calvo et al., 2001; Miller and Okkema, 2011; Peden et al., 2007; Winnier et al., 1999; Xia et al., 2007). Hypomorphic *unc-37* mutants display movement defects resulting from misspecification of particular motor neurons, while null mutants exhibit sterility and maternal effect lethality (Miller et al., 1993; Pflugrad et al., 1997). TBX-2 is the sole *C. elegans* member of the Tbx2 sub-family, and it is most closely related to the human transcriptional repressors *TBX2* and *TBX3* (Pocock et al., 2004). *C. elegans* TBX-2 is required for formation of the subset of pharyngeal muscles induced in the ABa-lineage, as well as for olfactory adaptation and neuronal fate specification in the HSN/PHB lineage (Miyahara et al., 2004; Roy Chowdhuri et al., 2006; Singhvi et al., 2008; Smith and Mango, 2007). *tbx-2* null mutants lack the ABa-derived muscles that make up the anterior region of the pharynx, and they arrest shortly after hatching as L1 larvae due to an inability to feed.

Here we show that TBX-2 functions as an UNC-37 dependent transcriptional repressor. TBX-2 interacts with UNC-37 via a conserved eh1 motif located near the TBX-2 C-terminus, and blocking this interaction disrupts function of TBX-2 in development. Moreover, reducing *unc-37* activity leads to derepression of a *tbx-2::gfp* reporter that is normally repressed by TBX-2 through a negative autoregulatory mechanism (Milton and Okkema, 2015). Complete knockdown of *unc-37* leads to embryonic arrest with a decreased number of pharyngeal muscles, consistent with a loss of ABa-derived pharyngeal muscles. We observe strong genetic interaction between *unc-37* and *tbx-2* hypomorphic mutations, indicating UNC-37 is crucial for TBX-2 activity *in vivo*. Finally, we show that SUMO pathway components, SMO-1 and UBC-9,

and UNC-37 regulate a *tbx-2::gfp* reporter in similar tissues, suggesting SUMOylation may promote TBX-2 interaction with UNC-37. Because diverged eh1 motifs are also present in human *TBX2* and *TBX3* (Copley, 2005), we suggest these repressors may similarly depend on Groucho-family corepressors.

4.3 Materials and Methods

4.3.1 Nematode handling, strains, and transformation

C. elegans were grown under standard conditions (Lewis and Fleming, 1995). The following strains were used in this study: N2 wild type Bristol, DP38 *unc-119(ed3)* (Maduro and Pilgrim, 1995), OK0460 *tbx-2(ok529)/ dpy-17(e164) unc-32(e189)* (Roy Chowdhuri et al., 2006), OK0507 *cuIs21[ceh-22::gfp] III* (Roy Chowdhuri et al., 2006), OK0640 *cuIs31[ceh-22::gfp] X*, CB262 *unc-37(e262) I* (Brenner, 1974), OK0660 *tbx-2(bx59) III* (Huber et al., 2013).

The following strains were generated for this study: OK1061 *tbx-2(ok529) III; cuEx809[tbx-2::TY1::EGFP::3xFLAG+unc-119(+)]*, OK1065 *tbx-2(ok529) III; cuEx810[tbx-2::TY1::EGFP::3xFLAG+unc-119(+)]*, OK1054 *tbx-2(ok529); cuEx814[tbx-2$^{FDV->ADA}$::TY1::EGFP::3xFLAG+unc-119(+)]*, OK1033 *unc-37(e262); tbx-2(bx59)*, OK0998 *unc-119(ed3); cuIs34 [Ptbx-2::gfp+unc-119(+)]*, OK1025 *unc-37(e262); cuIs34*, OK1055 *unc-37(e262) I; tbx-2(bx59) III; cuIs31/+ X*.

Germline transformation was performed by biolistic transformation using a PDS-1000/He (Bio-Rad) particle delivery system equipped with a Hepta adapter (Bio-Rad) with modifications suggested by the TransgeneOme project (Sarov et al., 2012) (https://transgeneome.mpi-cbg.de/transgeneomics/manuals.html). NEP plates seeded with *E. coli* NA22 were used to grow larger populations of DP38 worms for transformation (Merritt and Seydoux, 2010).

4.3.2 Genotyping *tbx-2* mutants

To generate rescue strains in the *tbx-2(ok529)* background, individual animals were PCR genotyped for the *tbx-2(ok529)* allele as previously described (Roy Chowdhuri et al., 2006). *tbx-2(ok529)* homozygotes were distinguished from heterozygotes by progeny tests in which rescued hermaphrodites were crossed into N2 males, and 100% of male progeny possessed the *ok529* allele. To generate the synthetic lethal *unc-37(e262); tbx-2(bx59)* strain, individual animals were PCR genotyped for *tbx-2(bx59)* allele as previously described (Huber et al., 2013).

4.3.3 General methods for nucleic acid manipulations and plasmid construction

Standard methods were used to manipulate plasmid DNAs and oligonucleotides (Ausubel, 1990), and all sequences are available from the authors.

Plasmid pOK291.03, which contains *Ptbx-2::gfp* and *unc-119(+)*, was constructed for biolistic transformation by inserting a 5968 bp SphI-AflII fragment containing *Ptbx-2::gfp* from plasmid pOK206.33 (Milton et al., 2013) into the SphI-AflII digested pSV41 vector containing *unc-119(+)* (Spencer et al., 2011).

Plasmid pOK222.11 for expressing TBX-2$^{FDV->ADA}$ in yeast two-hybrid assays was constructed by site-directed mutagenesis of the wild-type TBX-2 bait plasmid pOK187.01 (Roy Chowdhuri et al., 2006) with oligos PO796 (CCCAAAAAGGGAGGTGCTGATGCTCTCGATTTGTTGTCAAAG) and PO797 (CTTTGACAACAAATCGAGAGCATCAGCACCTCCCTTTTTGGG) using the Stratagene QuikChange II Kit, and plasmids were sequenced to verify the presence of the mutation.

4.3.4 Fosmid handling and recombineering

The *tbx-2::gfp* containing fosmid was obtained from M. Sarov, and DNA was isolated as described (Sarov et al., 2012). The *tbx-2::TY1::EGFP::3xFLAG* region was sequenced using

primers PO1403 (GCAAATGGCAACACTCTTC), PO1404 (CCATCTAATTCAACAAGAATTGGG), PO1405 (ACGGGAACTACAAGACAC), PO1406 (GTTTGTCCGCCATGATGT), and PO1407 (GAGTTTGTAACAGCTGCTGGG).

Two step recombineering was performed to mutate the eh1 motif in this *tbx-2::gfp* fosmid (Dolphin and Hope, 2006; Hirani et al., 2013). For the positive-selection recombineering step, MW005 *E. coli* (a gift from C. Dolphin, Addgene #24545) containing this fosmid were transformed by electroporation with the RT cassette fragment amplified from the plasmid pNH034 (a gift from C. Dolphin, Addgene #42150) using primers PO1415 (CTGAAGTGAAGAAAGAGCAAAAGTCAGTGACACCACCCAAAAAGGGAGGTTCGCTGTCGAGATATGACGGTG) and PO1416 (ACTTCATCCAGCGGGTCCTGATTGGTATGCACTTCAGGCTTTGACAACAAGATGATAAGCTGTCAAACATGAG), which produce an RT cassette fragment with 50 bp of *tbx-2* flanking the sequence encoding the eh1 motif. For the negative-selection recombineering step, a small fragment containing the mutated eh1 motif was prepared by annealing and end-filling oligos PO1417 (CTGAAGTGAAGAAAGAGCAAAAGTCAGTGACACCACCCAAAAAGGGAGGTGCTGATGCTCTCGAT) and PO1418 (ACTTCATCCAGCGGGTCCTGATTGGTATGCACTTCAGGCTTTGACAACAAATCGAGAGCATCAGC), and this was transformed by electroporation into MW005 competent *E. coli* cells containing the *tbx-2* fosmid with RT cassette insertion. 7/8 colonies selected were confirmed to have the eh1 motif mutation by sequencing with PO1403, and this fosmid was named pOK313.07.

4.3.5 Yeast two-hybrid assays

The yeast two-hybrid screen that identified the *unc-37* prey plasmid was described previously (Roy Chowdhuri et al., 2006). Yeast two-hybrid assays were carried out in L40 yeast containing *HIS3* and *lacZ* reporters regulated by LexA binding sites with the *unc-37* prey plasmid pOK195.18 in the pACT vector and *tbx-2* bait plasmids pOK187.01 (wild-type *tbx-2*) or pOK222.11 (*tbx-2*$^{FDV->ADA}$) in the pLexA-NLS vector (Roy Chowdhuri et al., 2006). These experiments were performed by co-author Sinchita Roy Chowdhuri.

4.3.6 RNAi experiments

Feeding RNAi was performed as previously described using *E. coli* expressing genomic fragments of *ubc-9* (clone F29B9.6, location IV-2K06) or *smo-1* (clone K12C11.2, location I-1O13) in L4440, or *E. coli* HT115(DE3) transformed with the *unc-37* plasmid pOK247.03 at 20˚C (Kamath et al., 2001; Miller and Okkema, 2011). To assess the effect of *unc-37* knockdown on *Ptbx-2::gfp* expression, L4 OK0998 *unc-119(ed3); cuIs34 [Ptbx-2::gfp+unc-119(+)]* worms were plated to *unc-37(RNAi)* plates, and L4 and young adult progeny were examined after 72-96 hours for ectopic GFP expression. To assess the effect of *unc-37* knockdown on *ceh-22::gfp* expression, L4 OK0507 *cuIs21[ceh-22::gfp]* worms were pre-fed for 24 hours on *unc-37(RNAi)* plates, shifted to new *unc-37(RNAi)* plates, and arrested progeny were examined by DIC and fluorescence microscopy.

4.3.7 Microscopy

Worms were visualized using Zeiss Axioskop and AxioImager microscopes equipped for DIC and fluorescence microscopy. Images were captured using Zeiss Axiocam MRm or QImaging Rolera em-c^2 cameras using Zeiss Zen software. To count *ceh-22::gfp* positive nuclei,

Z-series images were collected. Maximum intensity Z projections were produced using Fiji/ImageJ (Schindelin et al., 2012).

4.4 Results

4.4.1 TBX-2 interacts with UNC-37/Groucho via a conserved eh1 motif

We carried out a yeast two-hybrid screen of a *C. elegans* cDNA library using full-length TBX-2 as bait and identified the Groucho-family protein UNC-37 as a candidate TBX-2 interacting factor (Roy Chowdhuri et al., 2006). The cDNA identified in this screen encoded a large C-terminal fragment of the UNC-37 protein (residues 20-612) fused in-frame to the GAL4 activation domain. This region includes the entire WD domain, which mediates Groucho-family factor interactions with transcription factors (Pflugrad et al., 1997). The interaction detected in yeast was specific, as the *unc-37* prey did not interact with the empty bait plasmid.

UNC-37 interacts with eh1 motifs in the homeodomain factors UNC-4 and UNC-30 and the T-box factor MLS-1 (Miller and Okkema, 2011; Peden et al., 2007; Winnier et al., 1999). We found a slightly diverged eh1 motif near the TBX-2 C-terminus (Figure 18), which differs from the consensus by having an aspartate rather than serine or threonine at residue 2 (Yaklichkin et al., 2007). While charged residues at this position are predicted to have a negative influence on Groucho-family factor binding (Dalafave, 2009), UNC-37 interacts well with the UNC-30 eh1 motif, which contains an arginine in this position (Peden et al., 2007), suggesting UNC-37 can interact with divergent motifs.

The TBX-2 eh1 motif mediates interaction with UNC-37 in yeast two-hybrid assays. Mutating two consensus residues in the TBX-2 eh1 motif (Figure 18B) eliminated interaction of the TBX-2 bait with the UNC-37 prey (this finding was contributed by co-author Tanya Crum).

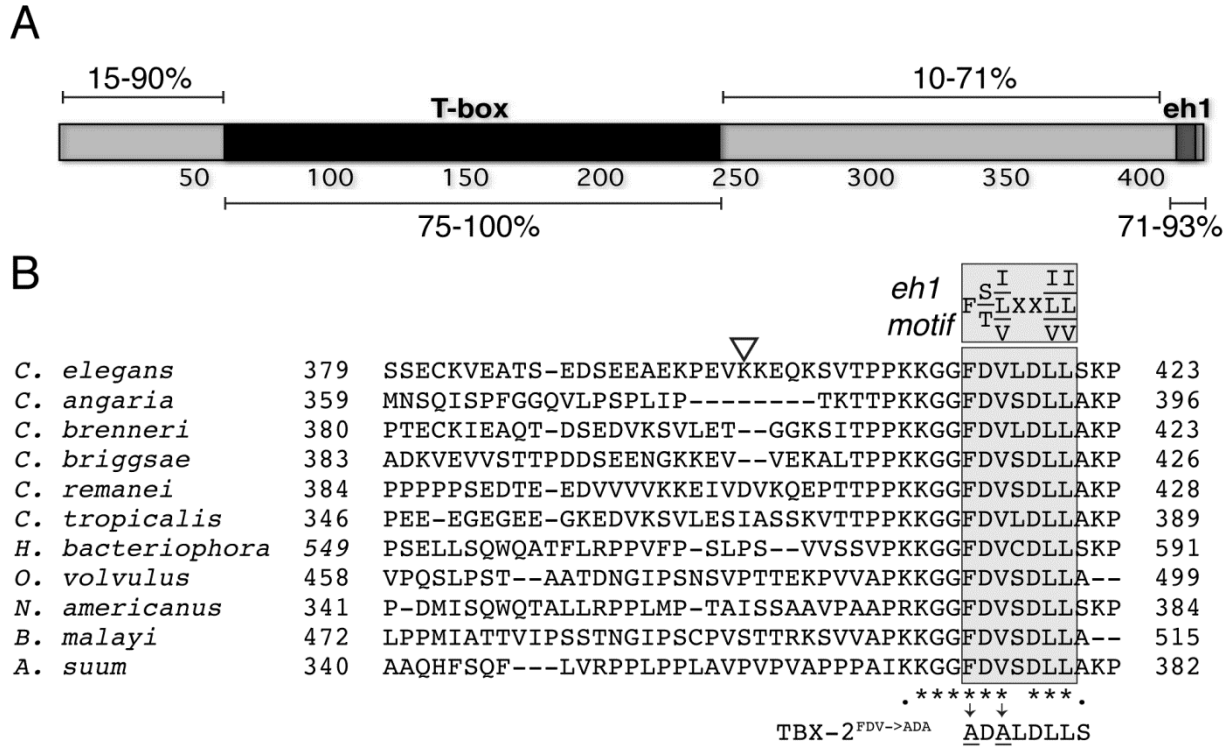

Figure 18. An eh1 motif in *C. elegans* TBX-2 is conserved in other nematode species.

A) Schematic diagram of TBX-2 protein (Wormbase ID WP:CE01245) indicating the positions of the T-box DNA-binding domain and the eh1-like motif. The percent sequence identity between nematode TBX-2 orthologs in different regions is indicated. B) ClustalW multiple sequence alignment of the C-terminus of TBX-2 from various nematode species including *C. elegans*, *C. angaria* (Wormbase ID CA:Cang_2012_03_13_00255.g7972.t1), *C. brenneri* (Wormbase ID CN:CN29328), *C. briggsae* (WormBase ID BP:CBP05056), *C. remanei* (WormBase ID RP:RP21057), *C. tropicalis* (Wormbase ID CT:Csp11.Scaffold629.g12511.t1), *H. bacteriophora* (Wormbase ID HB:Hba_14542), *O. volvulus* (Wormbase ID OV:OVP04186), *N. americanus* (Wormbase ID NA:NECAME_13239), *B. malayi* (Wormbase ID BM:BM26493), *A. suum* (Wormbase ID AS:GS_22659). The position of the eh1 motif is shaded grey with a consensus indicated above. Asterisks indicate identical residues, and periods indicate similar residues. The sequence in TBX-2$^{FDV->ADA}$ with mutated residues underlined is below. The SUMOylated lysine (K400) in *C. elegans* TBX-2 sequence is indicated (unfilled arrowhead).

In contrast, this mutation did not affect the interaction between TBX-2 and the E2 SUMO conjugating enzyme UBC-9, which binds a site near the eh1 motif (Huber et al., 2013), indicating that the mutant TBX-2 is expressed in yeast. A similar mutation in MLS-1 eliminates interaction with UNC-37 (Miller and Okkema, 2011), and in subsequent experiments we refer to this mutation as TBX-2$^{FDV->ADA}$.

The TBX-2 C-terminus including the eh1 motif is highly conserved among many of its nematode orthologs, while other regions outside the T-box DNA-binding domain are less well conserved (Figure 18). This conservation strongly suggests that the eh1 motif is important for TBX-2 function *in vivo*.

4.4.2 Knockdown of *unc-37* phenocopies *tbx-2* mutants

If interaction with UNC-37 is necessary for TBX-2 function, we expect that knocking down *unc-37* activity will produce phenotypes similar to those observed in *tbx-2* mutants. *unc-37(RNAi)* animals have been previously shown to exhibit highly penetrant embryonic lethality (Miller and Okkema, 2011; Simmer et al., 2003), but the arrest phenotype has not been characterized. We found these arrested *unc-37(RNAi)* animals exhibited defects in hypodermal enclosure and were incompletely elongated (Figure 19). Differentiated gut and pharyngeal cells were visible, but the amount of pharyngeal tissue appeared reduced compared to wild-type animals.

tbx-2 null mutants arrest as L1 larvae with a reduced number of pharyngeal muscle nuclei resulting from a loss of those derived from the ABa lineage (Roy Chowdhuri et al., 2006). To count the number of pharyngeal muscles in *unc-37(RNAi)* animals, we examined expression of a chromosomally integrated *ceh-22::gfp* reporter *cuIs21*, which is specifically expressed in pharyngeal muscles (Okkema and Fire, 1994; Roy Chowdhuri et al., 2006). The *ceh-22* gene is

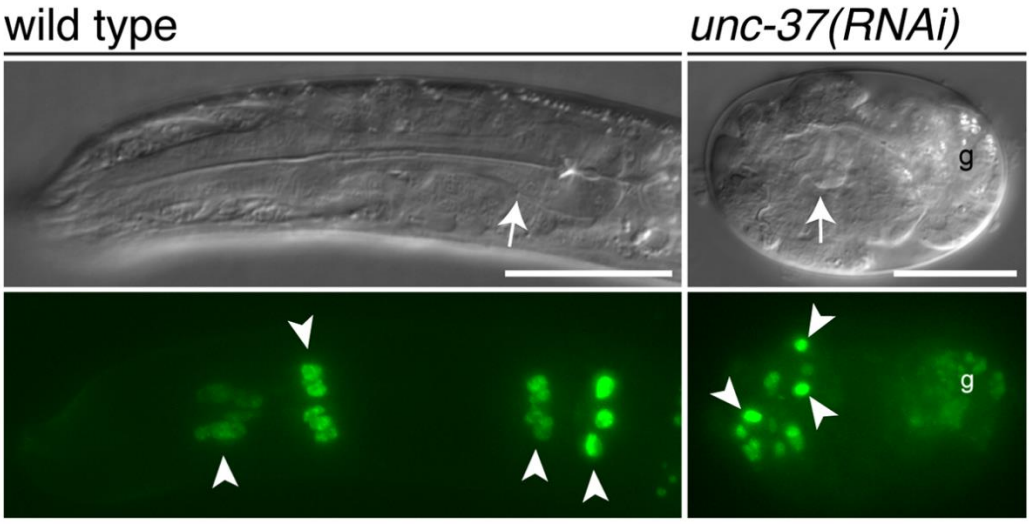

Figure 19. *unc-37* is required for a subset of pharyngeal muscles

DIC (top) and fluorescence (bottom) images of a wild-type L1 and a terminally arrested *unc-37(RNAi)* embryo of the same developmental age expressing *ceh-22::gfp*. Arrowheads indicate representative *ceh-22::gfp*-expressing pharyngeal muscle nuclei. The basement membrane surrounding the pharynx is indicated in both DIC images (arrow), and autofluorescent gut granules (g) are marked in *unc-37(RNAi)*. These fluorescence images are maximal intensity projections of representative z-series that were used to count pharyngeal muscle nuclei expressing *ceh-22::gfp*. The scale bar size is 20 microns.

expressed in 21 pharyngeal muscles, of which 7 are derived from the ABa lineage, and 14 are derived from the MS lineage (Okkema and Fire, 1994; Sulston et al., 1983). Wild-type late stage embryos and L1 larvae contained an average of 18.3 ± 1.7 *ceh-22::gfp* expressing nuclei (Figure 19; n=42 animals). This is slightly less than the total number of *ceh-22* expressing pharyngeal muscles due to somewhat mosaic expression of this reporter, and it is similar to the number of *ceh-22::gfp* expressing cells previously observed in wild-type animals (Roy Chowdhuri et al., 2006). In comparison, the number of *ceh-22::gfp* positive nuclei was significantly reduced to 13.2 ± 1.9 in terminally arrested *unc-37(RNAi)* embryos and L1s of the same developmental age as the wild-type animals (Figure 19; n=40 animals) ($p<0.0001$). This number is very similar to the number of MS-derived muscles observed previously in *tbx-2(RNAi)* animals (Roy Chowdhuri et al., 2006). We conclude that like TBX-2, UNC-37 is required for development of a subset of pharyngeal muscles, although UNC-37 has additional functions required for embryonic elongation.

We next examined expression of a *tbx-2::gfp* promoter fusion in animals with reduced UNC-37 activity. TBX-2 directly represses its own expression in a negative autoregulatory loop, and *Ptbx-2::gfp* exhibits derepressed expression in *tbx-2* mutants in the hypodermis, seam cells, and gut in L4 and adult animals (Milton and Okkema, 2015). We observed a similar pattern of derepressed expression of the *Ptbx-2::gfp* transgene *cuIs34* in both *unc-37(e262)* hypomorphs and in partially affected *unc-37(RNAi)* animals that escaped embryonic arrest and progressed through larval development (Figure 20; Table V). We note that gut expression was less frequent and often in fewer cells than expression in the seam cells, and that derepressed expression in both tissues was more frequent in *unc-37(e262)* mutants than in *unc-37(RNAi)* animals, suggesting that the *unc-37(RNAi)* animals that escape embryonic lethality retain more UNC-37

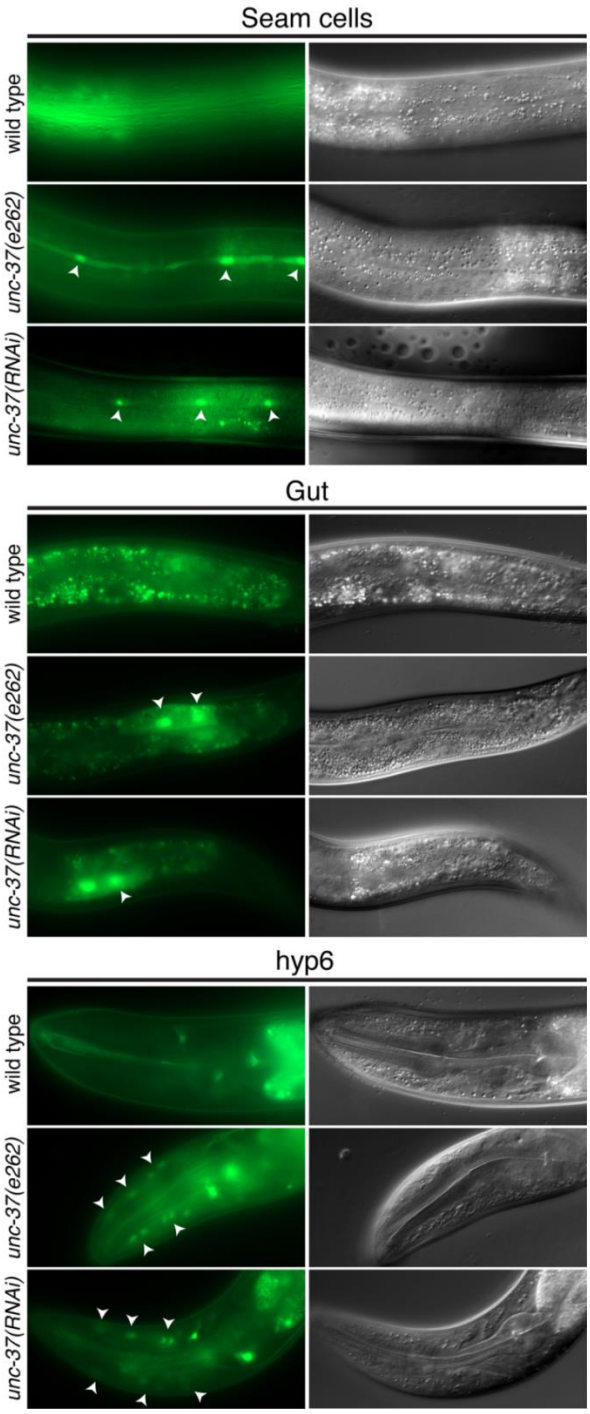

Figure 20. The *tbx-2* promoter is derepressed in *unc-37* mutants

Fluorescence and DIC images of L4 to young adult animals of the indicated genotypes expressing *Ptbx-2::gfp*. Ectopic expression is indicated by arrowheads in seam, gut, and hyp6 hypodermal cell nuclei in *unc-37(e262)* and *unc-37(RNAi)* mutants. Autofluorescent granules are visible in the gut cell cytoplasm in wild-type animals, but no nuclear localized GFP fluorescence is present.

TABLE V: *unc-37* NEGATIVELY REGULATES *tbx-2* EXPRESSION.

Genotype [a]	% animals expressing GFP in seam cells	% animals expressing GFP in gut	% animals expressing GFP in Hyp6	n
+/+	8	2	3	106
unc-37(e262)	80	47	42	135
unc-37(RNAi) [b]	26	12	31	58

[a] All animals were also homozygous for the chromosomally integrated *Ptbx-2::gfp* transgene *cuIs34*.

[b] For feeding RNAi, L4 stage animals grown at 20°C were transferred to plates with *E. coli* expressing *unc-37* dsRNA, and F1 progeny reaching the L4 stage were scored for ectopic *Ptbx-2::gfp* expression.

activity than the hypomorphic *unc-37(e262)* mutants. We also observed derepressed *Ptbx-2::gfp* expression in the head syncytial hypodermal cell hyp6 in *unc-37(e262)* and *unc-37(RNAi)* animals, and this had only been described in *tbx-2* mutants at the L1 stage (Milton and Okkema, 2015). These results demonstrate UNC-37 activity is necessary for repression of the *Ptbx-2::gfp* reporter, and the similar tissue distribution of this derepressed expression is consistent with our hypothesis that TBX-2 function depends on interaction with UNC-37.

4.4.3 Reduced *unc-37* enhances lethality of the *tbx-2(bx59)* hypomorph

We have previously used the hypomorphic mutant *tbx-2(bx59)* as a sensitized genetic background to ask if mutations in other genes affect TBX-2 activity *in vivo* (Huber et al., 2013; Milton et al., 2013). To test if UNC-37 affects TBX-2 activity, we compared the phenotype of the *tbx-2(bx59)* and *unc-37(e262)* single mutants to that of *unc-37(e262); tbx-2(bx59)* double mutants.

Most *tbx-2(bx59)* and *unc-37(e262)* single mutants hatched at the non-permissive temperature for *tbx-2(bx59)* (25˚C) (Table VI). *unc-37(e262)* mutants exhibit movement defects, but they grew well, and the majority of the hatched animals reached adulthood. *tbx-2(bx59)* mutants exhibited partially penetrant L1 arrest and slow larval growth phenotypes, but significant numbers of these animals did reach adulthood (Table VI) (Huber et al., 2013; Milton et al., 2013). In contrast, *unc-37(e262); tbx-2(bx59)* double mutants exhibited a strongly enhanced, synthetic lethal phenotype. Most of these animals arrested as embryos, and all the remaining animals that hatched arrested shortly after hatching at the L1 stage (Table VI).

We examined the pharynx in newly hatched animals and found that *unc-37(e262): tbx-2(bx59)* double mutants exhibited much more severe pharyngeal defects than either single mutant

TABLE VI: *unc-37(e262); tbx-2(bx59)* MUTANTS EXHIBIT SYNTHETIC LETHALITY

Genotype	% Embryonic arrest	% Adults	n
+/+	7	88	82
tbx-2(bx59)	10	14	106
unc-37(e262)	23	56	102
unc-37(e262); tbx-2(bx59)	73	0	113

L4 animals raised at 16°C were shifted to the non-permissive temperature, 25°C, and F1 progeny were scored for embryonic arrest after 12 hours and adulthood after 2.5 days.

(Figure 21; Table VII). Most *tbx-2(bx59)* mutants have anterior pharyngeal muscles but exhibit morphological defects in the pharynx which include a short, thick pharyngeal isthmus, while relatively few animals exhibited the severe loss of anterior muscles observed in *tbx-2(ok529)* null mutants. *unc-37(e262)* mutants generally had a wild-type pharynx, with a few animals exhibiting mild morphological defects similar to those of *tbx-2(bx59)*. In comparison, hatched *unc-37(e262); tbx-2(bx59)* exhibited strong and completely penetrant loss of the anterior pharynx resembling the phenotype of *tbx-2(ok529)* null mutants.

We next examined the number of pharyngeal muscles in these animals using the chromosomally integrated *ceh-22::gfp* reporter *cuIs31*. Wild-type L1 larvae contained 21.3 ± 0.9 nuclei expressing this *ceh-22::gfp* (Figure 22; n=17 animals), while terminally arrested *unc-37(e262); tbx-2(bx59)* embryos and larvae contained only 13.4 ± 1.9 GFP expressing nuclei (Figure 22; n=14 animal) ($p<10^{-10}$).

Together these results indicate that partially reducing both *tbx-2* and *unc-37* leads to synthetic lethality and a synergistic increase in the severity of pharyngeal defects, and they indicate that TBX-2 function depends on UNC-37 activity *in vivo*. Moreover, the fact that the number of *ceh-22::gfp* expressing nuclei in *unc-37(e262); tbx-2(bx59)* double mutants was nearly identical to what we observed in *unc-37(RNAi)* animals (compare Figures 19 and 22), strongly suggests that TBX-2 and UNC-37 are each required for the same set of ABa-derived pharyngeal muscles.

4.4.4 TBX-2 function in pharyngeal development depends on the eh1 motif

The severity of pharyngeal defects differs between various *tbx-2* mutants. *tbx-2(ok529)* null mutants lack the anterior pharyngeal muscles derived from the ABa lineage and arrest as

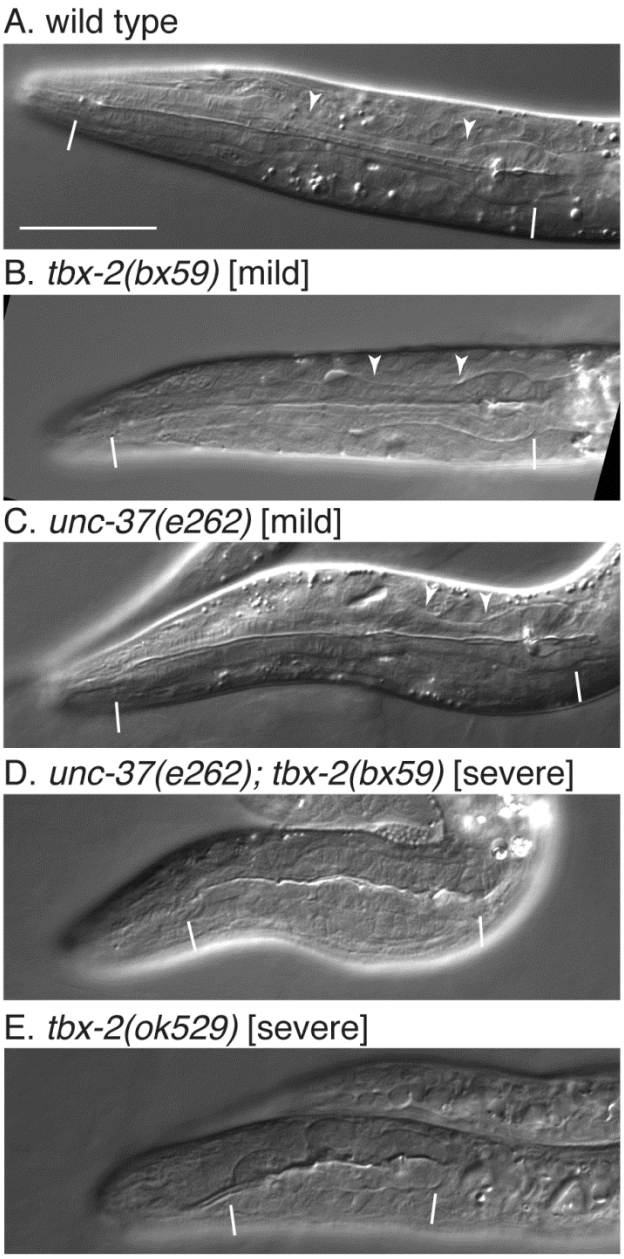

Figure 21. Pharyngeal defects in *tbx-2* and *unc-37* mutants

DIC images of the pharynx in L1 stage larvae of the indicated genotype grown at non-permissive temperature. A) Wild type. B, C) *tbx-2(bx59)* and *unc-37(e262)* mutants exhibiting mild pharyngeal morphological defects. D, E) *unc-37(e262); tbx-2(bx59)* double mutant and *tbx-2(ok529)* single mutant exhibiting severe pharyngeal defects. The length of the pharynx (A-E) and the pharyngeal isthmus (A-C) are indicated with lines and arrowheads, respectively.

TABLE VII: *unc-37(e262); tbx-2(bx59)* MUTANTS EXHIBIT SEVERE PHARYNGEAL DEFECTS

Genotype	% wild type pharynx	% mild Tbx-2 pharynx [a]	% severe Tbx-2 pharynx [b]	n
+/+	100	0	0	38
tbx-2(bx59)	10	80	10	40
unc-37(e262)	80	18	2	44
unc-37(e262); tbx-2(bx59)	0	0	100	42

L4 animals raised at 16°C were shifted to the non-permissive temperature, 25°C, and hatched F1 progeny were subsequently scored at L1 stage for severity of pharyngeal defects.

[a] Animals exhibiting a mild Tbx-2 phenotype had a complete pharynx extending to the anterior tip of the head but had an abnormally short and thick isthmus.

[b] Animals exhibiting a severe Tbx-2 phenotype had a clear decrease in the amount of anterior pharyngeal tissue and more extensive morphological defects in the pharynx.

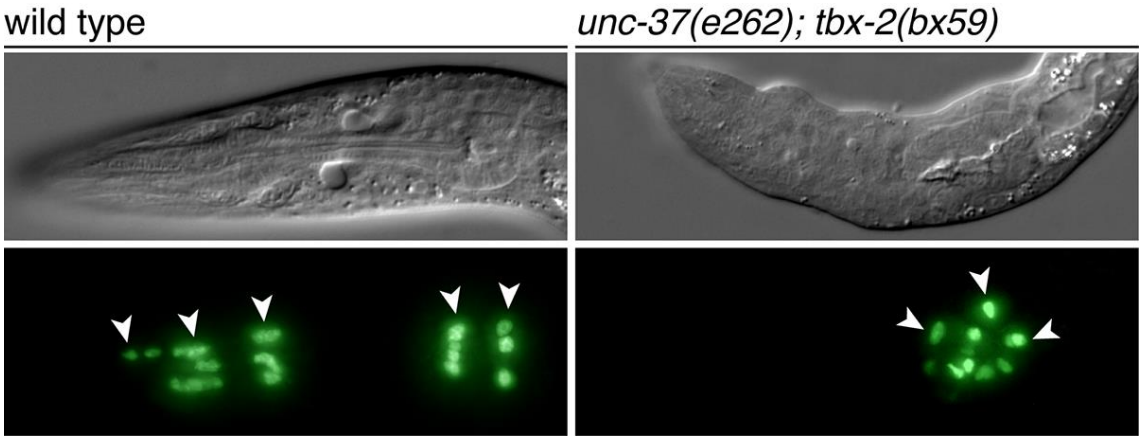

Figure 22. *unc-37(e262); tbx-2(bx59)* mutants lack anterior pharyngeal muscles

DIC (top) and fluorescence (bottom) images of L1 stage worms of the indicated genotypes expressing *ceh-22::gfp*. Arrowheads indicate *ceh-22::gfp*-expressing pharyngeal muscle nuclei. These fluorescence images are maximal intensity projections of representative z-series that were used to count pharyngeal muscle nuclei expressing *ceh-22::gfp*.

newly hatched L1 larvae (Figure 21E) (Roy Chowdhuri et al., 2006). In contrast, *tbx-2(bx59)* hypomorphs contain a complete pharynx, but they exhibit pharyngeal defects that include a wider and shorter pharyngeal isthmus than wild-type animals (Figure 21B) (Huber et al., 2013; Milton et al., 2013). We and others have previously been unable to rescue these mutants with a variety of genomic DNA or cDNA clones. However, we have now found that *tbx-2(ok529)* can be rescued by transgenes containing a *tbx-2::gfp* translational fusion in the fosmid WRM063aG09. WRM063aG09 contains ~36 kb of genomic DNA roughly centered on *tbx-2* (http://www.wormbase.org/species/c_elegans/clone/WRM063aG09#02--10). This fosmid was modified by the TransgeneOme Project with a *gfp* marker fused in frame at the 3' end of *tbx-2* (Sarov et al., 2012) (clone # 9347172996193398 G10, transgeneome.mpi-cbg.de/transgeneomics/public/clone.html?wellId=32604125). Two independent extrachromosomal transgenes *cuEx809* and *cuEx810* containing this modified WRM063aG09 fosmid were generated by microparticle bombardment and were crossed into *tbx-2(ok529)*. We were able to propagate viable *tbx-2(ok529)* homozygous strains rescued with each of these transgenes. We note that both of these strains also segregate a significant number of arrested embryos, a phenotype that has not been observed in *tbx-2(ok529)* mutants (Roy Chowdhuri et al., 2006; Smith and Mango, 2007). Extrachromosomal transgenes generally contain numerous copies of the transforming DNA (Praitis et al., 2001), and we suggest that this embryonic lethality may result from *tbx-2* over-expression.

To test if UNC-37/Groucho interaction affects TBX-2 function *in vivo*, we used recombineering to introduce the *tbx-2*$^{FDV->ADA}$ mutation affecting the eh1 motif into this *tbx-2::gfp* fosmid (Dolphin and Hope, 2006; Hirani et al., 2013), and we generated one extrachromosomal transgene *cuEx814* containing *tbx-2*$^{FDV->ADA}$*::gfp*. We note that the *cuEx814*

tbx-2$^{FDV->ADA}$*::gfp* transgene was more difficult to isolate than the transgenes containing wild-type *tbx-2::gfp*, and homozygous *tbx-2(ok529)* bearing *cuEx814* were underrepresented in our crosses. Despite these difficulties, we were able to isolate and propagate a viable *tbx-2(ok529); cuEx814* strain. This strain segregates arrested embryos similar to the *tbx-2(ok529)* strains rescued with wild-type *tbx-2::gfp*, but it also segregates arrested larvae and grows very slowly.

Both wild-type *tbx-2::gfp* and *tbx-2*$^{FDV->ADA}$*::gfp* transgenes restored production of the anterior pharyngeal muscles of *tbx-2(ok529)*. However, animals rescued with *tbx-2*$^{FDV->ADA}$*::gfp* exhibited frequent L1 arrest and abnormal pharyngeal morphologies characteristic of hypomorphic *tbx-2* mutants (Figure 23: Table VIII). While approximately 95% of *tbx-2(ok529)* - animals rescued with wild-type *tbx-2::gfp* had a normal pharyngeal morphology, only 29% of animals rescued with *tbx-2*$^{FDV->ADA}$*::gfp* had normal pharyngeal morphology (Table VIII). To more precisely evaluate the pharyngeal phenotype of these animals, we compared the dimensions of the isthmuses of L1 animals rescued with these transgenes with those of wild-type and *tbx-2(bx59)* L1s (Table IX). Newly hatched *tbx-2(ok529)* animals rescued with *tbx-2*$^{FDV->ADA}$*::gfp* had significantly wider and shorter pharyngeal isthmuses than wild-type animals, while *tbx-2(ok529)* mutants rescued with wild-type *tbx-2::gfp* were much more similar to wild-type. Strikingly, the animals rescued with *tbx-2*$^{FDV->ADA}$*::gfp* appeared nearly identical to *tbx-2(bx59)* (Table 22; compare Figures 21B and 23C). Both wild-type TBX-2::GFP and TBX-2$^{FDV->ADA}$ are expressed at similar levels in all strains (Figure 23), and we suggest the *tbx-2*$^{FDV->ADA}$ mutation causes a partial loss of TBX-2 activity.

Together, these results strongly suggest that interaction with UNC-37/Groucho is necessary for full TBX-2 function in the pharynx. We note that many of the L1 animals rescued with *tbx-2*$^{FDV->ADA}$ arrested shortly after hatching despite having a complete pharynx, suggesting

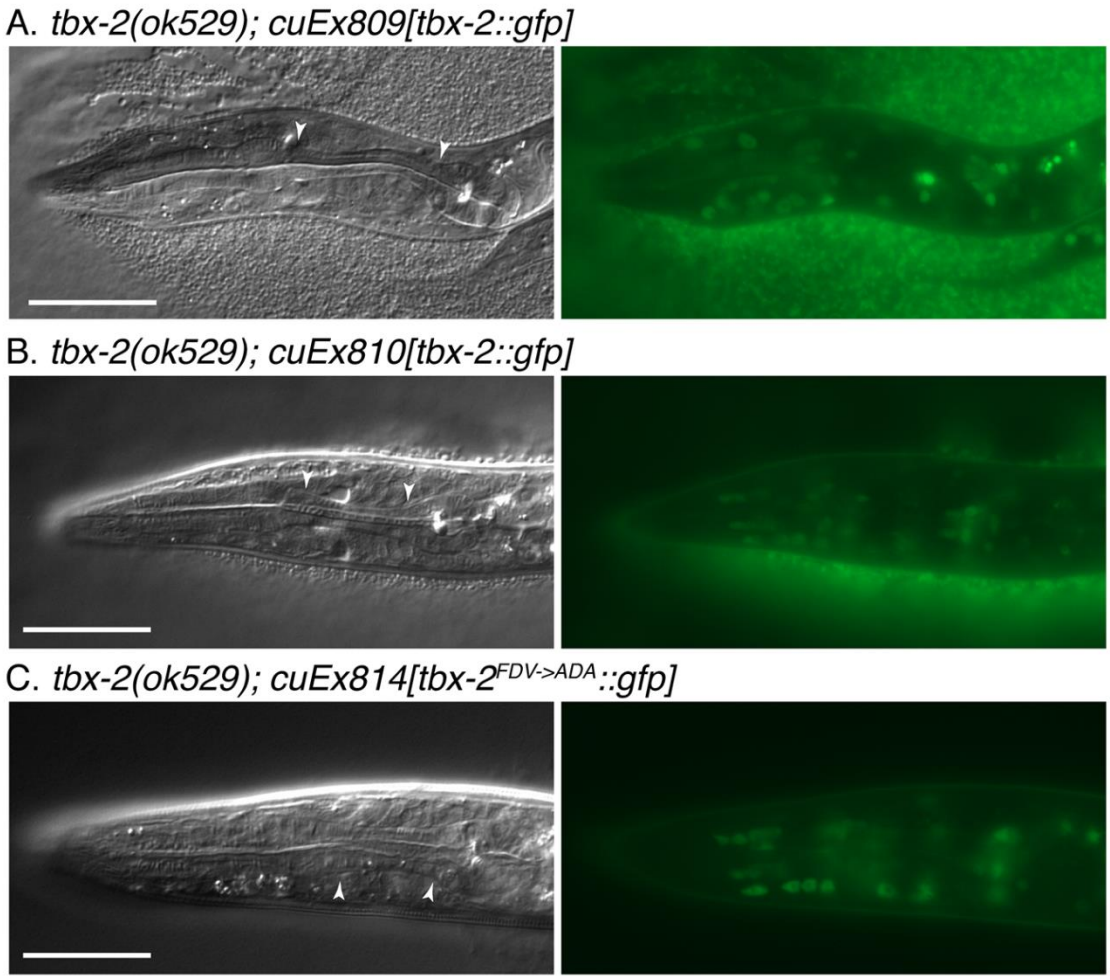

Figure 23. Pharyngeal morphology of *tbx-2(ok529)* mutants rescued with *tbx-2* fosmid transgenes

DIC (left) and GFP fluorescence (right) images of *tbx-2(ok529)* homozygotes expressing the indicated rescue constructs. The length of the pharyngeal isthmus is indicated with arrowheads. Fluorescence images were captured using identical microscope set up and exposure times, and the levels of TBX-2::GFP fluorescence are very similar.

TABLE VIII: PHARYNGEAL MORPHOLOGY OF L1 ANIMALS RESCUED WITH WILD-TYPE *tbx-2::gfp* AND *tbx-2*$^{FDV->ADA}$ FOSMID TRANSGENES

Genotype	% wild type pharynx	% mild Tbx-2 pharynx [a]	% severe Tbx-2 pharynx [b]	n
+/+	100	0	0	36
tbx-2(ok529); cuEx809[tbx-2::gfp]	95	5	0	42
tbx-2(ok529); cuEx810[tbx-2::gfp]	94	6	0	47
tbx-2(ok529); cuEx814[tbx-2$^{FDV->ADA}$*::gfp]*	29	71	0	35

[a] Animals exhibiting a mild Tbx-2 phenotype had a complete pharynx extending to the anterior tip of the head but had an abnormally short and thick isthmus.

[b] Animals exhibiting a severe Tbx-2 phenotype had a clear decrease in the amount of anterior pharyngeal tissue and more extensive morphological defects in the pharynx.

TABLE IX: COMPARISON OF ISTHMUS WIDTH AND LENGTH IN *tbx-2* MUTANTS AND RESCUED STRAINS

Genotype	isthmus width (µm)	isthmus length (µm)	n
+/+	3.8 ± 0.5	23.2 ± 1.5	11
tbx-2(bx59)	4.7 ± 0.7**	15.0 ± 3.2***	23
tbx-2(ok529); cuEx809[tbx-2::gfp]	3.9 ± 0.4	23.4 ± 1.0	21
tbx-2(ok529); cuEx810[tbx-2::gfp]	4.2 ± 0.6	21.2 ± 2.1*	11
tbx-2(ok529); c*uEx814[tbx-2$^{FDV->ADA}$::gfp]*	5.1 ± 0.6***	15.8 ± 3.4***	26

Significance of differences from wild-type (+/+) animals was estimated using a two-tailed Student's t-test.
* denotes significantly different from wild-type animals ($p < 0.05$)
** denotes significantly different from wild-type animals ($p < 0.001$)
*** denotes significantly different from wild-type animals ($p < 1x10^{-6}$).

that *tbx-2* and *unc-37* have additional essential roles beyond specifying ABa-derived pharyngeal muscles.

4.4.5 SUMO pathway enzymes and UNC-37 regulate *tbx-2* in a tissue-specific manner

We previously reported that TBX-2 function in ABa-derived pharyngeal development relies on SUMO-dependent mechanisms (Huber et al., 2013; Roy Chowdhuri et al., 2006), although exactly how SUMOylation affects TBX-2 activity remains to be elucidated. TBX-2 can be SUMOylated at K(400), just near its eh1 motif (Figure 18B), and we hypothesize that SUMOylation of TBX-2 may promote interaction with UNC-37. TBX-2 and SUMO pathway components, SMO-1 and UBC-9, repress *Ptbx-2::gfp* expression in seam, gut, and hyp6 hypodermal nuclei in late larval and early adult stages (Milton and Okkema, 2015), and we observed similar ectopic expression patterns in *unc-37* loss of function animals (Figure 20). To ask if reduction of *unc-37* and SUMOylation leads to a synergistic derepression of *Ptbx-2::gfp* in the same tissues, we compared *Ptbx-2::gfp* in *unc-37(262), smo-1(RNAi),* and *ubc-9(RNAi)* single mutants to *unc-37(e262);smo-1(RNAi)* and *unc-37(e262);ubc-9(RNAi)* double mutants and found that double mutants expressed *tbx-2::gfp* in seam cells, gut, and hyp6 nuclei in a slightly more than additive number than the single mutants combined, except for in seam cells, which was observed in a large majority of the *unc-37(e262)* single mutants (Figure 24, Table X). Double mutants also exhibited increased expression in hyp7 hypodermal nuclei, which we rarely observed in *smo-1, ubc-9,* or *unc-37* single mutants (Table X), but *Ptbx-2::gfp* expression was not expanded to any other tissues. These results suggest that UNC-37 and SUMO pathway enzymes, SMO-1 and UBC-9, likely do not function in independent pathways to repress *tbx-2*.

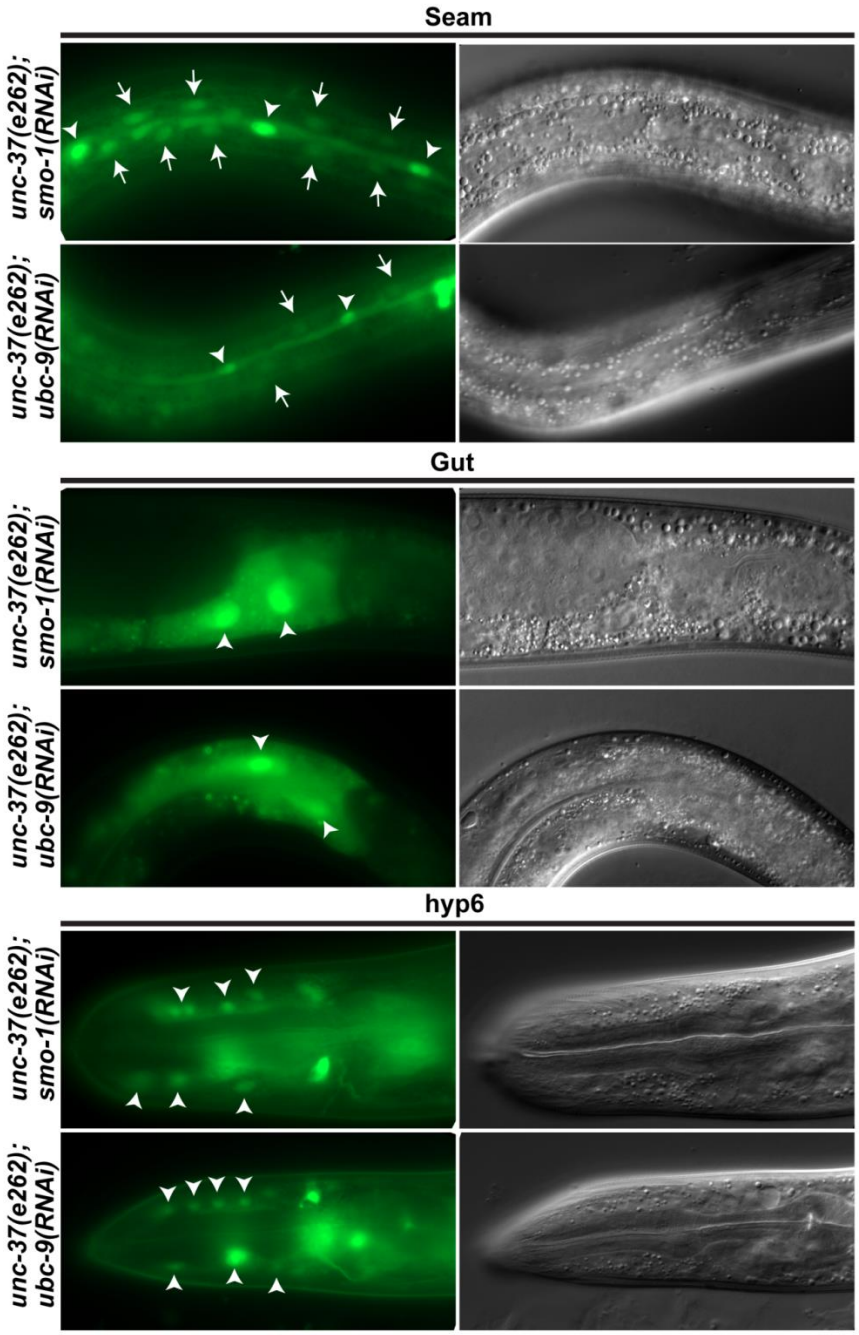

Figure 24. SUMO pathway enzymes and UNC-37 regulate *tbx-2* in a tissue-specific manner

Fluorescence (left) and DIC (right) images of L4 to young adult animals of the indicated genotypes expressing *Ptbx-2::gfp*. Ectopic expression is indicated by arrowheads in seam, gut, and hyp6 hypodermal cell nuclei, and by arrows in hyp7 hypodermal cell nuclei. Autofluorescent granules are visible in the gut cell cytoplasm in wild-type animals, but no nuclear localized GFP fluorescence is present.

TABLE X: *unc-37* AND SUMO PATHWAY COMPONENTS NEGATIVELY REGULATE *tbx-2* EXPRESSION.

Genotype [a]	% animals expressing GFP in seam cells	% animals expressing GFP in gut	% animals expressing GFP in Hyp6	% animals expressing GFP in Hyp7	n
+/+	8	2	3	0	106
unc-37(e262)	80	47	42	1.5	135
smo-1(RNAi) [b]	17	2	13	1	94
unc-37(e262); smo-1(RNAi)	82	60	80	48	71
ubc-9(RNAi)	24	21	0	0	103
unc-37(e262); ubc-9(RNAi)	67	74	68	5.5	91

[a] All animals were also homozygous for the chromosomally integrated *Ptbx-2::gfp* transgene *cuIs34*.

[b] For all RNAi feeding experiments, L4 stage animals grown at 20°C were transferred to plates with *E. coli* expressing *smo-1* or *ubc-9* dsRNA, and F1 progeny reaching the L4 stage were scored for ectopic *Ptbx-2::gfp* expression.

4.5 Discussion

Here we show that *C. elegans* TBX-2 interacts with the Groucho-family corepressor UNC-37 through a conserved eh1 motif located near the TBX-2 C-terminus. This interaction is essential for normal TBX-2 function, as the *tbx-2*$^{FDV->ADA}$ mutation disrupts interaction with UNC-37 and reduces the ability of the WRM063aG09 *tbx-2::gfp* fosmid transgene to fully rescue the *tbx-2(ok529)* null mutant. *tbx-2* and *unc-37* loss-of-function results in very similar phenotypes, including a loss of anterior pharyngeal muscles and derepression of the *tbx-2* promoter, consistent with TBX-2 and UNC-37 sharing common functions. Moreover, reducing *unc-37* activity strongly enhanced the lethality and pharyngeal defects of the *tbx-2(bx59)* hypomorphic mutant so that they resemble *tbx-2* null mutants. Taken together, these results indicate that TBX-2 activity *in vivo* depends on UNC-37 and that TBX-2 functions as a Groucho-dependent transcriptional repressor. Finally, SUMOylation may be a mechanism to promote TBX-2 interaction with UNC-37, as reduction of SUMO pathway components and UNC-37 leads to derepression of *tbx-2* in the same tissues.

4.5.1 Transgene rescue of *tbx-2* null mutants

Transgenes containing the WRM063aG09 *tbx-2::gfp* fosmid are the first to completely rescue pharyngeal defects and lethality of the null mutant *tbx-2(ok529)*. In contrast, previous rescue attempts with smaller *tbx-2(+)* transgenes failed to rescue lethality, although partial rescue of neuronal and pharyngeal defects were reported (Miyahara et al., 2004; Roy Chowdhuri et al., 2006; Singhvi et al., 2008; Smith and Mango, 2007). We suggest WRM063aG09 contains distal regulatory elements necessary for full *tbx-2* expression that were lacking in other transgenes. Consistent with this, the GFP expression pattern from this transgene is both

temporally and spatially more widespread than previously observed with shorter *tbx-2::gfp* reporters (Roy Chowdhuri et al., 2006; Smith and Mango, 2007).

While the WRM063aG09 *tbx-2::gfp* transgenes do rescue *tbx-2(ok529)* lethality and pharyngeal defects, these strains also segregate a significant number of arrested embryos. This lethality could result from *tbx-2* overexpression, as extrachromosomal transgenes typically contain high copy number of the transforming DNA. Phenotypic characterization and transcript profiling of these arrested embryos might reveal the basis of this embryonic arrest.

4.5.2 *tbx-2* function *in vivo* depends on *unc-37*

We present two lines of genetic evidence that *tbx-2* function *in vivo* depends on *unc-37*. First, we found that reducing either *tbx-2* or *unc-37* results in very similar phenotypes. Partial loss results in ectopic expression of the direct TBX-2 target *Ptbx-2::gfp* in seam cells and the gut, while a more severe reduction leads to lethality and a loss of *tbx-2* anterior pharyngeal muscles. Second, we observed a strong genetic interaction between *tbx-2* and *unc-37* hypomorphic mutants. *unc-37(e262); tbx-2(bx59)* double mutants exhibit an enhanced, synthetic lethal phenotype, which produces a pharyngeal phenotype nearly identical to that of *tbx-2* null mutants. Importantly, *unc-37(e262); tbx-2(bx59)* double mutants retain the same number of pharyngeal muscles as strongly affected *tbx-2* mutants or *unc-37(RNAi)* animals. Together, these results indicate that *tbx-2* and *unc-37* are both required for development of the pharyngeal muscles induced in the ABa lineage and suggest these genes are required for the same function (Herman and Yochem, 2005). We note also that *unc-37(e262); tbx-2(bx59)* exhibit an embryonic lethal phenotype that is not observed in *tbx-2* null mutants, indicating that the synthetic lethality of these double mutants does not simply result from a complete loss of *tbx-2* function. While we do not know the basis for this embryonic lethality, it suggests *tbx-2* may

have additional embryonic functions that are redundant with those of other UNC-37 interacting transcription factors.

tbx-2(bx59) and *unc-37(e262)* are hypomorphic mutations encoding single amino acid substitutions in key protein interaction domains, but it is unlikely that they affect specific interaction between these factors. *tbx-2(bx59)* is a histidine to tyrosine mutation in the so-called "dimerization domain" of the T-box (Huber et al., 2013), while *unc-37(e262)* is a histidine to tyrosine mutation of a conserved residue in WD repeat 5 of the ß propeller domain (Pflugrad et al., 1997). *unc-37(e262)* has previously been shown to interact genetically with mutations in a variety of transcription factor genes, including the homeobox gene *unc-4* and the mediator complex genes *sop-1, sop-3,* and *sur-2* (Winnier et al., 1999; Zhang and Emmons, 2002). These observations are consistent with the previous hypothesis that *unc-37(e262)* results in a general conformational disruption in the ß propeller rather than defective interaction with specific transcription factors (Jennings et al., 2006).

We have previously shown that *tbx-2(bx59)* lethality is also enhanced by reducing SUMOylation or the NF-Y transcription factor (Huber et al., 2013; Milton et al., 2013). Knockdown of the NF-Y B subunit gene *nfyb-1* in *tbx-2(bx59)* resulted in L1 arrest, but the pharyngeal defects in these animals were not enhanced and resembled the morphological defects observed in *tbx-2(bx59)* single mutants. In contrast, *tbx-2(bx59)* mutants knocked down for either *smo-1* encoding SUMO or *ubc-9* encoding the SUMO E2-conjugating enzyme produced embryonic lethality and severe pharyngeal defects identical to those observed in *unc-37(e262); tbx-2(bx59)* animals. We suggest that SUMOylation and UNC-37 have similar, direct effects on TBX-2 function, while reducing NF-Y has a different and perhaps less direct effect on TBX-2.

4.5.3 UNC-37 interaction is necessary for full TBX-2 activity

Our data indicates that TBX-2 function depends on interaction with UNC-37. Mutating the eh1 motif near the TBX-2 C-terminus eliminated interaction with UNC-37 in yeast two-hybrid assays and disrupted the ability to fully rescue *tbx-2(ok529)* mutants. While these mutants rescued with *tbx-2*$^{FDV->ADA}$ produced anterior pharyngeal muscles and were viable, they exhibited morphological defects in the pharynx resembling those of *tbx-2(bx59)* or partially affected *tbx-2(RNAi)* animals, and most of these animals arrested as larvae. This partial rescue phenotype may indicate TBX-2$^{FDV->ADA}$ still retains sufficient interaction with UNC-37 to specify ABa-derived muscles. Alternatively, TBX-2 may have both UNC-37 dependent and independent functions, which would be differently affected by eh1 motif mutation. In many cases, Groucho interaction converts a transcriptional activator to a repressor (Turki-Judeh and Courey, 2012), and this conversion has recently been shown for the mouse T-box factor Tbx20 (Kaltenbrun et al., 2013). Perhaps *C. elegans* TBX-2 activates some genes to specify anterior pharyngeal fate, but functions with UNC-37 to repress other genes necessary for normal pharyngeal morphology and larval growth.

eh1 motifs are found in many T-box factors, and several other *C. elegans* T-box factors contain potential eh1 motifs, including MLS-1, MAB-9, TBX-7, SEA-1, and TBX-34 (Copley, 2005). Both MLS-1 and MAB-9 interact with UNC-37, and this interaction is essential for MLS-1 function *in vivo* (Jafari et al., 2011; Miller and Okkema, 2011). Likewise, eh1 motifs are present in a variety of mammalian T-box factors, including the TBX2 and TBX3 orthologs of *C. elegans* TBX-2 (Copley, 2005). While these mammalian factors have not been shown to interact with Groucho-family corepressors, the mouse TBX2 eh1 motif is located within a potent repression domain located near the C-terminus (Paxton et al., 2002), and the human TBX3 eh1

motif is located in a peptide that can function as a repression domain in combination with other transcription factors (He et al., 1999). As *TBX2* and *TBX3* are overexpressed in several aggressive human cancers, we suggest that compounds targeting their interaction with Groucho-like corepressors could be explored as novel cancer therapies.

4.5.4 UNC-37 binds TBX-2 near a SUMOylation site

TBX-2 function in pharyngeal development depends on SUMOylation, and we have mapped two sites in TBX-2 that can be SUMOylated (Huber et al., 2013). One of these sites (VKKE) is located near the C-terminus just upstream of the TBX-2 eh1 motif (Figure 18B), and we suggest SUMOylation can affect UNC-37 interaction with TBX-2. While SUMOylation has been shown to both promote and inhibit transcription factor interaction with Groucho-family proteins (Lee et al., 2012; Sung et al., 2005), our genetic results indicate that SUMOylation and Groucho interaction promote TBX-2 repressor activity, and we suggest that SUMO conjugation helps to initiate or stabilize interaction with UNC-37. SUMOylation of Xenopus SoxE promotes recruitment of the Groucho-family Grg4 (Lee et al., 2012). SoxE lacks a functional eh1 interaction motif and SUMO protein is believed to provide a structural interface that allows a multi-valent mechanism for Groucho to specifically interact with SUMOylated SoxE. Perhaps binding of UNC-37 to the diverged eh1 motif in *C. elegans* TBX-2 is similarly stabilized by SUMOylation.

SUMOylation often promotes formation of protein complexes, and in some cases SUMOylation of multiple proteins within a complex can facilitate their interaction [reviewed in (Chymkowitch et al., 2015)]. Xenopus Groucho is SUMOylated at multiple sites, and SUMOylation enhances its corepressor activity (Ahn et al., 2009). Similarly, the yeast Groucho ortholog Tup1 has recently been shown to be SUMOylated, and although mutation of its SUMO

sites does not affect initial recruitment to target promoters, it does affect its ability to remain on the promoters, suggesting SUMO stabilizes the corepressor complex (Ng et al., 2015). Interestingly, Tup1 interaction partners histone H3, Cti6, Gcn5, Gal11, and Cyc8 also become SUMOylated under similar conditions as Tup1, and SUMO may generally hold together transcriptional repressor complexes in the same manner that SUMO protein functions to hold together DNA repair systems and PML nuclear bodies (Psakhye and Jentsch, 2012; Shen et al., 2006). In *C. elegans*, SUMOylation of multiple components of the dosage compensation complex is also required for complex assembly, but it is not required for initial targeting of the this complex to the X chromosome (Pferdehirt and Meyer, 2013). Our evidence that UNC-37 and SUMO pathway components regulate *tbx-2* in a similar manner to TBX-2 is consistent with the notion that SUMO binding may hold together TBX-2 and the Groucho-like homolog UNC-37 in a repressor complex to regulate target genes. As a growing number of T-box factors are known to be affiliated with SUMO and Groucho (Andreou et al., 2007; Beketaev et al., 2014; Farin et al., 2007; Huber et al., 2013; Kaltenbrun et al., 2013; Miller and Okkema, 2011; Roy Chowdhuri et al., 2006), we propose this as a novel mechanism of T-box factor activity.

5 GENERAL DISCUSSION OF TBX-2, SUMO, and GROUCHO

The focus of my project in the Okkema laboratory has been to extend the knowledge of how TBX-2 protein functions in *C. elegans* pharyngeal development by examining the effect of SUMOylation and interaction with the Groucho-like corepressor UNC-37 on TBX-2 activity. Over-expression of human TBX2 has been observed in numerous cancers (Mahlamaki et al., 2002; Sinclair et al., 2002; Vance et al., 2005; Wanslebena et al., 2014), while haplo-insuffiency of the related Tbx2 subfamily members *TBX3*, *TBX4*, and *TBX5* underlie Ulnar-mammary, Small patella, and Holt-Oram syndromes, respectively (Bamshad et al., 1997; Basson et al., 1997; Bongers et al., 2004; Li et al., 1997), indicating that proper modulation of T-box protein activity is necessary throughout development. Understanding how TBX-2 functions in the highly cellular diversified pharynx of *C. elegans* has offered us a glimpse of how the human Tbx2 subfamily may be regulated post-translationally, and it is my hope that it will one day lead to the development of novel therapies for the diseases and cancers associated with misregulation of their activity. In this work, I have presented a multitude of data indicating that both SUMOylation and interaction with UNC-37 promote TBX-2 function, and here I will discuss likely models by which they may affect TBX-2 activity, experiments to be performed in the future which could corroborate these models, as well as implications for the regulation of mammalian Tbx2 subfamily members.

5.1 Does SUMOylation affect TBX-2 interaction with Groucho?

I provided biochemical evidence showing that TBX-2, as well as its mammalian counterparts TBX2 and Tbx3, can be SUMOylated in COS-1 cells, and that two SUMO consensus sites in *C. elegans* TBX-2, LKIE and VKKE, mediate SUMOylation (Huber et al., 2013). Although genetic evidence strongly suggests that TBX-2 function depends on

SUMOylation, we still do not fully understand how the covalent attachment of SUMO moieties affects TBX-2 protein (Huber et al., 2013; Roy Chowdhuri et al., 2006). In COS-1 cells, I performed luciferase transcriptional assays, protein turnover assays, cellular localization assays, and, *in vivo*, rescue assays, and in these experiments neither the SUMOylation-defective TBX-$2^{LKIE/VKKE->AAAA}$ or TBX-2^{K400R} mutants displayed significant differential activity compared to the wild type protein (Huber et al., 2013). Since the discovery of the first SUMO-modified protein, RanGAP1, nearly two decades ago (Matunis et al., 1996), the mechanism of SUMO conjugation and its targets have been studied heavily, and surmounting evidence argues that SUMO plays a large role in transcriptional repression, particularly in the recruitment of repressor complex components and chromatin-modifying enzymes (Garcia-Dominguez and Reyes, 2009). At the end of the discussion in the previous chapter, I briefly touched on the possibility that SUMO may function to recruit or stabilize TBX-2 in a repressive complex with the Groucho corepressor UNC-37, and multiple lines of evidence are consistent with this model. Like *tbx-2* nulls, worms completely lacking the SUMO-conjugating enzyme *ubc-9* or *unc-37* both lack ABa-derived pharyngeal muscles (Roy Chowdhuri et al., 2006). Furthermore, combining the partial loss of function allele *tbx-2(bx59)* with a partial loss of *ubc-9* or *unc-37* leads to an enhanced *tbx-2* null-like phenotype, suggesting they may be functioning in the same pathway as *tbx-2* to regulate downstream target genes (Huber et al., 2013). Indeed, TBX-2, SUMO, and UNC-37 similarly regulate the downstream target gene *tbx-2*, as a reduction of any of their activity leads to de-repression of a *tbx-2:gfp* reporter in seam, gut, and hypodermis cells (Milton and Okkema, 2015). Because TBX-2 directly interacts with UNC-37 in yeast two-hybrid assays and can be SUMOylated in COS-cells, the physical interaction of TBX-2, SUMO, and UNC-37

in a repressor complex seems to be a plausible explanation for how they can similarly repress the target gene *tbx-2* (Figure 25A) (Huber et al., 2013).

In addition to mapping the SUMOylation sites in TBX-2, the site required for interaction with UNC-37, FDVLDLL, was also mapped, and interestingly, this eh1-like motif resides just 12 amino acids from the VKKE SUMO site at the C-terminus (Figure 25B), which raises the question, how could conjugation of SUMO protein affect the way TBX-2 interacts with UNC-37? Sometimes, SUMO blocks interaction with Groucho. For example, the SUMO target homeodomain-interacting protein kinase 2, HIPK2, which is a part of the homeodomain protein NK-3 repressor complex and interacts directly with Groucho in this context, does not bind to GST-Groucho in GST pull-down assays when HIPK2 is modified to be constitutively SUMOylated (Choi et al., 1999; Sung et al., 2005). Conversely, SUMOylation of SoxE family transcription factors is absolutely necessary to provide an interface which facilitates interaction with Grg4, the Xenopus Groucho ortholog, as SoxE factors do not possess a functional eh1 domain and SUMO-deficient mutants are unable to interact with Grg4 in Co-IP experiments (Lee et al., 2012). Because SUMO and UNC-37 exhibit a similar promotion of TBX-2 function in ABa-derived pharyngeal muscle development, it seems unlikely that SUMO inhibits interaction with UNC-37, but rather enhances TBX-2 and UNC-37 interaction. If this is true, I would expect that in-frame fusion of the *smo-1* gene to the 3' end of *tbx-2* (producing a constitutively SUMOylated TBX-2) in the *tbx-2*$^{FDV->ADA}$*::gfp* fosmid, which only partially rescues *tbx-2(ok529)*, would allow this mutant to more proficiently interact with UNC-37 and thereby fully rescue pharyngeal defects. The approach of comparing activity of a constitutively SUMOylated target to its non-SUMOylatable mutant allows for a clear distinction of how SUMO alters protein

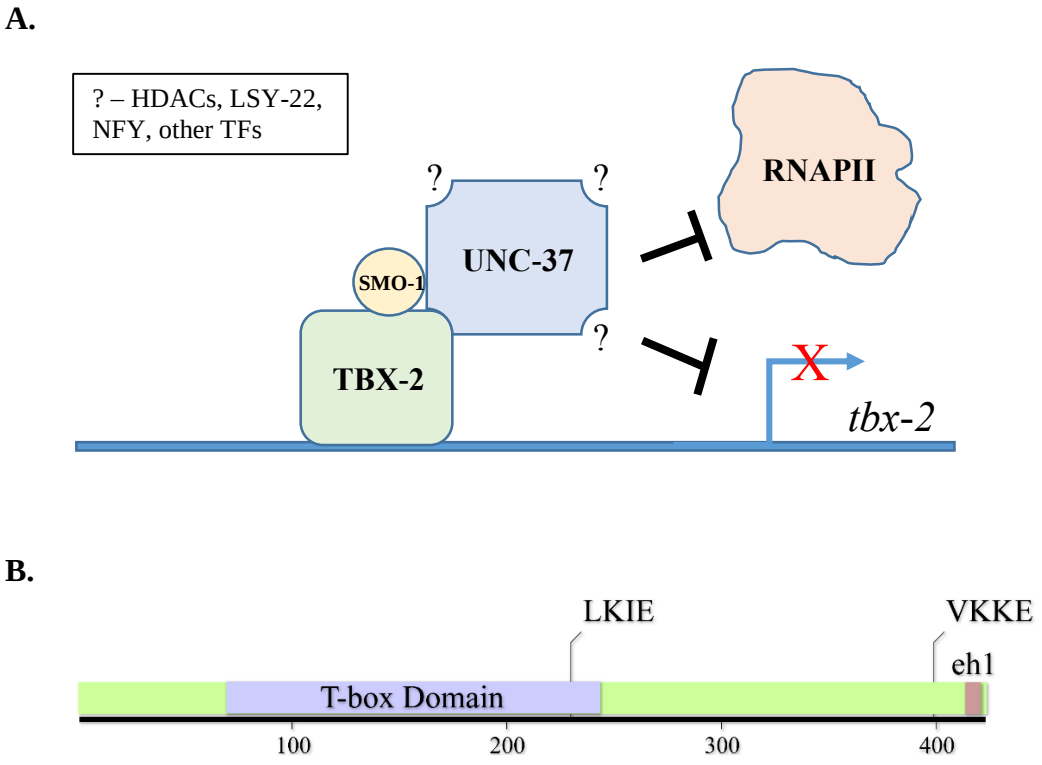

Figure 25. Model for interaction of TBX-2, SUMO, and Groucho at target promoter

A) Model of hypothesized protein-protein interactions at TBX-2 target promoter, *tbx-2*. In this model, SUMOylated TBX-2 is bound to DNA, and then recruits UNC-37 (likely also SUMOylated, although that is not represented here) or stabilizes interaction between TBX-2 and UNC-37. SUMO may also promote interaction with other repressor complex components, such as histone deacetylases (HDACs), short Groucho-like proteins (LSY-22), nuclear transcription factor Y (NFY) repressor complex subunits, or other unknown transcription factors and chromatin-modifying enzymes, leading to increased repression by inhibition of RNA polymerase II occupancy at target promoters. B) Schematic of full length TBX-2 peptide with the location of the two SUMO consensus sites, LKIE and VKKE, noted. LKIE resides near the C-terminal end of the DNA binding domain and VKKE resides near the C-terminal of TBX-2 just 12 amino acids upstream of the eh1-like motif, FDVLDLL, which facilitates interaction with the Groucho corepressor, UNC-37.

activity, and although the mutation in *tbx-2*$^{FDV->ADA}$*::gfp* does not inhibit TBX-2 SUMOylation [based on a positive yeast two-hybrid interaction of TBX-2$^{FDV->ADA}$ with UBC-9 (Roy Chowdhuri et al., 2006)], the ratio of SUMOylated TBX-2 to non-SUMOylated TBX-2 is likely to be very low in *C. elegans* [even when TBX-2 was over-expressed with human SUMO-1 in COS-1 cells, only about 10% of purified TBX-2 protein was modified by SUMO-1 (Huber et al., 2013)], so if SUMO does enhance TBX-2 interaction with UNC-37, and TBX-2 does depend on interaction with UNC-37 *in vivo*, we should see a difference when comparing the ability of *tbx-2*$^{FDV->ADA}$*::smo-1::gfp* or *tbx-2*$^{FDV->ADA}$*::gfp* to rescue *tbx-2(ok529).*

Although the SUMOylation-defective *tbx-2*^{K400R}*::gfp* fosmid rescued *tbx-2(ok529)* better than the *tbx-2*$^{FDV->ADA}$*::gfp* mutant, a small percentage of animals still exhibited weak pharyngeal defects, suggesting both mutant rescue strains lack full TBX-2 activity. Based on the model that TBX-2, SUMO, and UNC-37 function in a repressive complex together, I would expect that transcript profiling of these two rescue lines via RNA-seq would reveal a subset of genes overexpressed in both of the *tbx-2*^{K400R}*::gfp* and *tbx-2*$^{FDV->ADA}$*::gfp* mutant-rescue lines. These genes might be good candidates for direct TBX-2 targets (besides *tbx-2*), and this information could be useful in ChIP assays to further define how SUMO and UNC-37 affect the regulatory network of TBX-2.

One of the most well characterized examples of a SUMO-dependent complex is that of PML nuclear bodies (NBs) [reviewed in (Cheng and Kao, 2013)]. The presence of a SUMO interaction motif (SIM) and SUMO-conjugation sites in the PML protein contribute to PML NB formation, as this assembly is mediated by the combination of non-covalent interactions between SUMOylated substrates as well as SUMOylation of PML (and many of the other NB components) (Ishov et al., 1999; Seeler and Dejean, 2003; Shen et al., 2006; Zhong et al., 2000).

Recent studies in yeast showed that, in a SUMO-dependent Groucho co-repressor complex, many of the individual components become SUMOylated, including the yeast Groucho ortholog TUP1 (Ng et al., 2015), and I propose that the coordinated SUMOylation of both TBX-2 and UNC-37 (and potentially other proteins involved in this repressive complex) likely contributes to ABa-derived pharyngeal muscle development. We have shown that TBX-2 can be SUMOylated (Huber et al., 2013), and an analysis of the TBX-2 protein using GPS-SUMO [an updated version of SUMOsp which predicts SUMO sites and SUMO interaction motifs (SIMs) by comparison of an input peptide sequence with nearly a thousand known SUMOylation sites and just over 150 SIMs (Zhao et al., 2014)] reveals it possesses a putative SIM, VLDLL, and surprisingly, it resides within the eh1 motif. Although we haven't asked experimentally if UNC-37 is SUMOylated, it has been demonstrated that Groucho can be SUMOylated, and furthermore, Groucho depends on SUMOylation for its co-repressor activity and recruitment of HDACs to the promoter region of repressed genes (Ahn et al., 2009; Nie et al., 2009).

Perhaps SUMOylation of UNC-37 can provide an additional interface with which it can interact with TBX-2, such that when UNC-37 is SUMOylated, it can potentially interact with the C-terminus of TBX-2 via a SUMO-conjugated moiety, or its ß propeller domain, thereby enhancing its ability to interact with TBX-2 and repress target genes. Such a possibility could explain why *tbx-2*$^{FDV->ADA}$*::gfp* is able to partially rescue *tbx-2* nulls, and can be tested in mammalian cell culture assays by expressing recombinant TBX-2 and UNC-37 (containing the proper tags to permit Co-IP), performing native pulldowns of TBX-2, followed by subsequent probing of purified lysates for UNC-37. One could then introduce a mutation within the ß propeller domain of UNC-37 which would abrogate interaction with TBX-2, such as the missense mutation in the *unc-37(e262)* allele, which causes a histidine to tyrosine conversion at a

conserved residue in WD repeat 5 of the ß propeller domain (Pflugrad et al., 1997). I would expect then, that if SUMOylation of UNC-37 does provide an alternative interaction interface, fusion of SMO-1 to the N-terminus of UNC-37 should restore interaction with TBX-2.

In *C. elegans*, repression of target genes by UNC-37 depends on interaction of its N-terminal coiled-coil Q domain with a nearly identical Q domain in the N-terminus of the short Groucho-like protein LSY-22 (Flowers et al., 2010). Analysis of the LSY-22 and UNC-37 proteins (and Groucho orthologs from other species) using GPS-SUMO indicates that both proteins possess a high scoring SUMO consensus site (IKKE in LSY-22 and IKDE in UNC-37) at a similar position within their coiled-coil domains, which is a type of structure known to both permit SUMOylation and be functionally involved in Groucho tetramerization (Pinto and Lobe, 1996; Saul et al., 2015; Zhao et al., 2014). Interestingly, LSY-22 peptide sequence analysis reveals it also contains a high scoring SIM in this domain, and although SUMOylation has not been investigated as a mechanism mediating UNC-37 and LSY-22 interaction, SUMOylation of Groucho has been shown to lead to the recruitment of HDAC1 through a SIM (Ahn et al., 2009), and perhaps SUMOylation of UNC-37 similarly promotes oligomerization with LSY-22 through its N-terminal SIM. Because UNC-37 absolutely depends on interaction with LSY-22 for its ability to repress multiple target genes, this would be an intriguing possibility to explore via a combination of Co-IP, SUMOylation, and luciferase transcriptional assays, as corroboration of such a model could indicate SUMOylation as a novel mechanism for Groucho oligomerization (Flowers et al., 2010).

5.2 Does SUMOylation affect TBX-2 cellular localization?

It is possible that SUMO and Groucho could promote TBX-2 activity independently of each other. Although the non-SUMOylatable mutant TBX-2$^{LKIE/VKKE->AAAA}$ displayed similar

nuclear patterning compared to wild type protein in COS-1 cells, another group has observed cytoplasmic localization of TBX-2::GFP *in vivo* (Smith and Mango, 2007). Perhaps SUMO affects an interaction for TBX-2 which alters its cellular localization. The Tbx2 subfamily member Tbx5 shifts from a nuclear to cytoplasmic distribution and becomes sequestered to actin filaments when interacting with the PDZ-LIM domain protein, LMP4, and it is possible that post-translational modifications, such as SUMOylation, could be factors affecting this interaction (Camarata et al., 2006). Recently, another group showed Tbx5 can be SUMOylated, and although mutations affecting cellular localization did not affect SUMOylation, the authors showed that Tbx5 displayed a "moving" nature of SUMO sites in their assays, such that mutation of one site led to SUMO modification at another, so the localization of a bona fide SUMO-deficient Tbx5 has not yet been examined (Beketaev et al., 2014; Fan et al., 2003). Our lab previously reported preferential mislocalization of a TBX-2::GFP fusion to subnuclear puncta in *ubc-9(RNAi)* animals, suggesting a possible role for SUMOylation in the nuclear partitioning of *C. elegans* TBX-2 protein (Roy Chowdhuri et al., 2006). We now have multiple viable *tbx-2::gfp* fosmid rescued *tbx-2(ok529)* strains, which contain the best functional *tbx-2* transgene to date, and allow us to observe all functional TBX-2 protein *in vivo* because it is fused to GFP. I propose performing *ubc-9(RNAi)* to ask if depletion of SUMOylation affects localization of TBX-2::GFP in these rescue strains. I would also perform *ubc-9(RNAi)* on a *tbx-2::smo-1::gfp* rescue strain to ask if mislocalization was specific to a lack of TBX-2 SUMOylation. These experiments could be the first to show SUMOylation directly affects localization of a Tbx2 subfamily member.

APPENDIX A - TBX-2 and SMO-1 BiFC INTERACTION IS NOT DEPENDENT ON SUMOylation

Introduction

Bimolecular fluorescence complementation (BiFC) is a technique which allows for the identification of protein-protein interactions based on structural complementation of N- and C-terminal fragments of a fluorescent protein [reviewed in (Kerppola, 2008)]. TBX-2 interaction with SMO-1 produces a fluorescent signal in *in vivo* BiFC assays when they are fused to complementing halves of the Venus fluorescent protein (VC and VN) (Figure 26), although it is unclear whether this signal is an indication of SUMOylation of TBX-2 or a non-covalent physical interaction between TBX-2 and SMO-1 (Crum, 2012). The next set of experiments described will address this uncertainty by examining BiFC interaction of TBX-2 with a non-conjugatable mutant of SMO-1.

Results and discussion

Covalent attachment of SUMO occurs via a C-terminal Gly-Gly motif, and deletion of this motif renders SUMO protein non-conjugatable (Xu and Au, 2005). To ask if TBX-2::VC / VN::SMO-1 BiFC signal is dependent on SUMOylation, we created 2 independent transgenic lines carrying TBX-2::VC and VN::SMO-1(ΔGG) [a stop codon was introduced in the SMO-1 construct just before the bases encoding the C-terminal Gly-gly, producing a non-conjugatable VN::SMO-1(ΔGG) mutant]. A 2 hour heat shock was performed at 33°C for 5 transgenic lines expressing either TBX-2::VC/VN::SMO-1 (3 lines) or TBX-2::VC/VN::SMO-1(ΔGG) (2 lines), followed by a 1 hour recovery at 20°C before observing worms on a fluorescent scope

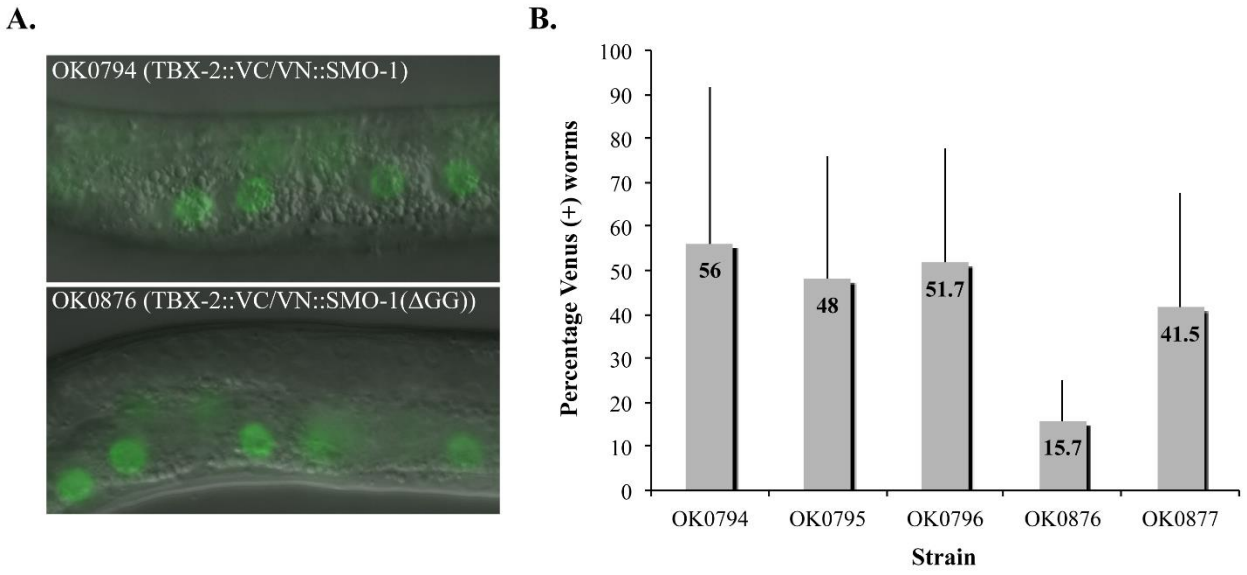

Figure 26. TBX-2 BiFC interaction with SMO-1 is not SUMOylation-dependent

BiFC assay expressing TBX::VC with either VN::SMO-1 or VN::SMO-1(ΔGG) under heat shock promoter. In panel A, compare fluorescence and DIC merged images of Venus expression in gut nuclei of L4 animals for the indicated strains 1 hour after heat shock. Panel B is a bar graph of average percentage of Venus (+) animals for the indicated strains (OK794-796 express TBX-2::VC/VN::SMO-1 and OK876-877 express TBX-2::VC/ VN::SMO-1(ΔGG)).

(Shyu et al., 2008). This duration of heat shock produced a strong GFP signal in nearly all worms for all lines. False positive BiFC interactions can happen as a result of high overexpression of fluorescent protein fragments, and sometimes lower expression levels need to be attained in order to identify specific interactions (Shyu et al., 2008). We found that a shorter heat shock of 30 minutes could permit better comparison from line to line because only approximately half of the animals expressing TBX-2::VC/VN::SMO-1 were GFP(+). Even still, the TBX-2::VC/VN::SMO-1(ΔGG) lines produced BiFC signal similar to that of the 3 strains carrying TBX-2::VC/VN::SMO-1 (Figure 26). This observation suggests that the signal seen in those strains expressing w/t SMO-1 is not indicative of SUMOylation of TBX-2, but rather a non-covalent interaction between SMO-1 and TBX-2. Conversely, the signal may be a result of non-specific interaction due to high levels of overexpression of the TBX-2 and SMO-1 BiFC constructs.

We also performed BiFC assays in COS-1 cells using fusions of TBX-2 and human SUMO-1 [TBX-2 can be SUMOylated by SUMO-1 in COS-1 cells (Huber et al., 2013)] to the C-terminus of cyan fluorescent protein (CC) and the N-terminus of yellow fluorescent protein (YN), respectively (Kerppola, 2006). Recombination of CC and YN due to BiFC interaction produces a green fluorescent signal and indicates a direct interaction between protein fusion partners. We co-transfected TBX-2::CC or non-SUMOylatable TBX-2$^{LKIE/VKKE->AAAA}$::CC, and YN::SUMO-1 or YN::SUMO-1(ΔGG), although transfections of all 4 combinations of wild type or mutant TBX-2 / SMO-1 BiFC constructs produced no specific GFP signal.

Material and Methods

Nematode strain construction

To generate a TBX-2::VC / VN::SMO-1(ΔGG) expressing strain for BiFC in *C. elegans*, we injected N2 young adult hermaphrodites with 2.5 ng/µl pOK266.11 (HA::TBX-2::VC), 2.5 ng/µl pOK286.01 [VN::myc::SMO-1(ΔGG)], and 100 ng/µl pRF4 in 1x injection buffer. The SMO-1(ΔGG) mutation in plasmid pOK286.01 was confirmed by sequencing with primers PO1073 and PO1089 prior to injection. We obtained two independent transgenic lines containing both HA::TBX-2::VC and VN::myc::SMO-1(ΔGG), and these strains were named OK0876 (*cuEx699*) and OK0877 (*cuEx700*).

General methods for nucleic acid manipulations and plasmid construction

BiFC plasmids pUbFC-YN173-SUMO-1(pOK323.08) and pBiFC-JunCC155 (pOK323.09) containing a CMV promoter for expression in mammalian cell culture were gifts from the Kerppola lab. To generate pUbFC-YN173-SUMO-1(ΔGG), pOK323.08 was mutated using the Stratagene QuikChange II Kit with the mutagenesis primer pair PO1067/PO1068 according to manufacturer's instructions. The PCR program used was as follows: step (1) 95°C for 30 seconds, 16 x [(2) 95°C for 30 seconds, (3) 55°C for 1 minute, (4) 68°C for 9 minute]. Sequencing primer PO4 was used to verify only the ΔGG mutation was present (the pUbFC-YN173-SUMO-1(ΔGG) plasmid unfortunately was lost before it could be given a name).

To generate pBiFC-TBX-2::CC155 and pBiFC-TBX-2$^{LKIE/VKKE->AAAA}$::CC155, *tbx-2* cDNA was amplified from pOK241.05 (TBX-2) and pOK241.17 (TBX-2$^{LKIE/VKKE->AAAA}$), respectively, and inserted upstream of, and in frame with CC155 after removal of Jun cDNA from plasmid pOK323.09 by restriction digest. Primers used for amplification were PO1222 (with an MscI linker) and PO1223 (with a KpnI linker). The PCR program used was as follows:

step (1) 94°C for 2 minutes, 5 x [(2) 94°C for 45 seconds, (3) 55°C for 45 seconds, (4) 72°C for 1.5 minutes], 30 x [(5) 94°C for 45 seconds, (6) 65°C for 45 seconds, (7) 72 °C for 1.5 minutes], (8) 72°C for 8 minutes. PCR reactions contained 1 µl DNA template (1/10 dilution of mini-prep in dH_2O), 5 µl 10x PCR buffer, 1.5 µl $MgCl_2$, 0.5 µl 25 mM dNTPs, 1 µl PO1222 (100ng/µl), 1 µl PO1223 (100 ng/µl), 0.5 µl Platinum Taq, and 39.5 µl dH_2O. PCR products and vector pOK323.09 were double digested with MscI and KpnI, and the 1.3 kb PCR insertions were ligated into the resulting 4 kb vector, transformed into dH5α *E. coli*, and plated on 2xTY+Amp (100ng/µl). Single colonies were then picked, grown overnight in selective media, and DNA was isolated from the pelleted culture. DNA was then subjected to restriction digest with MfeI to confirm the ligations were successful (insertion of TBX-2 introduced an additional MfeI site, so successful clones were identified by a 2 band pattern rather than just 1 band). Wild type and mutant TBX-2::CC155 clones were sequenced with primers PO448, PO623, and PO1078 to confirm no point mutations were introduced during insertion amplification (the pBiFC-TBX-2::CC155 and pBiFC-TBX-$2^{LKIE/VKKE->AAAA}$::CC155 plasmids unfortunately were lost before they could be given a name).

Bimolecular fluorescence complementation assays

BiFC assays in *C. elegans* were performed essentially as described (Shyu et al., 2008) with minor modifications. Briefly, 30-40 rolling L4 hermaphrodites of 3 strains carrying HA::TBX-2::VC / VN::myc::SMO-1 [OK0794 (*cuEx638*), OK0795 (*cuEx639*), OK0796 (*cuEx640*)], and 2 strains carrying HA::TBX-2::VC / VN::myc::SMO-1(ΔGG) (OK0876 and OK0877) were picked to small NGM plates with OP50, wrapped in parafilm, and placed (agar side down) in a 33°C water bath for 30 minutes (Crum, 2012). The plates were then removed from the bath and allowed to recover at 20°C for 1 hour. Worms were then scored for (+) or (-)

Venus expression in gut nuclei and images displaying Venus expression for one of each SMO-1 construct were obtained. This assay was performed on three separate occasions and averages with standard deviations of the percentage of Venus (+) animals within each strain over the three trials were determined.

BiFC assays in COS-1 cells were performed essentially as previously described (Kerppola, 2006). Briefly, COS-1 cells were maintained in D-MEM with 10% FBS, 10 mM HEPES, and 1x Antibiotic-Antimycotic (Invitrogen). ~$4x10^5$ cells were seeded into the wells of 2-chamber Lab-Tek chamber slides (Cat.# 177380, Nunc) 24 hours prior to transfection. Wells were transfected with plasmids expressing wild type pBiFC-TBX-2::CC155 or pBiFC-TBX-$2^{LKIE/VKKE->AAAA}$::CC155 (800 ng), and pUbFC-YN173-SUMO-1 (pOK323.08) or pUbFC-YN173-SUMO-1(ΔGG) (800 ng), using Lipofectamine 2000 in OPTI-MEM according to manufacturer's instructions (Invitrogen). For control transfections of single BiFC constructs, 800 ng empty pCDNA vector (pOK237.15) was transfected to keep total DNA concentrations the same. After 24 hours, the media was aspirated and chambers were removed from the slides. 60 µl of COS-1 media was immediately added to each well, and cover slips were placed over each well before visualizing cells using a Zeiss Axioskop microscope equipped for DIC and fluorescence microscopy. Images were captured using an Axiocam MRm camera and AxioVision software.

APPENDIX B - PULLDOWN ANALYSIS OF SMO-1 and TBX-2

Introduction

Consistent with TBX-2 function being SUMO-dependent, our lab has demonstrated that TBX-2 can interact with SUMO conjugating enzymes in yeast and be SUMOylated in mammalian cell cultures (Huber et al., 2013; Roy Chowdhuri et al., 2006). We wanted to ask if TBX-2 can be SUMOylated in *C. elegans*, so we designed an *in vivo* Co-IP experiment to answer this question. The results of this experiment are described here.

Results and discussion

We generated a strain carrying an integrated TBX-2::GFP::FLAG (*wgIs59*) fosmid and an integrated His::FLAG::SMO-1 (*tvEx25*) construct in a *smo-1*(*ok359*) background (so the only functional SMO-1 protein in the worms is His-tagged) to perform a Co-IP experiment in which we pulled down His::FLAG::SMO-1 with Ni-NTA beads under denaturing conditions, and probed western blots of His-purified worm extracts for TBX-2 with antibodies against GFP (Kaminsky et al., 2009). We verified we could pull down His-tagged proteins by detection with anti-FLAG (Figure 27A), but we did not detect TBX-2 in Ni-NTA purified extracts (ability to detect TBX-2 with anti-GFP was verified using crude worm extracts) (Figure 27B). It is estimated that there are at least 250 SUMO targets in *C. elegans* (although TBX-2 was not initially identified as a SUMO target in this proteomics screen, suggesting additional targets exist), and this fact combined with the fact that SUMOylated targets exist in nature in low abundance (including TBX-2), it is likely that our detection methods are not sensitive enough to detect TBX-2 protein in His::SMO-1 purified worm extracts (Huber et al., 2013; Kaminsky et al., 2009).

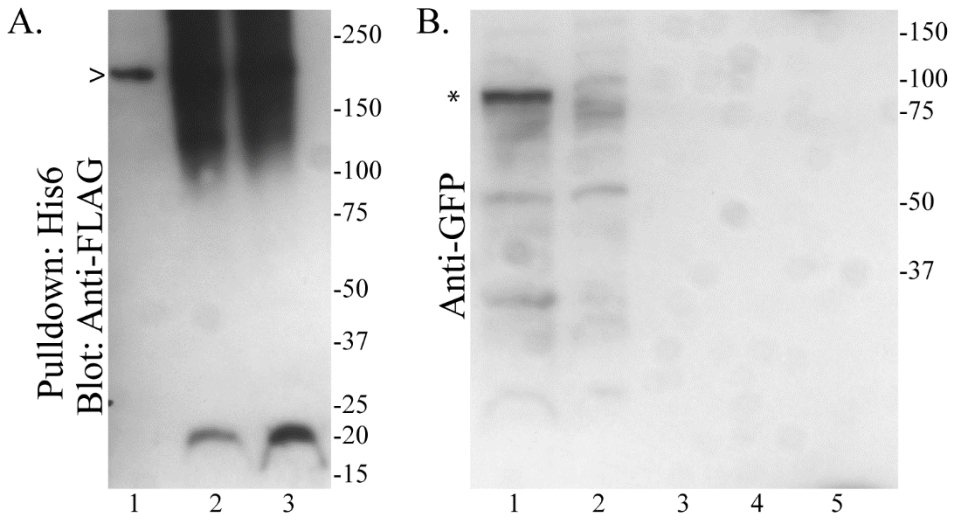

Figure 27. Western blots of purified His-tagged SMO-1 protein

Western blots of Ni-NTA purified worm lysates. The position of molecular weight markers are indicated in kDa (bars). Panel A is a western blot of Ni-NTA purified worm lysates probed with anti-FLAG. In lane 1 the strain is OP159 (TBX-2::GFP::FLAG), and only a cross-reactive band is detected around 200 kDa (indicated by ">"). In lane 2 is NX25 (His::FLAG::SMO-1), lane 3 is OK0874 (TBX-2::GFP::FLAG & His::FLAG::SMO-1), in both lanes SMO-1 (single band around 20 kDa) and a smear of SUMOylated proteins (extending 100-250 kDa) were detected. Panel B is a western blot of crude and Ni-NTA purified worm lysates probed with anti-GFP. In lanes 1 & 2 are crude lysates of OP159 and NX25, respectively, and only in lane 1 is TBX-2 detected (single band around 80 kDa, indicated by asterisk). Lanes 3-5 are Ni-NTA purified worm lysates of OP159, NX25, and OK0874, no protein was detected in any of these lanes.

Materials and Methods

Nematode strain construction

Strains NX25 [*smo-1(ok359)*; *tvEx25* (psmo-1:His::FLAG::SMO-1); *rol-6*] and OP159 [*wgIs159* (tbx-2::TY1::EGFP::3xFLAG+unc-119)] were gifts from the Limor Broday and Valerie Reinke labs, respectively, and were used to generate OK0874 [*smo-1(ok359)*; *tvEx25*; *wgIs159*; *rol-6*]. Briefly, *wgIs159/wgIs159* males were crossed into NX25 hermaphrodites (rollers) in the P_0 generation, and 40 F_1 rolling L4 hermaphrodites the same age as their male siblings [*smo-1(ok359)/+*; *wgIs159/+*; *tvEx25*; *rol-6*] were individually picked to small NGM plates. Then 50 F_2 rolling L4 hermaphrodites were individually picked to small NGM plates, allowed to lay eggs for 2 days, then the F_2 hermaphrodites were genotyped for *smo-1(ok359)* by single worm PCR using primers PO1296, PO1297, and PO1298, followed by separation on 2% agarose gel electrophoresis. The *ok539* mutation is a deletion of approximately 1.5 kb, and if this allele is homozygous, PO1296 and PO1298 will only amplify a single 702 bp product, and this is how we identified worms homozygous for this allele. PCR reactions contained 2.5 µl single worm lysis reaction, 1X PCR buffer, 2.5 mM MgCl2, 0.2 mM dNTPs, 100 ng each of PO1296, PO1297, and PO1298, and 0.1 µl Platinum Taq DNA polymerase (Invitrogen) in dH_2O to a final volume of 25 µl. PCR program used was as follows: 94°C for 30 seconds, (92°C for 30 seconds, 53°C for 30 seconds, 72°C for 30 seconds) X 40, 72°C for 5 minutes. Those plates with F_2 hermaphrodites which were homozygous for *ok359* were examined for TBX-2::GFP expression in F_3 progeny on a fluorescent microscope, and one plate with 100% of GFP(+) F_3 hermaphrodites was kept as OK0874 [*smo-1(ok359); wgIs159; tvEx25; rol-6*].

SMO-1 pulldown assays

For Ni-NTA purification of His::SMO-1, 4-6 L4 hermaphrodites of each strain (OP159, NX25, and OK0874) were picked to 5 large NGM plates seeded with 0.5 ml OP50. Once plates were nearly starved, worms were rinsed off the plates in 1 ml M9 buffer and pelleted by centrifugation at 2K RPM for 2 minutes. The pellet was washed 3 times with M9, and after aspiration of final wash, 0.75 ml of lysis buffer [8 M urea, 0.5 M NaCl, 45 mM Na_2HPO_4, 5 mM NaH_2PO_4,10 mM imidazole, 10 mM NEM (pH 8.0)] was added to each tube, and lysate was transferred to a 1.5 ml screw-top Eppendorf tube (Thermo-fisher) along with 100 mg 0.5 mm glass beads (Sigma, cat#G8772). The tubes were placed in a Mini-Beadbeater (Biospec products) at 4°C for five 3 minute beating intervals on the "homogenize" setting, and tubes were placed on ice for 2 minutes between each interval. Tubes were then centrifuged at 14K RPM and 4°C for 5 minutes, and supernatant was transferred to fresh Eppendorf tubes. The supernatants were then sonicated for 20 seconds, and centrifuged at 14K RPM for 15 minutes at 4°C. The supernatant was transferred to fresh Eppendorf tubes, and incubated with 50 µl Ni-NTA magnetic beads (Qiagen, cat#36111) for 1 hour on an end-over-end shaker. The beads were then washed twice with 1 ml wash buffer [8 M urea, 0.4 M NaCl, 17.6 mM Na_2HPO_4, 32.4 mM NaH_2PO_4, 10 mM imidazole, 10 mM NEM (pH 6.75)]. For each wash, the tubes were placed directly next to the magnets on a MagnaRack (Invitrogen), and the supernatant was aspirated. The tubes were moved away from the magnet, at which point 1 ml of wash was added to all tubes, which were then briefly vortexed and placed back against the magnets. After aspiration of the final wash, the tubes were kept against the magnets, and proteins were eluted by addition of 50 µl elution buffer (250 mM imidazole, 5% SDS, 0.15 M Tris pH6.7, 30% glycerol, 0.72 M ßME). The eluate was transferred to fresh Eppendorf tubes with 50 µl 2x SDS sample buffer,

and heated at 95°C for 5 minutes. Protein samples were then resolved by SDS-PAGE, and transferred to PVDF membrane by western blot. Proteins were detected using anti-GFP (1:1,000) (Roche) or anti-FLAG (1:1000) (Sigma), HRP-conjugated secondary antibody (1:2000) (Goat anti-mouse, Millipore), and ECL Plus (GE Healthcare) detection reagent. Chemilluminescence was recorded on film using Amersham ECL hyperfilm (GE Healthcare).

APPENDIX C - TBX-2 GAIN OF FUNCTION ASSAYS

Introduction

In luciferase transcriptional reporter assays in COS-1 cells, TBX-2 acts as a transcriptional repressor, although in these assays mutation of consensus SUMOylation sites LKIE and VKKE does not affect repressor activity (Huber et al., 2013). This observation contradicts *in vivo* genetic evidence which suggests that TBX-2 function is dependent on SUMOylation, although the COS-1 assays measured the repressor activity of a TBX-2::GAL4 fusion on a non-native basal thymidine kinase promoter with 5 upstream GAL4 binding sites. In order to determine a requirement for intact SUMO sites on TBX-2 repressor activity in the worm, we sought to first develop an *in vivo* transcriptional assay using a reporter of a bona fide downstream TBX-2 target. One such target our lab identified is the pharyngeal-expressed gene *D2096.6*. *D2096.6* expression onsets in numerous cell types within the pharynx beginning around the 1.5 fold stage of embryogenesis, and it is over-expressed in hypomorphic *tbx-2(bx59)* mutants in both microarray and GFP reporter analyses (Gaudet and Mango, 2002; Huber et al., 2013). Interestingly, *ubc-9* loss of function animals over-express a *D2096.6::gfp* promoter fusion in similar tissues as *tbx-2* mutants, suggesting that SUMOylation is required for repressor activity. To ask whether or not it is the TBX-2 protein specifically which requires SUMOylation, we devised a TBX-2 gain-of-function assay using *D2096.6::gfp* fluorescence as a readout for over-expressed TBX-2 transcriptional repressor activity which would thereby allow us to determine if there is a dependence on TBX-2 SUMO sites.

Results and discussion

TBX-2 represses the pharyngeal gene *D2096.6*

We first compared GFP intensity in the pharyngeal nuclei of two strains carrying an integrated *D2096.6::gfp* promoter fusion and extrachromosomal arrays expressing either *hsp-16.41::mCherry* or *hsp-16.41::mCherry::tbx-2* after induction of TBX-2 via the heat shock promoter. The *hsp-16.41* gene promoter specifically was chosen for over-expression of the mCherry constructs as it is known to be expressed strongly in the pharynx (and gut) and becomes highly active at 33°C (Stringham et al., 1992) facilitating robust elevation of mCherry or mCherry::TBX-2 protein levels in the same pharyngeal cells in which *D2096.6::gfp* is normally expressed without killing the worms (Figure 28A). 24 hours after heat shock treatment, there is an observable decrease in the intensity of pharyngeal GFP in the strain expressing mCherry::TBX-2 versus mCherry alone, and quantification of the difference reveals GFP levels are decreased by approximately 80% (Figure 28B,C). This reduction of GFP indicates that TBX-2 can repress the *D2096.6* gene when over-expressed in the pharynx, which coincides with the aforementioned *tbx-2* loss-of-function data.

TBX-2$^{LKIE/VKKE->AAAA}$ mutant does not repress the pharyngeal gene *D2096.6*

We next asked whether SUMO sites LKIE and VKKE were required for TBX-2 repression of *D2096.6::gfp.* The LKIE/VKKE->AAAA mutation which abolishes SUMOylation was introduced into *hsp-16.41::mCherry::tbx-2* and we generated a strain carrying *D2096.6::gfp* and *hsp-16.41::HA::mCherry::tbx-2*$^{LKIE/VKKE->AAAA}$. We examined *D2096.6::gfp* expression 24 hours after heat shock induction of this mutant [shown as mCherry::TBX-2(AAAA) in Figure 28] in the same manner as was done for strains expressing mCherry and mCherry::TBX-2, and

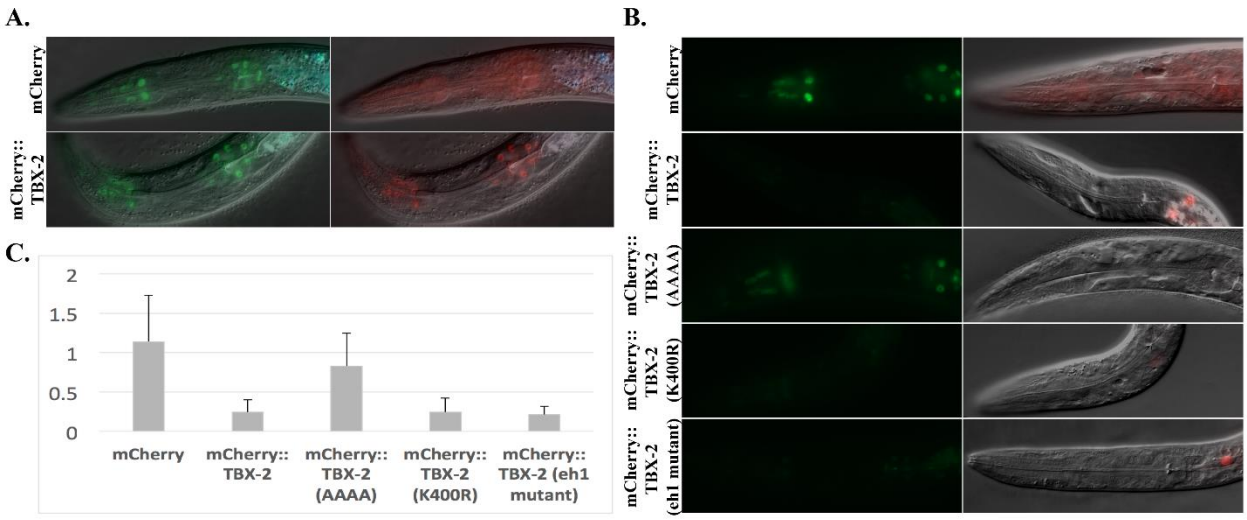

Figure 28. LKIE and VKKE mediate TBX-2 repression of *D2096.6::gfp*

In a TBX-2 gain-of-function assay, over-expression of TBX-2 via heat shock promoter reduces *D2096.6::gfp* expression *in vivo*. A) DIC and fluorescence merged images of *D2096.6::gfp* reporter strains expressing the indicated mCherry construct 4 hours after heat shock. The left panels show *D2096.6::gfp* expression in the pharynx in green and auto-fluorescent gut granules in blue. The right panels show mCherry expression in red (mCherry is dispersed throughout the cytoplasm, while the mCherry::TBX-2 fusion is localized to pharyngeal nuclei, also expressing *D2096.6::gfp*) and auto-fluorescent gut granules in blue. B) Fluorescence and DIC/fluorescence merged images of *D2096.6::gfp* reporter strains expressing the indicated mCherry construct 24 hours after heat shock. The left panels show *D2096.6::gfp* expression in the pharynx, all images were captured with 200 millisecond exposure times. The right panels show DIC with mCherry expression in red (those worms which still expressed mCherry in gut nuclei 24 hours after heat shock treatment were considered to have the highest expression levels of the mCherry::TBX-2 fusion strains and consequently were chosen for imaging and quantification of GFP intensity). C) Bar graph depiction of normalized (GFP of pharyngeal nuclei in the posterior bulb of mCherry(+) worms were normalized to that of mCherry(-) worms off the same heat shock plates) *D2096.6::gfp* expression for the strains displayed in part B. $n \geq 26$ for mCherry(+) and mCherry(-) worms for all strains. Error bars represent standard deviation of each normalized value, and was solved for as 'dx' in the equation $(dx/x)=\sqrt{((dA/A)^2+(dB/B)^2)}$, where, for each strain, x is the average GFP intensity of mCherry(+)/mCherry(-) worms (or A/B), dA is the standard deviation of GFP intensity in mCherry(+) worms, A is the average GFP intensity in mCherry(+) worms, dB is the standard deviation of GFP intensity in mCherry(-) worms, and B is the average GFP intensity in mCherry(-) worms.

observed only a partial reduction of GFP intensity (Figure 28B). Quantification of this difference reveals GFP levels are decreased by approximately 20% in the strain expressing mCherry::TBX-2$^{LKIE/VKKE->AAAA}$ compared to the strain expressing mCherry alone (Figure 28C). This indicates that mCherry::TBX-2$^{LKIE/VKKE->AAAA}$ mutants only weakly repress *D2096.6::gfp* compared to mCherry::TBX-2, which decreased GFP intensity by approximately 80% compared to the strain expressing mCherry alone.

Although we hypothesize that TBX-2$^{LKIE/VKKE->AAAA}$ does not repress *D2096.6* in these assays as well as TBX-2 because SUMOylation is required for repressor activity, we cannot rule out the possibility that it lacks repressor activity because it is DNA-binding defective. Mutation of the lysine residue in the highly conserved LKIE site of other T-box factors, such as TBX-22 and T-bet, eliminates transcriptional activity because they are DNA-binding defective (Andreou et al., 2007; Jang et al., 2013). DNA binding assays could indicate whether or not TBX-2$^{LKIE/VKKE->AAAA}$ mutants are able to make proper DNA contacts.

TBX-2^{K400R} and TBX-2$^{FDV->ADA}$ mutants repress the pharyngeal gene *D2096.6*

In our COS-1 SUMOylation assays, the K400R mutation significantly reduces SUMOylation of TBX-2 (Huber et al., 2013), and because Lys-400 is well outside of the T-box it should not affect DNA binding, so we decided to introduce this mutation into *hsp-16.41::mCherry::tbx-2* and generated a strain carrying *D2096.6::gfp* and *hsp-16.41::HA::mCherry::tbx-2^{K400R}*. We examined GFP levels 24 hours after heat shock induction of this mutant and found that it represses *D2096.6::gfp* expression by approximately 80%, similarly to wild type TBX-2 (Figure 28), indicating that either SUMOylation of Lys-400 is not required for repression of *D2096.6* in this over-expression assay, or that SUMOylation at other sites, such as LKIE, can facilitate TBX-2 repressor activity.

We have recently established that TBX-2 function in pharyngeal development depends on interaction with the Groucho-like corepressor UNC-37, and that this interaction is mediated through a conserved eh1 motif at the C-terminal of TBX-2, FDVLDLLS. TBX-2$^{FDV->ADA}$ mutants are unable to interact with UNC-37 in yeast, and only partially rescue *tbx-2* null mutants *in vivo*, and we wanted to ask if this mutation affects TBX-2 repressor activity in our gain-of-function assays. We introduced the FDV->ADA mutation in *hsp-16.41::mCherry::tbx-2* and generated a strain carrying *D2096.6::gfp* and *hsp-16.41::HA::mCherry::tbx-2*$^{FDV->ADA}$. We examined GFP levels 24 hours after heat shock induction of this mutant and found that it represses *D2096.6::gfp* expression by approximately 80%, similarly to wild type TBX-2 (Figure 28). This result is surprising because we hypothesized that TBX-2 requires UNC-37 to regulate target genes, however it is possible that over-expression of TBX-2 above endogenous levels negates the need for the UNC-37 corepressor. Conversely, UNC-37 may modulate TBX-2 repressor activity of target genes other than *D2096.6*, and this assay would therefore be insensitive to that possibility.

Material and Methods

Nematode strain construction

A chromosomally integrated *D2096.6::gfp* reporter strain, OK0999 *cuIs35 [PD2096.6::gfp; unc-119(+)]; unc-119(ed3)*, was generated by germline transformation of strain DP38 *unc-119(ed3)* animals with plasmid pOK291.01. Germline transformation was performed by biolistic transformation using a PDS-1000/He (Bio-Rad) particle delivery system equipped with a Hepta adapter (Bio-Rad) with modifications suggested by the TransgeneOme project (Sarov et al., 2012) (https://transgeneome.mpi-cbg.de/transgeneomics/manuals.html).

Extrachromosomal transgenic strains OK0983 *cuEx799 [hsp-16.41::HA::mCherry::unc-54 3'UTR]*, OK0984 *cuEx800 [hsp-16.41::HA::mCherry::tbx-2::unc-54 3'UTR]*, OK0985 *cuEx801 [hsp-16.41::HA::mCherry::tbx-2$^{LKIE/VKKE->AAAA}$::unc-54 3'UTR]*, OK0986 *cuEx802 [hsp-16.41::HA::mCherry::tbx-2^{K400R}::unc-54 3'UTR]*, and OK1008 *cuEx806 [hsp-16.41::HA::mCherry::tbx-2$^{FDV->ADA}$::unc-54 3'UTR]* were generated by micro-injection of 2.5 ng/µl plasmids pOK283.05, pOK283.03, pOK283.04, pOK294.01, and pOK293.05, respectively, with pRF4 containing *rol-6(su1006)* as a dominant marker for transformation.

To generate strains carrying the *D2096.6::gfp* insertion and heat shock mCherry arrays for use in TBX-2 gain-of-function assays, strains OK0983, OK0984, OK0985, OK0986, and OK1008 were crossed with N2 males and rolling male progeny (with genotypes of *cuEx799*, *cuEx800*, *cuEx801*, *cuEx802*, and *cuEx806*, respectively) were crossed with strain OK0999 (*cuIs35/cuIs35*). Rolling hermaphrodite progeny (all heterozygous for *cuIs35*) were then individually picked onto small NGM plates, and again the rolling hermaphrodite progeny were individually transferred to small NGM plates. Those plates with 100% GFP(+) rolling progeny were considered to be homozygous for *D2096.6::gfp* and given the following strain names: OK1000 *cuIs35; cuEx799*, OK1001 *cuIs35; cuEx800*, OK1002 *cuIs35; cuEx801*, OK1003 *cuIs35; cuEx802*, OK1011 *cuIs35; cuEx806*.

Plasmid construction

Plasmid pOK291.01, which contains *PD2096.6::gfp* and *unc-119(+)*, was constructed for biolistic transformation by inserting a PCR-amplified fragment containing *unc-119(+)* from plasmid pOK271.13 into a 5275 bp PciI-SphI digested vector fragment containing *PD2096.6::gfp* from plasmid pOK253.01. The *unc-119(+)* cassette was amplified using primers PO1383 and PO1385, containing PciI and SphI linkers, respectively, using the following PCR

program: step (1) 94°C for 30 seconds, 39 x [(2) 92°C for 30 seconds, (3) 52.8°C for 30 seconds, (4) 72°C for 2.5 minutes], (5) 72°C for 5 minutes. Sequencing with primers PO1158, PO1388, PO1389, PO1390, and PO1391 confirmed there were no mutations in the *unc-119(+)* cassette in plasmid pOK291.01.

Plasmids pOK283.05 (*hsp-16.41::HA::mCherry::unc-54 3'UTR*), pOK283.03 (*hsp-16.41::HA::mCherry::tbx-2::unc-54 3'UTR*), pOK283.04 (*hsp-16.41::HA::mCherry::tbx-2$^{LKIE/VKKE->AAAA}$::unc-54 3'UTR*), pOK294.01 (*hsp-16.41::HA::mCherry::tbx-2^{K400R}::unc-54 3'UTR*), and pOK293.05 (*hsp-16.41::HA::mCherry::tbx-2$^{FDV->ADA}$::unc-54 3'UTR*) were constructed using an In-Fusion HD cloning kit (Clontech) according to manufacturer's instructions. Briefly, *mCherry* cDNA (about 0.7 kb) was PCR amplified from plasmid pOK254.01 using primers PO1299/PO1301 or primers PO1299/PO1303 to generate mCherry::TBX-2 fusion or mCherry alone constructs, respectively. *tbx-2* cDNA (about 1.2 kb) was PCR amplified using primers PO1300/PO1302 from plasmids pOK241.17 (w/t *tbx-2*), pOK241.19 (*tbx-2$^{LKIE/VKKE->AAAA}$*), pOK244.18 (*tbx-2^{K400R}*), and pOK222.10 (*tbx-2$^{FDV->ADA}$*). The PCR program for amplifying *mCherry* and *tbx-2* inserts was as follows: step (1) 94°C for 30 seconds, 39 x [(2) 92°C for 30 seconds, (3) 54°C for 30 seconds, (4) 72°C for 1 minute], (5) 72°C for 5 minutes. Plasmid pOK257.02 containing the *hsp-16.41* heat shock promoter, HA tag, and *unc-54* 3'UTR was linearized with EcoRI and EcoRV, and the resultant 4174 bp vector was incubated with amplified inserts in a 1:2:2 molar ratio in the In-Fusion reaction. Reactions were then transformed and positive clones were sequenced with primers PO448, PO997, PO998, PO1323, and PO1324 to confirm *mCherry* and *tbx-2* cDNAs were present and no point mutations were induced during PCR.

Assay for TBX-2 repressor activity *in vivo*

To assay the effect of TBX-2 over-expression on *D2096.6::gfp* expression *in vivo*, worms carrying *mCherry* or *mCherry::tbx-2* fusions and *PD2096.6::gfp* constructs (strains OK1000, OK1001, OK1002, OK1003, OK1011) were heat shocked to induce TBX-2 expression, then examined for a difference in GFP fluorescence between the different strains. Briefly, L4/YA moms were allowed to lay eggs on small NGM plates with freshly seeded OP50 for 5 hours, then the moms were removed and the plates were incubated at 20°C for 16 hours. The plates were wrapped in parafilm, then placed agar side down in a 33°C water bath for 2 hours. Plates were shifted to 20°C and after 24 hours, L1/L2 larva still expressing mCherry in gut nuclei were imaged using a Zeiss Axioskop microscope equipped for DIC and fluorescence microscopy. Images were captured using a Zeiss Axiocam MRm camera and fluorescence intensity of GFP in the pharyngeal nuclei within the posterior bulb (with an $n \geq 26$ for all strains) was measured using Zeiss Zen software. When quantifying the *D2096.6::gfp* intensity for each different mCherry construct strain, we normalized GFP levels of mCherry(+) to mCherry(-) worms from the same heat shock plates to account for fluorescence intensity variability between strains.

APPENDIX D - TBX-2 GEL SHIFT ASSAYS

Introduction

In *in vivo* overexpression assays, the TBX-2$^{LKIE/VKKE->AAAA}$ double mutant lacks the ability to repress an indirect downstream target *D2096.6::gfp* reporter that wild type TBX-2 possesses (refer to Appendix C), however, it is unclear whether this is due to an inability of the mutant to properly bind DNA or a lack of SUMO-dependent repression. In another T-box factor, T-bet, mutation of only the conserved lysine of the LKIE site (which is actually LKID in T-bet, D and E residues are interchangeable in this conserved SUMO consensus motif) to arginine abolishes DNA binding ability (Jang et al., 2013). We wanted to ask if the TBX-2$^{LKIE/VKKE->AAAA}$ double mutant also lacks DNA binding ability, and we performed gel shift assays in an attempt to answer this question.

Results and discussion

Members of the T-box family can bind to the DNA consensus sequence AGGTGTGA (Wilson and Conlon, 2002), although to date, the only proven direct target of TBX-2 *in vivo* is *tbx*-2 itself, and it binds a similar sequence, AGGTGGCA (Milton and Okkema, 2015), so we synthesized ^{32}P-labelled probes with wild type and mutant TBX-2 binding sites [AGGTGGCA (probe 1) and ATTGTGCA (probe 2), respectively] and performed a gel shift assay with Ni-NTA natively purified TBX-2::V5::His or TBX-2$^{LKIE/VKKE->AAAA}$::V5::His proteins from transiently transfected COS-1 cells. We did not detect any difference in probe binding between mock transfected purifications and TBX-2::V5::His or TBX-2$^{LKIE/VKKE->AAAA}$::V5::His transfected purifications, or wild type vs. mutant probes (Figure 29A). Thus we could not detect binding of TBX-2 in this assay.

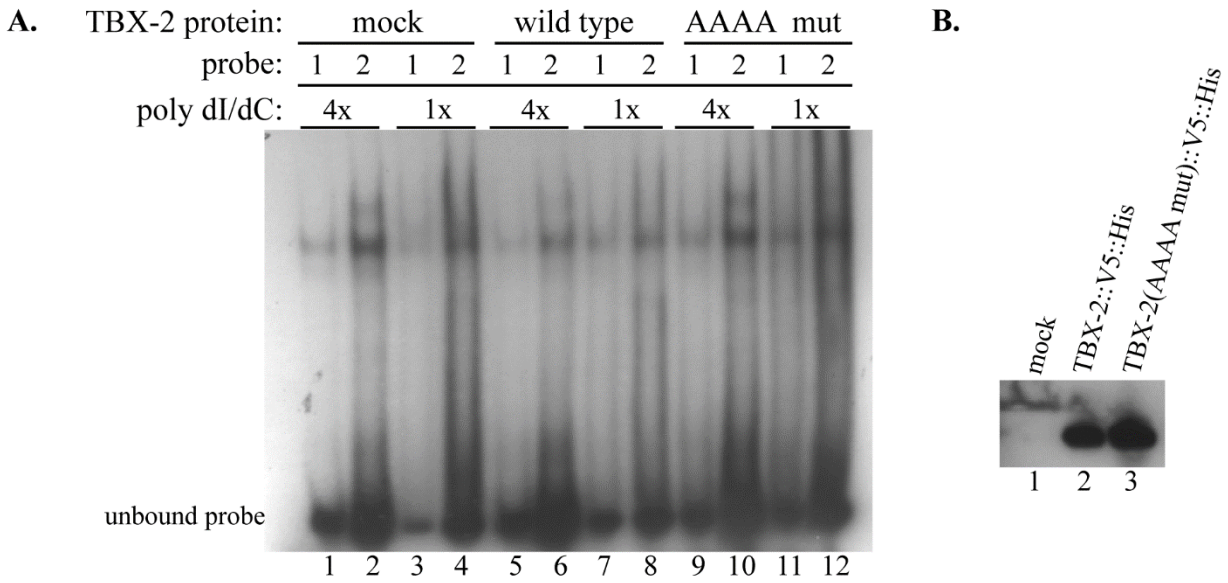

Figure 29. TBX-2::V5::His fusion does not detectably bind a TBX-2 binding site in *tbx-2*

Gel shift assay of Ni-NTA purified TBX-2::V5::His or TBX-2$^{LKIE/VKKE->AAAA}$::V5::His proteins incubated with ^{32}P-labelled probes containing wild type or mutant TBX-2 binding sites. Full length *tbx-2* cDNA fusions were used for transfection in COS-1 cells. A) Gel shift with mock (lanes 1-4), TBX-2::V5::His (lanes 5-8), and TBX-2$^{LKIE/VKKE->AAAA}$::V5::His (lanes 9-12) transfected COS-1 purifications indicated along with the probe used (probe 1 is wild type, probe 2 is mutant) and varied concentration of poly dI/dC used in binding reactions. Probe remains unbound in all lanes, no specific shift is noticeable. B) Western blot (using an anti-V5 antibody) of the indicated transfected construct in COS-1 cells after Ni-NTA protein purification.

Materials and Methods

TBX-2 protein sample preparation

To obtain TBX-2 protein for gel shift assays, ~$2x10^6$ COS-1 cells were seeded into six 10 cm plates 24 hours prior to transfection. For each construct, 2 plates were transfected with either no DNA (for mock transfection), 20 µg wild type TBX-2::V5::His (pOK241.05), or 20 µg TBX-2 $^{LKIE/VKKE->AAAA}$::V5::His (pOK241.17), and 4 µg pEGFP-N3 (Clontech) using Lipofectamine 2000 in OPTI-MEM according to manufacturer's instructions (Invitrogen). After 48 hours, transfected plates were checked on a Leica inverted microscope for GFP expression as a transfection control. Then COS-1 cells were harvested with a cell scraper in PBS, and transferred to 50 ml conical tubes (BD Falcon). Once all six plates were harvested, the tubes were spun down at 1K RPM to obtain cell pellets, then the pellets were resuspended in 1 ml PBS and transferred to 1.5 ml Eppendorf tubes, which were centrifuged for 5 minutes at 2K RPM. The supernatant was aspirated and 1 ml lysis buffer [0.345 g NaH_2PO_4, 0.877 g NaCl, 0.034 g imidazole, 25 µl Tween 20 in 50 ml dH_20, with freshly added 1x Protease Inhibitor Cocktail (Sigma P8465) made on the day of purification] was added. Cells were lysed by freeze-thaw on dry ice and thawing 3 times, then centrifuged at 14K RPM for 15 minutes at 4°C. The supernatant was transferred to fresh Eppendorf tubes, and incubated with 50 µl Ni-NTA magnetic beads (Qiagen) for 1 hour on an end-over-end shaker at 4°C. The beads were then washed twice with 1 ml wash buffer [50 mM NaH_2PO_4, 300 mM NaCl, 20 mM imidazole, 0.05% Tween 20 (pH 8.0)]. For each wash, the tubes were placed directly next to the magnets on a MagnaRack (Invitrogen), and the supernatant was aspirated. The tubes were moved away from the magnet, at which point 1 ml of wash was added to all tubes, which were then briefly vortexed and placed back against the magnets. After aspiration of the final wash, the tubes were

kept against the magnets, and proteins were eluted by addition of 50 µl elution buffer [50 mM NaH_2PO_4, 300 mM NaCl, 250 mM imidazole, 0.05% Tween 20 (pH 8.0)]. Most of the eluate was transferred to fresh Eppendorf tubes, placed on dry ice, and stored at -80°C until use in gel shift assay. 5 µl of each sample was placed in an Eppendorf tube with 5 µl 2x SDS sample buffer, heated on a 95°C heat block for 5 minutes, resolved by SDS-PAGE, and transferred to PVDF membrane by western blot. Proteins were detected using anti-V5 primary antibody (1:5,000) (Invitrogen), HRP-conjugated secondary antibody (1:2000) (Goat anti-mouse, Millipore), and ECL Plus (GE Healthcare) detection reagent. Chemilluminescence was recorded using Amersham ECL hyperfilm (GE Healthcare) or a STORM 860 Molecular Imager and ImageQuant software (Molecular Dynamics).

Radioactive-labeled probe preparation

Radioactive probes for gel shift assays were designed based on the TBX-2 binding site (Milton and Okkema, 2015). Probe 1 possessed the wild type binding site, AGGTGGCA, and was generated by annealing of primers PO1419 and PO1420. Probe 2 possessed the mutated binding site, ATTGTGCA, and was generated by annealing of primers PO1421 and PO1422. All primers were ordered through IDT (Integrated DNA Technologies) and were purified under standard desalting conditions. For annealing reactions, 4 µl of forward and reverse primer (1 µg/µl), 2 µl of 10x TE buffer, and 10 µl dH_20 (giving a final concentration of 0.4 µg/µl) was added to an Eppendorf tube and placed in a heat block at 100°C for 3 minutes. The block was removed from heat and the samples were allowed to slowly cool to room temperature before freezing at -20°C. Annealed probes were labeled with α-^{32}P dCTP (Perkin Elmer) in an end-filling reaction containing 0.5 µl double stranded oligo (0.4 µg/µl stock), 2 µl 10x REact buffer 2, 10 µl (0.5 mM dG, dA, dT mix), 5 µl α-^{32}P dCTP (800ci/mmol), and 2.5 µl dH_20, to which 0.5

µl of Klenow fragment (3'-5' exo-) of DNA Polymerase I (NEB) was added and reactions were then placed in a 37°C water bath. Reactions were stopped after 1 hour by addition of 40 µl 2x TE buffer. To determine the incorporation of radioactive counts, 1 µl of each labeled probe was pipetted onto 3 separate DE81 Whatman circular filter papers and allowed to air dry. For each probe, 2 out of 3 filters were washed 3x with 75 ml 0.5 M Na_2HPO_4 for 5 minutes. The filters were rinsed with absolute ethanol, dried, and individually placed into scintillation vials for determination of radioactive counts in a scintillation counter. All remaining labeled probe was purified using a QIAquick Nucleotide Removal Kit (Qiagen) and eluted in 100 µl of elution buffer (provided in kit). Specific activity of probe 1 was $9.08x10^7$ dpm/µg, and $1.64x10^6$ dpm/µg for probe 2.

Gel Shift assay

Gel shift assays were performed essentially as described (Thatcher et al., 1999), and is described briefly here. 5 µl purified TBX-2 protein was incubated in 20 µl binding reactions in buffer 2 [10 mM Tris (pH 7.8), 50 mM NaCl, 5 mM EDTA (pH 8.0), 10% glycerol] with 10-40 ng poly dI/dC for 15 minutes at room temperature. 500,000 cpm of probe was added and the reactions were incubated at room temperature for an additional 30 minutes before being electrophoresed on a 5% non-denaturing acrylamide gel at 4°C. Blue juice was loaded in the first lane, and once bands were about halfway down the gel, the gel was removed, dried on a gel dryer, imprinted on a phosphorimager, and recorded using Amersham ECL hyperfilm (GE Healthcare) or a STORM 860 Molecular Imager and ImageQuant software (Molecular Dynamics).

APPENDIX E - TBX-2 PROTEIN EXPRESSION IN E. COLI

Introduction

Mutation of two SUMO consensus sites in TBX-2 eliminates interaction with UBC-9 as well as SUMOylation of TBX-2 (Huber et al., 2013), although we don't know for certain whether this is due to the loss of interaction with the SUMO conjugating enzyme or elimination of points of SUMO conjugation. Crystal structure data of SUMO target E2-25K shows that non-consensus sites can be SUMOylated (Pichler et al., 2005). One method which has been used to identify SUMO modification at such sites is tandem mass spectrometry (MS) analysis (Plant et al., 2010), which involves co-expression in bacteria (for large scale purification) of a His-tagged SUMO target with a tricistronic vector expressing SUMO activating and conjugating enzymes as well as SUMO-1(T95K) (this single amino acid substitution facilitates more efficient MS analysis by shortening the C-terminal tryptic peptide fragments used to identify SUMO-conjugated lysines), and enrichment for the SUMO-modified target, followed by trypsinization and MS analysis. We sought to use this method to determine which lysines are SUMOylated in TBX-2.

Results and discussion

We first generated a His::TEV::TBX-2 construct which would allow us to express and pull down SUMO modified TBX-2 using Ni-NTA beads, then cleave native TBX-2 protein from the His tag prior to MS via the TEV protease cleavage site. This plasmid was successfully transformed into Rosetta and BL21 *E. coli* strains, although we were unable to induce TBX-2 protein expression in these cells (Figure 30). However, we were able to induce expression of a GST::TBX-2 DNA binding domain fusion (Figure 30), suggesting that full length TBX-2 may be

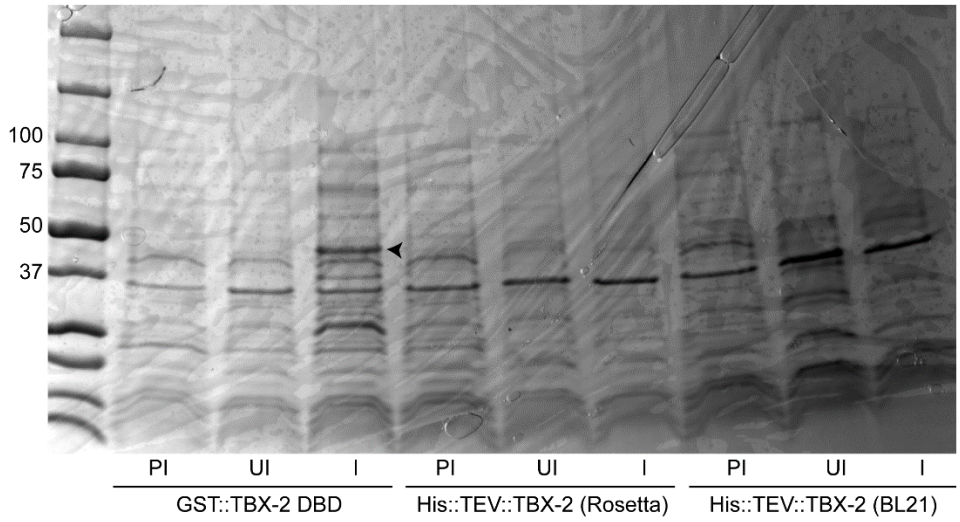

Figure 30. His::TEV::TBX-2 expression in *E. coli*

Coomassie stained gel of pre-induced (PI), uninduced (UI), and induced (I) expression of a GST::TBX-2 DBD fusion (in Rosetta cells) and His::TEV::TBX-2. Molecular weight markers (in kDa) are indicated on the left. Arrowhead indicates positive control GST::TBX-2 DBD fusion at 50 kDa in the induced lane only. His::TEV::TBX-2 size is expected to be approximately 50 kDa, although no observable expression is seen in the induced lanes when compared to pre-induced or uninduced lanes in each of the indicated bacteria strains.

degraded or proteolyzed in bacteria, a phenomenon that has been previously reported with human TBX2 (Sinha et al., 2000).

Material and Methods

General methods for nucleic acid manipulations and plasmid construction

Plasmids pT-E1E2S1(T95K), pOK280.01, and pET28a [His::TEV::K2P1(270-336)], pOK280.02, were gifts from the Goldstein Lab at University of Chicago. pOK280.02 was verified by sequencing with primers PO1305 and PO1306. To generate pET28a [His::TEV::TBX-2], pOK 241.07 was digested with SpeI and XhoI, and a 1342 bp band containing wild type TBX-2 cDNA was gel purified and ligated into a gel purified 5271 bp fragment of pOK280.02 after digestion with AvrII and Xho1. Proper insertion of TBX-2 into the vector was verified by restriction digest and this plasmid was named pOK281.07.

pOK281.07 was transformed into pre-made competent BL21 and Rosetta *E. coli* cells and plated on 2xTY+Kan (50 µg/ml). Plasmid pOK269.07 containing cDNA of the TBX-2 DNA binding domain fused to GST was also transformed into Rosetta competent cells (to be used as a positive control for induction) and plated on 2xTY+Amp (100 µg/ml).

TBX-2 protein induction and visualization

To induce protein expression, single colonies were then picked and grown overnight in 3 ml 2xTY with the appropriate selective antibiotic in 14 ml conical tubes (BD Falcon). The following day 250 µl of overnight culture was used to inoculate a sterile 125 ml flask with 25 ml 2xTY with 0.2% glucose and the appropriate antibiotic. This culture was then shaken at 37°C for about 2.5 hours, or until $OD_{600} = 0.6$. 1 ml was then transferred to a 1.5 ml Eppendorf tube, pelleted at 14K RPM for 2 minutes, and resuspended in 50 µl 1xSDS sample buffer, and kept on

ice to be used as a pre-induced control. 3 ml was also transferred to a 14 ml conical tube and placed back at 37°C with shaking for 2 hours, this culture would be used as the uninduced control. To the culture remaining in the flask, 11 µl 1 M IPTG was added for induction of TBX-2, and the flask was also placed back at 37°C with shaking for 2 hours. 1 ml of uninduced and induced cultures were then pelleted in 1.5 ml Eppendorf tubes at 14K RPM for minutes, and resuspended in 100 µl 1xSDS sample buffer. Pre-induced, uninduced, and induced samples were then heated for 5 minutes at 95°C and centrifuged for 15 minutes at 14K RPM. The supernatant was then transferred to fresh 1.5 ml Eppendorf tubes, and stored at -20°C or immediately separated by SDS-PAGE (loaded 15 µl) and subjected to Coomassie staining to visualize protein expression.

APPENDIX F - ULP RNAI ANALYSES

Introduction

The regulation of protein function and/or localization by SUMOylation is a reversible, dynamic process, requiring the activities of SUMO-conjugating enzymes and SUMO-specific proteases to maintain proper levels of modified substrates within the cell (Gill, 2004). SUMO-specific proteases, which are members of the C48 cysteine protease family, have responsibilities in SUMO maturation as well as SUMO-deconjugation from substrate proteins. Four of the six mammalian SUMO-specific proteases have been shown to reside in different cellular locations, and thereby deconjugate SUMO from different proteins (Nayak and Müller, 2014). In *C. elegans*, 5 ubiquitin-like proteases, ULP-1, ULP-2, ULP-3, ULP-4, and ULP-5, all contain a C48 peptidase catalytic domain, suggesting they confer SUMO-specific protease activity (Wormbase). We hypothesize that one or more of these ULPs function to de-conjugate SUMO/SMO-1 from TBX-2. In the set of experiments described here, we ask if a reduction of the five ULPs in *C. elegans* leads to misregulation of TBX-2 protein, causing L1 arrest or pharyngeal abnormalities.

Results and discussion

To test this, feeding RNAi was performed on N2 animals for each of the five ULPs. We did not observe any differences in growth or pharyngeal morphology in RNAi animals. This may be due to redundancy in the ability of ULPs to remove SUMO from TBX-2, so knockdown of a single protease would not eliminate deSUMOylation of TBX-2 because not just one single ULP is responsible for regulation of TBX-2 SUMOylation. To test this, multiple combinations with multiple ULPs could be knocked down simultaneously. Alternatively, feeding RNAi is the

not the most penetrant method for RNAi knockdown, so performing feeding RNAi with RNAi hyper-sensitive *rrf-3* mutants or the method of injecting synthesized dsRNA of the five ULPs could provide a stronger reduction of ULP mRNA.

Materials and Methods

RNAi analyses

For ubiquitin-like protease RNAi experiments, *ulp-1* (T10F2.3), *ulp-2* (Y38A8.3), *ulp-3* (Y48A5A.2), *ulp-4* (C41C4.6), and *ulp-5* (K02F2.4) individual feeding RNAi clones (in *E. coli* strain HT115(DE3)) were grown on 2xTY+Amp(50µg/ml)+Tet(15 µg/ml) and confirmed by sequencing with M13 forward sequencing primer (-20) (GTAAAACGACGGCCAGT). Feeding library locations for *ulp-1,2,3,4,5* are III-2N21, II-4K17, IV-1J09, II-6A07, I-3102, respectively. Feeding RNAi experiments were then performed as previously described (Kamath and Ahringer, 2003). Briefly, N2 L4 hermaphrodites were plated with the appropriate RNAi clone on feeding RNAi plates, which were labelled A. 24 hours later, moms were moved to the appropriate RNAi feeding plates, labelled B, and allowed to lay embryos for 12 hours, at which point the moms were again moved to appropriate RNAi plates, labelled C. 12 hours later, moms on C plates were flamed, and progeny on the B plates were examined by DIC microscopy for embryonic lethality and pharyngeal defects. The C plate progeny were examined in a similar manner 12 hours later.

APPENDIX G – OLIGONUCLEOTIDES

TABLE XI – OLIGONUCLEOTIDES USED IN THIS STUDY

Oligo	Sequence (5'->3')	Description
PO3	AGCGGATAACAATTTCACACAGGA	M13 reverse sequencing primer
PO4	TAATACGACTCACTATAGGG	T7 promoter sequencing primer
PO448	CATTGGATGTCAAAAGGCG	*tbx-2*/F21H11.3 sequencing primer
PO449	GAAGAGTGTTGCCATTTGC	*tbx-2*/F21H11.3 sequencing primer
PO587	TTTGGAGAGTAATGAAGCAGCA	*tbx-2::Gal4* sequencing primer
PO593	CAGACGGATATTCCCAGCAT	*tbx-2::Gal4* sequencing primer
PO604	TTTTGTGCGAACATCGACC	*tbx-2(ok529)* genotyping primer
PO605	ACACACACACCTACAGTAATGCG	*tbx-2(ok529)* genotyping primer
PO606	TCAGGCGAGCATTGGATG	*tbx-2(ok529)* genotyping primer
PO623	TCAGTGGATGTTGCCTTTAC	BiFC TBX-2::CC155 sequencing primer
PO796	CCCAAAAAGGGAGGTGCTGATGCTCTCGA TTTGTTGTCAAAG	(+) strand oligo for mutating eh1 site in *tbx-2*
PO797	CTTTGACAACAAATCGAGAGCATCAGCAC CTCCCTTTTTGGG	(-) strand oligo for mutating eh1 site in *tbx-2*
PO821	GGAATGGCATTCAATCCATTTG	upstream primer for amplifying *tbx-2* orf + Kozak sequence and cloning into pCDNA3.1
PO822	AGGCTTTGACAACAAATCGAGAAC	downstream primer for amplifying *tbx-2* orf with no stop codon and cloning in pCDNA

PO824	TTAAGGCTTTGACAACAAATCGAG	downstream primer for amplifying *tbx-2* orf with natural stop codon and cloning in pCDNA
PO833	GCTGAAAAGCCTGAAGTGCGGAAAGAGCAAAAGTCAGTGAC	(+) strand oligo for mutating *tbx-2* SUMO site 2 VKKE->VRKE in pCDNA
PO834	GTCACTGACTTTTGCTCTTTCCGCACTTCAGGCTTTTCAGC	(-) strand oligo for mutating *tbx-2* SUMO site 2 VKKE->VRKE in pCDNA
PO835	TGGCAAATGGCAACACTC	Forward sequencing primer for 3' end of *tbx-2*
PO859	GCCATGGCTTACCACCCGTTCC	upstream oligo for amplifying Hs *TBX2* and kozak sequence
PO860	CTTGGGCGACTCCCGGCCTG	downstream oligo for amplifying Hs *TBX2* orf without stop codon
PO861	GTGGATGAGCCTCTCCATGAGA	upstream oligo for amplifying Mm *Tbx3* and kozak sequence
PO862	AGGGGACCCGCTGCAAG	downstream oligo for amplifying Mm *Tbx3* orf without stop codon
PO871	TCCACATCGTCAGAGCCAAC	sequencing primer for Mm *Tbx3*
PO876	CGGCTTCACCATCCTAAAC	sequencing primer for Hs *TBX2*
PO877	ATAGGGGCTGAAACGCAGTC	sequencing primer for Hs *TBX2*
PO931	AGTTTGACACCGATTTTCTCG	*tbx2(bx59)* genotyping primer
PO932	GTGATGATGGATCTTGTTCCG	*tbx2(bx59)* genotyping primer
PO933	GATCTAGAATGGCATTCAATCCATTTGC	upstream primer for amplifying *tbx-2* orf + XbaI linker
PO934	GAGGATCCAGGCTTTGACAACAAATCGAGAAC	downstream primer for amplifying *tbx-2* orf with no stop codon + BamHI linker
PO1021	GAAGGTGACGGAGCTGAGAATCGAAAACAATCCGT	*tbx-2* SUMO site 1 LKIE->LRIE forward mutagenesis primer
PO1022	ACGGATTGTTTTCGATTCTCAGCTCCGTCACCTTC	*tbx-2* SUMO site 1 LKIE->LRIE reverse mutagenesis primer

PO1067	GAAGTTTATCAGGAACAAACGTAGGGTCATTCAACAGTTTAGGG	forward primer for mutating SUMO1 to SUMO1(ΔGG)
PO1068	CCCTAAACTGTTGAATGACCCTACGTTTGTTCCTGATAAACTTC	reverse primer for mutating SUMO1 to SUMO1(ΔGG)
PO1073	CATGAATTCGAATGGTGAGCAAGGGCGAGGAG	sequencing primer for BiFC clone with mutant SMO-1(ΔGG)
PO1078	CATGCCGGCCTTGTACAGCTCGTCCATGCC	sequencing primer for BiFC clone with TBX-2::CC155
PO1089	CATGTCGACGAGGACTAGAATCCGCCCAG	sequencing primer for BiFC clone with mutant SMO-1(ΔGG)
PO1158	CTTGGGGTACACATTAAGGTGAGAAAAAGTGAGCG	sequencing primer for plasmid pOK291.01
PO1222	TCATGGCCATGGCATTCAATCCATTTG	upstream primer for amplifying *tbx-2*, with Msc1 linker
PO1223	TCAGGTACCAGGCTTTGACAACAAATCGAGAAC	downstream primer for amplifying *tbx-2*, with Kpn1 linker
PO1296	TCAAGTTGGAGACATTTTGCG	upstream primer for genotyping *smo-1(ok359)*
PO1297	CATCCATCCCTTTTCCACTG	upstream primer for genotyping *smo-1(ok359)*
PO1298	TATCTTCCAGGCAATCACCAT	upstream primer for genotyping *smo-1(ok359)*
PO1305	TTAGGAAGCAGCCCAGTAG	upstream oligo for sequencing cloning region of plasmid pOK280.02
PO1306	CTAAATCGGAACCCTAAAGG	downstream oligo for sequencing cloning region of plasmid pOK280.02
PO1383	CAACATGTGGGCTGCAGAATTCGTTTT	upstream oligo for amplifying *unc-119(+)* from pOK271.13 with 5' PciI linker
PO1385	TCTGAGAAGCCCGACAGAAT	downstream oligo for amplifying *unc-119(+)* from pOK271.13

PO1388	TGTTGTTGTTGCTCTGCCT	sequencing primer for plasmid pOK291.01
PO1389	GCCTATGGAAAAACGCCA	sequencing primer for plasmid pOK291.01
PO1390	CTTTGCTACCAGTTTGAACC	sequencing primer for plasmid pOK291.01
PO1391	TTTGGATGTGCTCTGCGA	sequencing primer for plasmid pOK291.01
PO1403	GCAAATGGCAACACTCTTC	sequencing primer for *tbx-2* in *tbx-2::gfp* fosmid from modEncode
PO1404	CCATCTAATTCAACAAGAATTGGG	sequencing primer for *tbx-2* in *tbx-2::gfp* fosmid from modEncode
PO1405	ACGGGAACTACAAGACAC	sequencing primer for *tbx-2* in *tbx-2::gfp* fosmid from modEncode
PO1406	GTTTGTCCGCCATGATGT	sequencing primer for *tbx-2* in *tbx-2::gfp* fosmid from modEncode
PO1407	GAGTTTGTAACAGCTGCTGGG	sequencing primer for *tbx-2* in *tbx-2::gfp* fosmid from modEncode
PO1408	AAGTCGAAGCAACTTCTGAAGATTCTGAA GAAGCTGAAAAGCCTGAAGTGTCGCTGTC GAGATATGACGGTG	forward primer for amplifying RT cassette from pNH034 and recombineering near C-terminus of *tbx-2* in *tbx-2* fosmid
PO1409	AGAACATCAAAACCTCCCTTTTTGGGTGGT GTCACTGACTTTTGCTCTTTGATGATAAGC TGTCAAACATGAG	reverse primer for amplifying RT cassette from pNH034 and recombineering near C-terminus of *tbx-2* in *tbx-2* fosmid
PO1410	AAGTCGAAGCAACTTCTGAAGATTCTGAA GAAGCTGAAAAGCCTGAAGTGCGGAAAGA GCAAAAG	forward primer for replacement of RT cassette with VRKE in *tbx-2* fosmid
PO1411	AGAACATCAAAACCTCCCTTTTTGGGTGGT GTCACTGACTTTTGCTCTTTCCGCACTTCA GGCTT	reverse primer for replacement of RT cassette with VRKE in *tbx-2* fosmid

PO1415	CTGAAGTGAAGAAAGAGCAAAAGTCAGTG ACACCACCCAAAAAGGGAGGTTCGCTGTC GAGATATGACGGTG	RT cassette amplifying forward primer for insertion of RT cassette at the eh1 site of *tbx-2::gfp* fosmid from modEncode
PO1416	ACTTCATCCAGCGGGTCCTGATTGGTATGC ACTTCAGGCTTTGACAACAAGATGATAAG CTGTCAAACATGAG	RT cassette amplifying reverse primer for insertion of RT cassette at the eh1 site of *tbx-2::gfp* fosmid from modEncode
PO1417	CTGAAGTGAAGAAAGAGCAAAAGTCAGTG ACACCACCCAAAAAGGGAGGTGCTGATGC TCTCGAT	mutated eh1 site replacement primer forward for recombineering eh1 site mutant into *tbx-2::gfp* fosmid
PO1418	ACTTCATCCAGCGGGTCCTGATTGGTATGC ACTTCAGGCTTTGACAACAAATCGAGAGC ATCAGC	mutated eh1 site replacement reverse primer for recombineering eh1 site mutant into *tbx-2::gfp* fosmid
PO1419	CAAGCGTCCTCCTCCTTGCCACCTAAGCCC CGCCC	*tbx-2* proximal T-box binding site oligo for gel shifts with PO1420
PO1420	CTTGGGGCGGGGCTTAGGTGGCAAGGAGG AGGACG	*tbx-2* proximal T-box binding site oligo for gel shifts with PO1419
PO1421	CAAGCGTCCTCCTCCTTGCACAATAAGCCC CGCCC	*tbx-2* proximal T-box binding site mutant oligo for gel shifts with PO1422
PO1422	CTTGGGGCGGGGCTTATTGTGCAAGGAGG AGGACG	*tbx-2* proximal T-box binding site mutant oligo for gel shifts with PO1421

APPENDIX H – PLASMIDS

TABLE XII – PLASMIDS USED IN THIS STUDY

Plasmid	Description
pOK187.01	Complete *tbx-2* orf in plexA-NLS for yeast two hybrid. *tbx-2* cDNA was amplified from pOK165.07 with PO618 and PO619, cut with XmaI and XhoI, cloned into KS+, then cut again with XmaI and XhoI from pOK186.55 and cloned into XmaI and SalI digested plexA-NLS.
pOK193.11	Partial sequence of pOK193.11 insert in pACT w/ PO343. Encodes *ubc-9.*
pOK195.18	Yeast two-hybrid prey vector (pACT) containing *unc-37* cDNA cloned via XhoI site. *unc-37* cDNA is missing first ~200 bps according to sequencing. Sequencing covers only *unc-37* cDNA and areas around insertion.
pOK206.33	*tbx-2::gfp* translational fusion in exon 1 directly downstream of *tbx-2* ATG. *tbx-2* promoter amplified from pOK203.02 with PO752/754, cut with Pst-BglII and inserted into pPD95.69.
pOK222.01	Complete *tbx-2* orf in plexA-NLS for yeast two-hybrid with mutated SUMO site 1 (1774-1791,LKIE->AAAA). The mutation was introduced into pOK187.01 using primers PO792/793.
pOK222.06	Complete *tbx-2* orf in plexA-NLS for yeast two-hybrid with mutated SUMO site 2 (VKIE->AAAA,2281-2298). The mutation was introduced into pOK187.01 using primers PO794/PO795.
pOK222.10	Complete *tbx-2* orf in plexA-NLS for yeast two-hybrid with mutated eh1 site (FDVLDLL->ADALDLL,2323-2340). Mutation was introduced into pOK187.01 using primers PO796/797.
pOK222.11	Complete *tbx-2* orf in plexA-NLS for yeast two-hybrid with mutated eh1 site (FDVLDLL->ADALDLL,2323-2340). Mutation was introduced into pOK187.01 using primers PO796/797.
pOK225.02	Complete *tbx-2* orf in plexA-NLS for yeast two-hybrid with mutated SUMO sites 1 and 2.
pOK237.15	pCDNA3.1/V5/His Topo
pOK241.05	Wild-type *tbx-2* cDNA cloned into pCDNA3.1/V5/His Topo. For expressing TBX-2::V5::His fusion in mammalian cells.

pOK241.07	Wild-type *tbx-2* cDNA cloned into pCDNA3.1/V5/His Topo. For expressing native TBX-2 in mammalian cells.
pOK241.10	*tbx-2* cDNA SUMO site 1 mutant (LKIE->AAAA) cloned into pCDNA3.1/V5/His Topo. For expressing TBX-2 (SUMO site 1 mutant)::V5::His fusion in mammalian cells.
pOK241.13	*tbx-2* cDNA SUMO site 2 mutant (VKKE->AAAA) cloned into pCDNA3.1/V5/His Topo. For expressing TBX-2 (SUMO site 2 mutant)::V5::His fusion in mammalian cells.
pOK241.17	*tbx-2* cDNA SUMO sites 1 and 2 mutant cloned into pCDNA3.1/V5/His Topo. For expressing TBX-2 (SUMO sites 1 and 2 mutant)::V5::His fusion in mammalian cells.
pOK241.19	*tbx-2* cDNA SUMO sites 1 and 2 mutant cloned into pCDNA3.1/V5/His Topo. For expressing native TBX-2 (SUMO sites 1 and 2 mutant) in mammalian cells.
pOK244.18	*tbx-2* cDNA SUMO site 2 conservative mutant (VKKE->VRKE) in pCDNA3.1/V5/His Topo. For expressing mutant TBX-2::V5::His fusion in mammalian cells.
pOK245.01	Mm *Tbx3* cDNA in pCDNA 3.1/V5/His Topo. For expressing Tbx-3::V5::His fusion in mammalian cells.
pOK246.01	Hs *TBX2* cDNA in pCDNA3.1/V5/His Topo. For expressing TBX2::V5::His fusion in mammalian cells.
pOK247.03	Constructed from ligation of RNAi feeding vector (L4440) with *unc-37* orf from pOK214.05 using BamHI and PstI restriction sites.
pOK251.01	pCDNA HA/SUMO1. For expressing HA::SUMO1 in mammalian cells.
pOK251.02	pCDNA HA/SUMO2. For expressing HA::SUMO2 in mammalian cells.
pOK251.03	pCDNA HA/SUMO3. For expressing HA::SUMO3 in mammalian cells.
pOK251.04	pCDNA HA/Gal4(1-100). For expressing GAL4 fusions in mammalian cells.
pOK253.01	Ce *tbx-2* fused to Gal4(1-100) in pCDNA. For expression of HA::TBX-2::GAL4 fusion in mammalian cells.

pOK253.04	Ce *tbx-2* SUMO sites 1 and 2 mutant (LKIE/VKKE->AAAA) fused to Gal4(1-100) in pCDNA. For expression of HA::TBX-2(LKIE/VKKE->AAAA)::GAL4 fusion in mammalian cells.
pOK254.01	*mls-1* rescue plasmid with an mCherry gene inserted at the C-terminus of *mls-1*.
pOK257.02	Plasmid is a BiFC cloning vector containg C-terminal fragment of Venus FP. In order, it is HSP > HA Tag > MCS > Venus C-terminal fragment. Insert protein coding sequence of interest in MCS. Obtained from Dr. Hu's lab at Purdue July 2009.
pOK261.03	*tbx-2* mutant for SUMO sites 1 (LKIE->LRIE) and 2 (VKKE->VRKE) in pCDNA3.1/V5/His Topo. For expressing double conservative mutant TBX-2::V5::His fusion in mammalian cells.
pOK263.01	*tbx-2* mutant for SUMO site 1 (LKIE->LRIE) cloned into pCDNA3.1/V5/His Topo. For expressing mutant TBX-2::V5::His fusion in mammalian cells.
pOK263.05	Mutated pCDNA HA/SUMO1. For expressing HA::SUMO1(ΔGG) in mammalian cells.
pOK266.11	Plasmid is a BiFC cloning vector containg C-terminal fragment of Venus FP and *tbx-2* cDNA. In order it is HSP > HA Tag > *tbx-2* cDNA > Venus C-terminal fragment. Parental vector from Hu lab at Purdue.
pOK267.10	*smo-1* without diglycines was amplified from pOK261.07 with PO1088 and PO1089/bglII, salI and cloned into pOK266.04/BglII/XhoI (BifC vector for N-terminal labeling with VN173 and myc). Clone contains Phsp::myc::VN173::flexible linker:: *smo-1* in MCS::*unc-54* 3'UTR.
pOK269.04	Gal4::5xtk::luciferase reporter plasmid for luciferase assays.
pOK269.07	pGEX-4T2 cloning vector, containing the DNA binding domain of *tbx-2*.
pOK269.09	CMV-Beta-Gal plasmid for normalizing luciferase assays.
pOK271.13	*ser-7b* promoter driving expression of FLAG tagged Poly A Binding protein. This construct was generated by cloning ser-7b promoter from pOK271.09 into pOK264.17/pSV41 destination vector using gateway LR reaction.
pOK280.01	pT-E1E2SUMO1(T95K) from Goldstein lab for expression in *E. coli*.
pOK280.02	pET28 His-TEV K2P1 (270-336) 1D4 vector from Goldstein lab. For expression in *E. coli*.

pOK281.07	Vector for expressing His:TBX-2 in bacterial cells. Made by subcloning spe1/xho1 fragment of pOK241.07 into avrII/xho1 of pOK280.02.
pOK283.03	HA::mCherry::TBX-2 driven by heat shock promoter. For expression in worms, created using INFUSION reaction. mCherry and TBX-2 inserts amplified from plasmids pOK254.01 and pOK241.07, respectively, using primers PO1299/PO1301 and PO1300/PO1302, respectively, and cloned by INFUSION enzyme into pOK257.02 after digesting it with EcoRI and EcoRV. Sequenced through both inserts.
pOK283.04	HA::mCherry::TBX-2(LKIE/VKKE to AAAA) driven by heat shock promoter. For expression in worms, created using INFUSION reaction. mCherry and TBX-2 inserts amplified from plasmids pOK254.01 and pOK241.19, respectively, using primers PO1299/PO1301 and PO1300/PO1302, respectively, and cloned by INFUSION enzyme into pOK257.02 after digesting it with EcoRI and EcoRV. Sequenced through both inserts.
pOK283.05	HA::mCherry driven by heat shock promoter. For expression in worms, created using INFUSION reaction. mCherry insert amplified from pOK254.01 using primers PO1299/PO1303 and cloned by INFUSION enzyme into pOK257.02 after digesting it with EcoRI and EcoRV. Sequenced through mCherry insert.
pOK286.01	pOK267.10 was mutagenized to insert a TAG (stop codon) just before C-terminal Gly-Gly motif. Clone contains Phsp::myc::VN173::flexible linker:: *smo-1*(ΔGG) in MCS::*unc-54* 3'UTR. Verified by sequencing.
pOK291.01	*D2096.6::gfp::his2B* received from Jeb Gaudet, constructed from pAP.10. Contains about 1 kb of upstream sequence and also *unc-119(+)* from pOK271.13.
pOK291.03	*tbx-2::gfp* translational fusion in exon 1 directly downstream of *tbx-2* ATG. *tbx-2* promoter amplified from pOK203.02 with PO752/754, cut with Pst-BglII and inserted into Pst-Bam sites of pPD95.69, also contains *unc-119(+)* from pOK271.13 via AflII and Sph1.
pOK293.03	Originally plasmid pOK251.04, pCDNA HA/Gal4(1-100), the HA/GAL4(1-100) was removed by restriction digest with Pme1 for use in reporter alone samples in luciferase assays.

pOK294.01	HA::mCherry::TBX-2 (VKKE->VRKE) driven by heat shock promoter. For expression in worms, created using INFUSION reaction. mCherry and TBX-2 inserts amplified from plasmids pOK254.01 and pOK244.14, respectively, using primers PO1299/PO1301 and PO1300/PO1302, respectively, and cloned by INFUSION enzyme into pOK257.02 after digesting it with EcoRI and EcoRV. Sequenced through both inserts.
pOK313.01	pNH034, contains RT cassette for recombineering.
pOK313.02	pBAC-RT, contains RT cassette for recombineering.
pOK313.03	*ubc-9* in L4440 vector for feeding RNAi.
pOK313.04	*smo-1* in L4440 vector for feeding RNAi.
pOK313.05	*tbx-2::ty1::eGFP::FLAG* fosmid with *unc-119(+)* rescue cassette.
pOK313.06	*tbx-2(VKRE mut)::ty1::eGFP::FLAG* fosmid with *unc-119(+)* rescue cassette.
pOK313.07	*tbx-2(eh1 site mutant)::ty1::eGFP::FLAG* fosmid with *unc-119(+)* rescue cassette.
pOK323.06	peGFP-N3. for GFP expression in mammalian cells.
pOK323.08	pUbFC-YN173::SUMO-1
pOK323.09	pBIFC-Jun::CC155

APPENDIX I - *C. ELEGANS* STRAINS

TABLE XIII – C. ELEGANS STRAINS USED IN THIS STUDY

Strain	Genotype	Description
CB262	*unc-37(e262)I*	Worms display extreme Col/Unc phenotype (pile o' worms). Maintain strain by passaging at 25°C.
DP38	*unc-119(ed3) III; daf-?.*	Unc. Contains an unlinked dauer constitutive mutation. See HT1593 for a stock with the Daf mutation removed.
NX25	*smo-1(ok359);tvEx25[psmo-1::His-FLAG-SMO-1; rol-6]*	*smo-1* mutant rescued with integrated his-tagged *smo-1* construct (from Limor Broday).
OK0460	*tbx-2(ok529)/dpy-17(e164) unc-32(e189)*	Balanced hermaphrodite segregating WT heterozygotes, dpy unc, and *ok529* homozygotes.
OK0507	*cuIs21 III*	*ceh-22::gfp* integrated strain expressing nuclear localized GFP integrated from OK0469 by EMS mutagenesis. Out-crossed 2x to N2. Segregates almost 100% rollers. Maintain by picking rollers.
OK0640	*cuIs31 X*	*ceh-22::gfp* plasmid (pOK185.01) integrated from cuEx355. Nuclear GFP, pick rollers.
OK0660	*tbx-2(bx59) III*	*tbx-2* mutant outcrossed from *him-5(e1490).* Wild type at 16°C, weak temperature sensitive at 25°C.
OK0666	*cuEx553*	Plasmid constructed from pAP.10 contains 1kb of *D2096.6* upstream sequence (obtained from Jeb Gaudet). WT carrying *D2096.6::gfp::his2B* (2ng/ul) and *pRF4* (100ng/ul) as an extrachromosomal array (plasmid pOK253.05), segregates 50% rollers.
OK0692	*tbx-2(bx59)III; cuEx553*	Wild type at 16°C, weak temperature sensitive at 25°C, carrying *D2096.6::gfp::his2B* (2ng/ul) and *pRF4* (100ng/ul) as an extrachromosomal array (plasmid pOK253.05).

OK0741	*tbx-2(ok529)/dpy-17(e164) unc-32(e189); cuEx553*	OK0460 crossed into OK0666 carrying *D2096.6::gfp::his2B* (2ng/ul) and *pRF4* (100ng/ul) as extrachromosomal array (pOK253.05). Balanced hermaphrodite segregating WT heterozygotes, dpy unc, and *ok529* homozygotes, passage WT rollers.
OK0794	*cuEx638*	N2 worms injected with 2.5ng/ul pOK267.10 (VN173::SMO-1), 2.5ng/ul pOK266.11 (HA::TBX-2::VC155), and 100ng/ul *pRF4*. Pick rollers. Heat shock for Venus expression. Maintain at 20°C.
OK0795	*cuEx639*	N2 worms injected with 2.5ng/ul pOK267.10 (VN173::SMO-1), 2.5ng/ul pOK266.11 (HA::TBX-2::VC155), and 100ng/ul *pRF4*. Pick rollers. Heat shock for Venus expression. Maintain at 20°C.
OK0796	*cuEx640*	N2 worms injected with 2.5ng/ul pOK267.10 (VN173::SMO-1), 2.5ng/ul pOK266.11 (HA::TBX-2::VC155), and 100ng/ul pRF4. Pick rollers. Heat shock for Venus expression. Maintain at 20°C.
OK0873	*tbx-2(ok529); wgIs159*	*tbx-2(ok529)* rescued by the *wgIs159* allele (expressing fosmid containing TBX-2::TY1::GFP::FLAG). Worms look w/t, may still have *unc-119(ed3)* from OP159 strain.
OK0874	*smo-1(ok359); wgIs159; tvEx25*	*smo-1(ok359); wgIs159* homozygotes, with extrachromosomal array *tvEx25* (containing *psmo-1*:: HIS-FLAG-*smo-1*), *wgIs159* expresses fosmid with TBX-2::TY1-GFP-FLAG fusion. Pick rollers.
OK0875	*cuEx698*	N2 worms injected with 2.5ng/ul pOK267.10 (VN173::SMO-1), 2.5ng/ul pOK271.07 (HA::TBX-2(LKIE/VKKE->AAAA)::VC155), and 100ng/ul *pRF4*. Pick rollers. Heat shock for Venus expression. Maintain at 20°C.
OK0876	*cuEx699*	N2 worms injected with 2.5ng/ul pOK286.01 (VN173::SMO-1(ΔGG), 2.5ng/ul pOK271.07 (HA::TBX-2::VC155), and 100ng/ul *pRF4*. Pick rollers. Heat shock for Venus expression. Maintain at 20°C.

OK0877	*cuEx700*	N2 worms injected with 2.5ng/ul pOK286.01 (VN173::SMO-1(ΔGG), 2.5ng/ul pOK271.07 (HA::TBX-2::VC155), and 100ng/ul *pRF4*. Pick rollers. Heat shock for Venus expression. Maintain at 20°C.
OK0878	*cuEx701*	N2 worms injected with 2.5 ng/ul pOK283.05 (HA::mCherry), 2.5 ng/ul pOK253.05 (D2096.6::gfp), and 100 ng/ul pRF4. HS for mCherry expression, pick rollers. Maintain at 20°C.
OK0879	*cuEx702*	N2 worms injected with 2.5 ng/ul pOK283.05 (HA::mCherry), 2.5 ng/ul pOK253.05 (*D2096.6::gfp*), and 100 ng/ul *pRF4*. HS for mCherry expression, pick rollers. Maintain at 20°C.
OK0880	*cuEx703*	N2 worms injected with 2.5 ng/ul pOK283.03 (HA::mCherry::TBX-2), 2.5 ng/ul pOK253.05 (*D2096.6::gfp*), and 100 ng/ul *pRF4*. HS for mCherry expression, pick rollers. Maintain at 20°C.
OK0881	*cuEx704*	N2 worms injected with 2.5 ng/ul pOK283.03 (HA::mCherry::TBX-2), 2.5 ng/ul pOK253.05 (*D2096.6::gfp*), and 100 ng/ul *pRF4*. HS for mCherry expression, pick rollers. Maintain at 20°C.
OK0882	*cuEx705*	N2 worms injected with 2.5 ng/ul pOK283.04 (HA::mCherry::TBX-2(LKIE/VKKE to AAAA)), 2.5 ng/ul pOK253.05 (*D2096.6::gfp*), and 100 ng/ul *pRF4*. HS for mCherry expression, pick rollers. Maintain at 20°C.
OK0883	*cuEx706*	N2 worms injected with 2.5 ng/ul pOK283.04 (HA::mCherry::TBX-2(LKIE/VKKE to AAAA)), 2.5 ng/ul pOK253.05 (*D2096.6:gfp*), and 100 ng/ul *pRF4*. HS for mCherry expression, pick rollers. Maintain at 20°C.
OK0981	*cuEx797*	N2 worms injected with 2.5 ng/ul pOK283.05 (HA::mCherry) and 100ng/ul *pRF4*. Heat shock for mCherry expression, pick rollers. Maintain at 20°C.

OK0982	*cuEx798*	N2 worms injected with 2.5 ng/ul pOK283.05 (HA::mCherry) and 100ng/ul *pRF4*. Heat shock for mCherry expression, pick rollers. Maintain at 20°C.
OK0983	*cuEx799*	N2 worms injected with 2.5 ng/ul pOK283.05 (HA::mCherry) and 100ng/ul *pRF4*. Heat shock for mCherry expression, pick rollers. Maintain at 20°C.
OK0984	*cuEx800*	N2 worms injected with 2.5 ng/ul pOK283.03 (HA::mCherry::TBX-2) and 100ng/ul *pRF4*. Heat shock for mCherry expression, pick rollers. Maintain at 20°C.
OK0985	*cuEx801*	N2 worms injected with 2.5 ng/ul pOK283.04 (HA::mCherry::TBX-2 (LKIE/VKKE to AAAA)) and 100ng/ul *pRF4*. Heat shock for mCherry expression, pick rollers. Maintain at 20°C.
OK0986	*cuEx802*	N2 worms injected with 2.5 ng/ul pOK294.01 (HA::mCherry:TBX-2 (VKKE to VRKE)) and 100ng/ul *pRF4*. Heat shock for mCherry expression, pick rollers. Maintain at 20°C.
OK0987	*wgIs159 II; stIs10226 IV*	modEncode *tbx-2::gfp* in the *wgIs159* allele is a fosmid encoding for a TBX-2::TY1::GFP::FLAG fusion. Ubiquitous histone-mCherry expression from *stIs10226* [*his-72* promoter expressing HIS-24::mCherry translational fusion with *let-858* 3' UTR + *unc-119(+)*]. May also have *itIs37* [*pie-1:mCherry::H2B*].
OK0998	*cuIs34; unc-119(ed3) III*	*unc-119* worms carrying pOK291.03 (*Ptbx-2::gfp*), 4 kb of *tbx-2* promoter fragment driving expression of GFP, also carries *unc-119(+)*, obtained by microparticle bombardment. *cuIs34* allele causes slight egl phenotype. Passage non Uncs.
OK0999	*cuIs35; unc-119(ed3) III*	*unc-119* worms carrying pOK291.01 (*D2096.6::gfp*), *D2096.6* promoter driving expression of GFP, also carries *unc-119(+)*, obtained by microparticle bombardment. Passage non Uncs.

OK1000	*cuIs35; unc-119(ed3) III; cuEx799*	*unc-119* worms carrying pOK291.01 (*D2096.6::gfp*), *D2096.6* promoter driving expression of GFP, also carries *unc-119(+)*, obtained by microparticle bombardment. Crossed into worms injected with 2.5 ng/ul pOK283.05 (HA::mCherry) and 100ng/ul *pRF4*. Heat shock for mCherry expression, pick rollers. Maintain at 20°C. Not sure if this strain still has *unc-119(ed3)*.
OK1001	*cuIs35; unc-119(ed3) III; cuEx800*	*unc-119* worms carrying pOK291.01 (*D2096.6::gfp*), *D2096.6* promoter driving expression of GFP, also carries *unc-119(+)*, obtained by microparticle bombardment. Crossed into worms injected with 2.5 ng/ul pOK283.03 (HA::mCherry::TBX-2) and 100ng/ul *pRF4*. Heat shock for mCherry expression, pick rollers. Maintain at 20°C. Not sure if this strain still has *unc-119(ed3)*.
OK1002	*cuIs35; unc-119(ed3) III; cuEx801*	*unc-119* worms carrying pOK291.01 (*D2096.6::gfp*), *D2096.6* promoter driving expression of GFP, also carries *unc-119(+)*, obtained by microparticle bombardment. Crossed into worms injected with 2.5 ng/ul pOK283.04 (HA::mCherry::TBX-2 (LKIE/VKKE to AAAA)) and 100ng/ul *pRF4*. Heat shock for mCherry expression, pick rollers. Maintain at 20°C. Not sure if this strain still has *unc-119(ed3)*.
OK1003	*cuIs35; unc-119(ed3) III; cuEx802*	*unc-119* worms carrying pOK291.01 (*D2096.6::gfp*), *D2096.6* promoter driving expression of GFP, also carries *unc-119(+)*, obtained by microparticle bombardment. Crossed into worms injected with 2.5 ng/ul pOK294.01 (HA::mCherry::TBX-2 (VKKE to VRKE)) and 100ng/ul *pRF4*. Heat shock for mCherry expression, pick rollers. Maintain at 20°C. Not sure if this strain still has *unc-119(ed3)*.

OK1004	*cuIs34; unc-119(ed3) III; cuEx799*	*unc-119* worms carrying pOK291.03 (*Ptbx-2::gfp*), 4 kb *tbx-2* promoter fragment driving expression of GFP, also carries *unc-119(+)*, obtained by microparticle bombardment. Crossed into worms injected with 2.5 ng/ul pOK283.05 (HA::mCherry) and 100ng/ul *pRF4*. Heat shock for mCherry expression, pick rollers. Maintain at 20°C. Not sure if this strain still has *unc-119(ed3)*.
OK1005	*cuIs34; unc-119(ed3) III; cuEx800*	*unc-119* worms carrying pOK291.03 (*Ptbx-2::gfp*), 4 kb *tbx-2* promoter fragment driving expression of GFP, also carries *unc-119(+)*, obtained by microparticle bombardment. Crossed into worms injected with 2.5 ng/ul pOK283.03 (HA::mCherry::TBX-2) and 100ng/ul *pRF4*. Heat shock for mCherry expression, pick rollers. Maintain at 20°C. Not sure if this strain still has *unc-119(ed3)*.
OK1006	*cuIs34; unc-119(ed3) III; cuEx801*	*unc-119* worms carrying pOK291.03 (*Ptbx-2::gfp*), 4 kb *tbx-2* promoter fragment driving expression of GFP, also carries *unc-119(+)*, obtained by microparticle bombardment. Crossed into worms injected with 2.5 ng/ul pOK283.04 (HA::mCherry::TBX-2 (LKIE/VKKE to AAAA)) and 100ng/ul *pRF4*. Heat shock for mCherry expression, pick rollers. Maintain at 20°C. Not sure if this strain still has *unc-119(ed3)*.
OK1007	*cuIs34; unc-119(ed3) III; cuEx802*	*unc-119* worms carrying pOK291.03 (*Ptbx-2::gfp*), 4 kb *tbx-2* promoter fragment driving expression of GFP, also carries *unc-119(+)*, obtained by microparticle bombardment. Crossed into worms injected with 2.5 ng/ul pOK294.01 (HA::mCherry::TBX-2 (VKKE to VRKE)) and 100ng/ul *pRF4*. Heat shock for mCherry expression, pick rollers. Maintain at 20°C. Not sure if this strain still has *unc-119(ed3)*.
OK1008	*cuEx806*	N2 worms injected with 2.5 ng/ul pOK295.03 (HA::mCherry::TBX-2(eh1 site mutant)) and 100ng/ul *pRF4.* Heat shock for mCherry expression, pick rollers. Maintain at 20°C.

OK1009	*cuEx807*	N2 worms injected with 2.5 ng/ul pOK295.03 (HA::mCherry::TBX-2(eh1 site mutant)) and 100ng/ul *pRF4.* Heat shock for mCherry expression, pick rollers. Maintain at 20°C.
OK1010	*unc-119(ed3) III; wgIs159 II; cuEx800*	*unc-119* worms homozygous for *wgIs159* allele, expresses a fosmid containing a TBX-2::TY1::GFP::FLAG fusion. Crossed into worms injected with 2.5 ng/ul pOK283.03 (HA::mCherry::TBX-2) and 100ng/ul *pRF4*. Heat shock for mCherry expression, pick rollers. Maintain at 20°C. Not sure if this strain still has *unc-119(ed3)*.
OK1011	*cuIs35; unc-119(ed3) III; cuEx806*	*unc-119* worms carrying pOK291.01 (*D2096.6::gfp*), *D2096.6* promoter driving expression of GFP, also carries *unc-119(+)*, obtained by microparticle bombardment. Crossed into worms injected with 2.5 ng/ul pOK295.03 (HA::mCherry::TBX-2 (eh1 site mutant)) and 100ng/ul *pRF4*. Heat shock for mCherry expression, pick rollers. Maintain at 20°C. Not sure if this strain still has *unc-119(ed3).*
OK1012	*unc-119(ed3) III; wgIs159 II; cuEx806*	*unc-119* worms homozygous for *wgIs159* allele, expresses a fosmid containing a TBX-2::TY1::GFP::FLAG fusion. Crossed into worms injected with 2.5 ng/ul pOK295.03 (HA::mCherry::TBX-2 (eh1 site mutant)) and 100ng/ul *pRF4.* Heat shock for mCherry expression, pick rollers. Maintain at 20°C. Not sure if this strain still has *unc-119(ed3).*
OK1024	*unc-37(e262)I; wgIs159 II; unc-119(ed3)III*	homozygous for *wgIs159* allele, expresses a fosmid containing a TBX-2::TY1::GFP::FLAG fusion. *unc-119(ed3)* mutation may have been lost in cross into *unc-37(e262)*. *unc-37* mutation causes worms to display extreme Col/Unc phenotype. Maintain strain by passaging at 25°C.

OK1025	*cuIs34; unc-37(e262)I; unc-119(ed3) III*	homozygous for *cuIs34* allele (*Ptbx-2::gfp*), 4 kb *tbx-2* promoter fragment driving expression of GFP, also carries *unc-119(+)*. *cuIs34* allele causes slight egl phenotype. *unc-119(ed3)* mutation may have been lost in cross into *unc-37(e262)*. *unc-37* mutation causes worms to display extreme Col/Unc phenotype. Maintain strain by passaging at 25°C.
OK1026	*cuIs35; unc-37(e262)I; unc-119(ed3) III*	homozygous for *cuIs35* allele (*D2096.6::gfp*), *D2096.6* promoter driving expression of GFP, also carries *unc-119(+)*. *unc-119(ed3)* mutation may have been lost in cross with *unc-37(e262)*. *unc-37* mutation causes worms to display extreme Col/Unc phenotype (pile o' worms). Maintain strain by passaging at 25°C.
OK1033	*unc-37(e262) I; tbx-2(bx59) III*	*unc-37* mutation causes worms to display extreme Col/Unc phenotype. *tbx-2* mutant outcrossed from *him-5(e1490)*. Temperature sensitive lethality at 25°C, all animals will perish. Pick hermaphrodites and maintain at 16°C.
OK1034	*unc-119(ed3) III; cuIs38*	*unc-119* worms carrying pOK313.05 (TBX-2::TY1::GFP::FLAG fosmid with *unc-119(+)*), obtained by microparticle bombardment. Not on chromosome III, confirmed by mapping, and rescues *ok529*.
OK1035	*unc-119(ed3)III; cuEx808*	*unc-119* worms carrying pOK313.05 (TBX-2::TY1::GFP::FLAG fosmid with *unc-119(+)*), obtained by microparticle bombardment, but appears to be extrachromosomal, segregates 50% non-unc/GFP (+) worms.
OK1036	*unc-119(ed3)III; cuEx809*	*unc-119* worms carrying pOK313.05 (TBX-2::TY1::GFP::FLAG fosmid with *unc-119(+)*), obtained by microparticle bombardment, appears to be extrachromosomal, segregates 50% non-unc/GFP (+) worms.
OK1037	*unc-119(ed3)III; cuEx810*	*unc-119* worms carrying pOK313.05 (TBX-2::TY1::GFP::FLAG fosmid with *unc-119(+)*), obtained by microparticle bombardment, appears to be extrachromosomal, segregates 70% non-unc/GFP (+) worms.

OK1038	*unc-119(ed3)III; cuEx811*	*unc-119* worms carrying pOK313.06 (TBX-2(VRKE)::TY1::GFP::FLAG fosmid with *unc-119(+)*), obtained by microparticle bombardment, appears to be extrachromosomal, segregates 30% non-unc/GFP (+) worms.
OK1039	*unc-119(ed3)III; cuIs39*	*unc-119* worms carrying pOK313.06 (TBX-2(VRKE)::TY1::GFP::FLAG fosmid with *unc-119(+)*), obtained by microparticle bombardment, not on chromosome III, confirmed by mapping.
OK1040	*unc-119(ed3)III; cuEx812*	*unc-119* worms carrying pOK313.06 (TBX-2(VRKE)::TY1::GFP::FLAG fosmid with *unc-119(+)*), obtained by microparticle bombardment, appears to be extrachromosomal, segregates 60% non-unc/GFP (+) worms.
OK1041	*unc-119(ed3)III; cuEx813*	*unc-119* worms carrying pOK313.06 (TBX-2(VRKE)::TY1::GFP::FLAG fosmid with *unc-119(+)*), obtained by microparticle bombardment, appears to be extrachromosomal, segregates 60% non-unc/GFP (+) worms.
OK1042	*unc-119(ed3)III; cuIs40*	*unc-119* worms carrying pOK313.07 (TBX-2(eh1 site mutant)::TY1::GFP::FLAG fosmid with *unc-119(+)*), obtained by microparticle bombardment, on chromosome III, confirmed by mapping. Oddly enough, this strain seems to exhibit temperature sensitivity at 25°C, passage at 16°C.
OK1043	*unc-119(ed3)III; cuEx814*	*unc-119* worms carrying pOK313.07 (TBX-2(eh1 site mutant)::TY1::GFP::FLAG fosmid with *unc-119(+)*), obtained by microparticle bombardment, appears extrachromosomal, segregates 80% non-unc/GFP (+) worms.
OK1044	*tbx-2(ok529) III; cuIs38*	*tbx-2(ok529)* mutant phenotype rescued by *cuIs38* allele, *cuIs38* allele expresses fosmid with TBX-2::TY1::GFP::FLAG fusion, pOK313.05. Worms look w/t.

OK1051	*tbx-2(ok529) III; cuIs39*	*tbx-2(ok529)* mutant phenotype rescued by *cuIs39* allele, *cuIs39* allele expresses fosmid with TBX-2(VRKE)::TY1::GFP::FLAG fusion, pOK313.06. Worms look w/t.
OK1052	*dpy-17(e164) unc-32(e189) III; cuEx814*	dpy unc worms carrying pOK313.07 (TBX-2(eh1 site mutant)::TY1::GFP::FLAG fosmid with *unc-119(+)*), obtained by microparticle bombardment, appears extrachromosomal, segregates 80% GFP (+) worms. Maintain by passaging GFP (+) dpy unc worms.
OK1053	*glp-1(e2141) III; cuIs31*	*glp-1* mutant, temperature sensitive lethal at 25°C, *cuIs31* carries a nuclear-localized and integrated *ceh-22::gfp* (plasmid 185.01) on chromosome X. Pick rollers, maintain at 16°C.
OK1054	*tbx-2(ok529) III; cuEx814*	*tbx-2(ok529)* mutant phenotype rescued by *cuEx814* array, which carries pOK313.07 (TBX-2(eh1 site mutant)::TY1::GFP::FLAG fosmid with *unc-119(+)*). Many arrest as embryos, less than 10% of worms grow past L1 larval stage.
OK1055	*unc-37(e262) I; tbx-2(bx59) III; cuIs31/+ X*	*unc-37* mutation causes worms to display extreme Col/Unc phenotype. *tbx-2* mutant outcrossed from *him-5(e1490)*. Temperature sensitive lethality at 25°C, all animals will perish. Heterozygous for *cuIs31*, which carries a nuclear-localized and integrated *ceh-22::gfp* (plasmid 185.01) on chromosome X. Pick rolling GFP (+) hermaphrodites and maintain at 16°C.
OK1056	*dpy-17(e164) unc-32(e189) III; cuEx808*	dpy unc worms carrying pOK313.05 (TBX-2::TY1::GFP::FLAG fosmid with *unc-119(+)*), obtained by microparticle bombardment, appears extrachromosomal, segregates 50% GFP (+) worms. Maintain by passaging GFP (+) dpy unc worms.
OK1057	*dpy-17(e164) unc-32(e189) III; cuEx809*	dpy unc worms carrying pOK313.05 (TBX-2::TY1::GFP::FLAG fosmid with *unc-119(+)*), obtained by microparticle bombardment, appears extrachromosomal, segregates 50% GFP (+) worms. Maintain by passaging GFP (+) dpy unc worms.

OK1058	*dpy-17(e164) unc-32(e189) III; cuEx810*	dpy unc worms carrying pOK313.05 (TBX-2::TY1::GFP::FLAG fosmid with *unc-119(+)*), obtained by microparticle bombardment, appears extrachromosomal, segregates 70% GFP (+) worms. Maintain by passaging GFP (+) dpy unc worms.
OK1061	*tbx-2(ok529) III; cuEx809*	*tbx-2(ok529)* mutant phenotype rescued by *cuEx809* array, which carries pOK313.05 (TBX-2::TY1::GFP::FLAG fosmid with *unc-119(+)*). Many arrest as embryos.
OK1065	*tbx-2(ok529) III; cuEx810*	*tbx-2(ok529)* mutant phenotype rescued by *cuEx810* array, which carries pOK313.05 (TBX-2::TY1::GFP::FLAG fosmid with *unc-119(+)*). Many arrest as embryos.
OP159	*unc-119(ed3); wgIs159*	Homozygous for *wgIs159* allele, carries a fosmid containing TBX-2::TY1::GFP::FLAG fusion and *unc-119(+)*. Worms look w/t, *wgIs159* mapped to chromosome II.
RW10226	*unc-119(ed3) III; stIs10226; itIs37*	Ubiquitous histone-cherry expression suitable for lineage analysis. *itIs37*[*pie-1::mCherry::H2B-pie-1 3'*UTR + *unc-119(+)*]. *stIs10226*[*his-72* promoter driving HIS-24::mCherry translational fusion with *let-858* 3' UTR + *unc-119(+)*]. Mapped to chromosome IV.
SP1052	*dpy-13(e184) unc-5(e53) IV*	dpy unc

APPENDIX J - COPYRIGHT

GNC Free Documentation License

0. PREAMBLE

The purpose of this License is to make a manual, textbook, or other functional and useful document "free" in the sense of freedom: to assure everyone the effective freedom to copy and redistribute it, with or without modifying it, either commercially or noncommercially. Secondarily, this License preserves for the author and publisher a way to get credit for their work, while not being considered responsible for modifications made by others.

This License is a kind of "copyleft", which means that derivative works of the document must themselves be free in the same sense. It complements the GNU General Public License, which is a copyleft license designed for free software.

We have designed this License in order to use it for manuals for free software, because free software needs free documentation: a free program should come with manuals providing the same freedoms that the software does. But this License is not limited to software manuals; it can be used for any textual work, regardless of subject matter or whether it is published as a printed book. We recommend this License principally for works whose purpose is instruction or reference.

1. APPLICABILITY AND DEFINITIONS

This License applies to any manual or other work, in any medium, that contains a notice placed by the copyright holder saying it can be distributed under the terms of this License. Such a notice grants a world-wide, royalty-free license, unlimited in duration, to use that work under the conditions stated herein. The "Document", below, refers to any such manual or work. Any member of the public is a licensee, and is addressed as "you". You accept the license if you copy, modify or distribute the work in a way requiring permission under copyright law.

A "Modified Version" of the Document means any work containing the Document or a portion of it, either copied verbatim, or with modifications and/or translated into another language.

A "Secondary Section" is a named appendix or a front-matter section of the Document that deals exclusively with the relationship of the publishers or authors of the Document to the Document's overall subject (or to related matters) and contains nothing that could fall directly within that overall subject. (Thus, if the Document is in part a textbook of mathematics, a Secondary Section may not explain any mathematics.) The relationship could be a matter of historical connection with the subject or with related matters, or of legal, commercial, philosophical, ethical or political position regarding them.

The "Invariant Sections" are certain Secondary Sections whose titles are designated, as being those of Invariant Sections, in the notice that says that the Document is released under this License. If a section does not fit the above definition of Secondary then it is not allowed to be designated as Invariant. The Document may contain zero Invariant Sections. If the Document does not identify any Invariant Sections then there are none.

The "Cover Texts" are certain short passages of text that are listed, as Front-Cover Texts or Back-Cover Texts, in the notice that says that the Document is released under this License. A Front-Cover Text may be at most 5 words, and a Back-Cover Text may be at most 25 words.

A "Transparent" copy of the Document means a machine-readable copy, represented in a format whose specification is available to the general public, that is suitable for revising the document straightforwardly with generic text editors or (for images composed of pixels) generic paint programs or (for drawings) some widely available drawing editor, and that is suitable for input to text formatters or for automatic translation to a variety of formats suitable for input to text formatters. A copy made in an otherwise Transparent file format whose markup, or absence of markup, has been arranged to thwart or discourage subsequent modification by readers is not Transparent. An image format is not Transparent if used for any substantial amount of text. A copy that is not "Transparent" is called "Opaque".

Examples of suitable formats for Transparent copies include plain ASCII without markup, Texinfo input format, LaTeX input format, SGML or XML using a publicly available DTD, and standard-conforming simple HTML, PostScript or PDF designed for human modification. Examples of transparent image formats include PNG, XCF and JPG. Opaque formats include proprietary formats that can be read and edited only by proprietary word processors, SGML or XML for which the DTD and/or processing tools are not generally available, and the machine-generated HTML, PostScript or PDF produced by some word processors for output purposes only.

The "Title Page" means, for a printed book, the title page itself, plus such following pages as are needed to hold, legibly, the material this License requires to appear in the title page. For works in formats which do not have any title page as such, "Title Page" means the text near the most prominent appearance of the work's title, preceding the beginning of the body of the text.

A section "Entitled XYZ" means a named subunit of the Document whose title either is precisely XYZ or contains XYZ in parentheses following text that translates XYZ in another language. (Here XYZ stands for a specific section name mentioned below, such as "Acknowledgements", "Dedications", "Endorsements", or "History".) To "Preserve the Title" of such a section when you modify the Document means that it remains a section "Entitled XYZ" according to this definition.

The Document may include Warranty Disclaimers next to the notice which states that this License applies to the Document. These Warranty Disclaimers are considered to be included by reference in this License, but only as regards disclaiming warranties: any other implication that these Warranty Disclaimers may have is void and has no effect on the meaning of this License.

2. VERBATIM COPYING

You may copy and distribute the Document in any medium, either commercially or noncommercially, provided that this License, the copyright notices, and the license notice saying this License applies to the Document are reproduced in all copies, and that you add no other conditions whatsoever to those of this License. You may not use technical measures to obstruct or control the reading or further copying of the copies you make or distribute. However, you may accept compensation in exchange for copies. If you distribute a large enough number of copies you must also follow the conditions in section 3.

You may also lend copies, under the same conditions stated above, and you may publicly display copies.

3. COPYING IN QUANTITY

If you publish printed copies (or copies in media that commonly have printed covers) of the Document, numbering more than 100, and the Document's license notice requires Cover Texts, you must enclose the copies in covers that carry, clearly and legibly, all these Cover Texts: Front-Cover Texts on the front cover, and Back-Cover Texts on the back cover. Both covers must also clearly and legibly identify you as the publisher of these copies. The front cover must present the full title with all words of the title equally prominent and visible. You may add other material on the covers in addition. Copying with changes limited to the covers, as long as they preserve the title of the Document and satisfy these conditions, can be treated as verbatim copying in other respects.

If the required texts for either cover are too voluminous to fit legibly, you should put the first ones listed (as many as fit reasonably) on the actual cover, and continue the rest onto adjacent pages.

If you publish or distribute Opaque copies of the Document numbering more than 100, you must either include a machine-readable Transparent copy along with each Opaque copy, or state in or with each Opaque copy a computer-network location from which the general network-using public has access to download using public-standard network protocols a complete Transparent copy of the Document, free of added material. If you use the latter option, you must take

reasonably prudent steps, when you begin distribution of Opaque copies in quantity, to ensure that this Transparent copy will remain thus accessible at the stated location until at least one year after the last time you distribute an Opaque copy (directly or through your agents or retailers) of that edition to the public.

It is requested, but not required, that you contact the authors of the Document well before redistributing any large number of copies, to give them a chance to provide you with an updated version of the Document.

4. MODIFICATIONS

You may copy and distribute a Modified Version of the Document under the conditions of sections 2 and 3 above, provided that you release the Modified Version under precisely this License, with the Modified Version filling the role of the Document, thus licensing distribution and modification of the Modified Version to whoever possesses a copy of it. In addition, you must do these things in the Modified Version:

- A. Use in the Title Page (and on the covers, if any) a title distinct from that of the Document, and from those of previous versions (which should, if there were any, be listed in the History section of the Document). You may use the same title as a previous version if the original publisher of that version gives permission.
- B. List on the Title Page, as authors, one or more persons or entities responsible for authorship of the modifications in the Modified Version, together with at least five of the principal authors of the Document (all of its principal authors, if it has fewer than five), unless they release you from this requirement.
- C. State on the Title page the name of the publisher of the Modified Version, as the publisher.
- D. Preserve all the copyright notices of the Document.
- E. Add an appropriate copyright notice for your modifications adjacent to the other copyright notices.
- F. Include, immediately after the copyright notices, a license notice giving the public permission to use the Modified Version under the terms of this License, in the form shown in the Addendum below.
- G. Preserve in that license notice the full lists of Invariant Sections and required Cover Texts given in the Document's license notice.
- H. Include an unaltered copy of this License.
- I. Preserve the section Entitled \"History\", Preserve its Title, and add to it an item stating at least the title, year, new authors, and publisher of the Modified Version as given on the Title Page. If there is no section Entitled \"History\" in the Document, create one stating the title, year, authors, and publisher of the Document as given on its Title Page, then add an item describing the Modified Version as stated in the previous sentence.
- J. Preserve the network location, if any, given in the Document for public access to a Transparent copy of the Document, and likewise the network locations given in the Document for previous versions it was based on. These may be placed in the \"History\" section. You may omit a network location for a work that was published at least four

years before the Document itself, or if the original publisher of the version it refers to gives permission.

- K. For any section Entitled \"Acknowledgements\" or \"Dedications\", Preserve the Title of the section, and preserve in the section all the substance and tone of each of the contributor acknowledgements and/or dedications given therein.
- L. Preserve all the Invariant Sections of the Document, unaltered in their text and in their titles. Section numbers or the equivalent are not considered part of the section titles.
- M. Delete any section Entitled \"Endorsements\". Such a section may not be included in the Modified Version.
- N. Do not retitle any existing section to be Entitled \"Endorsements\" or to conflict in title with any Invariant Section.
- O. Preserve any Warranty Disclaimers.

If the Modified Version includes new front-matter sections or appendices that qualify as Secondary Sections and contain no material copied from the Document, you may at your option designate some or all of these sections as invariant. To do this, add their titles to the list of Invariant Sections in the Modified Version's license notice. These titles must be distinct from any other section titles.

You may add a section Entitled "Endorsements", provided it contains nothing but endorsements of your Modified Version by various parties--for example, statements of peer review or that the text has been approved by an organization as the authoritative definition of a standard.

You may add a passage of up to five words as a Front-Cover Text, and a passage of up to 25 words as a Back-Cover Text, to the end of the list of Cover Texts in the Modified Version. Only one passage of Front-Cover Text and one of Back-Cover Text may be added by (or through arrangements made by) any one entity. If the Document already includes a cover text for the same cover, previously added by you or by arrangement made by the same entity you are acting on behalf of, you may not add another; but you may replace the old one, on explicit permission from the previous publisher that added the old one.

The author(s) and publisher(s) of the Document do not by this License give permission to use their names for publicity for or to assert or imply endorsement of any Modified Version.

5. COMBINING DOCUMENTS

You may combine the Document with other documents released under this License, under the terms defined in section 4 above for modified versions, provided that you include in the combination all of the Invariant Sections of all of the original documents, unmodified, and list them all as Invariant Sections of your combined work in its license notice, and that you preserve all their Warranty Disclaimers.

The combined work need only contain one copy of this License, and multiple identical Invariant Sections may be replaced with a single copy. If there are multiple Invariant Sections with the same name but different contents, make the title of each such section unique by adding at the end of it, in parentheses, the name of the original author or publisher of that section if known, or else

a unique number. Make the same adjustment to the section titles in the list of Invariant Sections in the license notice of the combined work.

In the combination, you must combine any sections Entitled "History" in the various original documents, forming one section Entitled "History"; likewise combine any sections Entitled "Acknowledgements", and any sections Entitled "Dedications". You must delete all sections Entitled "Endorsements."

6. COLLECTIONS OF DOCUMENTS

You may make a collection consisting of the Document and other documents released under this License, and replace the individual copies of this License in the various documents with a single copy that is included in the collection, provided that you follow the rules of this License for verbatim copying of each of the documents in all other respects.

You may extract a single document from such a collection, and distribute it individually under this License, provided you insert a copy of this License into the extracted document, and follow this License in all other respects regarding verbatim copying of that document.

7. AGGREGATION WITH INDEPENDENT WORKS

A compilation of the Document or its derivatives with other separate and independent documents or works, in or on a volume of a storage or distribution medium, is called an "aggregate" if the copyright resulting from the compilation is not used to limit the legal rights of the compilation's users beyond what the individual works permit. When the Document is included in an aggregate, this License does not apply to the other works in the aggregate which are not themselves derivative works of the Document.

If the Cover Text requirement of section 3 is applicable to these copies of the Document, then if the Document is less than one half of the entire aggregate, the Document's Cover Texts may be placed on covers that bracket the Document within the aggregate, or the electronic equivalent of covers if the Document is in electronic form. Otherwise they must appear on printed covers that bracket the whole aggregate.

8. TRANSLATION

Translation is considered a kind of modification, so you may distribute translations of the Document under the terms of section 4. Replacing Invariant Sections with translations requires special permission from their copyright holders, but you may include translations of some or all Invariant Sections in addition to the original versions of these Invariant Sections. You may include a translation of this License, and all the license notices in the Document, and any Warranty Disclaimers, provided that you also include the original English version of this License and the original versions of those notices and disclaimers. In case of a disagreement between the translation and the original version of this License or a notice or disclaimer, the original version will prevail.

If a section in the Document is Entitled "Acknowledgements", "Dedications", or "History", the requirement (section 4) to Preserve its Title (section 1) will typically require changing the actual title.

9. TERMINATION

You may not copy, modify, sublicense, or distribute the Document except as expressly provided for under this License. Any other attempt to copy, modify, sublicense or distribute the Document is void, and will automatically terminate your rights under this License. However, parties who have received copies, or rights, from you under this License will not have their licenses terminated so long as such parties remain in full compliance.

10. FUTURE REVISIONS OF THIS LICENSE

The Free Software Foundation may publish new, revised versions of the GNU Free Documentation License from time to time. Such new versions will be similar in spirit to the present version, but may differ in detail to address new problems or concerns. See http://www.gnu.org/copyleft/ .

Each version of the License is given a distinguishing version number. If the Document specifies that a particular numbered version of this License "or any later version" applies to it, you have the option of following the terms and conditions either of that specified version or of any later version that has been published (not as a draft) by the Free Software Foundation. If the Document does not specify a version number of this License, you may choose any version ever published (not as a draft) by the Free Software Foundation.

How to use this License for your documents

To use this License in a document you have written, include a copy of the License in the document and put the following copyright and license notices just after the title page:

```
Copyright (c)  YEAR  YOUR NAME.
Permission is granted to copy, distribute and/or modify this document
under the terms of the GNU Free Documentation License, Version 1.2
or any later version published by the Free Software Foundation;
with no Invariant Sections, no Front-Cover Texts, and no Back-Cover Texts.
A copy of the license is included in the section entitled "GNU
Free Documentation License".
```

If you have Invariant Sections, Front-Cover Texts and Back-Cover Texts, replace the "with...Texts." line with this:

```
   with the Invariant Sections being LIST THEIR TITLES, with the
   Front-Cover Texts being LIST, and with the Back-Cover Texts being LIST.
```

If you have Invariant Sections without Cover Texts, or some other combination of the three, merge those two alternatives to suit the situation.

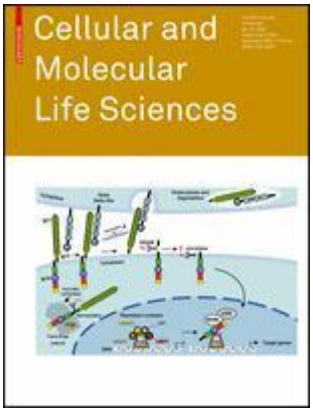

Title: Function of the C. elegans T-box factor TBX-2 depends on SUMOylation

Author: Paul Huber

Publication: Cellular and Molecular Life Sciences

Publisher: Springer

Date: Jan 1, 2013

Permissions Request

This is an open access article distributed under the terms of the Creative Commons Attribution License, which permits unrestricted use, distribution, and reproduction in any medium, provided the original work is properly cited.

Springer and BioMed Central offer a reprint service for those who require professionally produced copies of articles published under Creative Commons Attribution (CC BY) licenses. To obtain a quotation, please email reprints@springeropen.com with the article details, quantity(ies) and delivery destination. Minimum order 25 copies.

CLOSE WINDOW

Title:	T-Box Genes in Vertebrate Development
Author:	L.A. Naiche, Zachary Harrelson, Robert G. Kelly, et al
Publication:	Annual Review of Genetics
Publisher:	Annual Reviews
Date:	Dec 1, 2005

LOGIN

If you're a copyright.com user, you can login to RightsLink using your copyright.com credentials.

Already a RightsLink user or want to learn more?

Permission Not Required

Material may be republished in a thesis / dissertation without obtaining additional permission from Annual Reviews, providing that the author and the original source of publication are fully acknowledged.

BACK CLOSE WINDOW

CITIED LITERATURE

Agarwal, M., Kumar, P., Mathew, S., 2015. The Groucho/Transducin-like enhancer of split protein family in animal development. IUBMB Life 67, 472-481.

Ahn, J., Lee, Y., Ahn, J., Choi, C., 2009. Covalent conjugation of Groucho with SUMO-1 modulates its corepressor activity. Biochem Biophys Res Commun 379, 160-165.

Albertson, D.G., Thomson, J.N., 1976. The pharynx of Caenorhabditis elegans. Philos Trans R Soc Lond B Biol Sci 275, 299-325.

Allen, B., Taatjes, D., 2015. The Mediator complex: a central integrator of transcription. Nature reviews. Molecular Cell Biology 16, 155-166.

Amberg, D.C., Burke, D.J., Strathern, J.N., 2005. Methods in Yeast Genetics: A Cold Spring Harbor Laboratory Course Manual. Cold Spring Harbor Laboratory Press.

Anckar, J., Sistonen, L., 2007. Heat shock factor 1 as a coordinator of stress and developmental pathways. Advances in Experimental Medicine and Biology 594, 78-88.

Andreou, A.M., Pauws, E., Jones, M.C., Singh, M.K., Bussen, M., Doudney, K., Moore, G.E., Kispert, A., Brosens, J.J., Stanier, P., 2007. TBX22 missense mutations found in patients with X-linked cleft palate affect DNA binding, sumoylation, and transcriptional repression. American Journal of Human Genetics 81, 700-712.

Ausubel, F.M., 1990. Current protocols in molecular biology. Greene Pub. Associates and Wiley-Interscience : J. Wiley, New York.

Avery, L., Horvitz, H., 1987. A cell that dies during wild-type C. elegans development can function as a neuron in a ced-3 mutant. Cell, 1071-1078.

Avery, L., Thomas, J.H., 1997. Feeding and defication, C. elegans II. Cold Spring Harbor Laboratory Press.

Bakker, M., Boukens, B., Mommersteeg, M., Brons, J., Wakker, V., Moorman, A., Christoffels, V., 2008. Transcription factor Tbx3 is required for the specification of the atrioventricular conduction system. Circ Res 102, 1340-1349.

Bamshad, M., Lin, R.C., Law, D.J., Watkins, W.C., Krakowiak, P.A., Moore, M.E., Franceschini, P., Lala, R., Holmes, L.B., Gebuhr, T.C., Bruneau, B.G., Schinzel, A., Seidman, J.G., Seidman, C.E., Jorde, L.B., 1997. Mutations in human TBX3 alter limb, apocrine and genital development in ulnar-mammary syndrome. Nat Genet 16, 311-315.

CITIED LITERATURE (CONT.)

Basson, C.T., Bachinsky, D.R., Lin, R.C., Levi, T., Elkins, J.A., Soults, J., Grayzel, D., Kroumpouzou, E., Traill, T.A., Leblanc-Straceski, J., Renault, B., Kucherlapati, R., Seidman, J.G., Seidman, C.E., 1997. Mutations in human TBX5 cause limb and cardiac malformation in Holt-Oram syndrome. Nat Genet 15, 30-35.

Beaster-Jones, L., Okkema, P.G., 2004. DNA binding and in vivo function of C. elegans PEB-1 require a conserved FLYWCH motif. Journal of Molecular Biology 339, 695-706.

Beketaev, I., Kim, E.Y., Zhang, Y., Yu, W., Qian, L., Wang, J., 2014. Potentiation of Tbx5-mediated transactivation by SUMO conjugation and protein inhibitor of activated STAT 1 (PIAS1). The International Journal of Biochemistry & Cell Biology 50, 82-92.

Benjamini, Y., Hochberg, Y., 1995. Controlling the false discovery rate: A practical and powerful approach to multiple testing. Journal of the Royal Statistical Society. Series B (Methodological) 57, 289-300.

Bernier-Villamor, V., Sampson, D.A., Matunis, M.J., Lima, C.D., 2002. Structural basis for E2-mediated SUMO conjugation revealed by a complex between ubiquitin-conjugating enzyme Ubc9 and RanGAP1. Cell 108, 345-356.

Bolstad, B.M., Irizarry, R.A., Astrand, M., Speed, T.P., 2003. A comparison of normalization methods for high density oligonucleotide array data based on variance and bias. Bioinformatics 19, 185-193.

Bongers, E.M., Duijf, P.H., van Beersum, S.E., Schoots, J., Van Kampen, A., Burckhardt, A., Hamel, B.C., Losan, F., Hoefsloot, L.H., Yntema, H.G., Knoers, N.V., van Bokhoven, H., 2004. Mutations in the human TBX4 gene cause small patella syndrome. American journal of human genetics 74, 1239-1248.

Boogerd, C.J., Moorman, A.F., Barnett, P., 2009. Protein interactions at the heart of cardiac chamber formation. Annals of Anatomy 191, 505-517.

Bowerman, B., Draper, B.W., Mello, C.C., Priess, J.F., 1993. The maternal gene skn-1 encodes a protein that is distributed unequally in early C. elegans embryos. Cell, 443-452.

Bowerman, B., Eaton, B.A., Priess, J.R., 1992. skn-1, a maternally expressed gene required to specify the fate of ventral blastomeres in the early C. elegans embryo. Cell, 1061-1075.

Braybrook, C., Doudney, K., Marcano, A.C., Arnason, A., Bjornsson, A., Patton, M.A., Goodfellow, P.J., Moore, G.E., Stanier, P., 2001. The T-box transcription factor gene TBX22 is mutated in X-linked cleft palate and ankyloglossia. Nat Genet 29, 179-183.

Brenner, S., 1974. The genetics of Caenorhabditis elegans. Genetics 77, 71-94.

Broitman-Maduro, G., Lin, K.T., Hung, W.W., Maduro, M.F., 2006. Specification of the C. elegans MS blastomere by the T-box factor TBX-35. Development 133, 3097-3106.

Broitman-Maduro, G., Maduro, M.F., Rothman, J.H., 2005. The noncanonical binding site of the MED-1 GATA factor defines differentially regulated target genes in the C. elegans mesendoderm. Dev. Cell, 427-433.

Broitman-Maduro, G., Owraghi, M., Hung, W.W., Kuntz, S., Sternberg, P.W., Maduro, M.F., 2009. The NK-2 class homeodomain factor CEH-51 and the T-box factor TBX-35 have overlapping function in C. elegans mesoderm development. Development 136, 2735-2746.

Brummelkamp, T.R., Kortlever, R.M., Lingbeek, M., Trettel, F., MacDonald, M.E., van Lohuizen, M., Bernards, R., 2002. TBX-3, the gene mutated in Ulnar-Mammary Syndrome, is a negative regulator of p19ARF and inhibits senescence. The Journal of biological chemistry 277, 6567-6572.

Burgucu, D., Guney, K., Sahinturk, D., Ozbudak, I., Ozel, D., Ozbilim, G., Yavuzer, U., 2012. Tbx3 represses PTEN and is over-expressed in head and neck squamous cell carcinoma. BMC Cancer 12, 481.

Calvo, D., Victor, M., Gay, F., Sui, G., Luke, M.P., Dufourcq, P., Wen, G., Maduro, M., Rothman, J., Shi, Y., 2001. A POP-1 repressor complex restricts inappropriate cell type-specific gene transcription during Caenorhabditis elegans embryogenesis. The EMBO Journal 20, 7197-7208.

Camarata, T., Bimber, B., Kulisz, A., Chew, T.L., Yeung, J., Simon, H.G., 2006. LMP4 regulates Tbx5 protein subcellular localization and activity. J Cell Biol 174, 339-348.

Campbell, L.A., Faivre, E.J., Show, M.D., Ingraham, J.G., Flinders, J., Gross, J.D., Ingraham, H.A., 2008. Decreased recognition of SUMO-sensitive target genes following modification of SF-1 (NR5A1). Mol Cell Biol 28, 7476-7486.

Carlson, H., Ota, S., Campbell, C.E., Hurlin, P.J., 2001. A dominant repression domain in Tbx3 mediates transcriptional repression and cell immortalization: relevance to mutations in Tbx3 that cause ulnar-mammary syndrome. Hum Mol Genet 10, 2403-2413.

Chaffer, C., Weinberg, R., 2011. A perspective on cancer cell metastasis. Science 331, 1559-1564.

Chalfie, M., Tu, Y., Euskirchen, G., Ward, W., Prasher, D., 1994. Green fluorescent protein as a marker for gene expression. Science 263, 802-805.

Chang, S., Johnston, R., Hobert, O., 2003. A transcriptional regulatory cascade that controls left/right asymmetry in chemosensory neurons of C. elegans. Genes Dev 17, 2123-2137.

Chen, G., Fernandez, J., Mische, S., Courey, A., 1999. A functional interaction between the histone deacetylase Rpd3 and the corepressor groucho in Drosophila development. Genes Dev 13, 2218-2230.

Chen, J.N., Fishman, M.C., 1996. Zebrafish tinman homolog demarcates the heart field and initiates myocardial differentiation. Development, 3809-3816.

Chen, Y.Z., Chen, Z., Gong, Y.A., Ying, G., 2012. SUMOhydro: a novel method for the prediction of sumoylation sites based on hydrophobic properties. PloS one 7, e39195.

Cheng, X., Kao, H., 2013. Post-translational modifications of PML: consequences and implications. Front Oncol. 2.

Chiaretti, S., Li, X., Gentleman, R., Vitale, A., Vignetti, M., Mandelli, F., Ritz, J., Foa, R., 2004. Gene expression profile of adult T-cell acute lymphocytic leukemia identifies distinct subsets of patients with different response to therapy and survival. Blood 103, 2771-2778.

Choi, C., Kim, Y., Kwon, H.a., Kim, Y., 1999. The Homeodomain Protein NK-3 Recruits Groucho and a Histone Deacetylase Complex to Repress Transcription. The Journal of biological chemistry 274, 33194–33197

Christensen, S., Kodoyianni, V., Bosenberg, M., Friedman, L., Kimble, J., 1996. lag-1, a gene required for lin-12 and glp-1 signaling in Caenorhabditis elegans, is homologous to human CBF1 and Drosophila Su(H). Development, 1373-1383.

Christoffels, V.M., Hoogaars, W.M., Tessari, A., Clout, D.E., Moorman, A.F., Campione, M., 2004. T-box transcription factor Tbx2 represses differentiation and formation of the cardiac chambers. Dev Dyn 229, 763-770.

Chymkowitch, P., Nguea, P.A., Enserink, J.M., 2015. SUMO-regulated transcription: Challenging the dogma. Bioessays 37, 1095-1105.

Coll, M., Seidman, J.G., Muller, C.W., 2002. Structure of the DNA-bound T-box domain of human TBX3, a transcription factor responsible for ulnar-mammary syndrome. Structure 10, 343-356.

Copley, R.R., 2005. The EH1 motif in metazoan transcription factors. BMC Genomics 6, 169.

Corsi, A., 2006. A Biochemist's Guide to C. elegans. Anal Biochem 359, 1-17.

Costa, M.W., Lee, S., Furtado, M.B., Xin, L., Sparrow, D.B., Martinez, C.G., Dunwoodie, S.L., Kurtenbach, E., Mohun, T., Rosenthal, N., Harvey, R.P., 2011. Complex SUMO-1 regulation of cardiac transcription factor Nkx2-5. PloS one 6, e24812.

CITIED LITERATURE (CONT.)

Crum, T.L., 2011. SUMOylation is Required for Function of the Caenorhabditis elegans T-box Transcription Factor, TBX-2, Biological Sciences. University of Illinois at Chicago, Chicago, Illinois.

Dalafave, D.S., 2009. Prediction of functional engrailed homology-1 protein motif from sequence. Bioinformation 4, 229-232.

Desterro, J.M., Rodriguez, M.S., Kemp, G.D., Hay, R.T., 1999. Identification of the enzyme required for activation of the small ubiquitin-like protein SUMO-1. The Journal of Biological Chemistry 274, 10618-10624.

Dobrzycka, K., Kang, K., Jiang, S., Meyer, R., Rao, P., Lee, A., Oesterreich, S., 2006. Disruption of scaffold attachment factor B1 leads to TBX2 up-regulation, lack of p19ARF induction, lack of senescence, and cell immortalization. Cancer Res 66, 7859-7863.

Dolphin, C.T., Hope, I.A., 2006. Caenorhabditis elegans reporter fusion genes generated by seamless modification of large genomic DNA clones. Nucleic Acids Research 34, e72.

Eifler, K., Vertegaal, A.C.O., 2015. Mapping the SUMOylated landscape. FEBS Journal 282, 3669–3680.

El Omari, K., De Mesmaeker, J., Karia, D., Ginn, H., Bhattacharya, S., Mancini, E.J., 2011. Structure of the DNA-bound T-box domain of human TBX1, a transcription factor associated with the DiGeorge syndrome. Proteins, 80, 655-60.

Evans, T.C., Crittenden, S.L., Kodoyianni, V., Kimble, J., 1994. Translational control of maternal glp-1 mRNA establishes an asymmetry in the C. elegans embryo. Cell, 183-194.

Fan, C., Liu, M., Wang, Q., 2003. Functional analysis of TBX5 missense mutations associated with Holt-Oram syndrome. The Journal of Biological Chemistry 278, 8780-8785.

Farin, H.F., Bussen, M., Schmidt, M.K., Singh, M.K., Schuster-Gossler, K., Kispert, A., 2007. Transcriptional repression by the T-box proteins Tbx18 and Tbx15 depends on Groucho corepressors. The Journal of Biological Chemistry 282, 25748-25759.

Fire, A., Xu, S., Montgomery, M.K., Kostas, S.A., Driver, S.E., Mello, C.C., 1998. Potent and specific genetic interference by double-stranded RNA in Caenorhabditis elegans. Nature 391, 806-811.

Flowers, E.B., Poole, R.J., Tursun, B., Bashllari, E., Pe'er, I., Hobert, O., 2010. The Groucho ortholog UNC-37 interacts with the short Groucho-like protein LSY-22 to control developmental decisions in C. elegans. Development 137, 1799-1805.

Formaz-Preston, A., Ryu, J.R., Svendsen, P.C., Brook, W.J., 2012. The Tbx20 homolog Midline represses wingless in conjunction with Groucho during the maintenance of segment polarity. Developmental Biology 369, 319-329.

Garcia-Dominguez, M., Reyes, J.C., 2009. SUMO association with repressor complexes, emerging routes for transcriptional control. Biochimica Biophysica Acta 1789, 451-459.

Gareau, J.R., Lima, C.D., 2010. The SUMO pathway: emerging mechanisms that shape specificity, conjugation and recognition. Nature Reviews Molecular Cell Biology 11, 861-871.

Gaudet, J., Mango, S.E., 2002. Regulation of organogenesis by the Caenorhabditis elegans FoxA protein PHA-4. Science 295, 821-825.

Gentleman, R.C., Carey, V.J., Bates, D.M., Bolstad, B., Dettling, M., Dudoit, S., Ellis, B., Gautier, L., Ge, Y., Gentry, J., Hornik, K., Hothorn, T., Huber, W., Iacus, S., Irizarry, R., Leisch, F., Li, C., Maechler, M., Rossini, A.J., Sawitzki, G., Smith, C., Smyth, G., Tierney, L., Yang, J.Y., Zhang, J., 2004. Bioconductor: open software development for computational biology and bioinformatics. Genome Biology 5, R80.

Ghosh, T., Packham, E., Bonser, A., Robinson, T., Cross, S., Brook, J., 2001. Characterization of the TBX5 binding site and analysis of mutations that cause Holt-Oram syndrome. Hum Mol Genet 10, 1983-1994.

Giaever, G., Chu, A., Ni, L., Connelly, C., Riles, L., Véronneau, S., Dow, S., Lucau-Danila, A., Anderson, K., André, B., Arkin, A., Astromoff, A., El-Bakkoury, M., Bangham, R., Benito, R., Brachat, S., Campanaro, S., Curtiss, M., Davis, K., Deutschbauer, A., Entian, K., Flaherty, P., Foury, F., Garfinkel, D., Gerstein, M., Gotte, D., Güldener, U., Hegemann, J., Hempel, S., Herman, Z., Jaramillo, D., Kelly, D., Kelly, S., Kötter, P., LaBonte, D., Lamb, D., Lan, N., Liang, H., Liao, H., Liu, L., Luo, C., Lussier, M., Mao, R., Menard, P., Ooi, S., Revuelta, J., Roberts, C., Rose, M., Ross-Macdonald, P., Scherens, B., Schimmack, G., Shafer, B., Shoemaker, D., Sookhai-Mahadeo, S., Storms, R., Strathern, J., Valle, G., Voet, M., Volckaert, G., Wang, C., Ward, T., Wilhelmy, J., Winzeler, E., Yang, Y., Yen, G., Youngman, E., Yu, K., Bussey, H., Boeke, J., Snyder, M., Philippsen, P., Davis, R., Johnston, M., 2002. Functional profiling of the Saccharomyces cerevisiae genome. Nature 418, 387-391.

Gill, G., 2004. SUMO and ubiquitin in the nucleus: different functions, similar mechanisms? Genes Dev 18, 2046-2059.

Gill, G., 2005. Something about SUMO inhibits transcription. Current Opinion in Genetics & Development 15, 536-541.

Good, K., Ciosk, R., Nance, J., Neves, A., Hill, R.J., Priess, J.R., 2004. The T-box transcription factors TBX-37 and TBX-38 link GLP-1/Notch signaling to mesoderm induction in C. elegans embryos. Development 131, 1967-1978.

Goszczynski, B., McGhee, J.D., 2005. Reevaluation of the role of the med-1 and med-2 genes in specifying the Caenorhabditis elegans endoderm. Genetics, 545-555.

Greulich, F., Rudat, C., Kispert, A., 2011. Mechanisms of T-box gene function in the developing heart. Cardiovasc Res 91, 212-222.

Habets, P.E., Moorman, A.F., Clout, D.E., van Roon, M.A., Lingbeek, M., van Lohuizen, M., Campione, M., Christoffels, V.M., 2002. Cooperative action of Tbx2 and Nkx2.5 inhibits ANF expression in the atrioventricular canal: implications for cardiac chamber formation. Genes Dev 16, 1234-1246.

Harrelson, Z., Kelly, R.G., Goldin, S.N., Gibson-Brown, J.J., Bollag, R.J., Silver, L.M., Papaioannou, V.E., 2004. Tbx2 is essential for patterning the atrioventricular canal and for morphogenesis of the outflow tract during heart development. Development 131, 5041-5052.

Haun, C., Alexander, J., Stainier, D.Y., Okkema, P.G., 1998. Rescue of Caenorhabditis elegans pharyngeal development by a vertebrate heart specification gene. Proc. Natl. Acad. Sci. U.S.A., 5072-5075.

Hay, R.T., 2005. SUMO: a history of modification. Mol Cell 18, 1-12.

He, M., Wen, L., Campbell, C.E., Wu, J.Y., Rao, Y., 1999. Transcription repression by Xenopus ET and its human ortholog TBX3, a gene involved in ulnar-mammary syndrome. Proceedings of the National Academy of Sciences of the United States of America 96, 10212-10217.

Hendriks, I., D'Souza, R., Yang, B., Verlaan-de Vries, M., Mann, M., Vertegaal, A., 2014. Uncovering global SUMOylation signaling networks in a site-specific manner. Nature Structural & Molecular Biology 21, 927-936.

Herman, R.K., Yochem, J., 2005. Genetic enhancers. WormBook : the online review of C. elegans biology, 1-11.

Herrmann, B., 1991. Expression pattern of the Brachyury gene in whole-mount TWis/TWis mutant embryos. Development 113, 913-917.

Hirani, N., Westenberg, M., Gami, M.S., Davis, P., Hope, I.A., Dolphin, C.T., 2013. A simplified counter-selection recombineering protocol for creating fluorescent protein reporter constructs directly from C. elegans fosmid genomic clones. BMC Biotechnology 13, 1.

Hiroi, Y., Kudoh, S., Monzen, K., Ikeda, Y., Yazaki, Y., Nagai, R., Komuro, I., 2001. Tbx5 associates with Nkx2-5 and synergistically promotes cardiomyocyte differentiation. Nat Genet 28, 276-280.

Hitachi, K., Danno, H., Tazumi, S., Aihara, Y., Uchiyama, H., Okabayashi, K., Kondow, A., Asashima, M., 2009. The Xenopus Bowline/Ripply family proteins negatively regulate the transcriptional activity of T-box transcription factors. Int J Dev Biol 53, 631-639.

Hong, Y., Rogers, R., Matunis, M.J., Mayhew, C.N., Goodson, M.L., Park-Sarge, O.K., Sarge, K.D., 2001. Regulation of heat shock transcription factor 1 by stress-induced SUMO-1 modification. The Journal of Biological Chemistry 276, 40263-40267.

Hoogaars, W., Barnett, P., Rodriguez, M., Clout, D., Moorman, A., Goding, C., Christoffels, V., 2008. TBX3 and its splice variant TBX3 + exon 2a are functionally similar. Pigment Cell Melanoma Res 21, 379-387.

Hoogaars, W.M., Tessari, A., Moorman, A.F., de Boer, P.A., Hagoort, J., Soufan, A.T., Campione, M., Christoffels, V.M., 2004. The transcriptional repressor Tbx3 delineates the developing central conduction system of the heart. Cardiovasc Res 62, 489-499.

Huber, P., Crum, T., Clary, L.M., Ronan, T., Packard, A.V., Okkema, P.G., 2013. Function of the C. elegans T-box factor TBX-2 depends on SUMOylation. Cellular and Molecular Life Sciences : CMLS 70, 4157-4168.

Hutter, H., Schnabel, R., 1994. glp-1 and inductions establishing embryonic axes in C. elegans. Development, 2051-2064.

Ishov, A., Sotnikov, A., Negorev, D., Vladimirova, O., Neff, N., Kamitani, T., Yeh, E., Strauss, J.r., Maul, G., 1999. PML is critical for ND10 formation and recruits the PML-interacting protein daxx to this nuclear structure when modified by SUMO-1. J Cell Biol 147, 221-234.

Jacobs, J.J., Keblusek, P., Robanus-Maandag, E., Kristel, P., Lingbeek, M., Nederlof, P.M., van Welsem, T., van de Vijver, M.J., Koh, E.Y., Daley, G.Q., van Lohuizen, M., 2000. Senescence bypass screen identifies TBX2, which represses Cdkn2a (p19(ARF)) and is amplified in a subset of human breast cancers. Nat Genet 26, 291-299.

Jafari, G., Appleford, P.J., Seago, J., Pocock, R., Woollard, A., 2011. The UNC-4 homeobox protein represses mab-9 expression in DA motor neurons in Caenorhabditis elegans. Mechanisms of Development 128, 49-58.

Jang, E.J., Park, H.R., Hong, J.H., Hwang, E.S., 2013. Lysine 313 of T-box is crucial for modulation of protein stability, DNA binding, and threonine phosphorylation of T-bet. J Immunol 190, 5764-5770.

Jennings, B., Pickles, L., Wainwright, S., Roe, S., Pearl, L., Ish-Horowicz, D., 2006. Molecular recognition of transcriptional repressor motifs by the WD domain of the Groucho/TLE corepressor. Mol Cell 22, 645-655.

Johnson, E.S., 2004. Protein modification by SUMO. Annu Rev Biochem 73, 355-382.

Kalb, J.M., Lau, K.K., Goszczynski, B., Fukushige, T., Moons, D., Okkema, P.G., McGhee, J.D., 1998. pha-4 is Ce-fkh-1, a fork head/HNF-3alpha, beta, gamma homolog that functions in organogenesis of the C. elegans pharynx. Development, 2171-2180.

Kaletta, T., Hengartner, M., 2006. Finding function in novel targets: C. elegans as a model organism. Nature Reviews Drug Discovery, 387-399.

Kaltenbrun, E., Greco, T.M., Slagle, C.E., Kennedy, L.M., Li, T., Cristea, I.M., Conlon, F.L., 2013. A Gro/TLE-NuRD corepressor complex facilitates Tbx20-dependent transcriptional repression. J Proteome Res 12, 5395-5409.

Kamath, R.S., Ahringer, J., 2003. Genome-wide RNAi screening in Caenorhabditis elegans. Methods 30, 313-321.

Kamath, R.S., Martinez-Campos, M., Zipperlen, P., Fraser, A.G., Ahringer, J., 2001. Effectiveness of specific RNA-mediated interference through ingested double-stranded RNA in Caenorhabditis elegans. Genome Biology 2, 1.

Kaminsky, R., Denison, C., Bening-Abu-Shach, U., Chisholm, A., Gygi, S., Broday, L., 2009. SUMO regulates the assembly and function of a cytoplasmic intermediate filament protein in C. elegans. Developmental Cell 17, 724-735.

Kaul, A., Schuster, E., Jennings, B., 2014. The Groucho co-repressor is primarily recruited to local target sites in active chromatin to attenuate transcription. PLoS Genet 10.

Kaul, A., Schuster, E., Jennings, B., 2015. Recent insights into Groucho co-repressor recruitment and function. Transcription 6, 7-11.

Kawamura, A., Koshida, S., Takada, S., 2008. Activator-to-repressor conversion of T-box transcription factors by the Ripply family of Groucho/TLE-associated mediators. Mol Cell Biol 28, 3236-3244.

Kerppola, T.K., 2006. Design and implementation of bimolecular fluorescence complementation (BiFC) assays for the visualization of protein interactions in living cells. Nature Protocols 1, 1278-1286.

Kerppola, T.K., 2008. Bimolecular fluorescence complementation (BiFC) analysis as a probe of protein interactions in living cells. Annu Rev Biophys 37, 465-487.

Kimble, J., Hirsh, D., 1979. The postembryonic cell lineages of the hermaphrodite and male gonads in Caenorhabditis elegans. Developmental Biology 70, 396-417.

Knipscheer, P., Flotho, A., Klug, H., Olsen, J.V., van Dijk, W.J., Fish, A., Johnson, E.S., Mann, M., Sixma, T.K., Pichler, A., 2008. Ubc9 sumoylation regulates SUMO target discrimination. Mol Cell 31, 371-382.

Lambie, E.J., Kimble, J., 1991. Two homologous regulatory genes, lin-12 and glp-1, have overlapping functions. Development, 231-240.

Lee, P.C., Taylor-Jaffe, K.M., Nordin, K.M., Prasad, M.S., Lander, R.M., LaBonne, C., 2012. SUMOylated SoxE factors recruit Grg4 and function as transcriptional repressors in the neural crest. J Cell Biol 198, 799-813.

Leight, E.R., Glossip, D., Kornfeld, K., 2005. Sumoylation of LIN-1 promotes transcriptional repression and inhibition of vulval cell fates. Development 132, 1047-1056.

Lewis, J.A., Fleming, J.T., 1995. Basic Culture Methods, in: Biology, M.i.C. (Ed.), Caenorhabditis elegans: Modern Biological Analysis of an Organism. Academic Press, San Diego, CA, pp. 4-30.

Li, Q.Y., Newbury-Ecob, R.A., Terrett, J.A., Wilson, D.I., Curtis, A.R., Yi, C.H., Gebuhr, T., Bullen, P.J., Robson, S.C., Strachan, T., Bonnet, D., Lyonnet, S., Young, I.D., Raeburn, J.A., Buckler, A.J., Law, D.J., Brook, J.D., 1997. Holt-Oram syndrome is caused by mutations in TBX5, a member of the Brachyury (T) gene family. Nat Genet 15, 21-29.

Lin, D., Tatham, M.H., Yu, B., Kim, S., Hay, R.T., Chen, Y., 2002. Identification of a substrate recognition site on Ubc9. The Journal of Biological Chemistry 277, 21740-21748.

Lin, R., Thompson, S., Priess, J.R., 1995. pop-1 encodes an HMG box protein required for the specification of a mesoderm precursor in early C. elegans embryos. Cell, 599-609.

Lingbeek, M.E., Jacobs, J.J., van Lohuizen, M., 2002. The T-box repressors TBX2 and TBX3 specifically regulate the tumor suppressor gene p14ARF via a variant T-site in the initiator. The Journal of Biological Chemistry 277, 26120-26127.

Lo, M.C., Gay, F., Odom, R., Shi, Y., Lin, R., 2004. Phosphorylation by the beta-catenin/MAPK complex promotes 14–3-3-mediated nuclear export of TCF/POP-1 in signal-responsive cells in C. elegans. Cell, 95-106.

Lomelí, H., Vázquez, M., 2011. Emerging roles of the SUMO pathway in development. Cellular and molecular life sciences : CMLS 68, 4045-4064.

Lu, J., Li, X.P., Dong, Q., Kung, H.F., He, M.L., 2010. TBX2 and TBX3: the special value for anticancer drug targets. Biochimica Biophysica Acta 1806, 268-274.

Macindoe, I., Glockner, L., Vukasin, P., Stennard, F.A., Costa, M.W., Harvey, R.P., Mackay, J.P., Sunde, M., 2009. Conformational stability and DNA binding specificity of the cardiac T-box transcription factor Tbx20. Journal of Molecular Biology 389, 606-618.

Maduro, M., Pilgrim, D., 1995. Identification and cloning of unc-119, a gene expressed in the Caenorhabditis elegans nervous system. Genetics 141, 977-988.

Maduro, M.F., Broitman-Maduro, G., Mengarelli, I., Rothman, J.H.D.B., 2007. Maternal deployment of the embryonic SKN-1 to MED-1,2 cell specification pathway in C. elegans. Developmental Biology 301, 590-601.

Maduro, M.F., Lin, R., Rothman, J.H., 2002. Dynamics of a developmental switch: recursive intracellular and intranuclear redistribution of Caenorhabditis elegans POP-1 parallels Wnt-inhibited transcriptional repression. Dev. Biol. 248, 128-142.

Maduro, M.F., Meneghini, M.D., Bowerman, B., Broitman-Maduro, G., Rothman, J.H., 2001. Restriction of mesendoderm to a single blastomere by the combined action of SKN-1 and a GSK-3 beta homolog is mediated by MED-1 and -2 in C. elegans. Mol. Cell 7, 475-485.

Mahajan, R., Delphin, C., Guan, T., Gerace, L., Melchior, F., 1997. A small ubiquitin-related polypeptide involved in targeting RanGAP1 to nuclear pore complex protein RanBP2. Cell 88, 97-107.

Mahlamaki, E.H., Barlund, M., Tanner, M., Gorunova, L., Hoglund, M., Karhu, R., Kallioniemi, A., 2002. Frequent amplification of 8q24, 11q, 17q, and 20q-specific genes in pancreatic cancer. Genes Chromosomes Cancer 35, 353-358.

Mango, S., Lambie, E.J., Kimble, J., 1994. The pha-4 gene is required to generate the pharyngeal primordium of Caenorhabditis elegans. Development 120, 3019-3031.

Mango, S.E., 2007. The C. elegans pharynx: a model for organogenesis. WormBook : the online review of C. elegans biology, 1-26.

Mann, R.S., Carroll, S.B., 2002. Molecular mechanisms of selector gene function and evolution. Curr. Opin. Genet. Dev. 12, 592-600.

MarÁano, A.C., Doudney, K., Braybrook, C., Squires, R., Patton, M.A., Lees, M.M., Richieri-Costa, A., Lidral, A.C., Murray, J.C., Moore, G.E., Stanier, P., 2004. TBX22 mutations are a frequent cause of cleft palate. J Med Genet 41, 68 - 74.

Matunis, M.J., Coutavas, E., Blobel, G., 1996. A novel ubiquitin-like modification modulates the partitioning of the Ran-GTPase-activating protein RanGAP1 between the cytosol and the nuclear pore complex. J Cell Biol 135, 1457-1470.

Mello, C., Fire, A., 1995. DNA Transformation, in: Epstein, H.F., Shakes, D.C. (Eds.), Caenorhabditis elegans: Modern Biological Analysis of an Organism. Academic Press, San Diego, CA, pp. 451-482.

Merritt, C., Seydoux, G., 2010. Transgenic solutions for the germline. WormBook : the online review of C. elegans biology, 1-21.

Miller, D.M., 3rd, Niemeyer, C.J., Chitkara, P., 1993. Dominant unc-37 mutations suppress the movement defect of a homeodomain mutation in unc-4, a neural specificity gene in Caenorhabditis elegans. Genetics 135, 741-753.

Miller, R.R., Okkema, P.G., 2011. The Caenorhabditis elegans T-Box Factor MLS-1 Requires Groucho Co-Repressor Interaction for Uterine Muscle Specification. PLoS Genet 7, e1002210.

Milton, A.C., Okkema, P.G., 2015. Caenorhabditis elegans TBX-2 directly regulates its own expression in a negative autoregulatory loop. G3 5, 1177-1186.

Milton, A.C., Packard, A.V., Clary, L., Okkema, P.G., 2013. The NF-Y complex negatively regulates Caenorhabditis elegans tbx-2 expression. Developmental Biology 382, 38-47.

Miyahara, K., Suzuki, N., Ishihara, T., Tsuchiya, E., Katsura, I., 2004. TBX2/TBX3 transcriptional factor homologue controls olfactory adaptation in Caenorhabditis elegans. J Neurobiol 58, 392-402.

Moskowitz, I.P., Gendreau, S.B., Rothman, J.H., 1994. Combinatorial specification of blastomere identity by glp-1-dependent cellular interactions in the nematode Caenorhabditis elegans. Development 120, 3325-3338.

Muller, C.W., Herrmann, B.G., 1997. Crystallographic structure of the T domain-DNA complex of the Brachyury transcription factor. Nature 389, 884-888.

Nacerddine, K., Lehembre, F., Bhaumik, M., Artus, J., Cohen-Tannoudji, M., Babinet, C., Pandolfi, P., Dejean, A., 2005. The SUMO pathway is essential for nuclear integrity and chromosome segregation in mice. Developmental Cell 9, 769-779.

Naiche, L.A., Harrelson, Z., Kelly, R.G., Papaioannou, V.E., 2005. T-box genes in vertebrate development. Annu Rev Genet 39, 219-239.

Nakano, S., Ellis, R.E., Horvitz, H.R., 2010. Otx-dependent expression of proneural bHLH genes establishes a neuronal bilateral asymmetry in C. elegans. Development 137, 4017-4027.

Nayak, A., Müller, S., 2014. SUMO-specific proteases/isopeptidases: SENPs and beyond. Genome Biology 15.

Neves, A., Priess, J.R., 2005. The REF-1 family of bHLH transcription factors pattern C. elegans embryos through Notch-dependent and Notch-independent pathways. Dev. Cell 8, 867-879.

Ng, C., Akhter, A., Yurko, N., Burgener, J., Rosonina, E., Manley, J., 2015. Sumoylation controls the timing of Tup1-mediated transcriptional deactivation. Nat Commun.

Nie, M., Xie, Y., Loo, J., Courey, A., 2009. Genetic and proteomic evidence for roles of Drosophila SUMO in cell cycle control, Ras signaling, and early pattern formation. PloS One 4.

Notredame, C., Higgins, D.G., Heringa, J., 2000. T-Coffee: A novel method for fast and accurate multiple sequence alignment. Journal of Molecular Biology 302, 205-217.

Nowak, M., Hammerschmidt, M., 2006. Ubc9 regulates mitosis and cell survival during zebrafish development. Molecular Biology of the Cell 17, 5324-5336.

Ogg, S., Paradis, S., Gottlieb, S., Patterson, G., Lee, L., Tissenbaum, H., Ruvkun, G., 1997. The Fork head transcription factor DAF-16 transduces insulin-like metabolic and longevity signals in C. elegans. Nature 389, 994-999.

Okkema, P.G., Fire, A., 1994. The Caenorhabditis elegans NK-2 class homeoprotein CEH-22 is involved in combinatorial activation of gene expression in pharyngeal muscle. Development 120, 2175-2186.

Okkema, P.G., Ha, E., Haun, C., Chen, W., Fire, A., 1997. The Caenorhabditis elegans NK-2 homeobox gene ceh-22 activates pharyngeal muscle gene expression in combination with pha-1 and is required for normal pharyngeal development. Development 124, 3965-3973.

Okuma, T., Honda, R., Ichikawa, G., Tsumagari, N., Yasuda, H., 1999. In vitro SUMO-1 modification requires two enzymatic steps, E1 and E2. Biochem Biophys Res Commun 254, 693-698.

Packham, E.A., Brook, J.D., 2003. T-box genes in human disorders. Hum Mol Genet 12 Spec No 1, R37-44.

Papaioannou, V.E., 2001. T-box genes in development: from hydra to humans. Int Rev Cytol 207, 1-70.

Papaioannou, V.E., 2014. The T-box gene family: emerging roles in development, stem cells and cancer. Development 141, 3819-3833.

Papangeli, I., Scambler, P., 2013. The 22q11 deletion: DiGeorge and velocardiofacial syndromes and the role of TBX1. Wiley Interdiscip Rev Dev Biol 2, 393-403.

Park, I., Han, Y., Chung, H., Jung, Y., Kim, Y., Kim, H., 2016. SUMOylation regulates nuclear localization and stability of TRAIP/RNF206. Biochem Biophys Res Commun

Paxton, C., Zhao, H., Chin, Y., Langner, K., Reecy, J., 2002. Murine Tbx2 contains domains that activate and repress gene transcription. Gene 283, 117-124.

Peden, E., Kimberly, E., Gengyo-Ando, K., Mitani, S., Xue, D., 2007. Control of sex-specific apoptosis in C. elegans by the BarH homeodomain protein CEH-30 and the transcriptional repressor UNC-37/Groucho. Genes Dev 21, 3195-3207.

Pferdehirt, R.R., Meyer, B.J., 2013. SUMOylation is essential for sex-specific assembly and function of the Caenorhabditis elegans dosage compensation complex on X chromosomes. Proceedings of the National Academy of Sciences of the United States of America 110, E3810-3819.

Pflugfelder, G., Roth, H., Poeck, B., Kerscher, S., Schwarz, H., Jonschker, B., Heisenberg, M., 1992. The lethal(1)optomotor-blind gene of Drosophila melanogaster is a major organizer of optic lobe development: isolation and characterization of the gene. Proc Natl Acad Sci U S A. 89.

Pflugrad, A., Meir, J.Y., Barnes, T.M., Miller, D.M., 3rd, 1997. The Groucho-like transcription factor UNC-37 functions with the neural specificity gene unc-4 to govern motor neuron identity in C. elegans. Development 124, 1699-1709.

Pichler, A., Knipscheer, P., Oberhofer, E., van Dijk, W.J., Korner, R., Olsen, J.V., Jentsch, S., Melchior, F., Sixma, T.K., 2005. SUMO modification of the ubiquitin-conjugating enzyme E2-25K. Nature Structural & Molecular Biology 12, 264-269.

Pinto, M., Lobe, C., 1996. Products of the grg (Groucho-related gene) family can dimerize through the amino-terminal Q domain. The Journal of Biological Chemistry 271, 33026-33031.

Plant, L., Dementieva, I., Kollewe, A., Olikara, S., Marks, J., Goldstein, S., 2010. One SUMO is sufficient to silence the dimeric potassium channel K2P1. Proc Natl Acad Sci U S A. 107, 10743-10748.

Pocock, R., Ahringer, J., Mitsch, M., Maxwell, S., Woollard, A., 2004. A regulatory network of T-box genes and the even-skipped homologue vab-7 controls patterning and morphogenesis in C. elegans. Development 131, 2373-2385.

Portereiko, M.F., Mango, S.E., 2001. Early morphogenesis of the Caenorhabditis elegans pharynx. Dev. Biol., 482-494.

Praitis, V., Casey, E., Collar, D., Austin, J., 2001. Creation of low-copy integrated transgenic lines in Caenorhabditis elegans. Genetics 157, 1217-1226.

Priess, J.R., Schnabel, H., Schnabel, R., 1987. The glp-1 locus and cellular interactions in early C. elegans embryos. Cell 51, 601-611.

Priess, J.R., Thomson, J.N., 1987. Cellular interactions in early C. elegans embryos. Cell 48, 241-250.

Prince, S., Carreira, S., Vance, K.W., Abrahams, A., Goding, C.R., 2004. Tbx2 directly represses the expression of the p21(WAF1) cyclin-dependent kinase inhibitor. Cancer Res 64, 1669-1674.

Psakhye, I., Jentsch, S., 2012. Protein group modification and synergy in the SUMO pathway as exemplified in DNA repair. Cell 151, 807-820.

Ray, P., Schnabel, R., Okkema, P., 2008. Behavioral and synaptic defects in C. elegans lacking the NK-2 homeobox gene ceh-28. Dev Neurobiol. 68, 421-433.

Ren, J., Gao, X., Jin, C., Zhu, M., Wang, X., Shaw, A., Wen, L., Yao, X., Xue, Y., 2009. Systematic study of protein sumoylation: Development of a site-specific predictor of SUMOsp 2.0. Proteomics 9, 3409-3412.

Roy Chowdhuri, S., Crum, T., Woollard, A., Aslam, S., Okkema, P.G., 2006. The T-box factor TBX-2 and the SUMO conjugating enzyme UBC-9 are required for ABa-derived pharyngeal muscle in C. elegans. Developmental Biology 295, 664-677.

Ruvinsky, I., Silver, L.M., Gibson-Brown, J.J., 2000. Phylogenetic analysis of TBox genes demonstrates the importance of amphioxus for understanding evolution of the vertebrate genome. Genetics 156.

Sampson, D.A., Wang, M., Matunis, M.J., 2001. The small ubiquitin-like modifier-1 (SUMO-1) consensus sequence mediates Ubc9 binding and is essential for SUMO-1 modification. The Journal of Biological Chemistry 276, 21664-21669.

Sarov, M., Murray, J.I., Schanze, K., Pozniakovski, A., Niu, W., Angermann, K., Hasse, S., Rupprecht, M., Vinis, E., Tinney, M., Preston, E., Zinke, A., Enst, S., Teichgraber, T., Janette, J., Reis, K., Janosch, S., Schloissnig, S., Ejsmont, R.K., Slightam, C., Xu, X., Kim, S.K., Reinke, V., Stewart, A.F., Snyder, M., Waterston, R.H., Hyman, A.A., 2012. A genome-scale resource for in vivo tag-based protein function exploration in C. elegans. Cell 150, 855-866.

Saul, V., Niedenthal, R., Pich, A., Weber, F., Schmitz, M., 2015. SUMO modification of TBK1 at the adaptor-binding C-terminal coiled-coil domain contributes to its antiviral activity. Biochim Biophys Acta. 1853, 136-143.

Schindelin, J., Arganda-Carreras, I., Frise, E., Kaynig, V., Longair, M., Pietzsch, T., Preibisch, S., Rueden, C., Saalfeld, S., Schmid, B., Tinevez, J.Y., White, D.J., Hartenstein, V., Eliceiri, K., Tomancak, P., Cardona, A., 2012. Fiji: an open-source platform for biological-image analysis. Nature Methods 9, 676-682.

Seeler, J., Dejean, A., 2003. Nuclear and unclear functions of SUMO. Nature reviews. Molecular Cell Biology 4, 690-699.

Shen, T., Lin, H., Scaglioni, P., Yung, T., Pandolfi, P., 2006. The mechanisms of PML-nuclear body formation. Mol Cell. 24(3):331-9.

Shetty, P., Lo, M.C., Robertson, S.M., Lin, R., 2005. C. elegans TCF protein, POP-1, converts from repressor to activator as a result of Wnt-induced lowering of nuclear levels. Dev. Biol. 285, 584-592.

Showell, C., Binder, O., Conlon, F.L., 2004. T-box genes in early embryogenesis. Dev Dyn 229, 201-218.

Shyu, Y., Hiatt, S., Duren, H., Ellis, R., Kerppola, T., Hu, C., 2008. Visualization of protein interactions in living Caenorhabditis elegans using bimolecular fluorescence complementation analysis. Nature Protocols 3, 588-596.

Simmer, F., Moorman, C., Van Der Linden, A.M., Kuijk, E., Van Den Berghe, P.V., Kamath, R., Fraser, A.G., Ahringer, J., Plasterk, R.H., 2003. Genome-Wide RNAi of C. elegans Using the Hypersensitive rrf-3 Strain Reveals Novel Gene Functions. PLoS Biol 1, E12.

Sinclair, C.S., Adem, C., Naderi, A., Soderberg, C.L., Johnson, M., Wu, K., Wadum, L., Couch, V.L., Sellers, T.A., Schaid, D., Slezak, J., Fredericksen, Z., Ingle, J.N., Hartmann, L., Jenkins, R.B., Couch, F.J., 2002. TBX2 is preferentially amplified in BRCA1- and BRCA2-related breast tumors. Cancer Res 62, 3587-3591.

Singhvi, A., Frank, C.A., Garriga, G., 2008. The T-box gene tbx-2, the homeobox gene egl-5 and the asymmetric cell division gene ham-1 specify neural fate in the HSN/PHB lineage. Genetics 179, 887-898.

Sinha, S., Abraham, S., Gronostajski, R., Campbell, C., 2000. Differential DNA binding and transcription modulation by three T-box proteins, T, TBX1 and TBX2. Gene 258, 15-29.

Smith, P.A., Mango, S.E., 2007. Role of T-box gene tbx-2 for anterior foregut muscle development in C. elegans. Developmental Biology 302, 25-39.

Smyth, G.K., 2004. Linear models and empirical bayes methods for assessing differential expression in microarray experiments. Statistical Applications in Genetics and Molecular Biology 3, Article 3.

Spencer, W.C., Zeller, G., Watson, J.D., Henz, S.R., Watkins, K.L., McWhirter, R.D., Petersen, S., Sreedharan, V.T., Widmer, C., Jo, J., Reinke, V., Petrella, L., Strome, S., Von Stetina, S.E., Katz, M., Shaham, S., Ratsch, G., Miller, D.M., 3rd, 2011. A spatial and temporal map of C. elegans gene expression. Genome Research.

Sriramachandran, A.M., Dohmen, R.J., 2014. SUMO-targeted ubiquitin ligases. Biochim Biophys Acta. 1843, 75-85.

Stirnimann, C.U., Ptchelkine, D., Grimm, C., Muller, C.W., 2010. Structural basis of TBX5-DNA recognition: the T-box domain in its DNA-bound and -unbound form. Journal of Molecular Biology 400, 71-81.

Stringham, E., Dixon, D., Jones, D., Candido, E., 1992. Temporal and spatial expression patterns of the small heat shock (hsp16) genes in transgenic Caenorhabditis elegans. Molecular Biology of the Cell 3, 221-233.

Sulston, J.E., Horvitz, H.R., 1977. Post-embryonic cell lineages of the nematode, Caenorhabditis elegans. Developmental Biology 56, 110-156.

Sulston, J.E., Schierenberg, E., White, J.G., Thomson, J.N., 1983. The embryonic cell lineage of the nematode Caenorhabditis elegans. Developmental Biology 100, 64-119.

Sundaram, M., Greenwald, I., 1993. Suppressors of a lin-12 hypomorph define genes that interact with both lin-12 and glp-1 in Caenorhabditis elegans. Genetics, 765–783.

Sung, K.S., Go, Y.Y., Ahn, J.H., Kim, Y.H., Kim, Y., Choi, C.Y., 2005. Differential interactions of the homeodomain-interacting protein kinase 2 (HIPK2) by phosphorylation-dependent sumoylation. FEBS Letters 579, 3001-3008.

Takeuchi, J., Ohgi, M., Koshiba-Takeuchi, K., Shiratori, H., Sakaki, I., Ogura, K., Saijoh, Y., Ogura, T., 2003. Tbx5 specifies the left/right ventricles and ventricular septum position during cardiogenesis. Development 130, 5953-5964.

Thatcher, J., Haun, C., Okkema, P.G., 1999. The DAF-3 Smad binds DNA and represses gene expression in the Caenorhabditis elegans pharynx. Development 126, 91-107.

Timmons, L., Court, D.L., Fire, A., 2001. Ingestion of bacterially expressed dsRNAs can produce specific and potent genetic interference in Caenorhabditis elegans. Gene 263, 103-112.

Turki-Judeh, W., Courey, A.J., 2012. Groucho: a corepressor with instructive roles in development. Current Topics in Developmental Biology 98, 65-96.

Ureña, E., Pirone, L., Chafino, S., Pérez, C., Sutherland, J., Lang, V., Rodriguez, M., Lopitz-Otsoa, F., Blanco, F., Barrio, R., Martín, D., 2016. Evolution of SUMO function and chain formation in insects. Mol Biol Evol 33, 568-584.

van Wijk, S., Timmers, H., 2010. The family of ubiquitin-conjugating enzymes (E2s): deciding between life and death of proteins. FASEB Journal 24, 981-993.

Vance, K.W., Carreira, S., Brosch, G., Goding, C.R., 2005. Tbx2 is overexpressed and plays an important role in maintaining proliferation and suppression of senescence in melanomas. Cancer Res 65, 2260-2268.

Vormer, T., Foijer, F., Wielders, C., Reile, H., 2008. Anchorage-Independent growth of pocket protein-deficient murine fibroblasts requires bypass of G2 arrest and can be accomplished by expression of TBX2. Mol Cell Biol 28, 7263-7273

Wang, B., Lindley, L., Fernandez-Vega, V., Rieger, M., Sims, A., Briegel, K., 2012. The T box transcription factor TBX2 promotes epithelial-mesenchymal transition and invasion of normal and malignant breast epithelial cells. PloS One 7.

Wang, J., Feng, X.H., Schwartz, R.J., 2004. SUMO-1 modification activated GATA4-dependent cardiogenic gene activity. The Journal of Biological Chemistry 279, 49091-49098.

Wang, J., Li, A., Wang, Z., Feng, X., Olson, E.N., Schwartz, R.J., 2007. Myocardin sumoylation transactivates cardiogenic genes in pluripotent 10T1/2 fibroblasts. Mol Cell Biol 27, 622-632.

Wansleben, S., Peresa, J., Harea, S., Godingb, C., Prince, S., 2014. T-box transcription factors in cancer biology. Biochim Biophys Acta. 1846, 380-391.

Wilkinson, K.A., Henley, J.M., 2010. Mechanisms, regulation and consequences of protein SUMOylation. The Biochemical Journal 428, 133-145.

Wilson, V., Conlon, F.L., 2002. The T-box family. Genome Biology 3, REVIEWS3008.

Winnier, A., Meir, J., Ross, J., Tavernarakis, N., Driscoll, M., Ishihara, T., Katsura, I., Miller, D., 1999. UNC-4/UNC-37-dependent repression of motor neuron-specific genes controls synaptic choice in Caenorhabditis elegans. Genes Dev 13, 2774-2786.

Xia, D., Zhang, Y., Huang, X., Sun, Y., Zhang, H., 2007. The C. elegans CBFbeta homolog, BRO-1, regulates the proliferation, differentiation and specification of the stem cell-like seam cell lineages. Developmental Biology 309, 259-272.

Xu, Z., Au, S., 2005. Mapping residues of SUMO precursors essential in differential maturation by SUMO-specific protease, SENP1. The Biochemical Journal, 325-330.

Yaklichkin, S., Vekker, A., Stayrook, S., Lewis, M., Kessler, D.S., 2007. Prevalence of the EH1 Groucho interaction motif in the metazoan Fox family of transcriptional regulators. BMC Genomics 8, 201.

Zhang, H., Emmons, S.W., 2002. Caenorhabditis elegans unc-37/groucho interacts genetically with components of the transcriptional mediator complex. Genetics 160, 799-803.

Zhang, H., Smolen, G.A., Palmer, R., Christoforou, A., van den Heuvel, S., Haber, D.A., 2004. SUMO modification is required for in vivo Hox gene regulation by the Caenorhabditis elegans Polycomb group protein SOP-2. Nat Genet 36, 507-511.

Zhao, Q., Xie, Y., Zheng, Y., Jiang, S., Liu, W., Mu, W., Liu, Z., Zhao, Y., Xue, Y., Ren, J., 2014. GPS-SUMO: a tool for the prediction of sumoylation sites and SUMO-interaction motifs. Nucleic Acids Res. 42, 325-330.

Zhong, S., Müller, S., Ronchetti, S., Freemont, P., Dejean, A., Pandolfi, P., 2000. Role of SUMO-1-modified PML in nuclear body formation. Blood 95, 2748-2752.

Zweier, C., Sticht, H., Aydin-Yaylagul, I., Campbell, C.E., Rauch, A., 2007. Human TBX1 missense mutations cause gain of function resulting in the same phenotype as 22q11.2 deletions. American Journal of Human Genetics 80, 510-517.

VITA

Paul Huber, B.S.

EDUCATION

University of Illinois at Chicago, Chicago, IL

Doctor of Philosophy in Molecular, Cell, and Developmental Biology — **May 2016 (Expected)**

Bachelor of Science in Biological Sciences — **December 2006**

RESEARCH EXPERIENCE

Doctoral Researcher — **August 2007 - Present**

University of Illinois at Chicago, Department of Biological Sciences, MCDB

Laboratory of Dr. Peter Okkema

Identified two post-translational mechanisms, SUMOylation and interaction with a Groucho-like corepressor, which regulate activity of a T-box transcription factor, TBX-2, in pharyngeal development.

Research Assistant — **January – August 2007**

University of Illinois at Chicago, Department of Biological Sciences

Laboratory of Dr. Howard Buhse

Examined and compared growth kinetics of competing populations of two similar but distinct *tetrahymena* species.

TEACHING EXPERIENCE

Teaching Assistant

University of Illinois at Chicago, Department of Biological Sciences

Developmental Biology Laboratory — **Spring 2013, 2014, 2015**

Molecular Biology Laboratory — **Fall 2013, 2014**

Mendelian Genetics Laboratory — **Fall 2007 - Fall 2012**

Mentor — **Fall 2011 - Summer 2014**

University of Illinois at Chicago, Department of Biological Sciences

Trained and supervised three undergraduate researchers.

Trained and supervised two laboratory aides.

Lead Clinician — **May 1998 – August 2007**

Soccer Made in America, greater Chicago area, IL

Organized, promoted, and led team-based youth soccer skills training camps.

VOLUNTEER EXPERIENCE

Research Assistant — **June 2015 - Present**

The Chicago Field Museum

Helped to identify and classify several new species of tropical lichens collected in Sri Lankan forests.

Fundraiser — **Fall 1992 – Summer 1999**

Misericordia Heart of Mercy, Chicago, IL

Assisted in collecting and counting donations, as well as setting up and running special events.

SKILLS AND TECHNIQUES

Scientific: standard *C. elegans* and mammalian cell culture techniques, *Drosophila* handling and larval dissection, fresh and saltwater aquarium setup and maintenance, sea urchin growth and handling, planaria handling and dissection, fluorescence microscopy, luciferase gene reporter assay, bimolecular fluorescence complementation assay, gel shift assay, β-gal assay, microbial growth and handling, bacterial transformation, advanced molecular cloning, PCR and primer design, DNA sequence analysis, DNA and protein (native and denaturing) electrophoresis, DNA and protein purification and quantitation, immunoblotting, immunostaining.
Software: BLAST, MacVector, PyMOL, Wormbase, Axiovision, Zen lite, Fiji, Photoshop, Microsoft Office.

AWARDS AND HONORS

University of Illinois at Chicago, Chicago, IL

University Research Achievement Award	**2013, 2015**
Department of Biological Sciences Travel Award	**2009, 2012, 2013**
Liberal Arts and Sciences PhD Travel Award	**2012**
Dean's List	**Fall 2004, Spring 2006**

PROFESSIONAL ASSOCIATIONS

Genetics Society of America
UIC Developmental Biology Club
UIC *C. elegans* club

PEER-REVIEWED PUBLICATIONS

P. Huber, T. Crum, S. Roy Chowdhuri and Peter Okkema. "*C. elegans* T-box factor TBX-2 function in pharyngeal development depends on interaction with the Groucho-like corepressor UNC-37". (In review)

P. Huber, T. Crum, L. Clary, T. Ronan, A. Packard and Peter Okkema. "Function of the *C. elegans* T-box factor TBX-2 depends on SUMOylation" *Cellular and Molecular Life Sciences* 2013. 70(21):4157-68.

CONFERENCE PRESENTATIONS

Paul Huber, Tanya Crum, Lynn Clary, Tom Ronan, Adelaide Packard, Peter Okkema. Function of the *C. elegans* T-box factor TBX-2 depends on SUMOylation (June 2013). Genetics Society of America 19th International *C. elegans* meeting, UCLA, Los Angeles, CA. Poster presentation.

Paul Huber, Tanya Crum, Lynn Clary, Peter Okkema. Examining the role of SUMOylation in *C. elegans* T-box transcription factor TBX-2 function (February 2012). SUMO, Ubiquitin, UBL Proteins Conference, University of Texas MD Anderson Cancer Center, Houston, TX. Oral presentation.

Paul Huber, Tanya Crum, Peter Okkema. Examining the role of SUMOylation in C. elegans T-box transcription factor TBX-2 function (July 2011). Society for Developmental Biology 70th Annual meeting, Hyatt Regency, Chicago, IL. Poster presentation.

Tanya Crum, **Paul Huber**, Peter Okkema. SUMO and the T-box factor TBX-2 (June 2009). Genetics Society of America 17th International *C. elegans* meeting, UCLA, Los Angeles, CA. Poster presentation.